Niger. J. Physiol. Sci. 38 (December 2023): 135 – 143
www.njps.physiologicalsociety.com

Niger. J. Physiol. Sci.

Full length Research Article

Cerebellar and Olfactory Bulb Perturbations Induced by Vanadium Neurotoxicity in the African Giant Rat (*Cricetomys gambianus*, Waterhouse)

***Mustapha, O.A.[1], Omojola F.A.[1], Olaolorun F.A.[1] and Olude M.A.[1]**

[1]Neuroscience Unit, Department of Veterinary Anatomy, College of Veterinary Medicine, Federal University of Agriculture, Abeokuta, Ogun State, Nigeria.

Summary: The African giant rat, AGR (*Cricetomys gambianus*) is a unique rodent known for its keen sense of smell which has enabled its use in the diagnosis of tuberculosis and demining activities in war torn countries. This keen sense of smell and the ability to navigate tight spaces are skills modulated by the olfactory bulb and cerebellum. While the brain is generally susceptible to environmental pollutants such as heavy metals, vanadium has predilection for these two brain regions. This work was thus designed to investigate the probable neurotoxic effect of vanadium on the neuronal cytoarchitecture of the cerebellum and olfactory bulb in this rodent. To achieve this, twelve adults male AGRs were divided into two groups (vanadium and control groups) and were given intraperitoneal injections of 3mg/kg body weight sodium metavanadate and normal saline respectively for 14 days. After which they were sacrificed, and brains harvested for histological investigations using Nissl and Golgi staining techniques. Results from our experiment revealed Purkinje cell degeneration and pyknosis as revealed by a lower intact-pyknotic cell (I-P) ratio, higher pyknotic Purkinje cell density and poor dendritic arborizations in the molecular layer of the cerebellum in the vanadium treated group. In the olfactory bulb, neuronal loss in the glomerular layer was observed as shrunken glomeruli. These neuronal changes have been linked to deficits in motor function and disruption of odor transduction in the olfactory bulb. This work has further demonstrated the neurotoxic effects of vanadium on the cerebellum and olfactory bulb of the AGR and the likely threat it may pose to the translational potentials of this rodent. We therefore propose the use of this rodent as a suitable model for better understanding vanadium induced olfactory and cerebellar dysfunctions.

Keywords*: cerebellum, olfaction, olfactory dysfunction, glomeruli, vanadium, neurotoxicity*

**Authors for correspondence: mustaphaoa@funaab.edu.ng , Tel: +2348035915275*

Manuscript received- February, 2023; Accepted: October 2023

DOI: https://doi.org/10.54548/njps.v38i2.3

INTRODUCTION

The African giant rat (*Cricetomys gambianus*), also known as the giant pouched rat, HeroRAT, and Sniff Rat, is a common mammal belonging to the order Rodentia (Cooper 2008; Adekanmbi and Olude, 2021). They are indigenous to sub–Saharan Africa, distributed widely from regions of the West African savannah zones through the Guineo-Congolian forest to the savannahs of east and southern Africa (Musser and Carleton, 2005; Cooper 2008; Olayemi *et al*., 2022). This rodent is unique due to its sheer body size and some noteworthy attributes which include the large cheek pouches, high olfactory acumen and dexterous use of its limbs (Ibe *et al*., 2014; Mustapha *et al*., 2015). These qualities have aroused interest into the scientific and translational applications of these rats. One of such applications is the deployment of their keen sense of smell in successfully sniffing out tuberculosis-infected samples and detecting landmines during demining activities in war ravaged countries particularly in Africa. (Poling *et al*., 2015; Adekanmbi and Olude, 2021; Makoye, 2022). Recent experiments and trainings have seen the potential of these unique rodents in search and rescue operations to save human victims of disasters since they can adequately navigate narrow spaces owing to the adroit use of their limbs (Euronews and Reuters, 2022). The AGR's acute sense of smell and limb dexterity are modulated by the olfactory bulb and cerebellum respectively (Tufo *et al*., 2022; Thau *et al*., 2022).

Generally, the brain has been shown to be susceptible to various perturbations including environmental toxicants. The olfactory system, being the most rostral, most vulnerable, and most exposed part of the brain, is especially liable to neural injury because its primary sensory neurons are in direct contact with the external environment (Czarnecki *et al*., 2012; Rey *et al*., 2018; Calvo-Ochoa and Byrd-James 2019). Quite notably, environmental pollutants such as heavy metal neurotoxicity have been reported in literature (Garcia *et al*., 2005; Azubike *et al*., 2012; Li *et al*., 2021: Mustapha *et al*., 2022; Usende *et al*., 2022).

Heavy metals are naturally occurring elements that are found throughout the earth's crust. Though some have biological functions in trace amounts (Tchounwou *et al*., 2011; Jyothi 2020), bioaccumulation due to prolonged exposure to heavy metals can result in disruption of many biological system including the CNS where it has been shown to be neurotoxic and increase risk of neurodegenerative diseases (Naseri *et al*., 2021; Li *et al*., 2021).

Large quantities of vanadium compounds are released into the environment mainly through the burning of fossil fuels and gas flaring activities as in seen the Niger Delta region of Nigeria, with vanadium reported as the most abundant heavy metal in petroleum samples (Igado *et al*., 2012; Mustapha *et al*., 2018; Olaolorun *et al*., 2021). Vanadium accumulates in soil, groundwater, and plants, and is consumed by animals and humans (Pyrzynska and Wierzbicki, 2004; Chen *et al*., 2021). Vanadium exposure to humans has been shown to cause motor deficits (Li *et al*., 2013; Ngwa *et al*., 2014). Putatively, vanadium exerts its neurotoxic effects by causing oxidative damages to neural tissues in several regions within the brain (Ścibior *et al*., 2019; Rojas-Lemus *et al*., 2020; Xiong *et al*., 2020). Although, Mustapha *et al*., (2023) reported the effect of vanadium on the hippocampal-neuronal circuitry of the AGR, the neurotoxic effect of this metal on the olfactory bulb and cerebellum is yet to be documented. This work is thus designed to investigate the possible neurotoxic effect of vanadium on the neuronal cytoarchitecture of the cerebellum and olfactory bulb.

MATERIALS AND METHODS

Ethical consideration: All experimental procedures followed the criteria established by the College of Veterinary Medicine Research Ethics Committee (CREC) of the Federal University of Agriculture Abeokuta. Ethical Approval Reference Number: FUNNAB/COLVET/ CREC/007/18.

Animals: Twelve adult male AGRs were purchased from local hunters who had captured these rodents from the wild in Southwest, Nigeria. Physical examination was conducted on all animals to ensure they are devoid of any physical deformities that may interfere with the study. They were transferred to the Animal House of the Department of Veterinary Anatomy, Faculty of Veterinary Medicine, University of Ibadan, and housed in locally made cages (60cm long x 32cm wide x 21cm high) with a metal cap to mimic the nocturnal environment of the rodents and to provide them with a dark sleeping compartment. Feeding troughs containing nuts and rat pellets (Ladoke® type) and water troughs were fixed to the wall of this chamber. Screen wires were fixed at the other end of the cage to allow for light and proper ventilation.

Experimental procedure: Rats were stabilized for 48 hours before commencement of the experiment. Animals were randomly assigned into two groups of six animals each: vanadium (treatment) and control (sterile water). AGR in vanadium group were dosed with sodium metavanadate daily (Sigma-Aldrich, St. Louis, MO, USA; pH7.7; 3mg/kg body weight; intra peritoneally, IP) according to Garcia *et al*., (2004) and Olude *et al*., (2018) while control group were given sterile water, IP. All animals were dosed daily for a period of 14 days after which they were sacrificed. The rats were anaesthetized by intraperitoneal injections of 100mg/kg Ketamine (Ketanir®, Gujarat, India) and 10mg/kg Xylazine (Xylazine 20 Inj® KEPRO, Holland) after which they were perfused with 4% paraformaldehyde transcardia. Their brains were harvested with the aid of a pair of bone nippers as described by Olude *et al*., (2018). The olfactory bulbs and cerebellum were carefully dissected from the rest of the brain and later post fixed in 4% paraformaldehyde for 48 hours and subsequently processed histologically for Nissl (Cresyl Violet) and Golgi stains. Nissl stain was used for illustrating the neuronal somata and cytoarchitecture of the olfactory bulb and cerebellar cortex while the Rapid Golgi Technique was used to elucidate the Purkinje neurons with their axonal and dendritic projections in the cerebellum.

The Nissl Technique: The brain samples were passed through the serial process of washing, dehydration, clearing, and embedding in paraffin. The embedded samples were then cut into 5µm thick mid- and para-sagittal sections. Sections were stained following a standard Nissl protocol as described by Olude *et al*., (2014). Briefly, sections were deparaffinized in xylene for 5 min, followed by a hydration series in graded alcohols for 3 min each. After 3 min in distilled water, sections were stained in 0.1% cresyl violet solution for 10 min at 57°C. Sections were then differentiated in 95% alcohol for 20 min. After rinsing in distilled water, sections followed an ascending series of dehydration in graded alcohols for 3 min each, and finally 5 min in xylene. The sections were then covered with mounting medium and glass coverslip.

The Rapid Golgi Technique: Brain slices of not more than 4mm thickness were cut in horizontal and frontal planes and immersed in osmium-dichromate solution at room temperature for 7 days. The pieces were transferred into 0.75% aqueous silver nitrate and kept for 24 hours in the dark. Then the pieces were placed back into the same osmium-dichromate solution used in the first step in which they were left in for 6 days. This step was followed by the immersion of the pieces into silver nitrate solution for 48 hours in the dark. Then they were transferred into a new osmium-dichromate solution for 5 days. Again, the step with silver nitrate was repeated with increased time solution for 3 days. The pieces were then dehydrated in absolute alcohol for 5 minutes and embedded in soft paraffin matrix by pressing each piece gently into the melted paraffin. 200µm sections were made on a sliding microtome. The sections were transferred into absolute alcohol for 15 minutes, after which the sections were transferred into oil cloves for 15 minutes (Faulogy *et al*., 2008).

Photomicrography and Histology: All stained sections were examined and imaged under the light microscope with a built-in 1.3 megapixel digital camera (OMAX® MD82ES10) and advanced image software (OMAX ToupView Version x64, 4.11.19627). The observed histological features and cytoarchitecture in the cerebellum and olfactory bulbs were appropriately described.

Quantitative Densitometric Analysis of Purkinje Cells: Purkinje cell density (PCD) was estimated in the Purkinje cell layer of AGR cerebellum using a computer-based image analysis software (FIJI: ImageJ 1.53t; Java 1.8.0_172; 64bit NIH, USA). For each AGR, the number of Purkinje cells (intact and pyknotic) were counted from three different cerebellar folia of each section. Pyknotic neurons (with signs of injury) were identified and delineated from intact (healthy) neurons based on criteria described below (Kamal and Kamal, 2013; Ribeiro *et al*., 2017):

- **Cellular oedema:** represented by cells with visibly intact nuclei that showed an increase in cytoplasm/nucleus size ratio compared to adjacent cells
- **Autolysis:** anuclear cells or cells exhibiting abnormal nuclear morphology; and
- **Darkened and small cells:** shrunken cells with increased nuclear compactness

Number of intact and pyknotic neurons were counted over a surface length of 500µm using Nissl-stained sections at ×100 magnification according to methods described by Ribeiro *et al*., (2017). PCD was calculated as the sum of intact and pyknotic neurons in the Purkinje cell layer of the cerebellum over a surface length of 500µm while Intact-Pyknotic (I-P) ratio was also calculated for both control and vanadium groups.

Data Analysis: PCD were reported as mean ± standard error of mean. Inferential statistics was carried out with unpaired student t test. Differences in the means of intact and pyknotic neurons were analyzed using GraphPad Prism Software (version 7.00; GraphPad Software Inc., San Diego, CA, USA). A value of $p < 0.05$ was set to be statistically significant.

RESULTS

Effect of Vanadium Neurotoxicity on the histomorphology of the AGR Cerebellar Cortex: In Nissl stained sections, the cytoarchitecture of the cerebellar cortex was preserved in the control group, showing a distinct monolayer of intact Purkinje cells characterized by large pyriform shaped somata with prominent nucleoli and cytoplasm. These cells were located between an outer relatively hypocellular molecular layer and an inner densely packed granular cell layer (Plate 1). In contrast, the vanadium group showed a loss of cellular integrity of the Purkinje cells (Figure 1). Furthermore, granular cell degeneration was seen in the cerebellar cortex of vanadium-dosed AGR while the cytoarchitecture of these cells were preserved in control groups

Similarly, Golgi-stained sections of the vanadium group demonstrated Purkinje cells with poor dendritic arborizations into the molecular layer of the cerebellar cortex, while the control group had distinct and highly ramified dendritic projections in the molecular layer (Plate 2).

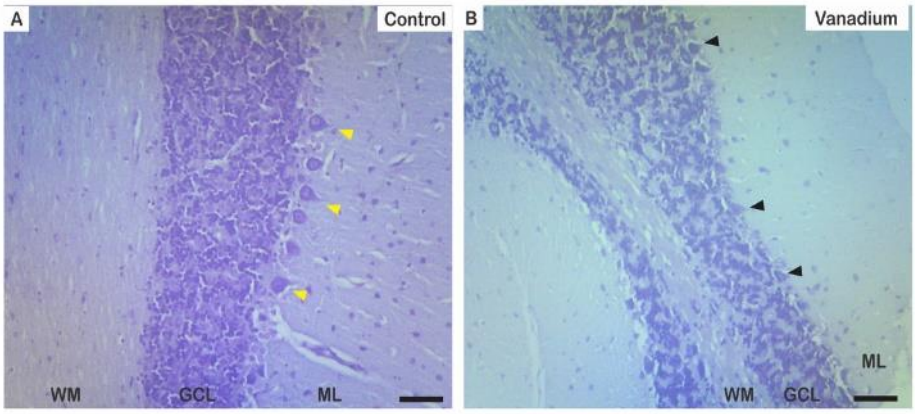

Plate 1:
Nissl-stained sections of AGR cerebellar cortex showing intact Purkinje cells (yellow arrows) in the control group [**A**], while a loss of Purkinje cells with numerous pyknotic cells (black arrows) in the vanadium dosed group. ML: molecular layer; GCL: granular cell layer; WM: white matter. Scale bar: 100µm.

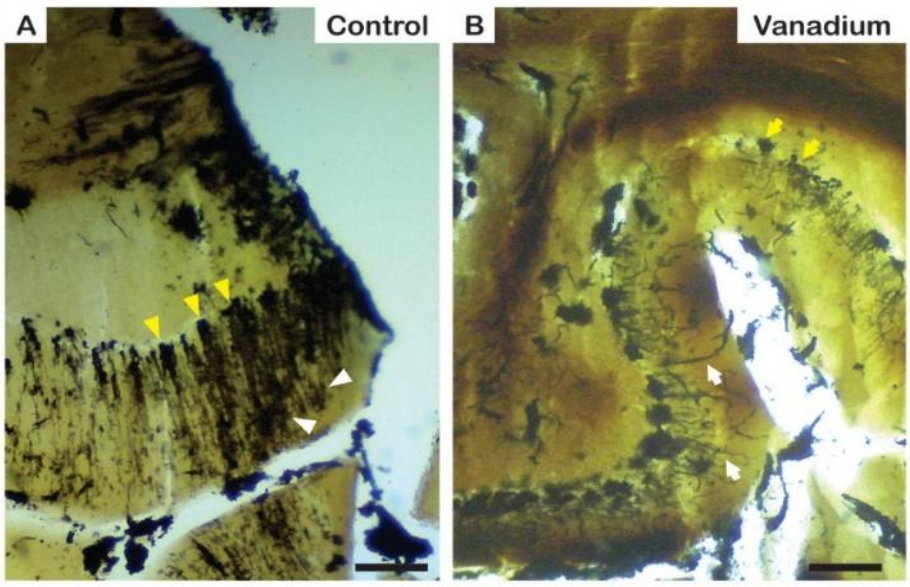

Plate 2:
Golgi-stained sections of the AGR cerebellar cortex. [A]: Control group - intact Purkinje somata (yellow arrowhead) with distinct dendritic projections (white arrowheads) into the molecular layer in the control group; [B]: Vanadium group - fewer Purkinje somata (yellow arrows) with reduced dendritic arborizations (white arrows). Scale bar: 50µm

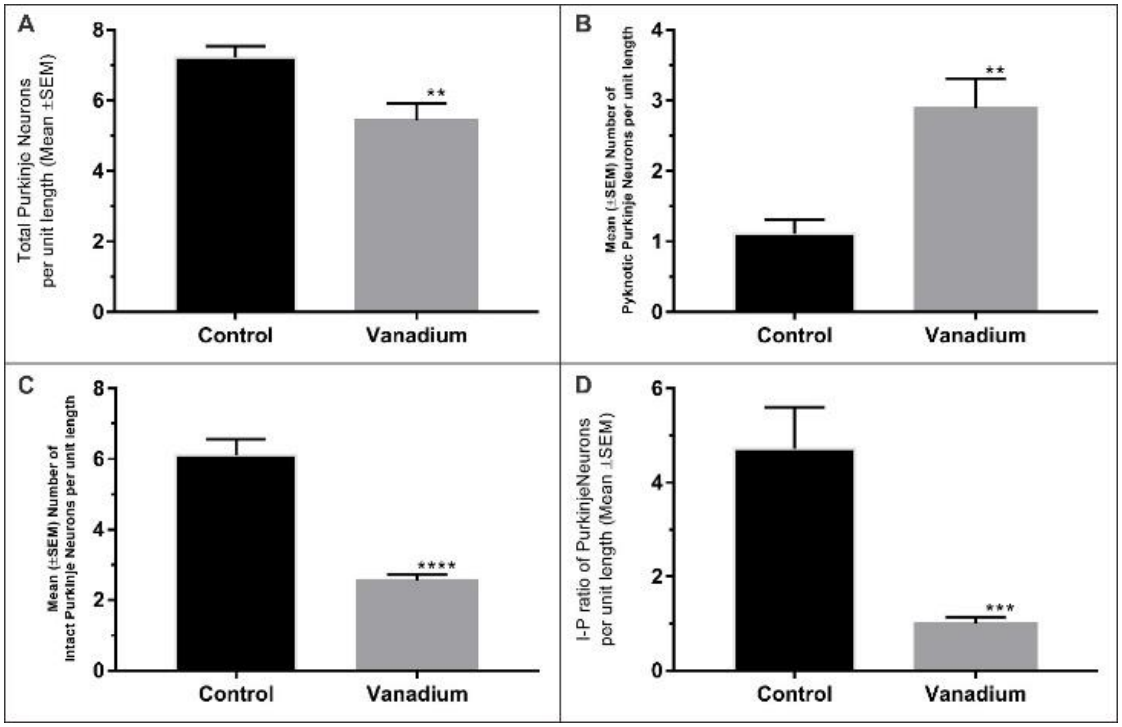

Figure 1:
Quantitative cell counts of: (A) total Purkinje neurons, (B): mean pyknotic Purkinje neurons, (C): mean intact Purkinje neurons, (D): Intact - Pyknotic Purkinje neuron ratio in the AGR cerebellar cortex. Cell count was done over a linear distance of approximately 500µm. Statistical significance was set @ $p < 0.05$.

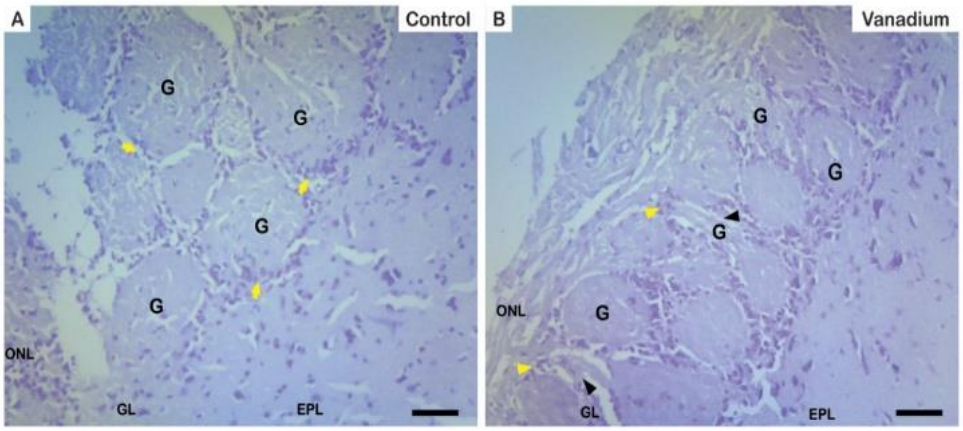

Plate 3:
Nissl-stained sections of the AGR olfactory bulb. Control group **[A]:** normal glomeruli (G) surrounded by periglomerular cells (yellow arrows) in the control group. Vanadium group **[B]** shrunken glomeruli (black arrowheads) surrounded by periglomerular cells (yellow arrowheads). ONL: olfactory nerve layer; GL: glomerular layer; EPL: external plexiform layer. Scale bar: 100µm

Effect of Vanadium Neurotoxicity on the Purkinje cell density in the AGR Cerebellar Cortex: Morphometric analysis revealed a statistically significant decrease in total PCD in the vanadium-dosed group compared to control ($P = 0.0070$; Figure 1a). A higher pyknotic PCD, lower intact PCD and lower I-P ratio was noted for AGR dosed with vanadium compared to the controls which had a lower pyknotic PCD, higher intact PCD and higher I-P ratio (Figure 1b - d). The observed differences in mean were statistically significant with P values given as $P=0.0016$, $P<0.0001$ and $P=0.0007$ respectively.

Effect of Vanadium Neurotoxicity on the histology of the AGR Olfactory Bulb: Disruption in the cellular integrity evidenced by the shrinkage of few glomeruli in the glomerular cell layer was noted for AGR dosed with vanadium. Compared to vanadium, the control group had intact, glomeruli surrounded by periglomerular cells (Plate 3).

DISCUSSION

This study documents vanadium induced neural perturbations in the cerebellum and olfactory bulb of the AGR – a rodent known for its profound olfactory acuity, cognition, and limb dexterity. We highlighted the neurotoxic effect of vanadium on the glomeruli (an important waystation in the pathway for signal transduction of odours) in the olfactory bulb, and the Purkinje neurons of the cerebellar cortex.

Vanadium has been shown to cross the blood-brain barrier and accumulate in the brain where it exerts its deleterious effect by generating reactive oxygen species and

causing lipid peroxidation (Mustapha *et al*., 2014; Azeez *et al*., 2016; Fatola *et al*., 2019). Current findings have established that vanadium has preferential predilection for the olfactory bulb, brain stem and cerebellum (Haider *et al*., 1998, Garcia *et al*., 2005; Ngwa *et al*., 2014; Colín-Barenque *et al*., 2015; Folarin *et al*., 2017; Rojas-Lemus *et al*., 2020).

In the olfactory bulb, for instance, vanadium has been shown to induce olfactory dysfunction typified by decreased olfactory bulb volume and, severe dopaminergic neuronal loss in the glomerular layer of the olfactory bulb (Ngwa *et al*., 2014). From this study, we observed focal lesions of glomeruli shrinkage at the glomerular layer of the OB of AGR dosed with vanadium. This observation may reflect a destruction and/or disruption of the dopaminergic neurotransmission system of the OB, and consequential reduction of the synaptic surface area in this layer. Indeed, dopamine plays a significant role in olfaction (Duchamp-Viret *et al*., 1997, Hsia *et al*., 1999, Koster *et al*., 1999; Ngwa *et al*., 2014) and have been shown to be expressed in high abundance in the glomerular layer of the OB (Halasz *et al*., 1981, Davila *et al*., 2003), with changes in dopamine levels shown to affect olfaction. Dopamine regulates transmission between the olfactory bulb epithelium and the olfactory bulb glomeruli to mediate entry of sensory olfactory information into the brain (Hsia *et al*., 1999). Ngwa *et al*., (2014) posited that the depletion of dopamine in the olfactory bulb may impair odor identification and discrimination by disinhibition of neural transmission in olfactory glomeruli consequently leading to impaired olfactory processing.

Purkinje neurons are the primary processing units and sole output neurons of the cerebellar circuitry (Kemp *et al*., 2016; White *et al*., 2021). They send inhibitory GABA-ergic inputs to the deep cerebellar nuclei in the cerebellum and play pivotal roles in motor coordination, control, and learning (Purves *et al*., 2001; Kano and Watanabe, 2020). These neurons have been shown to be susceptible to both genetic and environmental perturbations that may disrupt their regular functions (Garcia *et al*., 2005; Hegarty *et al*., 2020). Pathologies associated with Purkinje cell loss have been associated with motor deficits and incoordination. Thus, optimal Purkinje cell function is essential to the overall function of the cerebellum (Xia *et al*., 2013; Louis *et al*., 2014; Redondo *et al*., 2015; Folarin *et al*., 2017). From this study, Purkinje cell degeneration and pyknosis substantiated by a higher pyknotic PCD, lower total PCD, and lower I-P ratio in the Purkinje cell layer of the AGR cerebellum dosed with vanadium may suggest a likely deficit in motor coordination and learning – an essential neurobehavioural forte of this rodent. This Purkinje neuronal degeneration was further corroborated with Golgi stain which revealed significant loss of dendritic arborizations of the Purkinje neurons in the molecular layer. Reduction in dendritic arborizations is a structural change that is usually associated with neuronal dysfunction, leading to dysfunctional neural circuits and it is thought to precede neuronal death (Ferrer *et al*., 1984; Beckers and Moons, 2019). Previous works have reported a reduction of Purkinje cell dendritic branching in patients with essential tremor (Louis *et al*., 2014); hereditary ataxias (Shintaku and Kaneda, 2009), chronic alcoholics (Ferrer *et al*., 1984) and in Alzheimer's disease (Mavroudis *et al*., 2013).

Interestingly, olfactory dysfunction induced by the dopamine depletion has been shown to be associated with cerebellar motor deficits, as seen in Parkinson's disease patients, via the nigrostriatal dopaminergic system. More intriguing is that, recently the striatum has been shown to have a di-synaptic communication with the cerebellum via the cerebello-thalamo-cortical circuit (Bostan *et al*., 2010; Bostan and Strick, 2018) while the dentate nucleus of the cerebellum also has a di-synaptic projection to an input stage of the striatum (Bostan *et al*., 2010). Thus, providing an anatomical substrate for substantial two-way integrated functional network that play a pivotal role in a variety of motor and non-motor functions (Milardi *et al*., 2019).

Neuronal death is an important process in many neurodegenerative diseases that is associated with oxidative stress. One of the probable mechanisms by which vanadium might have caused the observed neuropathologies in this study is by ROS-mediated oxidative damages to cellular macromolecules such as lipids, proteins and DNA, leading to a cascade of cellular injuries and metabolic dysfunctions, and ultimately apoptosis and necrosis (Bandyopadhyay *et al*., 1999; Mustapha *et al*., 2014 & 2019; Rojas- Lemus *et al*., 2020; Xiong *et al*., 2021; Folarin *et al*., 2018; Usende *et al*., 2018 & 2022). Vanadium has been shown to increase the upregulation of apoptotic proteins such as p53, induce mitochondrial membrane permeability, mitochondrial membrane potential disruption, cytochrome c release, and activation of proteases such as caspase 9 and 3 (Chakraborty *et al*. 2005; Roos and Kaina, 2006; Caicedo *et al*., 2008; Zhao *et al*., 2010; Colín-Barenque *et al*., 2015; Xiong *et al*., 2021).

Although stereological analysis allows for an unbiased approach to tissue sampling (Choe *et al*., 2016), there remain real concerns on the feasibility for stereological studies of the entire brain region selected (case in point: the cerebellum), as the entire cerebellum or even a hemi-cerebellar study is rare if ever available, as is required for such analyses. Our results should thus be interpreted within the context of this limitation. Also, a detailed neurochemical profiling of these brain regions would provide more credence to these pathologies and will be considered in future studies.

In conclusion, this work has put together some evidences of the vanadium-induced neuropathology in the cerebellum and olfactory bulb of the AGR, characterized by neuronal degeneration, loss of dendritic arborizations, pyknosis, and neuronal cell loss. It has also demonstrated the potential threat environmental pollution may contribute to translational benefits of the rodent. We propose this rodent as a suitable model for a better understanding of olfactory dysfunctions and cerebellar disorders.

REFERENCES

Adekanmbi, A. J., and Olude, M. A. (2021). An alternate prospect in detecting presymptomatic and asymptomatic COVID-19 carriers through odor differentiation by HeroRATs. *J. Vet. Behav.* 42: 26-29. https://doi.org/10.1016/j.jveb.2020.12.001

Azeez, I. A., Olopade, F., Laperchia, C., Andrioli, A., Scambi, I., Onwuka, S. K., Bentivoglio, M., and Olopade, J. O. (2016). Regional myelin and axon damage and neuroinflammation in the adult mouse brain after long

exposure. *J. Neuropathol. Exp. Neurol*., 75(9):843-854. https://doi.org/10.1093/jnen/nlw058.

Ebokaiwe A. P., Adedara I. A., Owoeye O. and Farombi E. O. (2013). Neurotoxicity of Nigerian bonny light crude oil in rats. *Drug Chem. Toxicol*. 36(2): 187-195. doi: 10.3109/01480545.2012.710619

Bandyopadhyay U., Das D., and Banerjee R. K. (1999). Reactive oxygen species: Oxidative damage and pathogenesis. *Curr. Sci*. 77(5): 658-666.

Beckers, A., and Moons, L. (2019). Dendritic shrinkage after injury: a cellular killer or a necessity for axonal regeneration? Neural Regen. Res. 14(8): 1313–1316. https://doi.org/10.4103/1673-5374.253505

Bostan, A. C., and Strick, P. L. (2018). The basal ganglia and the cerebellum: nodes in an integrated network. *Nat. Rev. Neurosci*. 19: 338–350. doi: 10.1038/s41583-018-0002-7

Bostan, A. C., Dum, R. P., and Strick, P. L. (2010). The basal ganglia communicate with the cerebellum. Proc. Natl. Acad. Sci. USA. 107(18): 8452–8456. https://doi.org/10.1073/pnas.1000496107

Briffa, J., Sinagra, E., and Blundell, R. (2020). Heavy metal pollution in the environment and their toxicological effects on humans. Heliyon 6(9): e04691. https://doi.org/10.1016/j.heliyon.2020.e04691

Caicedo M., Jacobs J. J., Reddy A., and Hallab N. J. (2008). Analysis of metal ion-induced DNA damage, apoptosis, and necrosis in human (Jurkat) T-cells demonstrates Ni2+ and V3+ are more toxic than other metals: Al3+, Be2+, Co2+, Cr3+, Cu2+, Fe3+, Mo5+, Nb5+, Zr2+. *J. Biomed. Mater. Res*. 86: 905–913.

Calvo-Ochoa, E., and Byrd-Jacobs, C. A. (2019). The Olfactory System of Zebrafish as a Model for the Study of Neurotoxicity and Injury: Implications for Neuroplasticity and Disease. *Int. J. Mol. Sci.* 20(7): 1639. https://doi.org/10.3390/ijms20071639

Campbell J. (2011). 'HeroRATs' corner landmines and tuberculosis in Africa. https://www.cfr.org/blog/herorats-corner-landmines-and-tuberculosis-africa. Date accessed: January 6,2023

Chakraborty T., Samanta S., Ghosh B., Thirumoorthy N., and Chatterjee M. (2005). Vanadium induces apoptosis and modulates the expressions of metallothionein, Ki-67 nuclear antigen, and p53 during 2-acetylaminofluorene-induced rat liver preneoplasia. *J. Cell Biochem*. 94: 744–762.

Chen, L., Liu, J., Hu, W., Gao, J., and Yang, J. (2021). Vanadium in soil-plant system: Source, fate, toxicity, and bioremediation. *J. Hazard. Mater*. 405: 124200. https://doi.org/10.1016/j.jhazmat.2020.124200

Cheng A. (2022). Magawa, 'hero rat' who sniffed out 71 land mines with his tiny nose, dies in retirement. The Washington Post. https://www.washingtonpost.com/world/2022/01/12/magawa-african-landmine-rat-dies-cambodia/. Date accessed: January 6, 2023.

Choe, M., Cortés, E., Vonsattel, J. P., Kuo, S. H., Faust, P. L., and Louis, E. D. (2016). Purkinje cell loss in essential tremor: Random sampling quantification and nearest neighbor analysis. *Mov. Disord.* 31(3): 393–401. https://doi.org/10.1002/mds.26490

Colín-Barenque, L., Pedraza-Chaverri, J., Medina-Campos, O., Jimenez-Martínez, R., Bizarro-Nevares, P., González-Villalva, A., Rojas-Lemus, M., and Fortoul, T. I. (2015). Functional and morphological olfactory bulb modifications in mice after vanadium inhalation. *Toxicol. Pathol*. 43(2): 282–291. https://doi.org/10.1177/0192623314548668

Cooper, R.G. (2008). Care, husbandry and diseases of the African giant rat (*Cricetomys gambianus*): Review Article. *J. S. Afr. Vet. Assoc.* 79(2): 62-66. https://doi.org/10.4102/jsava.v79i2.245

Czarnecki L. A., Moberly A. H., Turkel D. J., Rubinstein T., Pottackal J., Rosenthal M. C., McCandlish E. M. K, Buckley B., and McGann J. P. (2012). Functional Rehabilitation of Cadmium-Induced Neurotoxicity Despite Persistent Peripheral Pathophysiology in the Olfactory System, *Toxicol. Sci.* 126(2): 534–544. https://doi.org/10.1093/toxsci/kfs030

Davila, N. G., Blakemore, L. J., and Trombley, P. Q. (2003). Dopamine modulates synaptic transmission between rat olfactory bulb neurons in culture. *J. Neurophysiol*. 90(1): 395-404.

Duchamp-Viret, P., Coronas, V., Delaleu, J. C., Moyse, E. and Duchamp, A. (1997). Dopaminergic modulation of mitral cell activity in the frog olfactory bulb: a combined radioligand binding–electrophysiological study. *Neurosc*i. 79(1): 203-216.

Euronews and Reuters (2022). Rodents to the rescue: Trained rats with hi-tech backpacks could save your life in a disaster. Biztech News. https://www.euronews.com/next/2022/11/11/rodents-to-the-rescue-trained-rats-with-hi-tech-backpacks-could-save-your-life-in-a-disast. Date accessed: January 6, 2023.

Fatola, O. I., Olaolorun, F. A., Olopade, F. E., and Olopade, J. O. (2019). Trends in vanadium neurotoxicity. *Brain Res. Bull*. 145: 75–80. https://doi.org/10.1016/j.brainresbull.2018.03.010

Faulogy, E. I., Kubikova, E. and Benuska, J. (2008). Microscopical structure of the hippocampus of the rat. *Bratisl. Med. J*. 109(3): 106-110.

Ferrer I, Fabregues I, Pineda M, Gracia I, and Ribalta T. A. (1984). Golgi study of cerebellar atrophy in human chronic alcoholism. *Neuropathol. Appl. Neurobiol*. 10(4): 245–253.

Folarin, O. R., Adaramoye, O. A., Akanni, O. O., and Olopade, J. O. (2018). Changes in the brain antioxidant profile after chronic vanadium administration in mice. *Metab. Brain Dis*. 33(2): 377–385. https://doi.org/10.1007/s11011-017-0070-9

Folarin, O. R., Snyder, A. M., Peters, D. G., Olopade, F., Connor, J. R., and Olopade, J. O. (2017). Brain Metal Distribution and Neuro-Inflammatory Profiles after Chronic Vanadium Administration and Withdrawal in Mice. *Front. Neuroanat*. 11:58. https://doi.org/10.3389/fnana.2017.00058

Garcia, G. B., Biancardi, M. E., and Quiroga, A. D. (2005). Vanadium (V)-induced neurotoxicity in the rat central nervous system: a histo-immunohistochemical study. *Drug Chem. Toxicol.* 28(3): 329–344. https://doi.org/10.1081/dct-200064496

Hagino-Yamagishi and Kimiko (2008). Diverse Systems for Pheromone Perception: Multiple Receptor Families in Two Olfactory Systems. *Zool. Sci.* 25(12): 1179–1189. https://doi.org/10.2108/zsj.25.1179

Haider S. S., Abdel-Gayoum A. A., el-Fakhri M. and Ghwarsha K. M. (1998). Effect of selenium on vanadium toxicity in different regions of rat brain. Hum. Exp. Toxicol. 17: 23–28. https://doi.org/10.1191/096032798678907784

Halász, N., Johansson, O., Hökfelt, T., Ljungdahl, Å. and Goldstein, M. (1981). Immunohistochemical identification of two types of dopamine neuron in the rat olfactory bulb as seen by serial sectioning. *J. Neurocytol*. 10(2): 251-259.

Hegarty, J. P., 2nd, Pegoraro, L. F. L., Lazzeroni, L. C., Raman, M. M., Hallmayer, J. F., Monterrey, J. C., Cleveland, S. C., Wolke, O. N., Phillips, J. M., Reiss, A. L., and Hardan, A. Y. (2020). Genetic and environmental influences on structural brain measures in twins with autism spectrum disorder. *Mol. Psychiatry* 25(10): 2556–2566. https://doi.org/10.1038/s41380-018-0330-z

Hsia, A. Y., Vincent, J. D., and Lledo, P. M. (1999). Dopamine depresses synaptic inputs into the olfactory bulb. *J. Neurophysiol*. 82(2): 1082-1085.

Ibe, C. S., Onyeanusi, B. I., and Hambolu, J. O. (2014). Functional morphology of the brain of the African giant pouched rat (*Cricetomys gambianus*) Waterhouse, 1840). *Onderstepoort. J. Vet. Res.* 81(1), e1–e7. https://doi.org/10.4102/ojvr.v81i1.644

Igado, Olumayowa O.; Olopade, James O.; Adesida, Adebukola; Aina, Oluwasanmi O.; Farombi, Ebenezer O. (2012). Morphological and biochemical investigation into the possible neuroprotective effects of kolaviron (Garcinia kola bioflavonoid) on the brains of rats exposed to vanadium. *Drug Chem. Toxicol.* 35(4): 371–380. https://doi.org/10.3109/01480545.2011.630005

Johnston, R. E. (2000). Chemical communication and pheromones: the types of chemical signals and the role of the vomeronasal system. *Neurobiol. Taste Smell* 2:101-127.

Jyothi, N. R. (2020). Heavy Metal Sources and Their Effects on Human Health. In M. K. Nazal, & H. Zhao (Eds.), Heavy Metals - Their Environmental Impacts and Mitigation. *IntechOpen*. https://doi.org/10.5772/intechopen.95370

Jennett, W. B. (1968). Blood flow techniques in clinical neurosurgery. In: Bain, W. H. and Harper, A. M. (eds). Blood flow through organs and tissues. E. S. Livingston Ltd., Edinburg, pp 349 - 354.

Kano M and Watanabe M (2020). Cerebellar circuits: Chapter 4. In: John Rubenstein, Pasko Rakic, Bin Chen, Kenneth Y. Kwan (eds). Neural Circuit and Cognitive Development (Second Edition), Academic Press. pp 79-102. https://doi.org/10.1016/B978-0-12-814411-4.00004-4.

Kemp, K.C., Cook, A.J., Redondo, J., Kurian, K. M., Scolding, N. J., and Wilkins, A. (2016). Purkinje cell injury, structural plasticity and fusion in patients with Friedreich's ataxia. *Acta Neuropathol. Commun*. 4:53. https://doi.org/10.1186/s40478-016-0326-3

Koster, N. L., Norman, A. B., Richtand, N. M., Nickell, W. T., Puche, A. C., Pixley, S. K., and Shipley, M. T. (1999). Olfactory receptor neurons express D2 dopamine receptors. *J. Comp. Neurol*. 411(4): 666-673.

Pyrzyńska K. and Wierzbicki T. (2004). Determination of vanadium species in environmental samples. Talanta. 64(4): 823–829. https://doi.org/10.1016/j.talanta.2004.05.007

Lang-Ouellette, D., Gruver, K.M., Smith-Dijak, A. Blot, F. G. C., Stewart, C. A., de Vanssay de Blavous, P., Li, C. H., Van Eitrem, C., Rosen, C., Faust, P. L., Schonewille, M., and Watt, A. J. (2021). Purkinje cell axonal swellings enhance action potential fidelity and cerebellar function. *Nat. Commun.* 12(1): 4129. https://doi.org/10.1038/s41467-021-24390-4

Li, B., Xia, M., Zorec, R., Parpura, V., and Verkhratsky, A. (2021). Astrocytes in heavy metal neurotoxicity and neurodegeneration. Brain Res. 1752:147234. https://doi.org/10.1016/j.brainres.2020.147234

Li H., Zhou D. Zhang Q., Feng C., Zheng W., He K. and Lan Y. (2013). Vanadium exposure-induced neurobehavioral alterations among Chinese workers. *Neurotoxicology* 36:49–54. https://doi.org/10.1016/j.neuro.2013.02.008

Louis, E. D., Lee, M., Babij, R., Ma, K., Cortés, E., Vonsattel, J. P., and Faust, P. L. (2014). Reduced Purkinje cell dendritic arborization and loss of dendritic spines in essential tremor. *Brain*, 137(12): 3142–3148. https://doi.org/10.1093/brain/awu314

Makoye K. (2022). Giant rats help scientists in Tanzania trying to snuff out tuberculosis. https://www.aa.com.tr/en/africa/giant-rats-help-scientists-in-tanzania-trying-to-snuff-out-tuberculosis/2466694. Data accessed: January 3, 2023.

Mavroudis, I. A., Manani, M. G., Petrides, F., Petsoglou, K., Njau, S. D., Costa, V. G., and Baloyannis, S. J. (2013). Dendritic and spinal pathology of the Purkinje cells from the human cerebellar vermis in Alzheimer's disease. *Psychiatr Danub*. 25: 221–226.

Milardi, D., Quartarone, A., Bramanti, A., Anastasi, G., Bertino, S., Basile, G. A., Buonasera, P., Pilone, G., Celeste, G., Rizzo, G., Bruschetta, D., and Cacciola, A. (2019). The Cortico-Basal Ganglia-Cerebellar Network: Past, Present and Future Perspectives. *Front. Syst. Neurosci.* 13: 61. https://doi.org/10.3389/fnsys.2019.00061

Musser G. G. and Carleton M. D. (2005). Family Muridae. In: Wilson DE, Reeder DM, (eds). Mammal species of the world: a taxonomic and geographic reference. Baltimore: The Johns Hopkins University Press. pp 745–752.

Mustapha O.A., Awala-Ajakaiye M., Taiwo B., Bello S. T., Olude M. A., and Olopade J. O. (2023). Vanadium impairs neuronal infrastructure of the hippocampal trisynaptic loop in the African Giant Rat (*Cricetomys gambianus*, Waterhouse). *Nig. J. Neurosci.* 14(1):1-9. http://doi.org/10.47081/njn2023.14.1/001

Mustapha O. A., Ayoade O. E., Ogunbunmi T. K., and Olude M. A. (2015). Morphology of the oral cavity of the African giant rat (*Cricetomys gambianus*, Waterhouse). *Bulg. J. Vet. Med*. 18(1): 19-30.

Mustapha O.A., Olude M.A., Bello S.T., Taiwo A, Jagun A., and Olopade J.O. (2018). Peripheral axonopathy in sciatic nerve of adult Wistar rats following exposure to vanadium. *J. Peripher. Nerv. Syst.* 24(1): 94-99. https://doi.org/10.1111/jns.12294.

Mustapha O.A., Olude M.A., Taiwo B., and Olopade J.O. (2019). Cytoarchitecture of the Hippocampal Formation in the African Giant Rat (*Cricetomys gambianus*, Waterhouse). *Niger. J. Physiol. Sci*. 34: 55-62.

Mustapha, O. A., Oke, B., Offen, N., Siren, A. L. and Olopade, J. O. (2014). Neurobehavioral and cytotoxic effects of vanadium during oligodendrocyte maturation: a protective role for erythropoietin. *Environ. Toxicol. Pharmacol*. 38(1): 98–111. doi: 10.1016/j.etap.2014.05.001.

Naga R.S.S.S. (2021). Anatomy of Cerebellum. In (Ed.), Spinocerebellar Ataxia - Concepts, Particularities and Generalities. *IntechOpen*. https://doi.org/10.5772/intechopen.97579

Naseri, K., Tahergorabi, Z., Khazdair, M. R., and Sadeghi, M. (2021). Toxic Mechanisms of Five Heavy Metals: Mercury, Lead, Chromium, Cadmium, and Arsenic. *Front. Pharmacol*. https://doi.org/10.3389/fphar.2021.643972

Ngwa, H. A., Kanthasamy, A., Jin, H., Anantharam, V., and Kanthasamy, A. G. (2014). Vanadium Exposure Induces Olfactory Dysfunction in an Animal Model of Metal Neurotoxicity. *Neurotoxicology*, 43: 73. https://doi.org/10.1016/j.neuro.2013.12.004

Olaolorun, F. A., Olopade, F. E., Usende, I. L., Lijoka, A. D., Ladagu, A. D., and Olopade, J. O. (2021). Neurotoxicity of vanadium. Adv. Neurotoxicol. 299–327. https://doi.org/10.1016/bs.ant.2021.01.002

Olayemi A., Nicolas V., Hulselmans J., Missoup A.D., Fichet-Calvet E., Amundala D., Dudu A., Dierckx T., Wendelen W., Leirs H., and Verheyen E. (2012). Taxonomy of The African Giant Pouched Rats (Nesomyidae: Cricetomys): Molecular and Craniometric Evidence Support An Unexpected High Species Diversity. *Zool. J. Linn. Soc.* 165(3): 700–719. https://doi.org/10.1111/j.1096-3642.2012.00823.x

Olude M. A., Mustapha O. A. and Olopade J. O. (2016). Morphological characterization of the African giant rat (*Cricetomys gambianus*, waterhouse) brain across age groups: gross features of cortices. *Niger. J. Physiol. Sci*. 31: 133-138.

Olude, M. A., Ogunbunmi, T. K., Olopade, J. O., and Ihunwo, A. O. (2014). The olfactory bulb structure of African giant rat (*Cricetomys gambianus*, Waterhouse 1840) I: cytoarchitecture. Anat. Sci. Int. 89(4): 224–231. https://doi.org/10.1007/s12565-014-0227-0

Poling A., Mahoney A., Beyene N., Mgode G., Weetjens B., Cox C., and Durgin A. (2015). Using giant african pouched rats to detect human tuberculosis: a review. *Pan Afr. Med. J*. 21:333. doi: 10.11604/pamj.2015.21.333.2977

Poling, A., Weetjens, B., Cox, C., Beyene, N., Durgin, A. and Mahoney, A. (2011). Tuberculosis Detection by Giant African Pouched Rats. *Behav. Anal*. 34(1): 47-54. https://doi.org/10.1007/BF03392234

Purves D, Augustine GJ, Fitzpatrick D, *et al*., editors. Neuroscience. 2nd edition. Sunderland (MA): Sinauer Associates; 2001. Circuits within the Cerebellum. Available from: https://www.ncbi.nlm.nih.gov/books/NBK10865/

Redondo, J., Kemp, K., Hares, K., Rice, C., Scolding, N., and Wilkins, A. (2015). Purkinje Cell Pathology and Loss in Multiple Sclerosis Cerebellum. *Brain Pathol*. (Zurich, Switzerland), 25(6): 692–700. https://doi.org/10.1111/bpa.12230

Rey, N. L., Wesson, D. W., and Brundin, P. (2018). The olfactory bulb as the entry site for prion-like propagation in neurodegenerative diseases. *Neurobiol. Dis*. 109: 226-248. https://doi.org/10.1016/j.nbd.2016.12.013

Rojas-Lemus, M., Bizarro-Nevares, P., López-Valdez, N., González-Villalva, A., Guerrero-Palomo, G., Cervantes-Valencia, M. E. , Tavera-Cabrera, O., Rivera-Fernández, N., Casarrubias-Tabarez, B., Ustarroz-Cano, M., Rodríguez-Zepeda, A., Pasos-Nájera, F., and Goes, T. F. d. (2020). Oxidative Stress and Vanadium. In S. Soloneski, & M. L. Larramendy (Eds.), Genotoxicity and Mutagenicity - Mechanisms and Test Methods. *IntechOpen*. https://doi.org/10.5772/intechopen.90861

Roos W. P. and Kaina B. (2006). DNA damage-induced cell death by apoptosis. *Trends Mol. Med*. 12: 440–450.

Ścibior, A., and Kurus, J. (2019). Vanadium and Oxidative Stress Markers - In Vivo Model: A Review. *Curr. Med. Chem*. 26(29): 5456–5500. https://doi.org/10.2174/0929867326666190108112255

Shintaku M, and Kaneda D. (2009). Chromosome 16q22.1-linked autosomal dominant cerebellar ataxia: an autopsy case report with some new observations on cerebellar pathology. *Neuropathol*. 29: 285–292.

Tchounwou, P. B., Yedjou, C. G., Patlolla, A. K., and Sutton, D. J. (2011). Heavy Metals Toxicity and the Environment. EXS 101:133. https://doi.org/10.1007/978-3-7643-8340-4_6

Thau L, Reddy V, and Singh P. (2022). Anatomy, Central Nervous System. [Updated 2022 Oct 10]. In: StatPearls [Internet]. Treasure Island (FL): StatPearls Publishing; 2022 Jan-. Available from: https://www.ncbi.nlm.nih.gov/books/NBK542179/

Tole, S., and Hébert, J. (2013). Telencephalon Patterning. Patterning and Cell Type Specification in the Developing CNS and PNS. Editors: John Rubenstein, Pasko Rakic (1st eds). *Comprehensive Developmental Neuroscience*, pp 3-24. https://doi.org/10.1016/B978-0-12-397265-1.00018-6

Tufo, C., Poopalasundaram, S., Dorrego-Rivas, A., Ford, M. C., Graham, A., and Grubb, M. S. (2022). Development of the mammalian main olfactory bulb. Development. 149(3): dev200210. doi: 10.1242/dev.200210

Usende, I. L., Alimba, C. G., Emikpe, B. O., Bakare, A. A., and Olopade, J. O. (2018). Intraperitoneal sodium metavanadate exposure induced severe clinicopathological alterations, hepato-renal toxicity and cytogenotoxicity in African giant rats (*Cricetomys gambianus*, Waterhouse, 1840). *Environ. Sci. Pollut. Res.* 25(26): 26383–26393. https://doi.org/10.1007/s11356-018-2588-8

Usende, I. L., Olopade, J. O., Azeez, I. A., Andrioli, A., Bankole, M. O., Olopade, F. E., Nafady, A. A., and Bentivoglio, M. (2022). Neuroecotoxicology: Effects of environmental heavy metal exposure on the brain of African giant rats and the contribution of vanadium to the neuropathology. *IBRO Neurosci. Reports*, 13: 215–234. https://doi.org/10.1016/j.ibneur.2022.08.008

van der Heijden, M. E., and Sillitoe, R. V. (2021). Interactions between Purkinje cells and granule cells coordinate the development of functional cerebellar circuits. *Neuroscience*, 462:4. https://doi.org/10.1016/j.neuroscience.2020.06.010

White, J. J., Arancillo, M., Stay, T. L., George-Jones, N. A., Levy, S. L., Heck, D. H., & Sillitoe, R. V. (2014). Cerebellar Zonal Patterning Relies on Purkinje Cell Neurotransmission. *J. Neurosci.* 34 (24):8231-8245. https://doi.org/10.1523/JNEUROSCI.0122-14.2014

White, J. J., Bosman, L. W. J., Blot, F. G. C., Osório, C., Kuppens, B. W., Krijnen, W. H. J. J., Andriessen, C., De Zeeuw, C. I., Jaarsma, D., and Schonewille, M. (2021). Region-specific preservation of Purkinje cell morphology and motor behavior in the ATXN1[82Q] mouse model of spinocerebellar ataxia 1. *Brain Pathol.* (Zurich, Switzerland), 31(5): e12946. https://doi.org/10.1111/bpa.12946

Xia, G., McFarland, K. N., Wang, K., Sarkar, P. S., Yachnis, A. T., & Ashizawa, T. (2013). Purkinje cell loss is the major brain pathology of spinocerebellar ataxia type 10. *J. Neurol. Neurosurg. Psychiatry*, 84(12): 1409–1411. https://doi.org/10.1136/jnnp-2013-305080

Xiong, Z., Xing, C., Xu, T., Yang, Y., Liu, G., Hu, G., Cao, H., Zhang, C., Guo, X., and Yang, F. (2021). Vanadium Induces Oxidative Stress and Mitochondrial Quality Control Disorder in the Heart of Ducks. *Front. Vet. Sci*. 8: 756534. https://doi.org/10.3389/fvets.2021.756534

Yan, X., Joshi, A., Zang, Y., Assunção, F., Fernandes, H. M., and Hummel, T. (2022). The Shape of the Olfactory Bulb Predicts Olfactory Function. *Brain Sci.* 12(2): https://doi.org/10.3390/brainsci12020128

Zhao Y., Ye L., Liu H., Xia Q., Zhang Y., Yang X., and Wang K. (2010). Vanadium compounds induced mitochondria permeability transition pore (PTP) opening related to oxidative stress. *J. Inorg. Biochem*. 104: 371–378.

Niger. J. Physiol. Sci. 38 (December 2023): 145 – 155
www.njps.physiologicalsociety.com

Niger. J. Physiol. Sci.

Full length Research Article

Protocatechuic Acid Modulates Hepatic Oxidative Stress and Inflammation Linked to Dimethyl Nitrosamine Exposure in Rat

Asejeje, F.O., Etim, S., Asejeje, G., Iwuoha, B.C., Akintade, S.I., Akanmu, T.Y., Adedara, I.A. and *Farombi, E.O.

Molecular Drug Metabolism & Toxicology Research Laboratories, Department of Biochemistry, College of Medicine, University of Ibadan, Ibadan, Nigeria

Summary: Dimethyl nitrosamine (DMN), a potent hepatotoxin, exerts carcinogenic effects and induces hepatic necrosis in experimental animals via CYP2E1 metabolic activation, and generation of reactive oxygen species (ROS). Protocatechuic acid (PCA), a plant-based simple phenolic compound and potent antioxidant, has been shown to affect the development of neoplasia in the rat liver and inhibit the initiation or progression phases of most cancers. In this study, the modulatory effects of PCA on DMN-induced hepatotoxicity, oxidative stress, inflammation, and selected phase I xenobiotic metabolizing enzymes were investigated in male Wistar rats. This study assessed biomarkers of hepatic injury (alanine transaminase, aspartate aminotransferase, alkaline phosphatase, and gamma- glutamyl transferase); oxidative stress (hydrogen peroxide concentration, lipid peroxidation, and reduced glutathione levels); measured activities of antioxidant enzymes (catalase, sodium dismutase, glutathione peroxidase, glutathione S-transferase); and inflammation (Tumor necrosis factor (TNF)-α, interleukin-1-Beta (IL-1β) and iNOS). The results of our investigation demonstrated that pretreatment with PCA at 50 and 100 mg/kg body weight p.o. reduced DMN (20 mg/kg bw) i.p. mediated hepatic injury, oxidative stress, and inflammation in a dose-dependent manner. In addition, the activities of phase I metabolizing enzymes were significantly induced except for aminopyrine-N-demethylase in the DMN-treated rats when compared with the DMN alone control group. This induction was also reversed by pre-treatment with PCA. The result of this study suggests that PCA is hepatoprotective against DMN-induced hepatic damage by its ability to suppress oxidative stress, inflammation, and modulate the activities of the selected phase I drug metabolizing enzymes. Thus, PCA may prove useful in combating DMN-induced hepatic damage.

Keywords*: Protocatechuic Acid, Hepatotoxicity, Antioxidant, Oxidative Stress, Dimethyl nitrosamine*

**Authors for correspondence: olatunde_farombi@yahoo.com , Tel: +2348023470333*

Manuscript received- March 2023; Accepted- September 2023

DOI: https://doi.org/10.54548/njps.v38i2.4

INTRODUCTION

Dimethyl nitrosamine (DMN) belongs to the family of compounds known as nitrosamines an important environmental carcinogen (Ray *et al*., 2014). Scientists have been motivated to investigate the role of DMN in the etiology and pathophysiology of liver damage following the report of two cases of liver cirrhosis in men working in the research laboratory of a large firm that introduced DMN as a solvent (Barnes and Magee, 1954). Several research reports have indicated that DMN can also affect the kidney, in addition to being a potent hepatotoxicant (Usunomena *et al*., 2012; Saricicek *et al*., 2016; Usunobun and Okolie, 2016; Shamsi *et al*., 2017; Abdur-Rahman *et al*., 2022).
Experimental studies have shown that DMN causes oxidative stress; a major factor implicated in the etiology of cancer, via reactive oxygen species (ROS) production which occurs during its CYP2E1-mediated metabolism and alteration of the antioxidant defense system in tissues (Farombi *et al*., 2008; Usunomena *et al*., 2012). These reactive oxygen species have the potential to damage DNA which can lead to mutations and chromosomal damage, and they also oxidize cellular thiols and abstract hydrogen atoms from unsaturated fatty acids to initiate the peroxidation of membrane lipids (Halliwell and Gutteridge, 2015).

Under normal physiological conditions, the production of reactive oxygen species (ROS) is balanced by the activity of antioxidant enzymes and other molecules that help to reduce oxidation. Antioxidants play a crucial role in safeguarding the body against damage resulting from oxidative stress induced by free radicals (Ozsoy *et al*., 2008; Halliwell and Gutteridge, 2015). Excessive ROS is promptly removed from the cell to prevent their potentially harmful effects. Numerous antioxidant enzymes, including superoxide dismutase (SOD), catalase (CAT), glutathione peroxidase (GPx), glutathione-S-transferase (GST), and glutathione reductase (GR), as well as non-enzymatic endogenous antioxidants like ascorbic acid, tocopherols, reduced glutathione (GSH), and uric acid, participate in mechanisms responsible for eliminating or regulating the levels of ROS within the cell (Halliwell and Gutteridge, 2015). Similarly, exogenous antioxidants like phenolic

phytochemicals have been shown to possess antioxidant activities owing to their capacity for scavenging free radicals (Costa *et al*., 2017; Engwa, 2018; Ortega and Campos, 2019; Shah *et al*., 2021; Abdur-Rahman *et al*., 2022).

Phenolic phytochemicals are secondary metabolites produced by plants; either as a component of their regular growth and maturation process or as a response to pathogen invasion or stress (Falcone Ferreyra *et al*., 2012; Gasmi *et al*., 2022). Consuming diets abundant in phenolic phytochemicals may have the potential to decrease the risk of diseases associated with oxidative damage, such as cancer, and could even act as a preventative measure (Singh *et al*., 2014; Sandoval-Yañez *et al*., 2018; Rojas and Buitrago, 2019; Rudrapal *et al*., 2022). One of such phytochemicals is 3, 4-dihydroxybenzoic acid, a simple phenolic compound; also known as protocatechuic acid (PCA). Like many other phenolic acids, PCA is present in most plants (especially fruit and vegetables) and thus a common component of the human diet (Liu *et al*., 2002; Liu, 2004; Tanaka *et al*., 2011; Khan *et al*., 2015; Singh *et al*., 2017; Liu *et al*., 2020). PCA has been shown to have strong antioxidant and antitumor promotion effects (Tseng *et al*., 2000; Lin *et al*., 2007; Xi *et al*., 2016; Liu *et al*., 2020). In addition, it has been demonstrated that PCA exhibits chemo preventive properties by impeding the carcinogenic effects of diverse chemicals in various tissues, including the liver (Gani *et al*., 2019; Punvittayagul *et al*., 2022), colon (Tanaka *et al*., 1993b; Tanaka *et al*., 1995; Farombi *et al*., 2016; Crespo *et al*., 2017), oral cavity (Babich *et al*., 2002), stomach tissue (Hu *et al*., 2020), and the bladder (Hirose *et al*., 1995).

The present study was undertaken to examine the modulatory effects of PCA on DMN-induced hepatic injury, oxidative stress, inflammation, and activities of selected phase I xenobiotic metabolizing enzymes involved in DMN metabolism.

MATERIALS AND METHODS

Materials: Dimethyl nitrosamine (≥ 98%) and protocatechuic acid (≥ 98%) were obtained from Sigma-Aldrich (St. Louis, MO, USA). Alanine amino transferase, asparatate amino transferase, bilirubin, alkaline phosphate and gamma glutamyl transferase assay kits obtained from Randox incorporated, UK. Rabbit polyclonal anti-iNOS antibody from Santa Cruz Biotechnology Inc. USA. Conjugated secondary antibodies obtained from Vector Labs, USA.
All other reagents used were of analytical grade and manufactured by Sigma-Aldrich (St. Louis, MO, USA) and British Drug Houses (Dorset, Poole, UK).

Animals: Sixty (60) male Wistar rats (150-220 g) were obtained from the Central Animal House of the College of Medicine, University of Ibadan and were housed at room temperature under a 12 h light/dark cycle in well-ventilated, plastic cages in the Animal House, Department of Biochemistry. They were acclimatized for a period of 2 weeks and provided with free access to rat pellets and water for the duration of the experiment.

Animal Treatment: Animals were randomly divided into six groups which were treated as follows: one group received only normal saline intraperitoneally (i.p.) for 7 days while two others were given only 50 mg/kg bw and 100 mg/kg bw PCA in normal saline orally (p.o.) respectively also for 7 days. Two groups were administered 50 mg/kg bw and 100 mg/kg bw PCA in normal saline orally (p.o.) respectively for 6 days together with a single i.p. injection of 20 mg/kg bw DMN on day 6. The last group received only 20 mg/kg bw DMN i.p. on day 6 of treatment. All animals were observed twice daily for any abnormal behavior and mortality. All the groups were sacrificed 48 hours after DMN administration.

Collection and Preparation of Serum and Tissues for Biochemical Analyses: The animals were humanely euthanized through cervical dislocation. Blood was obtained via cardiac puncture using a sterile needle and syringe, and then it was collected into clean, dry centrifuge tubes. The blood was left to coagulate by standing for 30 minutes. The blood samples were then centrifuged for 10 mins at 3000 g using a bench centrifuge. The clear supernatant (serum) was collected and stored in the refrigerator at 4Oc. The liver samples were quickly removed, rinsed in ice-cold 1.15% KCl, blotted, and weighed. The liver samples were then minced and homogenized in 4 volumes of ice-cold 0.1 M phosphate buffer, Ph 7.4. The homogenates were centrifuged at 10,000 g for 15 minutes at 4Oc and the supernatants were divided into aliquots and frozen until required for the enzyme assays.

Preparation of Samples used for Immunohistochemistry: Briefly, liver sections were submerged in a 4% phosphate buffer formalin solution, dehydrated through a series of alcohol gradients, and subsequently embedded in paraffin. Thin sections were then prepared and affixed onto glass slides treated with saline.

Preparation of Samples used for Histology: Liver samples were fixed in 10% formaldehyde, dehydrated in graded alcohol, and subsequently embedded in paraffin. Fine sections were obtained, mounted on glass slides, and stained with haematoxylin and eosin for light microscopic analyses.

Evaluation of biomarkers of hepatic injury: Serum alanine transaminase (ALT) and Serum aspartate aminotransferase (AST) activities were determined following the principle described by Reitman and Frankel (Reitman and Frankel, 1957). Alkaline phosphatase (ALP) was determined by the method of Englehardt (Englehardt, 1970). Gamma-glutamyl transferase (γ-GT) was determined using colorimetric method according to Szasz (Szasz, 1969).

Evaluation of biomarkers of oxidative stress: Hydrogen peroxide concentration was determined based on the method of Wolff (Wolff, 1994). Lipid peroxidation (LPO) was evaluated by measuring the level of thiobarbituric acid reactive substances (TBARS) by the method of Varshney and Kale (Varshney and Kale, 1990). The level of reduced glutathione (GSH) was estimated following the method of Beutler (Beutler, 1963).

Evaluation of Antioxidant Enzyme Activity: Catalase activity was determined according to Sinha (Sinha, 1972). SOD activity was assessed by the method of Misra and Fridovich (Misra and Fridovich, 1972). Glutathione peroxidase was assayed according to Rotruck *et al*. (Rotruck *et al*., 1973). Glutathione S-transferase activity was determined according to Habig *et al*. (Habig *et al*., 1974).

Evaluation of biomarkers of inflammation: Tumor necrosis factor (TNF)-α and interleukin-1-Beta (IL-1β) were analysed using specific enzyme-linked immunosorbent assay (ELISA) kits (Bioo Scientific Corporation®, USA) according to the manufacturer's instructions. The cytokines present in a serum sample conjugates with an immobilized IL-Iβ antibody when added into wells. Addition of a secondary antibody conjugated with horse radish peroxidase and TMB substrate to the well results in an antibody–antibody coloured complex. The intensity of colour developed at 450 nm is directly proportional to the concentration of IL-Iβ (measured in pg/mL) in the sample. Immunochemical analyses of iNOS expression were carried out according to the method previously described by Farombi *et al*. (Farombi *et al*., 2009).

Evaluation of Phase 1 Metabolizing Enzymes: Hepatic aniline hydroxylase activity was evaluated by the method of Schenkman *et al*. (Schenkman *et al*., 1967) based on the measurement of the quantity of p-aminophenol formed during the hydroxylation of aniline hydrochloride. Aminopyrine-n-demethylase activity was determined by the method of Holtzmann *et al*. (Holzmann *et al*., 1968). Hepatic p-nitroanisole-o-demethylase activity was estimated by the method of Netter and Seidel (Netter and Seidel, 1964).

Statistical Analysis: Data are expressed as mean ± SD and analyzed with Microsoft Excel and SPSS statistical packages. Statistical analyses were performed by Student t-test and one-way analyses of variance (ANOVA). P value of less than 0.05 was considered statistically significant.

RESULTS

Evaluation of Biomarkers of Hepatic Damage and Oxidative Stress: In summary, Table 1 shows a significant increase in the levels of serum ALT and AST with DMN treatment when compared with the control. Pre-treatment with PCA at both doses caused a significant reduction in the levels of these liver function enzymes. Also, DMN significantly increased the level of serum ALP, and γ-GT was increased by 37.50% when compared with the control. Again, pre-treatment with PCA, reduced ALP by 29.93% at 100 mg/kg and γ-GT was not affected by PCA at 100 mg/kg.

Figures 1, 2, and 3 showed that DMN caused a significant increase ($p<0.05$) in LPO, reduction in GSH, and 10.64% increase in H2O2 concentration. While PCA at both doses prevented DMN-induced LPO. PCA at 50 mg/kg increased GSH concentration by 2.58% and H2O2 generation was lowered by 11.80%. However, PCA at 100 mg/kg produced a significant ($p<0.05$) elevation in GSH level and reduction in H2O2 concentration.

Evaluation of Antioxidant Enzyme Activity and Biomarkers of Inflammation: Table 2 indicates that DMN caused a significant reduction ($p<0.05$) in the activities of CAT and SOD, while PCA at both doses induced CAT and SOD activities significantly. The table also shows that DMN caused the induction of GPX and GST activities. GPX was induced by about 4% and GST by about 10%, but PCA at 100 mg/kg reversed both activities significantly.
DMN significantly increased the serum levels of IL-1β and TNF-α while pre-treatment with PCA significantly reversed this observed elevation in serum levels of these cytokines as presented in Table 3. Furthermore, Table 3 indicates that DMN caused a significant induction in the activity of MPO, and PCA significantly inhibited the MPO activity at 100 mg/kg and by about 6% at 50mg/kg**.**

Evaluation of Phase 1 Drug Metabolizing Enzymes: Table 4 shows that DMN caused a significant increase in the activities of aniline hydroxylase and p-nitroanisole-O-demethylase, and a significant decrease in the activity of aminopyrine-N-demethylase. PCA at 50 mg/kg significantly inhibited the activity of aniline hydroxylase, reduced the activity of p-nitroanisole-O-demethylase by about 30%, and reduced the activities of aniline hydroxylase and p-nitroanisole-O-demethylase by about 12% and 8% respectively at 100 mg/kg. Both doses of PCA significantly induced the activity of aminopyrine-N-demethylase

Table 1:
Chemo protective effects of PCA on serum biomarkers of DMN-induced hepatic injury in rats

Groups	ALT (U/L)	AST (U/L)	ALP (U/L)	γ-GT (U/L)
Normal Saline (I.P.)	3.2±0.87	29.83±4.16	4.91 ± 0.53	1.93 ± 0.55
50mg/kg PCA	3.93±1.45	29.67±7.75	11.04 ± 4.87	1.29 ± 0.59
100mg/kg PCA	2.65±0.41	30.88±3.15	7.97 ± 1.06	1.93 ± 0.55
20mg/kg DMN	38.95±4.07*	66.88±3.54*	58.65 ± 14.46*	3.09 ± 1.02 (37.50%) ****
50mg/kg PCA + 20 mg/kg DMN	28.87±3.89**	51.33±6.01**	26.45 ± 3.48**	1.93 ± 0.32**
100mg/kg PCA + 20mg/kg DMN	25.2±2.09**	55.13±4.61**	41.09 ± 9.22 (29.93%) ***	3.22 ± 0.89 (4.17%) ***

* indicates $p < 0.05$ when compared with the Normal Saline
** indicates $p < 0.05$ when compared with the DMN group.
*** indicates percentage change when compared with the DMN group.
**** indicates percentage change when compared with the Normal Saline.

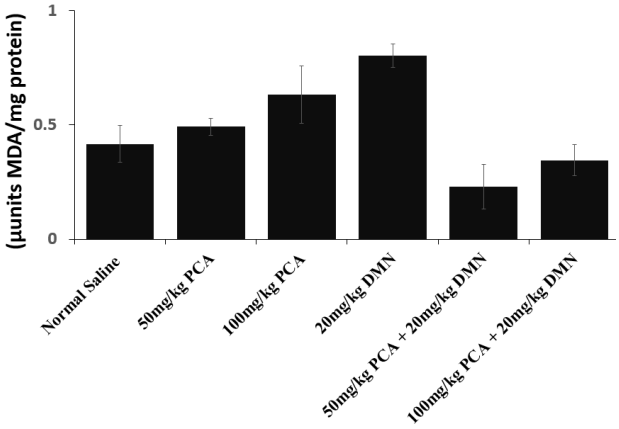

Figure 1
Chemo preventive effects of PCA on DMN-induced LPO
** indicates p < 0.05 when compared with Normal Saline (Control)*
*** indicates p < 0.05 when compared with the DMN alone group.*

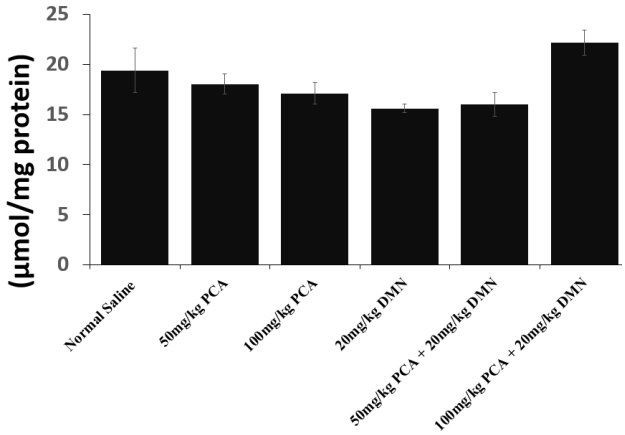

Figure 2
Chemo preventive effects of PCA on DMN-induced GSH
** indicatesp< 0.05 when compared with Normal Saline (Control)*
*** indicates p < 0.05 when compared with the DMN alone group*

.

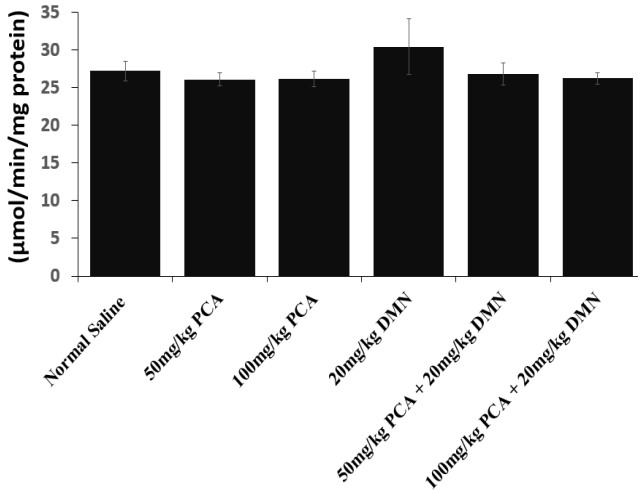

Figure 3
Chemo preventive effects of PCA on DMN-induced H_2O_2 generation
** indicates p< 0.05 when compared with Normal Saline (Control)*
*** indicates p < 0.05 when compared with the DMN alone group*

DISCUSSION

There has been considerable interest in N-nitrosamines because of the known carcinogenicity and mutagenicity of these compounds. N–Nitrosamines are long-established environmental/food contaminants (Poste *et al*., 2014; Park *et al*., 2015; Chen *et al*., 2018; Mazari *et al*., 2019; Suvorov *et al*., 2023). Several experimental studies have reported the hazards of nitrates and nitrites in food as precursors of carcinogenic nitrosamines such as DMN (Magee, 1971; Wolff and Wasserman, 1972; Sebranek and Cassens, 1973; Scanlan and Issenberg, 1975).

Table 2:
Chemo preventive effects of PCA on DMN-induced reduction antioxidant enzyme activities

Groups	CAT (µmol H2O2 consumed/min/mg protein)	SOD (units/mg protein)	GPX (µmol GSH consumed/mg protein)	GST (µmol/min/mg protein)
Normal Saline (I.P.)	510.71 ± 28.55	10.10 ± 0.59	156.71 ± 12.52	0.19 ± 0.03
50mg/kg PCA	481.84 ± 9.45	10.68 ± 0.49	151.89 ± 1.30	0.20 ± 0.02
100mg/kg PCA	468.78 ± 16.86	10.41 ± 0.82	145.85 ± 6.30	0.21 ± 0.02
20mg/kg DMN	379.41 ± 12.42*	8.84 ± 0.44*	122.61 ± 4.54*	0.10 ± 0.01*
50mg/kg PCA + 20mg/kg DMN	422.96 ± 24.98**	9.91 ± 0.66**	127.14 ± 5.63	0.11 ± 0.01
100mg/kg PCA + 20mg/kg DMN	542.01 ± 34.94**	12.41 ± 1.07**	177.53 ± 11.69**	0.16 ± 0.03**

* indicates p < 0.05 when compared with the Normal Saline ** indicates p < 0.05 when compared with the DMN alone group.

Table 3:
Chemo preventive effects of PCA on biomarkers of DMN-induced inflammation in rats

Groups	IL-1β (pg/ml)	TNF-α (pg/ml)	MPO (µmol H_2O_2 split/min/mg protein)
Normal Saline (I.P.)	550.61 ± 7.35	137.64 ± 38.05	1.37 ± 0.13
50mg/kg PCA	423.20 ± 94.22	289.95 ± 125.49	1.35 ± 0.21
100mg/kg PCA	408.05 ± 28.87	122.14 ± 9.93	1.34 ± 0.13
20mg/kg DMN	1685.30 ± 13.15*	699.35 ± 139.58*	2.48 ± 0.24*
50mg/kg PCA + 20 mg/kg DMN	672.74 ± 12.41**	246.23 ± 54.63**	2.32 ± 0.37 (6.48%) ***
100mg/kg PCA + 20mg/kg DMN	592.58 ±100.96**	181.74 ± 70.51**	2.18 ± 0.19**

* indicates p < 0.05 when compared with the Normal Saline ** indicates p < 0.05 when compared with the DMN group.
*** indicates percentage change when compared with the DMN group. **** indicates percentage change when compared with the Normal Saline

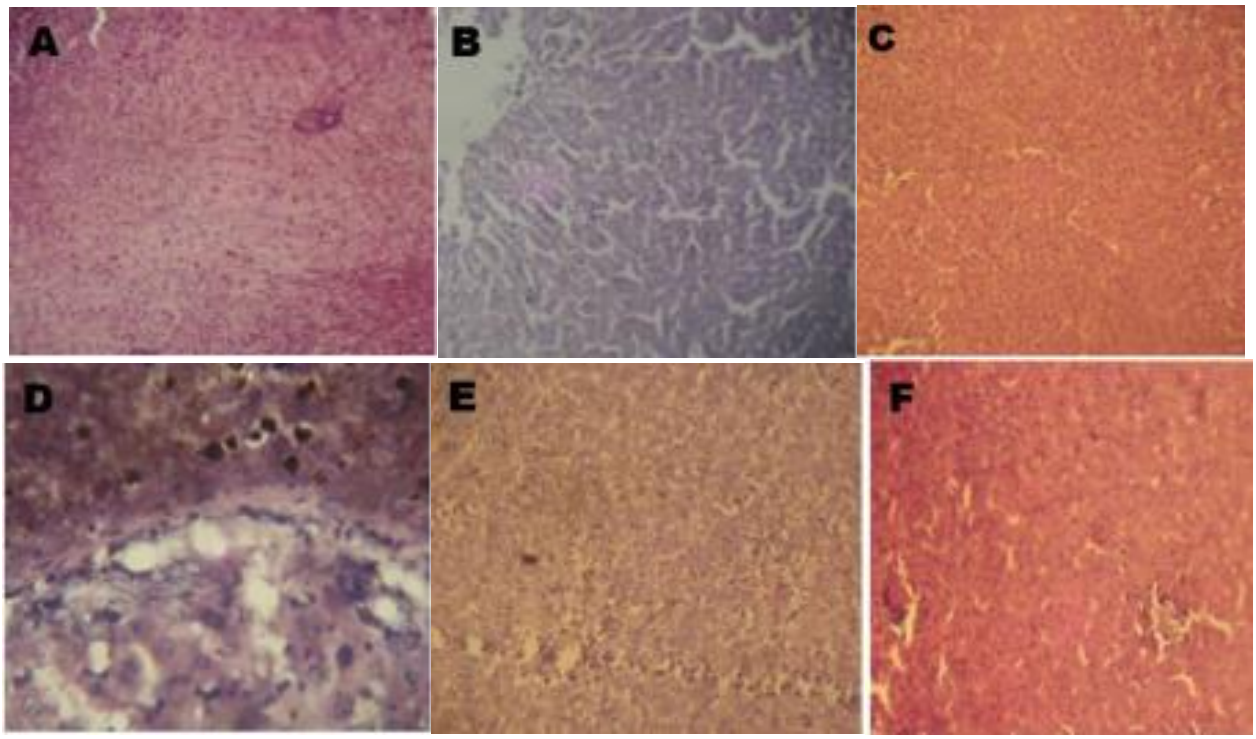

Plate 1A-F
(Histopathology): (A) Control Normal Saline – No visible lesions. (B) PCA (50mg/kg) – No visible lesions. (C) PCA (100mg/kg) – No visible lesions. (D) DMN Only – There is a severe portal congestion. There is also a severe diffuse vacuolar degeneration and necrosis of hepatocytes, with diffuse cellular infiltration by mononuclear cells. (E) PCA (50mg/kg) and DMN – There is a mild diffuse vacuolar degeneration and necrosis of hepatocytes, with diffuse cellular infiltration by mononuclear cells. (F) PCA (100mg/kg) and DMN – No visible lesions. *Magnification X100*

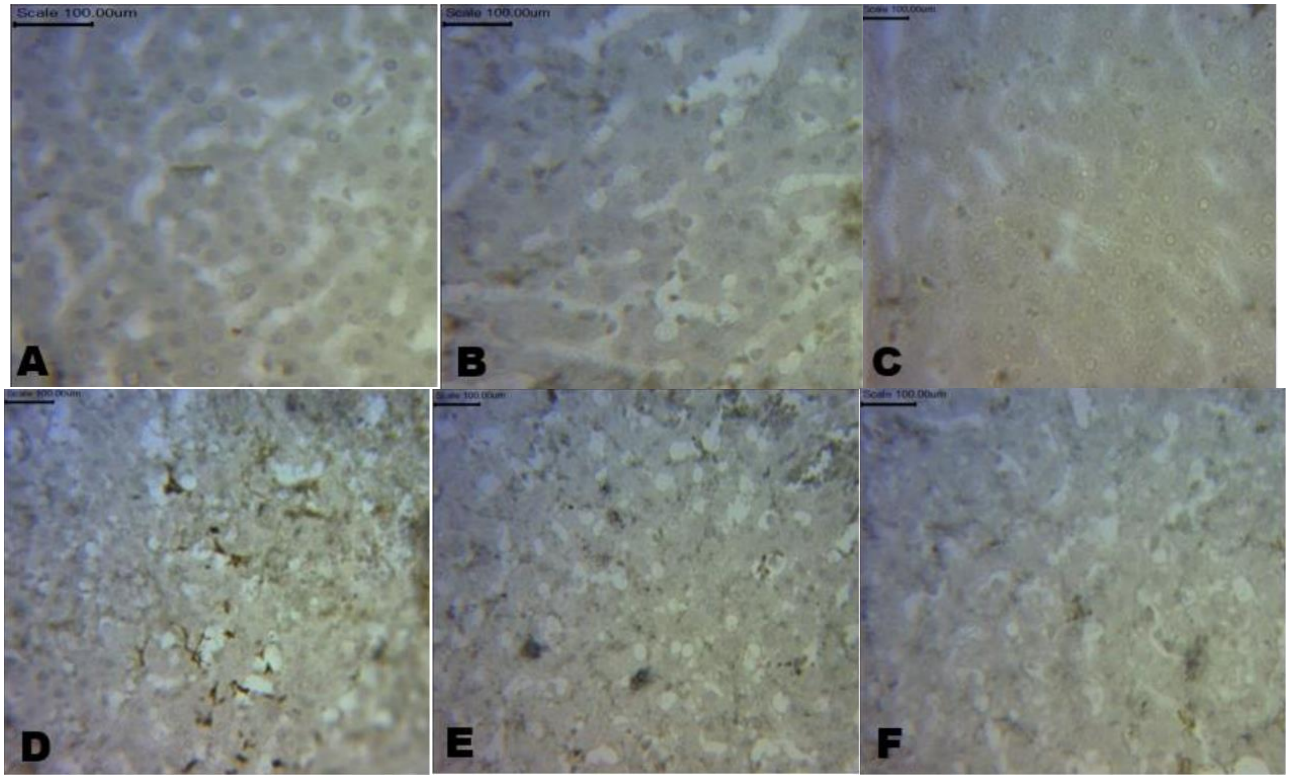

Plate 2A-F
(Immunohistochemistry results of iNOS expression): (A) Control Normal Saline. (B) PCA (50mg/kg). (C) PCA (100mg/kg). (D) DMN Only. (E) PCA (50mg/kg) and DMN. (F) PCA (100mg/kg) and DMN. iNOS expression is depicted by brown staining; the intensity of which determines the extent of enzyme expression. Results indicate that the DMN only group showed increased expression of iNOS compared to control while PCA was able to diminish this expression.

Table 4:
Chemo preventive effects of PCA on DMN-induced liver injury on Hepatic Phase I Drug Metabolizing Enzymes

Groups	ANILINE HYDROXYLASE (µmol p-aminophenol formed/mg protein/hr.)	P-NITRO ANISOLE-O-DEMETHYLASE (nmol p-nitro phenol formed/mg protein/hr.)	AMINOPYRINE-N-DEMTHYLASE (nmol HCHO formed/ mg protein/hr.)
Normal Saline (I.P.)	0.38 ± 0.03	2.54 ± 0.30	61.98 ± 11.74
50mg/kg PCA	0.38 ± 0.02	2.46 ± 0.30	80.60 ± 6.27
100mg/kg PCA	0.36 ± 0.02	1.76 ± 0.19	53.25 ± 6.56
20mg/kg DMN	0.59 ± 0.01*	4.12 ± 1.21*	36.40 ± 5.46*
50mg/kg PCA + 20mg/kg DMN	0.34 ± 0.04**	2.88 ± 0.42	54.25 ± 3.53**
100mg/kg PCA + 20mg/kg DMN	0.52 ± 0.08	3.79 ± 0.55	53.73 ± 4.65**

* indicates $p < 0.05$ when compared with the Normal Saline

** indicates $p < 0.05$ when compared with the DMN group.

Protocatechuic acid (PCA), also known as 3, 4-dihydroxybenzoic acid, is a potent antioxidant Thapa *et al*., 2023). It is a phenolic acid belonging to the broad class of polyphenols. It is widely available in oil, vegetables, fruits, and tea (Khan *et al*., 2015; Singh *et al*., 2017). It is mainly found in Roselle (Hibiscus sabdariffa) which is a species of hibiscus found in Old World tropics (Ali *et al*., 2005). PCA is a strong antioxidant that has been reported to show therapeutic potential as an anti-carcinogenic agent (Ali *et al*., 2005; Kakkar and Bais, 2014).

In the present study, we investigated the chemo-preventive effect, and possible mechanisms of chemoprevention of PCA on DMN-induced hepatotoxicity, oxidative stress, and inflammation. Our result, exemplified by the significantly elevated levels of serum AST, ALT, γ-GT, and ALP after the male rats were challenged with DMN; is in agreement with previous research reports that DMN is a potent hepatotoxin (George *et al*., 2001; Andrzejewski *et al*., 2005; Farombi *et al*., 2009; Choi *et al*., 2016; Rani *et al*., 2018).

Alanine aminotransferase (ALT) is an enzyme present in the hepatocytes. When the cell is damaged, this enzyme leaks into the blood. The serum level of ALT significantly increases during acute liver damage. ALT is considered a more dependable indicator of liver health and integrity in comparison to Aspartate Aminotransferase (AST). (Kaplan, 2002; Ojiako and Nwanjo, 2006). AST is also found in red blood cells, cardiac muscle, and skeletal muscle, making it less specific to liver damage as compared to ALT. It is also associated with liver parenchymal cells, and it requires acute liver damage to elevate blood AST levels (Moss *et al*., 1999; Vozarova *et al*., 2002). As a liver specific enzyme, ALT only significantly increases in the serum during hepatobiliary disease (Kaplan, 2002). Hence, the observed elevated serum ALT level in this present study is an indication that DMN caused hepatic injury. However, pre-treatment with PCA significantly lowered this rise in serum ALT level; with the 100 mg/kg treated group showing a greater decrease. Similarly, PCA pre-treated groups also showed a reduction in AST levels when compared with the DMN-treated group. Elevated levels of Alanine and Aspartate Aminotransferases are indicative of liver damage (Giboney, 2005; Chapman and Hostutler, 2013).

Alkaline Phosphatase (ALP) is an enzyme present in the cells lining the biliary ducts of the liver (Sharma *et al*., 2014; Poupon, 2015). The increased serum level of ALP in the DMN alone group observed in this present study may be attributed to damage in the structural integrity of hepatic cells causing the release of ALP into the circulation (McComb *et al*., 2013). However, in the groups pre-treated with 50 mg/kg PCA, we observed a statistically significant decrease in ALP levels; while the group that was pre-treated with 100 mg/kg PCA showed about a 30% decrease in ALP levels compared with the control group.

Gamma Glutamyl Transpeptidase (γ-GT or GGT) is relatively liver-specific and serves as a more sensitive indicator for cholestatic damage when compared to ALP. Elevated levels of γ-GT may occur even in cases of minor, sub-clinical liver dysfunction (Gowda *et al*., 2009; Anand and Mallick, 2019). The 37.50% elevation in γ-GT (Table 1) in the DMN-only treated rats when compared with the normal control may reflect the progress of carcinogenesis since the animals were sacrificed just 24 hours after treatment with 20 mg/kg DMN. However, the 50 mg/kg PCA pre-treatment caused a significant reduction in the γ-GT level. Unpredictably, 100 mg/kg PCA pretreatment could not reverse the elevated γ-GT caused by DMN. This might be due to the induction of γ-GT synthesis in the presence of chemical carcinogens (Vanisree and Shyamala, 1999; Lee *et al*., 2004).

To further validate damage to the liver, histopathology of the liver tissue was carried out. The results of the histopathological examination showed severe portal congestion, severe diffuse vacuolar degeneration, and necrosis of hepatocytes with diffuse cellular infiltration by mononuclear cells in the group that received DMN alone (PLATE D). In contrast, no lesion was observed in the control groups (PLATE A). However, PCA administration at both doses (PLATES E and F) reversed this hepatic degeneration and necrosis.

Furthermore, our results indicate increased H2O2 production and LPO in the group treated with DMN alone. Studies have shown that DMN mediates oxidative stress through the generation of reactive oxygen species (ROS), resulting in the alteration of the antioxidant defense system and attendant cellular injury (George *et al*., 2001; Zhang *et al*., 2016). Also, experimental studies suggest that when biological systems are subjected to oxidative stress, oxygen radicals like superoxide anion (.O2-), hydroxyl radical (.OH), and peroxyl radicals (˙OOH) are generated. These ROS oxidize cellular thiols, damaging protein structure and function, and abstracting hydrogen atoms from unsaturated fatty acids to initiate the peroxidation of membrane lipids (Halliwell and Gutteridge, 2015). This may explain the observed elevation of H2O2, and the statistically significant increase in LPO of the DMN alone group compared to the control. However, pretreatment with 50 mg/kg and 100 mg/kg PCA significantly reduces LPO.

Furthermore, our results demonstrated significant elevation of lipid peroxidation (LPO), lowered levels of reduced glutathione (GSH), lowered activity of catalase (CAT), decreased activity of superoxide dismutase (SOD), reduced activity of glutathione peroxidase (GPX), and decreased activity of glutathione S-transferase (GST) in the rats challenged with DMN when compared with the normal control. Under normal physiological conditions, a variety of antioxidant systems which include redox molecules like GSH; antioxidant enzymes like superoxide dismutase (SOD), catalase (CAT), glutathione S-transferase (GST), glutathione peroxidase (GPx), and glutathione reductase (GR) are employed by the mammalian system to eliminate cellular ROS, and thus offer protection against the harmful effect of ROS. During the oxidative assault of the cell, cellular ROS generation is exaggerated, and/or the antioxidant defense system is impeded resulting in an imbalance in the rate of generation versus the removal of cellular ROS (Halliwell and Gutteridge, 2015). The observed decrease in the investigated components of the antioxidant system in this present study can be attributed to the finding that ROS-generating xenobiotics like DMN can inhibit the activity of the antioxidant system (Liu, 2004; Hsu *et al*., 2008; Halliwell and Gutteridge, 2015; Rojas and Buitrago, 2019). It is worthy of note that our results show a correlation between the activity of CAT (an enzyme responsible for the removal of H2O2 by reduction to molecular oxygen and water) and the levels of H2O2. This is evidenced by the significantly lowered CAT activity, and increased levels of H2O2 and LPO in the DMN alone group. In the present study, we demonstrated that pretreatment with PCA prevented DMN-induced reduction of antioxidant enzyme activities (Table 2). Our observation aligns with the report of Masella *et al*. (Masella *et al*., 2004), that protocatechuic acid restores glutathione peroxidase activity and reduces glutathione to control levels. Similarly, our data demonstrated that PCA elicited antioxidant effects evidenced by restoration of GSH levels as previously reported by Liu *et al*., and Tsuda *et al*. (Tsuda *et al*., 1999; Liu *et al*., 2002).

In addition, our findings indicated that DMN treatment resulted in a significant elevation in the serum levels of pro-inflammatory cytokines, specifically TNF-α and IL-1β. Furthermore, hepatic myeloperoxidase (MPO) activity and the expression of inducible nitric oxide synthase (iNOS) in the liver were significantly increased. (Plate 2 and Table 3). On the other hand, PCA administration at both 100 mg/kg and 50 mg/kg lowered the serum levels of tumor necrosis factor-alpha (TNF-α) and interleukin-1beta (IL-1β) significantly. Similarly, MPO activity was statistically significantly lowered in the 100 mg/kg PCA pre-treated group, and about 6.5% decrease in the 50 mg/kg PCA pre-treated group when compared to their toxicant alone counterpart.

iNOS expression was increased in the DMN-treated animals and differential lowered expressions were observed in the animals pre-treated with PCA in a dose-dependent manner. Inflammatory cells, such as neutrophils, monocytes, macrophages, dendritic cells, eosinophils, mast cells, and lymphocytes, are typically mobilized in large numbers in response to damage or infection. This inflammatory response could potentially play a role in the initiation and advancement of cancer (Siaga *et al*., 1978; Allavena *et al*., 2008; Fernandes *et al*., 2015). Prostaglandins, cytokines, nuclear factor kappa B (NFκB), chemokines, and angiogenic factors are crucial molecular components that establish a connection between inflammation and genetic alterations. While on the other hand, the free radical species from oxygen (ROS) and nitrogen (RNS) are the key chemical effectors of these cellular insults (Tripathi and Aggarwal, 2006; Mantovani *et al*., 2010). This assertion is evident in the results of our present study wherein the levels of markers of inflammation were elevated significantly in the group challenged with DMN alone.

ROS and RNS are generated in response to pro-inflammatory cytokines, both in phagocytic and non-phagocytic cells, as a result of the activation of protein kinase signaling pathways (Moldogazieva *et al*., 2018). For example, TNF-α enhances the formation of ROS by neutrophils and other cells, while interleukin-1-β (IL-1-β), TNF-α and interferon (IFN)-γ stimulate the expression of inducible nitric oxide synthase (iNOS) in inflammatory and epithelial cells. This may account for the high expression of iNOS observed in this present study. To further substantiate the involvement of these cytokines in tumorigenesis, Moore *et al*. demonstrated that the knockout of the TNF-α gene in experimental animals significantly inhibits the development of skin tumors when exposed to DMBA and phorbol esters (Moore *et al*., 1999). This may explain the involvement of these cytokines in the hepato-pathogenesis observed in this present study. Therefore, from observations in this present study, and reports of previous investigators, these cytokines and proteins may have additive effects in hepatic injury.

To further probe the modulatory effect of PCA on DMN-induced liver injury in the present study, we investigated the roles of phase 1 drug-metabolizing enzymes. We determined the activities of liver microsomal cytochrome p450 enzymes aniline hydroxylase, aminopyrine-N-demethylase, and p-nitroanisole-O-demethylase. Our results showed that there were significant changes in the activities of these enzymes under different experimental conditions (Table 4). Aminopyrine-N-demethylase activity was inhibited in the DMN-only group, an observation which is in consonance with the findings of Kim *et al*., (Kim *et al*., 2009), where DMN caused a decrease in microsomal aminopyrine-N-demethylase activity. Since this enzyme is responsible for DMN metabolism and subsequent clearance, it can be suggested that DMN overwhelmed the enzyme, thereby enhancing the persistence of DMN in the tissue and causing damage. However, it was observed in this present study that pretreatment with PCA at both concentrations prevented DMN-induced loss in the activity of aminopyrine-N-demethylase.

On the other hand, the activities of aniline hydroxylase which is selective for cytochrome p450 2E1 (CYP 2E1) and p-nitroanisole-O-demethylase were significantly induced by DMN while the group treated with PCA at 50 mg/kg prior to DMN administration showed significant reduction of aniline hydroxylase activity when compared with the DMN-only group. This observation supports the report of Baer-Dubowska *et al*. (Baer-Dubowska *et al*., 1998) that protocatechuic acid inhibited the catalytic activity of certain cytochrome p450 enzymes better than chlorogenic acid, and propyl gallate more effectively than dodecyl gallate. Experimental studies have also shown that protocatechuic

acid administered at a dose of 50 mg/kg every 3 days for 2 weeks to rats that were exposed to 3-methylcholantrene on the 12th day of protocatechuic acid treatment resulted in decreases in activities and expression of CYP1A1, CYP1A2, and CYP2E1 (Krajka-Kuźniak *et al*., 2004). It is well-established that CYP2E1 plays a role in activating N-nitrosamines found in tobacco smoke, various compounds in food (Wang *et al*., 2002; Danko and Chaschin, 2005), numerous industrial carcinogens (Nakajima and Aoyama, 2000), as well as several endogenous carcinogens (Bartsch *et al*., 2000). In addition, CYP2E1 possesses the ability to reduce molecular oxygen to highly reactive compounds like superoxide anion radical, singlet oxygen, hydrogen peroxide, and hydroxyl radical even in the absence of substrate which can result in lipid and protein peroxidation, DNA damage, and carcinogenesis (Danko and Chaschin, 2005). Therefore, the inhibition of aniline hydroxylase and p-nitroanisole-O-demethylase by protocatechuic acid as observed in this present study indicates the ability of PCA to offer cytoprotection by preventing bio-activation of DMN.

The chemo-preventive ability of PCA observed in this present study is plausible because other studies have shown that protocatechuic acid (PCA) possesses the dual ability to inhibit the formation and scavenging of free radicals (Kakkar and Bais, 2014; Farombi *et al*., 2016; Hu *et al*., 2020; Thapa *et al*., 2023). The capacity of protocatechuic acid to create complexes with transition metal ions like Cu (II) and Fe (II), or to reduce the activity of enzymes involved in reactions that produce free radicals as by-products, such as xanthine oxidase, is linked to its ability to inhibit the generation of free radicals. The neutralization of free radicals occurs when they react with the hydroxyl groups present in protocatechuic acid. In vitro models have demonstrated that protocatechuic acid effectively prevents oxidative DNA damage and lipid peroxidation (Tanaka *et al*., 2011).

In conclusion, our results indicate that DMN is a potent hepatotoxin as evidenced by the elevated levels of serum liver enzymes, increased lipid peroxidation, and reduction in the antioxidant defense systems of the liver. In addition, we observed increased levels of pro-inflammatory cytokines (IL-1β and TNF-α), and increased expression of inflammatory biomarkers (iNOS and MPO) during DMN administration; indicating the involvement of inflammation in DMN-induced hepatic injury. Similarly, the group of rats challenged with DMN showed induced levels of phase 1 metabolizing enzymes except for aminopyrine-N-demethylase, thereby increasing the bioactivation and cytotoxicity of DMN. PCA however, acted as a potent hepatoprotective and chemo-preventive agent by ameliorating the various adverse hepatoxic conditions induced by DMN.

REFERENCES

Abdur-Rahman, M., Shams-Eldin, E. (2022). Modeling with Biomarkers: Nitrosamines and Phytochemical Protection. In: Patel, V.B., Preedy, V.R., Rajendram, R. (eds) Biomarkers in Toxicology. Biomarkers in Disease: Methods, Discoveries and Applications. Springer, Cham. https://doi.org/10.1007/978-3-030-87225-0_61-1

Ali, B. H., Wabel, N. A., and Blunden, G. (2005). Phytochemical, pharmacological and toxicological aspects of Hibiscus sabdariffa L.: a review. *Phytotherapy Research: An International Journal Devoted to Pharmacological and Toxicological Evaluation of Natural Product Derivatives*, 19, 369-375.

Allavena, P., Garlanda, C., Borrello, M. G., Sica, A. and Mantovani, A. (2008). Pathways connecting inflammation and cancer. *Current opinion in genetics & development*, 18, 3-10.

Anand, A. K. and Mallick, A. K. (2019). A comparative study of serum gamma-glutamyltranspeptidase, serum alkaline phosphatase and GGT/ALP ratio in different liver disorders. Int. *J. Contemp. Med. Res*, 6, 11-14.

Andrzejewski, P., Kasprzyk-Hordern, B. and Nawrocki, J. (2005). The hazard of N-nitrosodimethylamine (NDMA) formation during water disinfection with strong oxidants. *Desalination*, 176, 37-45.

Babich, H., Sedletcaia, A. and Kenigsberg, B. (2002). In Vitro Cytotoxicity of Protocatechuic Acid to Cultured Human Cells from Oral Tissue: Involvement in Oxidative Stress. *Pharmacology & Toxicology*, 91, 245-253.

Baer-Dubowska, W., Szaefer, H. and Krajka-Kuzniak, V. (1998). Inhibition of murine hepatic cytochrome P450 activities by natural and synthetic phenolic compounds. *Xenobiotica*, 28, 735-743.

Barnes, J. M. and Magee, P. (1954). Some toxic properties of dimethylnitrosamine. *British Journal of Industrial Medicine*, 11, 167.

Bartsch, H., Nair, U., Risch, A., Rojas, M., Wikman, H. and Alexandrov, K. (2000). Genetic polymorphism of CYP genes, alone or in combination, as a risk modifier of tobacco-related cancers. *Cancer Epidemiology and Prevention Biomarker*s, 9, 3-28.

Beutler, E. (1963). Improved method for the determination of blood glutathione. *J. lab. clin. Med*., 61, 882-888.

Chapman, S. E. and Hostutler, R. A. (2013). A laboratory diagnostic approach to hepatobiliary disease in small animals. Veterinary Clinics: *Small Animal Practice*, 43, 1209-1225.

Chen, X., Huang, G., An, C., Yao, Y. and Zhao, S. (2018). Emerging N-nitrosamines and N-nitramines from amine-based post-combustion CO2 capture–a review. *Chemical Engineering Journal*, 335, 921-935.

Choi, M. J., Zheng, H. M., Kim, J. M., Lee, K. W., Park, Y. H. and Lee, D. H. (2016). Protective effects of Centella asiatica leaf extract on dimethylnitrosamine-induced liver injury in rats. *Molecular medicine reports*, 14, 4521-4528.

Costa, C., Tsatsakis, A., Mamoulakis, C., Teodoro, M., Briguglio, G., Caruso, E., Tsoukalas, D., Margina, D., Dardiotis, E. and Kouretas, D. (2017). Current evidence on the effect of dietary polyphenols intake on chronic diseases. *Food and Chemical Toxicology*, 110, 286-299.

Crespo, I., San-Miguel, B., Mauriz, J. L., Ortiz De Urbina, J. J., Almar, M., Tuñón, M. J. and González-Gallego, J. (2017). Protective effect of protocatechuic acid on TNBS-induced colitis in mice is associated with modulation of the SphK/S1P signaling pathway. *Nutrients*, 9, 288.

Danko, I. and Chaschin, N. (2005). Association of CYP2E1 gene polymorphism with predisposition to cancer development. *Exp Oncol*, 27, 248-256.

Englehardt, A. (1970). Measurement of alkaline phosphatase. *Aerztl Labor*, 16, 1.

Engwa, G.A. (2018) Free Radicals and the Role of Plant Phytochemicals as Antioxidants Against Oxidative Stress-Related Diseases. Phytochemicals - Source of Antioxidants and Role in Disease Prevention. InTech. Available at: http://dx.doi.org/10.5772/intechopen.76719.

Farombi, E. O., Adedara, I. A., Awoyemi, O. V., Njoku, C. R., Micah, G. O., Esogwa, C. U., Owumi, S. E. and Olopade, J. O. (2016). Dietary protocatechuic acid ameliorates dextran sulphate sodium-induced ulcerative colitis and hepatotoxicity in rats. *Food Funct*, 7, 913-21.

Farombi, E. O., Shrotriya, S., Na, H.-K., Kim, S.-H. and Surh, Y.-J. (2008). Curcumin attenuates dimethylnitrosamine-induced liver injury in rats through Nrf2-mediated induction of heme oxygenase-1. *Food and Chemical Toxicology*, 46, 1279-1287.

Farombi, E. O., Shrotriya, S. and Surh, Y.-J. (2009). Kolaviron inhibits dimethyl nitrosamine-induced liver injury by suppressing COX-2 and iNOS expression via NF-κB and AP-1. *Life sciences*, 84, 149-155.

Fernandes, J. V., Cobucci, R. N. O., Jatobá, C. A. N., De Medeiros Fernandes, T. A. A., De Azevedo, J. W. V. & De Araújo, J. M. G. (2015). The role of the mediators of inflammation in cancer development. *Pathology & Oncology Research*, 21, 527-534.

Gani, S. A., Muhammad, S. A., Kura, A. U., Barahuie, F., Hussein, M. Z. and Fakurazi, S. (2019). Effect of protocatechuic acid-layered double hydroxide nanoparticles on diethylnitrosamine/phenobarbital-induced hepatocellular carcinoma in mice. *PloS one*, 14, e0217009.

Gasmi, A. Mujawdiya, P.K. Noor, S. Lysiuk, R. Darmohray, R. Piscopo, S. Lenchyk, L. Antonyak, H. Dehtiarova, K. Shanaida, M. *et al*. (2022). Polyphenols in Metabolic Diseases. Molecules, 27, 6280. https://doi.org/10.3390/molecules27196280

George, J., Rao, K. R., Stern, R. and Chandrakasan, G. (2001). Dimethylnitrosamine-induced liver injury in rats: the early deposition of collagen. *Toxicology*, 156, 129-138.

Giboney, P. T. (2005). Mildly elevated liver transaminase levels in the asymptomatic patient. *American family physician*, 71, 1105-1110.

Gowda, S., Desai, P. B., Hull, V. V., Math, A. A. K., Vernekar, S. N. and Kulkarni, S. S. (2009). A review on laboratory liver function tests. *The Pan african medical journal*, 3.

Habig, W. H., Pabst, M. J. and Jakoby, W. B. (1974). Glutathione S-transferases: the first enzymatic step in mercapturic acid formation. *Journal of Biological chemistry*, 249, 7130-7139.

Halliwell, B. and Gutteridge, J. M. (2015). Free radicals in biology and medicine, Oxford University Press, USA.

Hirose, Y., Tanaka, T., Kawamori, T., Olnishi, M., Makita, H., Mori, H., Satoh, K. and Hara, A. (1995). Chemoprevention of urinary bladder carcinogenesis by the natural phenolic compound protocatechuic acid in rats. *Carcinogenesis*, 16, 2337-2342.

Holzmann, H., Morsches, B. and Kabel, E. (1968). Enzymaktivitätsmuster im Serum von Kranken mit Psoriasis vulgaris. Archiv für klinische und experimentelle Dermatologie, 231, 335-343.

Hsu, C.-C., Lin, K.-Y., Wang, Z.-H., Lin, W.-L. and Yin, M.-C. (2008). Preventive effect of Ganoderma amboinense on acetaminophen-induced acute liver injury. *Phytomedicine*, 15, 946-950.

Hu, R., He, Z., Liu, M., Tan, J., Zhang, H., Hou, D.-X., He, J. and Wu, S. (2020). Dietary protocatechuic acid ameliorates inflammation and up-regulates intestinal tight junction proteins by modulating gut microbiota in LPS-challenged piglets. *Journal of Animal Science and Biotechnology*, 11, 92.

Kakkar, S. and Bais, S. (2014). A review on protocatechuic acid and its pharmacological potential. *International Scholarly Research Notices*, 2014.

Kaplan, M. M. (2002). Alanine aminotransferase levels: what's normal? *Annals of internal medicine*, 137, 49-51.

Khan, A., Rashid, R., Fatima, N., Mahmood, S., Mir, S., Khan, S., Jabeen, N. and Murtaza, G. (2015). Pharmacological activities of protocatechuic acid. *Acta poloniae pharmaceutica*, 72 4, 643-50.

Kim, S. K., Seo, J. M., Chae, Y. R., Jung, Y. S., Park, J. H. and Kim, Y. C. (2009). Alleviation of dimethylnitrosamine-induced liver injury and fibrosis by betaine supplementation in rats. *Chemico-biological interactions*, 177, 204-211.

Krajka-Kuźniak, V., Szaefer, H. and Baer-Dubowska, W. (2004). Modulation of 3-methylcholanthrene-induced rat hepatic and renal cytochrome P450 and phase II enzymes by plant phenols: protocatechuic and tannic acids. *Toxicology letters*, 152, 117-126.

Lee, D.-H., Blomhoff, R. and Jacobs, D. R. (2004). Is Serum Gamma Glutamyltransferase a Marker of Oxidative Stress? *Free Radical Research*, 38, 535-539.

Lin, H.-H., Chen, J.-H., Huang, C.-C. and Wang, C.-J. (2007). Apoptotic effect of 3,4-dihydroxybenzoic acid on human gastric carcinoma cells involving JNK/p38 MAPK signaling activation. *International Journal of Cancer*, 120, 2306-2316.

Liu, C.-L., Wang, J.-M., Chu, C.-Y., Cheng, M.-T. and Tseng, T.-H. (2002). In vivo protective effect of protocatechuic acid on tert-butyl hydroperoxide-induced rat hepatotoxicity. *Food and Chemical Toxicology*, 40, 635-641.

Liu, M., Zhu, K., Yao, Y., Chen, Y., Guo, H., Ren, G., Yang, X. and Li, J. (2020). Antioxidant, anti-inflammatory, and antitumor activities of phenolic compounds from white, red, and black Chenopodium quinoa seed. *Cereal Chemistry*, 97, 703-713.

Liu, R. H. (2004). Potential synergy of phytochemicals in cancer prevention: mechanism of action. *The Journal of nutrition*, 134, 3479S-3485S.

Magee, P. (1971). Toxicity of nitrosamines: Their possible human health hazards. Food and cosmetics toxicology, 9, 207-218.

Mantovani, A., Garlanda, C. and Allavena, P. (2010). Molecular pathways and targets in cancer-related inflammation. *Annals of medicine*, 42, 161-170.

Masella, R., Varì, R., D'archivio, M., Di Benedetto, R., Matarrese, P., Malorni, W., Scazzocchio, B. and Giovannini, C. (2004). Extra Virgin Olive Oil Biophenols Inhibit Cell-Mediated Oxidation of LDL by Increasing the mRNA Transcription of Glutathione-Related Enzymes. *The Journal of nutritio*n, 134, 785-791.

Mazari, S. A., Alaba, P. and Saeed, I. M. (2019). Formation and elimination of nitrosamines and nitramines in freshwaters involved in post-combustion carbon capture process. *Journal of Environmental Chemical Engineering*, 7, 103111.

Mccomb, R. B., Bowers Jr, G. N. and Posen, S. (2013). Alkaline phosphatase, Springer Science & Business Media.

Misra, H. P. and Fridovich, I. (1972). The univalent reduction of oxygen by reduced flavins and quinones. *Journal of Biological chemistry*, 247, 188-192.

Moldogazieva, N. T., Mokhosoev, I. M., Feldman, N. B. and Lutsenko, S. V. (2018). ROS and RNS signalling: adaptive redox switches through oxidative/nitrosative protein modifications. *Free Radical Research*, 52, 507-543.

Moore, R. J., Owens, D. M., Stamp, G., Arnott, C., Burke, F., East, N., Holdsworth, H., Turner, L., Rollins, B. and Pasparakis, M. (1999). Mice deficient in tumor necrosis factor-α are resistant to skin carcinogenesis. *Nature medicine*, 5, 828-831.

Morrissey, J. P. and Osbourn, A. E. (1999). Fungal resistance to plant antibiotics as a mechanism of pathogenesis. *Microbiology and Molecular Biology Reviews*, 63, 708-724.

Moss, D., Henderson, A. and Tietz, T. (1999). Textbook of Clinical Enzymology, Clinical Enzymology. WB Saunders Co, Philadelphia, PA, USA. p617-721.

Nakajima, T. and Aoyama, T. (2000). Polymorphism of drug-metabolizing enzymes in relation to individual susceptibility to industrial chemicals. *Industrial health*, 38, 143-152.

Netter, K. and Seidel, G. (1964). An adaptively stimulated O-demethylating system in rat liver microsomes and its kinetic properties. *Journal of pharmacology and experimental therapeutics*, 146, 61-65.

Ojiako, O. and Nwanjo, H. (2006). Is Vernonia amygdalina hepatotoxic or hepatoprotective? Response from biochemical and toxicity studies in rats. *African Journal of Biotechnology*, 5.

Ortega, A. M. M. and Campos, M. R. S. (2019). Bioactive Compounds as Therapeutic Alternatives. *Bioactive compounds*. Elsevier.

Ozsoy, N., Can, A., Yanardag, R. and Akev, N. (2008). Antioxidant activity of Smilax excelsa L. leaf extracts. *Food Chemistry*, 110, 571-583.

Park, J.-E., Seo, J.-E., Lee, J.-Y. and Kwon, H. (2015). Distribution of seven N-nitrosamines in food. *Toxicological research*, 31, 279-288.

Poste, A. E., Grung, M. and Wright, R. F. (2014). Amines and amine-related compounds in surface waters: a review of sources, concentrations and aquatic toxicity. Science of the total environment, 481, 274-279.

Poupon, R. (2015). Liver alkaline phosphatase: A missing link between choleresis and biliary inflammation. *Hepatology*, 61, 2080-2090.

Punvittayagul, C., Luangsuphabool, T., & Wongpoomchai, R. (2022). Protocatechuic acid as a potent anticarcinogenic compound in purple rice bran against diethylnitrosamine-initiated rat hepatocarcinogenesis. *Scientific reports*, 12(1), 10548. https://doi.org/10.1038/s41598-022-14888-2

Rani, V., Verma, Y., Rana, K. and Rana, S. V. S. (2018). Zinc oxide nanoparticles inhibit dimethylnitrosamine induced liver injury in rat. *Chemico-biological interactions*, 295, 84-92.

Ray, S., Brown, D. and Yang, N. (2014). Dimethylnitrosamine.

Reitman, S. and Frankel, S. (1957). A colorimetric method for the determination of serum glutamic oxalacetic and glutamic pyruvic transaminases. *American journal of clinical pathology*, 28, 56-63.

Rojas, J. and Buitrago, A. (2019). Antioxidant Activity of Phenolic Compounds Biosynthesized by Plants and Its Relationship With Prevention of Neurodegenerative Diseases. Bioactive Compounds. *Elsevier*.

Rotruck, J. T., Pope, A. L., Ganther, H. E., Swanson, A., Hafeman, D. G. and Hoekstra, W. (1973). Selenium: biochemical role as a component of glutathione peroxidase. *Science*, 179, 588-590.

Rudrapal, M., Khairnar, S. J., Khan, J., Dukhyil, A. B., Ansari, M. A., Alomary, M. N., Alshabrmi, F. M., Palai, S., Deb, P. K., & Devi, R. (2022). Dietary Polyphenols and Their Role in Oxidative Stress-Induced Human Diseases: Insights Into Protective Effects, Antioxidant Potentials and Mechanism(s) of Action. *Frontiers in pharmacology*, 13, 806470. https://doi.org/10.3389/fphar.2022.806470

Sandoval-Yañez, C., Mascayano, C. and Martínez-Araya, J. I. (2018). A theoretical assessment of antioxidant capacity of flavonoids by means of local hyper–softness. *Arabian journal of chemistry*, 11, 554-563.

Saricicek, E., Celik, A., Uremis, N. and Kilinc, M. (2016). Protective effects of simvastatin, Nigella sativa oil and thmoquinone against dimethylnitrosamine-induced oxidative stress in rat kidney.

Scanlan, R. A. and Issenberg, P. (1975). N-nitrosamines in foods. Critical *Reviews in Food Science & Nutrition*, 5, 357-402.

Schenkman, J. B., Frey, I., Remmer, H. and Estabrook, R. W. (1967). Sex differences in drug metabolism by rat liver microsomes. *Molecular pharmacology*, 3, 516-525.

Sebranek, J. and Cassens, R. (1973). Nitrosamines: A review. *Journal of Milk and Food Technology*, 36, 76-91.

Shamsi, A., Ahmed, A. and Bano, B. (2017). Structural transition of kidney cystatin in dimethylnitrosamine-induced renal cancer in rats: identification as a novel biomarker for kidney cancer and prognosis. *Journal of Biomolecular Structure and Dynamics*, 35, 1020-1029.

Sharma, U., Pal, D. and Prasad, R. (2014). Alkaline Phosphatase: An Overview. *Indian Journal of Clinical Biochemistry*, 29, 269-278.

Siaga, T., Lichti, U., Hennings, H., Elgjo, K. and Yuspa, S. (1978). Effects of tumor promoters and steroidal anti-inflammatory agents on skin of newborn mice in vivo and in vitro. *Journal of the National Cancer Institute*, 60, 425-431.

Singh, B., Parsaik, A. K., Mielke, M. M., Erwin, P. J., Knopman, D. S., Petersen, R. C. and Roberts, R. O. (2014). Association of mediterranean diet with mild cognitive impairment and Alzheimer's disease: a systematic review and meta-analysis. *Journal of Alzheimer's disease*, 39, 271-282.

Singh, B., Singh, J. P., Kaur, A. and Singh, N. (2017). Phenolic composition and antioxidant potential of grain legume seeds: A review. *Food research international*, 101, 1-16.

Sinha, A. K. (1972). Colorimetric assay of catalase. *Analytical biochemistry*, 47, 389-394.

Suvorov, D. V., Zaitseva, N. V., Shur, P. Z., Zelenkin, S. E., Ngoc, N. T. N., & Thanh, T. T. (2023). Voprosy pitaniia, 92(4), 38–48. https://doi.org/10.33029/0042-8833-2023-92-4-38-48

Szasz, G. (1969). A kinetic photometric method for serum γ-glutamyl transpeptidase. *Clinical chemistry*, 15, 124-136.

Tanaka, T., Kojima, T., Kawamori, T. and Mori, H. (1995). Chemoprevention of digestive organs carcinogenesis by natural product protocatechuic acid. *Cance*r, 75, 1433-1439.

Tanaka, T., Kojima, T., Suzui, M. and Mori, H. (1993b). Chemoprevention of colon carcinogenesis by the natural product of a simple phenolic compound protocatechuic acid: suppressing effects on tumor development and biomarkers expression of colon tumorigenesis. *Cancer Res*, 53, 3908-13.

Tanaka, T., Tanaka, T. and Tanaka, M. (2011) Potential Cancer Chemopreventive Activity of Protocatechuic Acid. *Journal of Experimental & Clinical Medicine*, 3, 27-33.

Thapa, R., Goyal, A., Gupta, G., Bhat, A. A., Singh, S. K., Subramaniyan, V., ... & Dua, K. (2023). Recent developments in the role of protocatechuic acid in neurodegenerative disorders. *EXCLI journal*, 22, 595.

Tripathi, P. & Aggarwal, A. (2006). NF-kB transcription factor: a key player in the generation of immune response. *Current science*, 519-531.

Tseng, T. H., Kao, T. W., Chu, C. Y., Chou, F. P., Lin, W. L. and Wang, C. J. (2000). Induction of apoptosis by hibiscus protocatechuic acid in human leukemia cells via reduction of retinoblastoma (RB) phosphorylation and Bcl-2 expression. *Biochem Pharmacol*, 60, 307-15.

Tsuda, T., Horio, F. and Osawa, T. (1999). Absorption and metabolism of cyanidin 3-O-β-D-glucoside in rats. FEBS Letters, 449, 179-182.

Usunobun, U. and Okolie, N. (2016). Effect of Annona muricata pre-treatment on liver synthetic ability, kidney function and hematological parameters in

dimethylnitrosamine (DMN)-administered rats. *Int. J. Med*, 4, 1-5.

Usunomena, U., Ademuyiwa, A. J., Tinuade, O. O., Uduenevwo, F. E., Martin, O. and Okolie, N. (2012). N-nitrosodimethylamine (NDMA), Liver function enzymes, renal function parameters and oxidative stress parameters: A Review. *British Journal of Pharmacology and Toxicology*, 3, 165-176.

Vanisree, A. and Shyamala, D. C. (1999). Effect of therapeutics strategy established by N-acetyl cysteine and vitamin C on the activities of tumour marker enzymes in vitro. *Indian Journal of Pharmacology*, 31, 275.

Varshney, R. and Kale, R. (1990). Effects of calmodulin antagonists on radiation-induced lipid peroxidation in microsomes. *International journal of radiation biology*, 58, 733-743.

Vozarova, B., Stefan, N., Lindsay, R. S., Saremi, A., Pratley, R. E., Bogardus, C. and Tataranni, P. A. 2002. High alanine aminotransferase is associated with decreased hepatic insulin sensitivity and predicts the development of type 2 diabetes. *diabetes*, 51, 1889-1895.

Wang, A.-H., Sun, C.-S., Li, L.-S., Huang, J.-Y. and Chen, Q.-S. (2002). Relationship of tobacco smoking, CYP1A1, GSTM1 gene polymorphism and esophageal cancer in Xi'an. World journal of gastroenterology, 8, 49.

Wolff, S. P. (1994). Ferrous ion oxidation in presence of ferric ion indicator xylenol orange for measurement of hydroperoxides. *Methods in enzymology*, 233, 182-189.

Xi, X., Hu, S., Zhou, Z., Liu, X., Tang, J. and Shen, Y. (2016). Dendrimers with the protocatechuic acid building block for anticancer drug delivery. *Journal of Materials Chemistry* B, 4, 5236-5245.

Zhang, W., Yin, L., Tao, X., Xu, L., Zheng, L., Han, X., Xu, Y., Wang, C. and Peng, J. (2016). Dioscin alleviates dimethylnitrosamine-induced acute liver injury through regulating apoptosis, oxidative stress and inflammation. *Environmental toxicology and pharmacology*, 45, 193-201.

Niger. J. Physiol. Sci. 38 (December 2023): 157 – 169
www.njps.physiologicalsociety.com

Niger. J. Physiol. Sci.

Full length Research Article

Brain Antioxidant Status and Gene Expressions of Nicotinic and Dopamine Receptors are Improved by Black Seed (*Nigella Sativa*) Oil Administration in Cigarette Smoke or Nicotine Vapour-Exposed Rats

***Adejare, A.A.[1], Oloyo, A.K.[1], Ishola, I.O.[2], Busari, A.A.[2], Ismail-Badmus, K.B.[1], Abdulrazaq, M.M.[3], Osifala, O.O.[1] and Salami, M.O.[4]**

[1]*Department of Physiology, College of Medicine, University of Lagos, Lagos, Nigeria.*
[2]*Department of Pharmacology, Therapeutics &Toxicology, College of Medicine, University of Lagos, Nigeria.*
[3]*Department of Biochemistry, College of Medicine, University of Lagos, Lagos, Nigeria.*
[4]*Department of Mechanical Engineering, Faculty of Engineering, University of Lagos, Lagos, Nigeria*

Summary: Smoking is associated with dysregulation of the antioxidant system and addiction. This study sought to ascertain the effect of *Nigella sativa* (NS) oil on the antioxidant system, nicotine/tobacco addiction as well as the expressions of α4β2 nicotinic (nAChR) and dopamine type-2 (DRD2) receptors in selected brain regions of the rat. Thirty (30) male Sprague-Dawley rats were divided into 6 groups (n=5/group) comprising of vehicle-treated control, NS oil only, Smoke only, Smoke + NS oil, Nicotine only and Nicotine + NS oil. Animals were passively exposed to cigarette smoke or nicotine vapour for 12 weeks (whole body exposure, 60min/session/day), however, NS oil treatment commenced from 9th-12th week of the experimental duration. Conditioned place preference test was carried out at the start and end of the experiment. Cotinine and antioxidants levels were assessed in the plasma. Quantitative RT-PCT was used to assess gene expressions of nicotine subtypes and dopamine receptor in the brain homogenates. Nicotine vapour and cigarette smoke-induced increase in cotinine level were significantly reduced by NS treatment. Cigarette smoke or nicotine vapour exposure significantly ($p<0.05$) decreased the level of antioxidant enzymes while increasing malondialdehyde level in the brain homogenates of the rats. Administration of NS oil significantly ($p<0.05$) reversed the reduced antioxidant level. Cigarette-smoke also significantly increased α4-nAChR expression in the frontal cortex and olfactory bulb of exposed rats compared to control. Nicotine vapour significantly increased DRD2 expression only in the olfactory cortex. NS oil administration reduced both the cigarette-smoke-induced increase in α4-nAChR and nicotine vapour-induced increase in DRD2 gene expression only in the olfactory cortex. Findings from this study suggest that NS oil improves brain antioxidant status while ameliorating nicotine vapour and cigarette smoke addiction through down-regulation of α4-nAChR and DRD2 gene expressions in discrete brain regions of Sprague-Dawley rats.

Keywords*: Antioxidants, cigarette smoke; dopamine receptor; nicotinic receptor; Nigella sativa oil*

**Authors for correspondence: aadejare@unilag.edu.ng , Tel: +234 8069651326*

Manuscript received- March 2023; Accepted- September 2023

DOI: https://doi.org/10.54548/njps.v38i2.5

INTRODUCTION

Tobacco addiction is the leading cause of preventable death worldwide (CDCP 2012). According to the World Health Organization (WHO 2013), smoking causes about 6 million deaths yearly. Based on previous studies, the main psychoactive component responsible for the positive reinforcing effects of tobacco use is nicotine (Hoffman and Evan 2013). Several studies have proven beyond any reasonable doubt that α4β2 nicotinic receptors (Kamens *et al*. 2013; Esterlis *et al*. 2016; Melroy-Greif *et al*. 2016) are the main receptors responsible for addiction due to cigarette smoke (Zoli *et al*. 1998; Pons *et al*. 2008) as these receptors are up-regulated during chronic exposure to nicotine and cigarette smoke (Brees *et al*. 1997; Perry *et al*. 1999).

Another gene that plays a very prominent role in addiction is the dopamine type 2 receptors (DRD2). These are G-protein coupled receptors (GPCRs) linked to the G-alpha-inhibitory (Gαi) arm of the receptor to bring about their effects on the reward pathways and addiction (Seamans and Yang 2004; Bronson and Konradi 2010). DRD2 receptors also act by inhibiting adenylate cyclase and activating beta arrestins and protein phosphatase 2A (PP2A) which inhibit protein kinase B (Akt), leading to the dephosphorylation and activation of glycogen synthase kinase 3 beta (GSK3β), a kinase involved in Wnt signaling (Cross *et al*. 1995; Beaulieu *et al*. 2009). Previous study had

earlier linked nicotine exposure to increase dopamine release in mesolimbic terminal fields to cause dependence (DiChiara 2000).

While there are several animal models of addiction, the two commonly used models are the conditioned place preference (CPP) and self-administration (SA) tests (Torres *et al*. 2008; Shram and Le 2010). Conditioned place preference, has been used to study rewarding properties of addictive substances in rodents (Le Foll and Goldberg 2005; Liu and Le Foll 2008; O'Dell and Khroyan 2009). Many smokers are on quit smoking therapies, but the success rates of these regimens remain disappointingly low. In an attempt to quit smoking, some smokers have resulted to the use of Electronic Nicotine Delivery Systems (ENDS) also called e-cigarettes (Singh *et al*. 2016). The primary aim of using the e-cigarettes is to aid quitting process in smokers (Bold *et al*. 2017; Chaffee *et al*. 2018; Leventhal *et al*. 2015; Weaver *et al*. 2015) but may also even escalate addiction to nicotine (Fong *et al*. 2019; Mathur and Dempsey 2018). There is thus, an urgent need for an intervention that would aid voluntary quitting in these individuals.

Nigella sativa L. (Ranunculaceae) oil also known as black seed or black cumin oil has been reported to possess immuno-stimulatory, anti-inflammatory, hypoglycemic, antihypertensive, anti-asthmatic, antimicrobial, anti-parasitic, antioxidant and anticancer properties (Randhawa and Alghamdi 2002; Ali and Blunden 2003; Salem 2005). Interestingly, black seed oil had been reported to be an effective non-opiate treatment for opioid dependence (Sangi *et al*. 2008). Abdel-Zaher *et al*. (2011) also, reported the inhibition of tramadol tolerance and dependence in rats following the use of *Nigella sativa* seed oil. Phytochemical analysis revealed the main active constituent of *Nigella sativa* seed oil to be thymoquinone which had been reported to be safe when used orally (Mansour 2001; Al-Ali *et al*. 2008). This study provides an insight into the mechanism(s) by which oral administration of *Nigella sativa* oil could modulate the mRNA expressions of nicotinic acetylcholine receptor (nAChR) and dopamine type 2 (DRD2) receptors in nicotine and cigarette smoke-induced addiction. The study demonstrates the potential use of black seed oil as an effective adjunct therapy to aid quitting and increase the chance of cessation in smokers.

MATERIALS AND METHODS

Experimental animals: Thirty (30) male Sprague-Dawley rats (80-100g, 4-5 weeks old) were obtained from the animal facility of the Faculty of Basic Medical Sciences, College of Medicine of the University of Lagos. Rats were fed normal rat chow ad libitum. They were housed five per cage under a 12-hour dark-12-hour light cycle in room temperature (30 ± 2ºC) and humidity (55 ± 5%) controlled animal room. Before the commencement of the study, the rats were acclimatized in the new room for a week. Ethical approval was obtained from the College of Medicine of the University of Lagos Animal Care and Use Research Ethics Committee (CMUL-ACUREC) with registration number: CMUL/HREC/08/19/568. All animal experiments complied with, and were carried out following the National Institutes of Health guide for the care and use of Laboratory animals (NIH 1996).

Study design: The chart below illustrates the selection process carried out in the choice of rats used for the study. Using computer generated numbers, Sprague-Dawley rats were randomly assigned into 6 groups consisting of: Vehicle control (Ctrl; 10 ml/kg): rats received only water ad-libitum without any cigarette smoke or nicotine vapour exposure.

Positive control (NS): NS oil (10ml/kg, p.o.) was administered for 4 weeks (9th to 12th week)

Cigarette-Smoke-exposure (SMK): passive whole-body exposure to cigarette smoke for 12 weeks, 60 min/session/day.

Nicotine vapour-exposure (NCV): passive whole-body exposure to nicotine vapour for 12 weeks, 60 min/session/day.

Nicotine vapour–exposure + NS (NCV+NS) passive whole-body exposure to nicotine vapour for 12 weeks, 60 min/session/day, then NS oil was administered for 4 weeks (9th to 12th week).

Cigarette-Smoke-exposure + NS (SMK+NS): passive whole-body exposure to cigarette smoke for 12 weeks, 60 min/session/day, then NS oil was administered for 4 weeks (9th to 12th week).

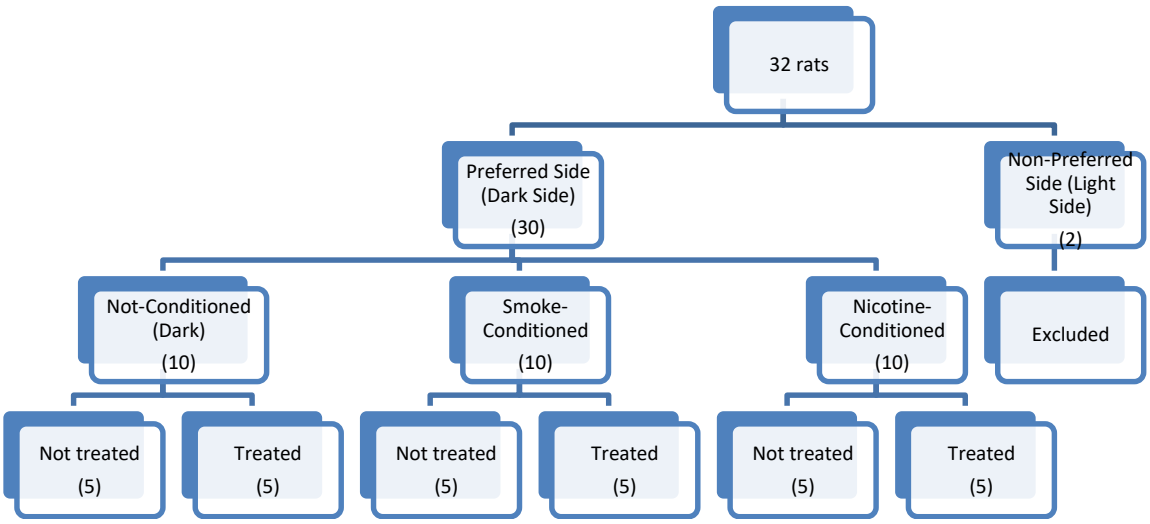

Figure 1:
Chart showing rat selection process.

Rats in groups III and IV were exposed to smoke from 3 sticks (Rothmans®) cigarette (Omotoso *et al*. 2012) daily over a period of 60 minutes for 12 weeks. The Rothmans® cigarette contained 0.738 g of tobacco and 1 mg of nicotine36 and was used because of its wide acceptability and use among Nigerian smokers.

Rats in groups II, IV and VI were administered with *Nigella sativa* (NS) oil (10 ml/kg, p.o) once daily (Kanter *et al*. 2005) during the last 4 weeks (9th to 12th week) of the experimental period.

Experimental procedures

Exposure Chamber: The conditioning chamber consisted of two Plexiglas chambers (l=40cm × b=25cm × w=30cm) each with a door (10cm × 10cm) in dimensions. The two chambers are connected by a central connecting chamber (10cm × 40cm × 10cm) which also has a (10cm × 10cm) door through which the animals were introduced into either side of the chamber. The first side was designated to be the non-preferred side and consisted of white-colored walls with a rough, black floor. On the wall of the first side is an extractor, with power rating of 1200 rpm to prevent excess accumulation of the vapour in the chamber. Also present in the chamber is a Multigas MSA detector (ALTAIR5X) containing a gas analyzer sensor which is used to ensure carbon monoxide level in the chamber is kept between acceptable 150 to 250 ppm during the exposures. The Multigas MSA detector also helped ensure the other gases like sulphur IV oxide and methane were maintained at zero while oxygen was maintained at 20.8%. The other side of the chamber was the dark side designed and designated as the preferred side. The side has a smooth floor and a small vent through which the side is aerated. For smoke exposure, the system consists of a pump (air pump) that has a direct connection to a syringe-system that blows air across the already lit cigarette. The air flow moves backward such that only filtered smoke gets into the chamber which directly mimics the kind of smoke inhaled by smokers in a passive whole-body exposure system.

For the nicotine vapour exposure, nicotine vapour was generated by bubbling air generated by an aerator (air pump) operating at a flow rate of 30 liters per minute through an Airistech vaporizer containing a solution of vaporized nicotine concentrations (80 mg/ml (FEELLiFE Vanilla Orange)) for 12 weeks (60 min/session/day) into the chamber. Nicotine vapour was produced by heating the nicotine solution to a temperature of 200ºC (392ºF) by the vaporizer. While there were other concentrations, it was observed that smokers preferred the 80 mg/ml concentration and that informed the choice of the concentration to mimic the likely effects observed in most smokers. Pure cotton wool was used to soak about 2mls of the pure nicotine and inserted into the vaporizer during each session that lasted for an hour per day for the two concerned groups of rats. Nicotine concentrations were selected putting the following factors into consideration: (1) the nicotine concentration (0-30 mg/mL) usually found in commercial e-cigarette liquids (Goniewicz *et al*. 2013), (2) companies' recommendation of e-cigarette liquids up to 60-100 mg/ml nicotine level; and (3) reported rapid metabolism of nicotine in rats compared to humans smokers (Matta *et al*. 2007). Identical chambers with controlled untreated air were used as the Control group. These chambers were either used for nicotine vapour exposure with the door closed during exposure or with the doors free to open during conditioned place preference assessment.

Conditioned Place Preference test: Conditioned Place Preference test was carried out at the start and end of the experiment using the methods of Okhuarobo *et al*. (2019) with little modifications. The preferred (dark side) and non-preferred side (light side) were first determined by the time spent in each side of the chamber by the rats and recorded as initial values. Rats that showed preference for the light side were removed from the experiment and replaced. The rats that showed preference for the dark side were divided into the different test groups accordingly. Smoke or nicotine vapour exposure was separately used to condition the rats to the initially non-preferred side (light side) and the reversal potential of NS oil tested accordingly. After the smoke or nicotine exposure that lasted for 12 weeks and the eventual application of the NS oil for 4 weeks (9th to 12th week) in the appropriate groups, the rats were placed at the central connecting chamber for free access to either of the main sides of the chamber. The rats were then left for 30 minutes, and the time spent on each sides of the chamber at the end of the 30 minutes was recorded.

Determination of Plasma Cotinine Concentration: Collection of blood samples for cotinine measurement in all groups of rats was performed on the last day of exposure. Plasma (150µL) was separated by centrifugation at 3000 rpm for 15 min and then stored at −80 °C until time for analysis. The concentration of cotinine (nicotine metabolite) was determined with Cotinine Direct ELISA (MBS580061), MyBioSource Inc., San Diego, CA 92195) according to the manufacturer's instructions.

Oxidative Stress Studies: The levels of reduced glutathione (GSH), catalase (CAT), superoxide dismutase (SOD), glutathione-S-transferase (GST) and malondialdehyde (MDA) were assessed in the brain homogenates of the rats using previously described standard methods (Morakinyo *et al*., 2011). Absorbance was recorded using Shimadzu recording spectrophotometer (UV 160) in all measurements. The reduced glutathione (GSH) content of the homogenates was determined using the method described by VanDooran *et al*. (1978). The GSH determination method is based on the reaction of Ellman's reagent 5,5' dithiobis (2-nitrobenzoic acid) DNTB) with the thiol group of GSH at pH 8.0 to produce 5-thiol-2-nitrobenzoate which is yellow at 412nm. The activity of the SOD enzyme was determined according to the method described by Sun and Zigman (1978). The reaction was carried out in 0.05M sodium carbonate buffer pH 10.3 and was initiated by the addition of epinephrine in 0.005N HCl. Catalase (CAT) activity was determined by measuring the exponential disappearance of H2O2 at 240nm and expressed in units/mg of protein as described by Aebi (1984). Absorbance was recorded using Shimadzu recording spectrophotometer (UV 160) in all measurement. For the malondialdehyde (MDA), it was estimated with the method of Uchiyama and Mihara (1978) which is based on its interaction with thiobarbituric acid (TBA) to form a pink complex with absorption maximum at 535nm. Absorbance

was recorded using Shimadzu recording spectrophotometer (UV 160) in all measurements.

Quantitative Reverse-Transcription Polymerase Chain Reaction (RT-PCR): At the end of the experiment, rats were sacrificed by cervical dislocation. The brains were quickly removed from the skull, immediately snap frozen in liquid nitrogen (-178ºC) and stored at -80ºC.

RNA extraction: Total RNA was extracted from the brain tissue with RNA extraction kit (ZYMO Quick-RNATM MiniPrep, (Cat. No: R1054, Lot No: ZRC203837)) following the manufacturer's instructions. Total RNA was quantified by measuring the absorbance at 260 nm (U-1100 spectrophotometer, Yokohama, Japan). All RNA samples were treated with amplification grade DNase 1 according to the manufacturer's instructions (ZYMO Quick-RNATM, CA) to eliminate residual DNA.

Reverse-transcription- qPCR (RT-qPCR): Complementary DNA (cDNA) synthesis and qPCR was performed in a single tube using gene-specific primers and total RNA by Protoscript First Strand cDNA Synthesis Kit (NEW ENGLAND BioLabs II E6300S/L) and LunaR Universal Quantitative PCR Master Mix (M3003) following the manufacturer's instruction. For the conversion of total RNA to cDNA, a 50-µl single-tube reaction mixture was prepared from a master mix containing 25µl of 2× reaction mix, 0.5 µg of template RNA. Then, 10 µM of each gene-specific primer pair was added to the tubes. Primer sequences were selected from the unique cytoplasmic domain region of each nicotinic acetylcholine or dopamine receptor as indicated below:

For α4:
Forward: 5'-GTCAAAGACAACTGCCGGAGACTT-3'
300 bp, 57ºC (Anneal temp.)
Reverse:5'TGATGAGCATTGGAGCCCCACTGC-3'

For β2:
Forward: 5'-ACGGTGTTCCTGCTGCTCATC-3'
507 bp, 57ºC (Anneal temp.)
Reverse: 5'-CACACTCTGGTCATCATCCTC-3'

For DRD2:
Forward: 5'-GCAGTCGAGCTTTCAGAGCC-3'
507 bp, 57ºC (Anneal temp.)
Reverse: 5'-TCTGCGGCTCATCGTCTTAAG-3'

For GAPDH:
Forward: 5'-ATGACAATGAATATGGCTACAG-3'
507 bp, 57ºC (Anneal temp.)
Reverse: 5'-CTCTTGCTCTCAGTATCCTT-3'

Glyceraldehyde-3-phosphate dehydrogenase (G3PDH) was used as an internal control to verify the quality of each RNA sample and its subsequent qRT-PCR analysis. The qRT-PCR cycling profiles using a Thermal Cycler (GeneAmp PCR System 9600; BIORAD CFX ConnectTM Real-Time System, USA) was as follows: 1 cycle at 50ºC for 30 min, 1 cycle at 94ºC for 2 min, 35 cycles at 94ºC for 1 min (46-57ºC), 72ºC for 1 min, and a final cycle at 72ºC for 7 min.

Statistical analyses: Intergroup comparisons were carried out using ANOVA to determine the level of significance. Values quantified from the expressions were represented as Mean ± SEM and Tukey post-hoc test was carried out with the significance level set at $p< 0.05$. STATA statistical software (version 13) was used for the analyses.

RESULTS

Impact of NS on rat conditioned place preference (CPP) for cigarette smoke or nicotine vapour: Figure 2 shows the time spent in the cigarette smoke or nicotine vapour-paired side of the chamber at the end of the experiment. The time spent in the drug-conditioned side was not statistically different ($p>0.05$) between the cigarette smoke-exposed group (SMK) and the control (Ctrl). Also, NS oil administration did not significantly change ($p>0.05$) the time spent in the drug-conditioned chamber between the SMK+NS group and SMK group. However, rats exposed to nicotine vapour stayed longer ($p<0.001$) in the nicotine vapour-paired side compared to the control group. The period of stay was equally longer in the NCV group when compared with the SMK group ($p<0.01$). Black seed oil administration caused a significant reduction ($p<0.05$) in the period of stay in the NCV+NS group compared to the NCV group.

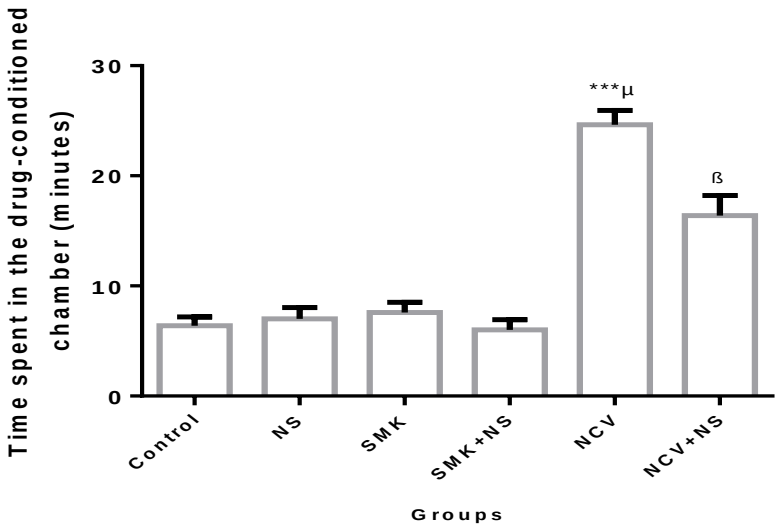

Figure 2:
Effect of treatments on conditioned place preference tests. Values are expressed as mean ± SEM (*n*=5 for each group). $^{***}p<0.001$ versus vehicle control, $^{µ}p<0.01$ versus SMK group, $^{ß}p<0.05$ versus NCV group. Control= Control group, NS= No exposure + black seed oil, SMK= Cigarette smoke exposed group, SMK+NS= Cigarette smoke exposed + black seed oil, NCV = Nicotine vapour exposed group, NCV+NS= Nicotine vapour exposed + black seed oil.

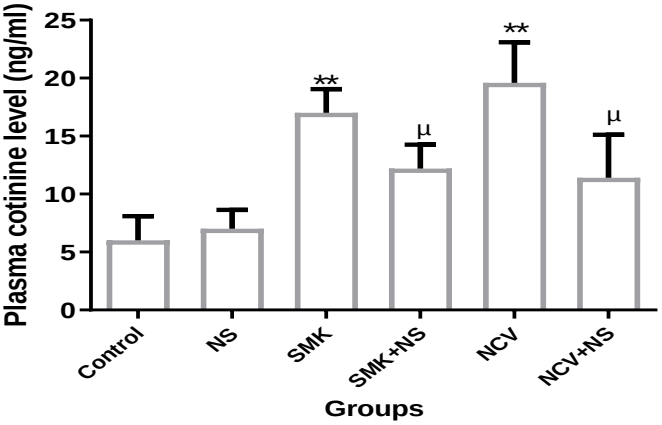

Figure 3:
Cotinine level across the group at the end of the experiment. Values are expressed as Mean ± SEM (*n*=5 for each group). **p<0.001 versus Control group, $^{\mu}$p<0.01 versus corresponding SMK and NCV groups. Control= Control group, NS= No exposure + black seed oil, SMK= Cigarette smoke exposed group, SMK+NS= Cigarette smoke exposed + black seed oil, NCV = Nicotine vapour exposed group, NCV+NS= Nicotine vapour exposed + black seed oil.

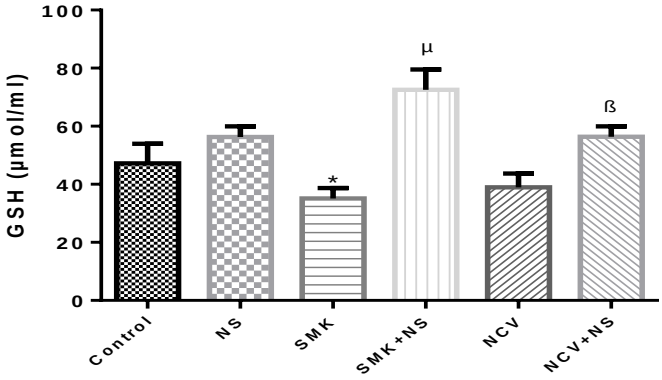

Figure 4:
Brain GSH level across the groups. Values are expressed as Mean ± SEM (*n*=5 for each group). *vs Control (*p<0.05), μ=vs SMK (p<0.0001), β=vs NCV (p<0.01). Control= Control group, NS= No exposure + black seed oil, SMK= Cigarette smoke exposed group, SMK+NS= Cigarette smoke exposed + black seed oil, NCV = Nicotine vapour exposed group, NCV+NS= Nicotine vapour exposed + black seed oil.

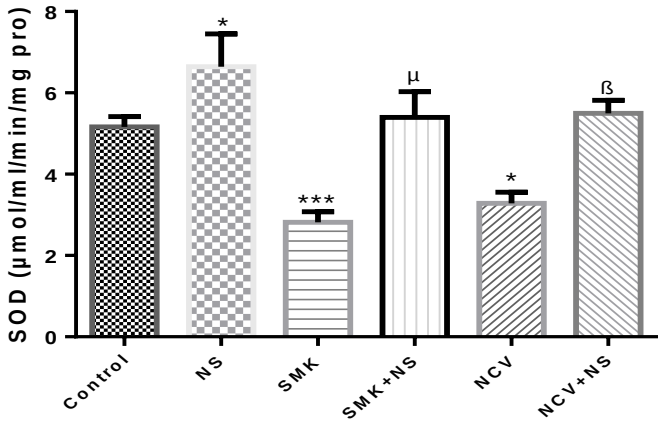

Figure 5:
Brain SOD level across the groups. Bars represent Mean ± SEM (*n*=5 for each group). *VS Ctrl (*p<0.05, ***p<0.001), μ=vs SMK (p<0.001), β=vs NCV (p<0.01). Control= Control group, NS= No exposure + black seed oil, SMK= Cigarette smoke exposed group, SMK+NS= Cigarette smoke exposed + black seed oil, NCV = Nicotine vapour exposed group, NCV+NS= Nicotine vapour exposed + black seed oil.

Effect of treatments on cotinine level: Figure 3 illustrates the plasma cotinine level at the end of the experiment. Both cigarette smoke and nicotine vapour exposure caused a statistically significant increase (p<0.01) in the level of cotinine in the SMK and NCV groups when compared with the control group. Black seed oil administration in both the cigarette smoke and nicotine vapour-exposed groups caused a statistically significant (p<0.01) reduction in cotinine level in the SMK+NS and NCV+NS groups compared to the SMK and NCV groups respectively.

Effect of smoke exposure, nicotine vapour exposure and oil administration on GSH level: In the brain tissue, GSH level was significantly lower (p<0.05) in the SMK group (35.12±3.58 μmol/ml) compared to the Control (47.23±6.73 μmol/ml). GSH level was however significantly higher (p<0.0001) in SMK+NS group (72.55±7.02 μmol/ml) compared to the SMK group. While there was no significant difference in the GSH level between the NCV group (38.94±4.81 μmol/ml) and Control, the level was significantly higher (p<0.01) in the NCV+NS group (56.34±3.64 μmol/ml) compared to the NCV group (Figure 4).

Effect of smoke exposure, nicotine vapour exposure and oil administration on SOD level: In the brain as well, SOD level was significantly lower (p<0.001) in the SMK group (2.81±0.26 μmol/ml/mg pro) compared to the Control (5.16±0.26 μmol/ml/mg pro). SOD level was however significantly higher (p<0.0001) in SMK+NS group (5.39±0.63 μmol/ml/mg pro) compared to the SMK group. The SOD level was also significantly lower (p<0.05) in the NCV group (3.29±0.29 μmol/ml/mg pro) when compared with the Control. However, the SOD level was significantly higher (p<0.01) in the NCV+NS group (5.50±0.32 μmol/ml/mg pro) compared to the NCV group (Figure 5).

Effect of smoke exposure, nicotine vapour exposure and oil administration on Catalase level: Catalase level was significantly lower (p<0.001) in the SMK group

(12.71±3.09 µmol/ml/mg pro) compared to the Control (31.45±1.79 µmol/m µmol/ml/mg pro). Catalase level was however significantly higher (p<0.001) in SMK+NS group (29.10±4.41 µmol/ml/mg pro) compared to the SMK group. The Catalase level was also significantly lower (p<0.001) in the NCV group (15.47±2.29 µmol/ml/mg pro) when compared with the Control. However, there was no significant difference (p>0.05) in the Catalase level between the NCV+NS group (19.02±1.51 µmol/ml/mg pro) compared to the NCV group (Figure 6).

Effect of smoke exposure, nicotine vapour exposure and oil administration on GST level: GST level was significantly lower (p<0.05) in the SMK group (0.68±0.13 µmol/ml/mg pro) compared to the Control (1.52±0.04 µmol/ml/mg pro). GST level was however significantly higher (p<0.001) in SMK+NS group (3.46±0.40 µmol/ml/mg pro) compared to the SMK group. The GST level was also significantly lower (p<0.05) in the NCV group (0.79±0.06 µmol/ml/mg pro) when compared with the Control. However, the GST level was significantly higher (p<0.001) in the NCV+NS group (2.56±0.39 µmol/ml/mg pro) compared to the NCV group (Figure 7).

Effect of smoke exposure, nicotine vapour exposure and oil administration on MDA level: In the brain as well, MDA level was significantly higher (p<0.05) in the SMK group (5.70±1.03 µmol/ml) compared to the Control (2.30±0.28 µmol/ml). MDA level was however significantly lower (p<0.05) in SMK+NS group (3.86±0.24 µmol/ml) compared to the SMK group. The MDA level was also significantly higher (p<0.001) in the NCV group (6.27±1.35 µmol/ml) when compared with the Control. However, the MDA level was significantly lower (p<0.001) in the NCV+NS group (3.23±0.46 µmol/ml) compared to the NCV group (Figure 8).

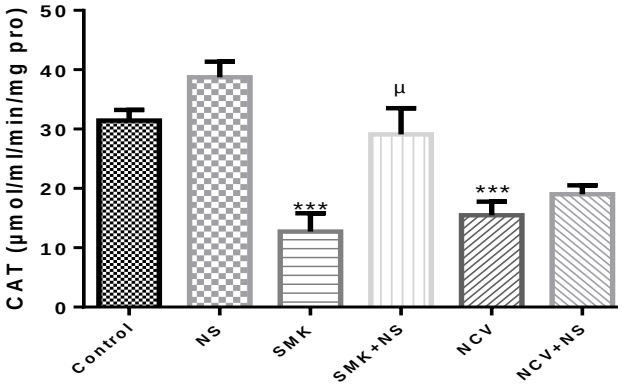

Figure 6:
Brain CAT level across the groups. Bars represent Mean ± SEM (*n*=5 for each group). *vs Control (***p<0.001), µ=vs SMK (p<0.001). Control= Control group, NS= No exposure + black seed oil, SMK= Cigarette smoke exposed group, SMK+NS= Cigarette smoke exposed + black seed oil, NCV = Nicotine vapour exposed group, NCV+NS= Nicotine vapour exposed + black seed oil.

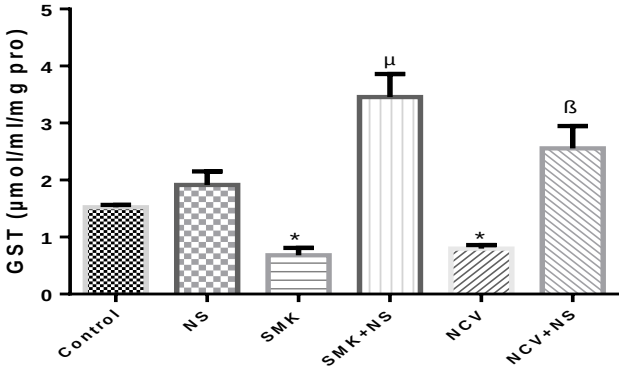

Figure 7:
Brain GST level across the groups. Values are expressed as Mean ± SEM (*n*=5 for each group). *vs Control (*p<0.05), µ=vs SMK (p<0.001), β=vs NCV (p<0.001). Control= Control group, NS= No exposure + black seed oil, SMK= Cigarette smoke exposed group, SMK+NS= Cigarette smoke exposed + black seed oil, NCV = Nicotine vapour exposed group, NCV+NS= Nicotine vapour exposed + black seed oil.

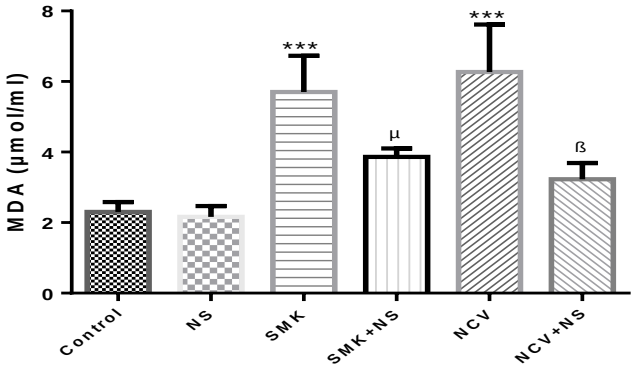

Figure 8:
Brain MDA level across the groups. Bars represent Mean ± SEM (*n*=5 for each group). *vs Control (***p<0.001), µ=vs SMK (p<0.001), β=vs NCV (p<0.001). Control= Control group, NS= No exposure + black seed oil, SMK= Cigarette smoke exposed group, SMK+NS= Cigarette smoke exposed + black seed oil, NCV = Nicotine vapour exposed group, NCV+NS= Nicotine vapour exposed + black seed oil

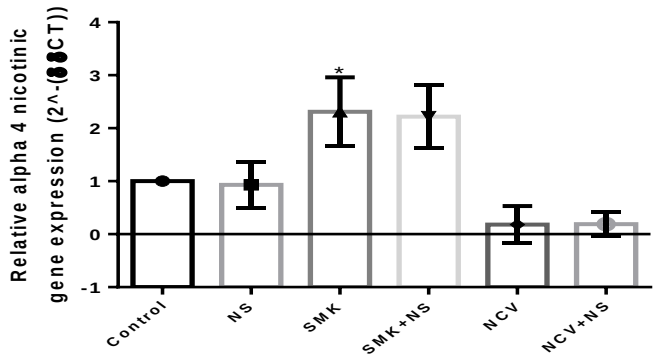

Figure 9:
Alpha-4 nicotinic gene expression in the frontal cortex. Values are expressed as Mean ± SEM (*n*=5). *p<0.05 versus Control group. Statistical level of significance analysis by one way ANOVA followed by Tukey *post hoc* multiple comparison test. Control= Control group, NS= No exposure + black seed oil, SMK= Cigarette smoke exposed group, SMK+NS= Cigarette smoke exposed + black seed oil, NCV = Nicotine vapour exposed group, NCV+NS= Nicotine vapour exposed + black seed oil

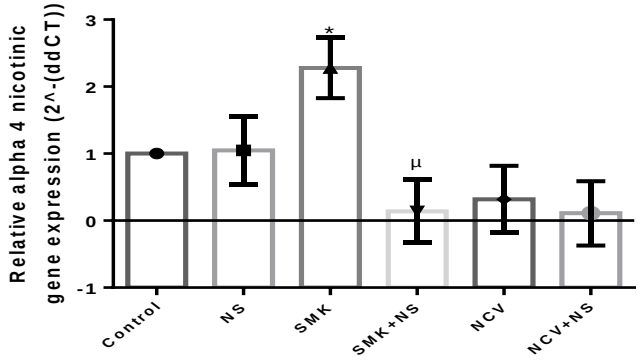

Figure 10:
α4 nicotinic gene expression in the olfactory cortex. Values are expressed as Mean ± SEM (*n*=5 for each group). *p<0.05 versus Control group; μp<0.05 versus SMK group. Statistical level of significance analysis by one way ANOVA followed by Tukey *post hoc* multiple comparison test. Control= Control group, NS= No exposure + black seed oil, SMK= Cigarette smoke exposed group, SMK+NS= Cigarette smoke exposed + black seed oil, NCV = Nicotine vapour exposed group, NCV+NS= Nicotine vapour exposed + black seed oil

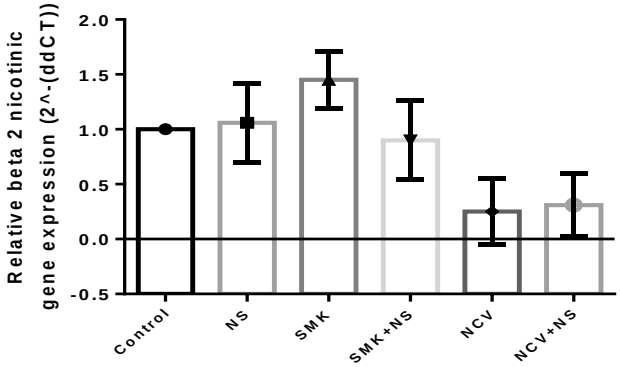

Figure 11:
β_2 nicotinic gene expression in the frontal cortex. Values are expressed as Mean ± SEM (*n*=5). Statistical level of significance analysis by one way ANOVA followed by Tukey *post hoc* multiple comparison test. Control= Control group, NS= No exposure + black seed oil, SMK= Cigarette smoke exposed group, SMK+NS= Cigarette smoke exposed + black seed oil, NCV = Nicotine vapour exposed group, NCV+NS= Nicotine vapour exposed + black seed oil

Alpha 4 subunit nicotinic gene expression in the frontal cortex: As illustrated in Figure 9, cigarette smoke exposure significantly (p<0.05) increased the expression of α4 subunit of nicotinic acetylcholine receptor in the SMK group when compared with the control group. There was no statistically significant (p>0.05) difference in the expression of the subunit in the SMK+NS group when compared with the SMK group. In essence, black seed oil administration failed to alter the expression of this subunit in rats exposed to cigarette smoke. In a similar manner, nicotine vapour caused no significant change (p>0.05) in the NCV group when compared with the control. Oil administration in the NCV+NS group did not significantly alter the level of the subunit expression when compared with the NCV group.

Alpha 4 subunit nicotinic gene expression in the olfactory cortex: Cigarette smoke exposure caused the expression of α4 subunit of nicotinic acetylcholine receptor to be significantly higher (p<0.05) in SMK group when compared with the control group. Its worthy of note that the expression of the subunit was significantly lower in the SMK+NS group compared to the SMK group indicating significant suppression effect on the expression of the subunit in the olfactory cortex. Exposure to nicotine vapour in the NCV group caused no statistically significant difference (p>0.05) in the level of expression of the subunit in the NCV group when compared to the control group. Black seed oil administration also failed to cause a statistically significant change in the level of expression of the subunit in the NCV+NS group compared to the NCV group (Figure 10).

β2 subunit nicotinic gene expression in the frontal cortex: Cigarette smoke exposure caused no statistically significant change (p>0.05) in the gene expression of β2 subunit of nicotinic acetylcholine receptor in the SMK group compared to the control (Figure 11). Black seed oil administration did not significantly change the expression of the subunit (SMKNS versus SMK, p>0.05). Nicotine vapour exposure caused no statistically significant (p>0.05) change in the expression level of the subunit in the NCV group compared to the control group. Black seed oil administration also did not cause a significant change in the expression of the subunit in the NCV+NS group when compared with the NCV group.

β2 subunit nicotinic gene expression in the olfactory cortex: Cigarette smoke exposure significantly increased ($p<0.05$) the expression of β2 subunit in the SMK group compared to the control group. There was no statistically significant ($p>0.05$) difference in the expression of the subunit in the SMK+NS group compared to the SMK group even though, there appears to be a slight reduction in the gene expression of the subunit following oil administration. In essence, black seed oil administration failed to alter the expression of this subunit in rats exposed to cigarette smoke. Nicotine vapour exposure caused no significant ($p>0.05$) change in the subunit expression in the NCV group compared to the control group. Black seed oil administration caused no significant change ($p>0.05$) in the subunit expression in the NCV+NS group compared to the NCV only group.

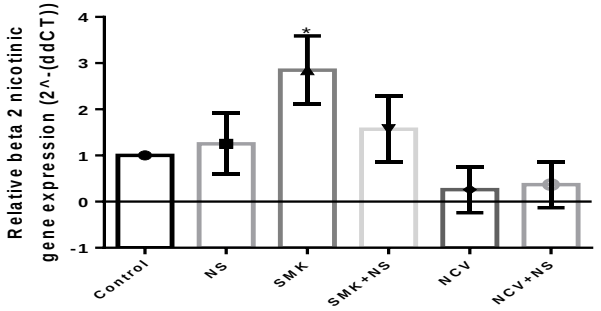

Figure 12:
Beta 2 nicotinic gene expression in the olfactory cortex. Values are expressed as Mean ± SEM (n=5 for each group). *p<0.05 versus Ctrl group. Statistical level of significance analysis by one way ANOVA followed by Tukey *post hoc* multiple comparison test. Control= Control group, NS= No exposure + black seed oil, SMK= Cigarette smoke exposed group, SMK+NS= Cigarette smoke exposed + black seed oil, NCV = Nicotine vapour exposed group, NCV+NS= Nicotine vapour exposed + black seed oil

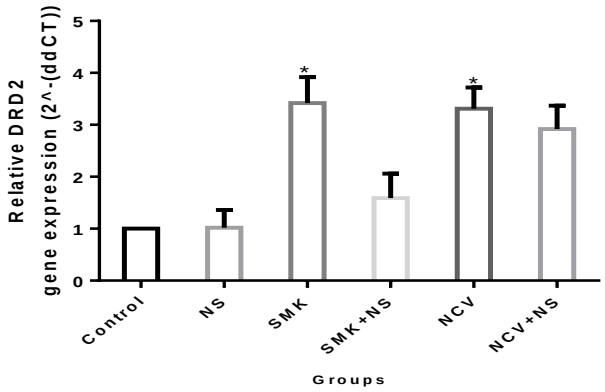

Figure 13:
Dopamine receptor type 2 gene expression in the frontal cortex. Values are expressed as Mean ± SEM (n=5 for each group). *p<0.05 versus Control group. Statistical level of significance analysis by one way ANOVA followed by Tukey *post hoc* multiple comparison test. Control= Control group, NS= No exposure + black seed oil, SMK= Cigarette smoke exposed group, SMK+NS= Cigarette smoke exposed + black seed oil, NCV = Nicotine vapour exposed group, NCV+NS= Nicotine vapour exposed + black seed oil.

Dopamine receptor type 2 (DRD2) gene expression in the frontal cortex: Cigarette smoke exposure caused the DRD2 gene expression to be higher ($p<0.05$) in the SMK group compared to the control group. Black seed oil administration did not cause a significant change ($p>0.05$) in the level of expression of the subunit. Nicotine vapour exposure caused significant increase in DRD2 gene expression ($p<0.05$) in the NCV group compared to the control group. In contrast, black seed oil failed to attenuate DRD2 gene expression in the NCV+NS group when compared with the NCV group (Figure 13).

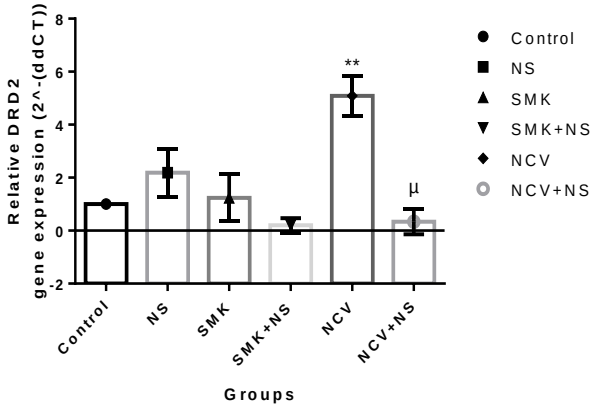

Figure 14:
Dopamine receptor type 2 gene expression in the olfactory cortex. Values are expressed as Mean ± SEM (n=5). *p<0.01 versus control group; μp<0.01 versus NCV-control group. Statistical level of significance analysis by one way ANOVA followed by Tukey *post hoc* multiple comparison test. Control= Control group, NS= No exposure + black seed oil, SMK= Cigarette smoke exposed group, SMK+NS= Cigarette smoke exposed + black seed oil, NCV = Nicotine vapour exposed group, NCV+NS= Nicotine vapour exposed + black seed oil.

Dopamine receptor type 2 (DRD2) gene expression in the olfactory cortex: Cigarette smoke exposure failed to cause a significant ($p>0.05$) change in the expression of the DRD2 gene in the SMK group compared to the control group. Black seed oil caused no significant change in the gene expression in the SMK+NS group compared to the SMK group. Exposure to nicotine vapour caused a marked statistically significant ($p<0.01$) increase in DRD2 gene expression in the NCV group compared to the control group. Black seed oil administration also caused a statistically significant reduction ($p<0.01$) in the level of DRD2 gene expression in the NCV+NS group when compared with the NCV group (Figure 14).

DISCUSSION

Our results did not only demonstrate the cigarette smoke and /or nicotine vapour induced-damage to the brain antioxidant systems and the gene expressions of the α4β2 nicotinic acetylcholine receptors and dopamine receptor type 2 (DRD2), it further showed the possible ameliorative effects of Black seed oil on the deranged brain antioxidant system and addictive genes expression. In this study, cigarette smoke exposure resulted in a general marked reduction in the brain antioxidant system of the animals as assessed from the brain homogenates. Our results further corroborate some earlier findings (Benowitz, 2014; Nielsen *et al*., 2000; Maritz, 2009). According to Nielsen *et al*. (2000), the degree of lipid peroxidation in the brain of the rats was observed to be high as well. In another study, Maritz (2009) reported marked reduction in the antioxidant capacity of other tissues exposed to cigarette smoke. Benowitz (2014) opined that these observations may be due to the presence of

carcinogens and heavy metals widely known to always lower the concentrations and activity of antioxidant micronutrients or the activation of vagocytic cells that generate potent oxidant species that worsen the degree of lipid peroxidation (Valavanidis *et al*., 2009).

In a similar manner, the brain antioxidant system was suppressed following exposure to nicotine vapour. The damaging effects appeared to be less intense however compared to that of exposure to cigarette smoke. This points to the fact that vaping can never be a better alternative to smoking based on its damaging effects on the antioxidant system. In support of these observations, Lerner *et al*. (2015) reported the ability of nicotine vapours to cause release of vapours that potentiate the oxidant system while suppressing the antioxidant system. Sussan *et al*. (2015) made similar observations. Beyond causing oxidative stress (Rubenstein *et al*., 2015; Ji *et al*., 2016), these vapours could therefore be responsible for the reduced brain antioxidant levels observed in this study. Consistent with these postulations, nicotine vapour and cigarette smoke had been reported to significantly increase cellular reactive oxygen species and decrease total cellular antioxidant capacity in other studies (Ganapathy *et al*., 2017; Biodi-Zoccai *et al*., 2019).

The fact that the success rates of the available quit-smoking therapies are disappointingly low makes it imperative to look for alternative drugs with smoking-quitting properties. However, the mechanisms underlying the therapeutic properties of such agents need to be unraveled. This study sought to provide the molecular basis for the possible therapeutic use of black seed oil as a smoking cessation regimen or as an adjunct therapy to aid the quitting process via modulation of α4β2 nicotinic acetylcholine receptors and dopamine receptor type 2 (DRD2) beyond its potent antioxidant effects. Our results showed that black seed oil administration could modulate the expressions of the selected genes and lower the levels of the major metabolite of cigarette smoke- cotinine. Moreso, young-adult rats were used in this study as they appeared to be more sensitive to the reinforcing effects of nicotine or cigarette smoke-induced addiction (Kota *et al*., 2007; Brielmaier *et al*., 2008).

To first ascertain addiction, we conducted a conditioned place preference (CPP) test which is one of the commonly used methods to assess the rewarding and cue-craving effects of drugs (Prokhorov, 1996; Tzschentke, 1998). The method had been shown to involve Pavlovian learning (Liu and Le Foll, 2008; Le Foll and Goldberg, 2005). What informed the choice of this method was the fact that the test is comparatively easy to perform unlike the self-administration test that requires a lot of technicalities among which is training the animals before the commencement of the study (Le Foll and Goldberg, 2005). In this study, all the rats initially preferred the dark side of the testing apparatus. This observation agrees with earlier studies (Biala and Budzynska, 2006; Brielmaier *et al*., 2008; Le Foll and Goldberg, 2009). After exposure to either cigarette smoke or nicotine vapour, their preference shifted to the light side which hitherto was non-preferred side in the nicotine groups to indicate their attachment to the drug-paired side (Picciotto, 2003) while there was a weakened preference to this drug-paired side in the cigarette smoke-exposed groups. An assessment of the period of stay for thirty minutes (Picciotto, 2003) in the drug-paired side at the start and end of the experiment also indicated the strong attachment of the groups exposed to nicotine vapour while there appeared to be aversion in the groups exposed to cigarette smoke. Earlier studies had shown the ability of nicotine to induce conditioned place preference (Fudala and Teoh, 1985; Horan and Smith, 1997; Le Foll and Goldberg, 2005). Our conditioned place preference result is in line with these earlier results. The "biased" place preference procedure used, whereby the drug of interest is paired with the initially non-preferred side made it easy to achieve the observed place preference (Le Foll and Goldberg, 2005). The observed place aversion after the long period of exposure in the cigarette smoke-exposed group may be due to many reasons among which is the presence of numerous other compounds apart from nicotine whose potential aversive or addictive actions have not been thoroughly investigated (Carter *et al*., 2009).

In the assessments, black seed oil administration significantly reduced the period of stay in the drug-paired side. To buttress this finding, both the cigarette smoke and nicotine vapour exposed groups had higher cotinine levels while black seed oil administration caused a significant reduction in the level of this bye-product of nicotine metabolism. In essence, it's either the oil reduced nicotine metabolism, reduced nicotine reuptake or enhanced the reuptake of cotinine into other tissues or probably caused degradation of cotinine into other metabolites that we could not assay for. Another possibility is the fact that the reduction in the cotinine level could be due to the reduced exposure to the source of nicotine which would consequently reduce the amount of nicotine available for metabolism and definitely its metabolite – cotinine. Sangi *et al*. (2008) had earlier reported the potential of black seed oil to ameliorate dependence caused by opioids. The ability of the oil to improve tramadol-induced tolerance and dependence had equally been established (Abdel-Zaher *et al*., 2011). Our observations for the ameliorative effects of the oil are thus in agreement with these earlier findings. It is worthy of note that the level of cotinine which happens to be the main bye-product of nicotine metabolism was found to be reduced in the test groups exposed to cigarette smoke or nicotine vapour. The cotinine level reported in this study could be extrapolated to that of human smokers. To the best of our knowledge, this report is among the first to indicate the direct effect of the black seed oil administration on this end-product of nicotine metabolism. Considering the other therapeutic benefits of black seed oil, our results indicate the potential use of the oil to improve the cessation rate. This explains the need to account for the molecular basis of such therapeutic potential on selected genes known to be associated with addiction.

The α4β2 receptors are a group of nicotinic acetylcholine receptors mainly responsible for nicotine addiction (Zoli *et al*., 1998; Gotti *et al*., 2006). They are found in large numbers in regions of the brain concerned with addiction and their subunits have been shown to play prominent roles in the modulation of addiction (Pons *et al*., 2008; Picciotto *et al*., 2008). These subunits are usually up-regulated whenever there is exposure to nicotine from cigarette smoke (Breese et a., 1997; Perry *et al*., 1999). Our results on these subunits indicated a significant increase in the gene expression of α4 subunit in the frontal and olfactory cortices

of smoke-exposed rats. Cigarette smoke exposure also increased the β2 subunit gene expression in the olfactory cortex without significantly changing the expression in the frontal cortex of the brain. Black seed oil administration only significantly reduced the α4 subunit expression in the olfactory cortex with minimal modulatory effects in the other regions. There were wide variations in the expressions of both the α4 and β2 subunits expression in the brain areas following exposure to nicotine vapour. Therefore, the likely modulatory effects of black seed oil administration on the expression of these subunits in these areas were minimal. In line with our results, previous studies had reported increased gene expressions of the α4β2 receptors following exposure to either cigarette smoke or nicotine vapour (Marks *et al*., 1983; Schwartz and Kellar, 1983; Flores *et al*., 1992; Marks *et al*., 2011). This was the same observation made in human tobacco users and cultured cells expressing the genes after transfection with nicotine (Lomazzo *et al*., 2011; Zambrano *et al*., 2012). The observed slight but not statistically significant reduction in the expression of the β2 subunit in the smoke-exposed group following black seed oil administration is an indicator of the potential therapeutic effect of reducing addiction caused by cigarette smoke as earlier reports indicated that deletion of some of the subunits of the nicotinic receptors are associated with reduced responsiveness to nicotine (Tapper *et al*., 2007) and nicotine self-administration in mice (Pons *et al*., 2008; Picciotto *et al*., 2008). In this study, the whole oil was used, and the period of oil administration was quite short. There is every possibility that this beneficial effect of the oil could be enhanced if the active component of the oil, which is thymoquinone was used and the period of administration prolonged. However, this study remains an eye-opener to the potential of the oil to cause reduction in the expression of the genes responsible for addiction and the potential use in smoking cessation and aiding the quitting process in smokers.

Another gene of interest is the dopamine receptor type 2 (DRD2). This is a G-protein coupled receptor (GPCR) with G-alpha inhibitory properties (Seamans and Yang, 2004). The dopamine system has been implicated in addiction and reward pathways (Kauer and Malenka, 2007). The established mechanism of action of DRD2 partly involves inhibition of adenylate cyclase (Enjalbert and Bockaert, 1983) and activation of beta arrestins and protein phosphatase 2A (PP2A) which inhibit protein kinase B (Akt), leading to the activation of glycogen synthase kinase 3 beta (GSK3β) involved in Wnt signaling (Beaulieu *et al*., 2009). Cigarette smoke and nicotine vapour exposure increased the mRNA expression of the DRD2 receptor in the frontal and olfactory cortices respectively. Again, black seed oil administration significantly reduced the expression of the gene in the olfactory cortex. In line with our observations, earlier reports had indicated attenuation of nicotine self-administration following disruption of dopamine in the ventral tegmental area of the brain (Corrigall and Coen, 1991; Huston-Lyons *et al*., 1993; Koob and LeMoal, 2008). Dopamine antagonists had earlier been reported to block nicotine-induced conditioned place preference (Acquas *et al*., 1989; Vizi *et al*., 2004). The marked reduction in DRD2 gene expression in group administered with black seed oil indicates the potential use of the oil in aiding the quitting process in smokers. However, further studies would be needed to ascertain this effect. The less attraction of the rats administered with the NS oil could further explain the observed marked reduction in the mRNA expression of the DRD2 receptor.

It is necessary to add that the source of nicotine vapour used in this study is the Electronic Nicotine Delivery Systems (ENDS) which is also known as e-cigarettes. These e-cigarettes were ordinarily intended to aid smoking cessation but the results from this study signal the possibility of the vapour worsening addiction instead of ameliorating it. Other studies had reported e-cigarettes not to be effective in smoking cessation (Leventhal *et al*., 2015; Weaver *et al*., 2015; Bold *et al*., 2017; Chaffee *et al*., 2018) while others even claim it facilitates smoking and dependence (Jensen *et al*., 2015; Sifat *et al*., 2018; Kulik *et al*., 2018; El-Hellani *et al*., 2019).

In conclusion, both smoke exposure from conventional cigarette and nicotine vapour from e-cigarettes have the potential to induce addiction through mechanisms that may involve up-regulation of the gene expressions of the α4β2 subunits of nicotinic acetylcholine receptor and dopamine receptor type 2 (DRD2) in the frontal and olfactory cortices. However, nicotine vapour appears to be more addictive than cigarette smoke. Black seed oil has the therapeutic potential to reduce the expression of these above-mentioned genes especially in the olfactory cortex of the brain. Black seed oil administration is a potential novel regimen that could be further investigated in the search for agents that could be used for smoking cessation. The study demonstrates the potential use of black seed oil as an effective adjunct therapy to aid quitting and increase the chance of cessation in smokers while boosting the antioxidant system. There would be a need to further investigate these potential ameliorative effects of Black seed oil on the antioxidant system and addiction in humans.

Acknowledgement

This work was supported by the College of Medicine of the University of Lagos BRAINS' mentored research grant (Year 5). The authors acknowledge the mentorship support from Prof. F. T. Ogunsola, Prof. A. S. Akanmu and Prof. N. U. Okubadejo.

REFERENCES

Abdel-Zaher, A. O., Abdel-Rahman, M. S., Elwasei, F. M. (2011) Protective effect of *Nigella sativa* oil against tramadol-induced tolerance and dependence in mice: role of nitric oxide and oxidative stress. *Neurotoxicology* 32: 725-733.

Acquas, E., Carboni, E., Leone, P., DiChiara, G. (1989). SCH23390 blocks drug-conditioned place-preference and place-aversion: anhedonia (lack of reward) or apathy (lack of motivation) after dopamine-receptor blockade? *Psychopharmacology*(Berl.); 99: 151–155.

Aebi H. (1984). Catalase in vitro. Methods in enzymology, 105, 121–126. https://doi.org/10.1016/s0076-6879(84)05016-3.

Al-Ali, A., Alkhawajah, A. A., Randhawa, M. A., Shaikh, N. A. (2008). Oral and intraperitoneal LD50 of thymoquinone, an active principle of *Nigella sativa*, in mice and rats. *J. Ayub. Med. Coll. Abbottabad*; 20: 25-27.

Ali, B. H., Blunden, G. (2003). Pharmacological and toxicological properties of *Nigella sativa*. *Phytother. Res*.; 17: 299-305.

Beaulieu, J. M., Gainetdinov, R. R., Caron, M. G. (2009). Akt/GSK3 signaling in the action of psychotropic drugs. Annu. *Rev. Pharmacol. Toxicol*.; 49:327–347.

Beaulieu, J. M., Gainetdinov, R. R., Caron, M. G. (2009). Akt/GSK3 signaling in the action of psychotropic drugs. *Annu. Rev. Pharmacol. Toxicol*.; 49:327–347.

Benowitz, N. L. (2014). "Emerging nicotine delivery products: implications for public health," *Annals of the American Thoracic Society*; 11(2): 231-235.

Biala, G., Budzynska, B. (2006). Reinstatement of nicotine-conditioned place preference by drug priming: effects of calcium channel antagonists. Eur. J. Pharmacol.; 537:85–93.

Biondi-Zoccai, G.; Sciarretta, S.; Bullen, C.; Nocella, C.; Violi, F.; Loffredo, L.; Pignatelli, P.; Perri, L.; Peruzzi, M.; Marullo, A.G.M.; De Falco, E.; Chimenti, I.; Cammisotto, V.; Valenti, V.; Coluzzi, F.; Cavarretta, E.; Carrizzo, A.; Prati, F.; Carnevale, R.; Frati, G., "Acute effects of heat-not-burn, electronic vaping, and traditional tobacco combustion cigarettes: the Sapienza University of Rome-Vascular Assessment of Proatherosclerotic Effects of Smoking (SUR – VAPES) 2 Randomized Trial," Journal of the American Heart Association 8(6): e010455, March 16, 2019.

Bold, K. W., Kong, G., Camenga, D. R. (2017). Trajectories of E-Cigarette and Conventional Cigarette Use Among Youth. *Pediatrics*. 141(1).

Breese, C. R., Adams, C., Logel, J., Drebing, C., Rollins, Y., Barnhart, M., Sullivan, B., Demasters, B. K., Freedman, R., Leonard, S. (1997). Comparison of the regional expression of nicotinic acetylcholine receptor alpha7 mRNA and [125I]-alpha-bungarotoxin binding in human postmortem brain. *J. Comp. Neurol*.; 387:385–398.

Brielmaier, J. M., McDonald, C. G., Smith, R. F. (2008). Nicotine place preference in a biased conditioned place preference design. Pharmacol. Biochem. Behav. 89:94–100.

Bronson, S. E., Konradi, C. (2010). Second Messenger Cascades. Handbook of basal ganglia structure and function. Vol. 20. Elsevier; Amsterdam: 447-460.

Carter, L. P., Stitzer, M. L., Henningfield, J. E., O'Connor, R. J., Cummings, K. M., Hatsukami, D. K. (2009). Abuse liability assessment of tobacco products including potential reduced exposure products. *Cancer Epidemiol. Biomarkers Prev*; 18:3241–3262.

Centers for Disease Control and Prevention (CDCP), Office on Smoking and Health, U.S Department of Health and Human Services (2012). Preventing Tobacco Use Among Young People: A Report of the Surgeon General. Atlanta, GA.

Chaffee, B. W., Watkins, S. L., Glantz, S. A. (2018). Electronic Cigarette Use and Progression From Experimentation to Established Smoking. *Pediatrics*. 141(4).

Corrigall, W. A., Coen, K. M. (1991). Opiate antagonists reduce cocaine but not nicotine self-administration. Psychopharmacology(Berl.); 104: 167–170.

Cross, D. A., Alessi, D. R., Cohen, P., Andjelkovich, M., Hemmings, B. A. (1995). Inhibition of glycogen synthase kinase-3 by insulin mediated by protein kinase B. *Nature*; 378:785–789.

DiChiara, G. (2000). Role of dopamine in the behavioural actions of nicotine related to addiction. *Eur. J. Pharmacol*.; 393, 295–314.

El-Hellani, A., Al-Moussawi, S., El-Hage, R., Talih, S, Salman, R., Shihadeh, A. (2019). Carbon monoxide and small hydrocarbon emissions from sub-ohm electronic cigarettes. *Chem. Res. Toxicol*.; 32:312–7.

Enjalbert, A., Bockaert J. (1983). Pharmacological characterization of the D2 dopamine receptor negatively coupled with adenylate cyclase in rat anterior pituitary. *Mol. Pharmacol*.; 23:576–584.

Esterlis, I., Hillmer, A. T., Bois, F., Pittman, B., McGovern, E., O'Malley, S. S. (2016). CHRNA4 and ANKK1 polymorphisms influence smoking-induced nicotinic acetylcholine receptor upregulation. *Nicotine Tob. Res*.; 18: 1845–1852.

Flores, C. M., Rogers, S. W., Pabreza, L. A., Wolfe, B. B., Kellar, K. J. (1992). A subtype of nicotinic cholinergic receptor in rat brain is composed of alpha 4 and beta 2 subunits and is up-regulated by chronic nicotine treatment. *Mol. Pharmacol*.; 41: 31–37.

Fong, G. T., Elton-Marshall, T., Driezen, P., Kaufman, A. R., Cummings, K. M., Choi, K. (2019). U.S. adult perceptions of the harmfulness of tobacco products: descriptive findings from the 2013–14 baseline wave 1 of the path study. *Addict Behav.;* 91 :180–7.

Fudala, P. J., Teoh, K. W. (1985). Pharmacologic characterization of nicotine-induced conditioned place preference. Pharmacol. *Biochem. Behav*. 22 (2), 237–241.

Ganapathy, V.; Manyanga, J.; Brame, L.; McGuire, D.; Sadhasivam, B.; Floyd, E.; Rubenstein, D.A.; Ramachandran, I.; Wagener, T.; Queimado, L., "Electronic cigarette aerosols suppress cellular antioxidant defenses and induce significant oxidative DNA damage," *PLOS One* 12(5): e0177780, May 18, 2017.

Goniewicz, M. L, Kuma, T., Gawron, M., Knysak, J., Kosmider, L. (2013) Nicotine levels in electronic cigarettes. *Nicotine Tob. Res*.; 15: 158-66.

Gotti, C., Zoli, M., Clementi, F. (2006). Brain nicotinic acetylcholine receptors: native subtypes and their relevance. *Trends Pharmacol. Sci*.; 27, 482–491.

Hoffman, A. C., Evans, S. E. (2013). Abuse potential of non-nicotine tobacco smoke components: acetaldehyde, nornicotine, cotinine, and anabasine. *Nicotine Tob. Res*.; 15, 622–632.

Horan, B., Smith, M. (1997). Nicotine produces conditioned place preference in Lewis, but not Fischer 344 rats. Synapse 26 (1), 93–94.

Huston-Lyons, D., Sarkar, M., Kornetsky, C. (1993). Nicotine and brain-stimulation reward: interactions with morphine. amphetamine and pimozide. Pharmacol. Biochem. Behav.; 46, 453–457.

Jensen, R. P., Luo, W., Pankow, J. F., Strongin, R. M., Peyton, D. H. (2015). Hidden formaldehyde in e-cigarette aerosols. *N. Engl. J. Med*.; 372:392–4.

Ji EH, Sun B, Zhao T, Shu S, Chang CH, Messadi D, *et al*. Characterization of Electronic Cigarette. Aerosol and Its Induction of Oxidative Stress Response in Oral Keratinocytes. PLoS One. 2016; 11(5): e0154447. PubMed Central PMCID: PMCPMC4880184. https://doi.org/10.1371/journal.pone.0154447. PMID: 27223106.

Kanter, M., Demir, H., Karakaya, C., Ozbek, H. (2005). Gastro-protective activity of *Nigella sativa* L oil and its constituent, thymoquinone against acute alcohol-induced gastric mucosal injury in rats. *World J. Gastroenterol*.; 11:6662–6666.

Kauer, J. A., Malenka, R. C.(2007). Synaptic plasticity and addiction. *Nat. Rev. Neurosci*.; 8:844–858.

Koob, G. F., LeMoal, M. (2008). Addiction and the brain anti-reward system. *Annu. Rev. Psychol*.; 59, 29–53.

Kota, D., Martin, B. R., Robinson, S. E. and Damaj, M. I. (2007). Nicotine dependence and reward differ between adolescent and adult male mice. *J. Pharmacol. Exp. Ther*.; 322, 399-407.

Kulik, M. C., Lisha, N. E., Glantz, S. A. (2018). E-cigarettes Associated with Depressed Smoking Cessation: A Cross-sectional Study of 28 European Union Countries. *Am. J. Prev. Med*.; 54(4): 603-609.

Le Foll, B., Goldberg, S. R. (2005). Nicotine induces conditioned place preferences over a large range of doses in rats. *Psychopharmacology* (Berl) 178:481–492.

Le Foll, B., Goldberg, S. R. (2009). Effects of nicotine in experimental animals and humans: an update on addictive properties. *Handb. Exp. Pharmacol*.; 192:335–367.

Lerner, C.A.; Sundar, I.K.; Watson, R.M.; Elder, A.; Jones, R.; Done, D.; Kurtzman, R.; Ossip, D.J.; Robinson, R.; McIntosh,

S.; Rahman, I., "Environmental health hazards of e-cigarettes and their components: oxidants and copper in e-cigarette aerosols," 198: 100-107, March 2015.

Leventhal, A. M., Strong, D. R., Kirkpatrick, M. G. (2015). Association of Electronic Cigarette Use With Initiation of Combustible Tobacco Product Smoking in Early Adolescence. *JAMA* 314(7): 700-707.

Liu, Y., Le Foll, B. (2008). Conditioned place preference induced by licit drugs: establishment, extinction, and reinstatement. *Scientific World Journal* 8, 1228–1245.

Lomazzo, E., Hussmann, G. P., Wolfe, B. B., Yasuda, R. P., Perry, D. C., Kellar, K. J. (2011). Effects of chronic nicotine on heteromeric neuronal nicotinic receptors in rat primary cultured neurons. *J. Neurochem*.; 119: 153–164.

Mansour, M. A., Ginwai, O. T., El-Hadiya, T., ElKhatib, A. S., Al-Shabanah, O. A. (2001). Effects of volatile oil constituents of *Nigella sativa* on carbon tetrachloride-hepatotoxicity in mice: evidence for antioxidant effects of thymoquinone. *Res. Commun. Mol. Pathol. Pharmacol*.; 110: 239-251.

Maritz, G. S. (2009). Are nicotine replacement therapy, varenicline or bupropion options for pregnant mothers to quit smoking? Effects on the respiratory system of the offspring. Ther. Adv. Respir. Dis.; 3(4):193-210. https://doi.org/10.1177/1753465809343712 PMID: 19706643.

Marks, M. J., Burch, J. B., Collins, A. C. (1983). Effects of chronic nicotine infusion on tolerance development and nicotinic receptors. *J. Pharmacol. Exp. Ther*. 226:817–825.

Marks, M. J., McClure-Begley, T. D., Whiteaker, P., Salminen, O., Brown, R. W., Cooper, J. (2011). Increased nicotinic acetylcholine receptor protein underlies chronic nicotine-induced up-regulation of nicotinic agonist binding sites in mouse brain. *J. Pharmacol. Exp. Ther*.; 337: 187–200.

Mathur, A., Dempsey, O. J. (2018). Electronic cigarettes: a brief update. J *R Coll. Physicians. Edinb*.; 48:346–51.

Matta, S. G., Balfour, D. J., Benowitz, N. L., Boyd, R. T., Buccafusco, J. J., Caggiula, A. R.(2007). Guidelines on nicotine dose selection for in vivo research. Psychopharmacology(Berl.) 190, 269–319.

Melroy-Greif, W. E., Stitzel, J. A., Ehringer, M. A. (2016). Nicotinic acetylcholine receptors: upregulation, age-related effects and associations with drug use. *Genes Brain Behav*.; 15: 89–107.

Mihara, M., & Uchiyama, M. (1978). Determination of malonaldehyde precursor in tissues by thiobarbituric acid test. Analytical biochemistry, 86(1), 271–278. https://doi.org/10.1016/0003-2697(78)90342-1

Morakinyo, A. O., Iranloye, B. O., Daramola, A. O., Adegoke, O. A. (2011). Antifertility effect of calcium channel blockers on male rats: association with oxidative stress. *Advances in Medical Sciences*; 56: 1-8.

Nielsen, F., Mikkelsen, B. B., Nielsen, J. B., Andersen, H. R., Grandjean, P. (2000) Plasma malondialdehyde as biomarker for oxidative stress: reference interval and effects of life-style factors. *Clinical Chemistry*;43(7):1209–1214.

NIH Publications No. 8023, revised 1996.

O'Dell, L.E., Khroyan, T.V. (2009). Rodent models of nicotine reward: what do they tell us about tobacco abuse in humans? *Pharmacol. Biochem. Behav*. 91 (4), 481–488.

Okhuarobo, A., Igbe, I., Yahaya, A. and Sule, Z. (2019). Effect of caffeine on alcohol consumption and alcohol-induced conditioned place preference in rodents. *J. Basic Clin. Physiol. Pharmacol*.; 30(1): 19–28.

Omotoso, G.O., Olagunju, A.A., Enaibe, B. U., Oyabambi, A. O., Balogun, O. R., Olawuyi, S. (2012). Alteration in Semen Characteristics and Testicular Histology of male Wistar Rats following exposure to Cigarette Smoke. *West African Journal of Assisted Reproduction*. https://www.researchgate.net/publication/256437770.

Perry, D. C., Davila-Garcia, M. I., Stockmeier, C. A., Kellar, K. J. (1999). Increased nicotinic receptors in brains from smokers: membrane binding and autoradiography studies. *J. Pharmacol. Exp. Ther*.; 289:1545–1552

Picciotto, M. R. (2003). Nicotine as a modulator of behavior: beyond the inverted U. *Trends Pharmacol. Sci*. 24 (9), 493–499.

Picciotto, M. R., Addy, N. A., Mineur, Y.S., Brunzell, D. H. (2008). It is not "either / or": activation and desensitization of nicotinic acetylcholinereceptors both contribute to behaviors related to nicotine addiction and mood. *Prog. Neurobiol*.; 84, 329–342.

Pons, S., Fattore, L., Cossu, G., Tolu, S., Porcu, E., Mcintosh, J. M. (2008). Crucial role of a4 and a6 nicotinic acetylcholine receptor subunits from ventral tegmental area in systemic nicotine self-administration. *J. Neurosci*. 28, 12318–12327.

Prokhorov, A. V., Pallonen, U. E., Fava, J. L., Ding, L. and Niaura, R. (1996). Measuring nicotine dependence among high-risk adolescent smokers. Addict. Behav.; 21, 117-127.

Randhawa, M. A. Alghamdi, M. S. (2002). A review of the pharmaco-therapeutic effects of *Nigella sativa*. *Pak. J. Med. Res*.; 41: 77-83.

Rubenstein, D.A.; Hom, S.; Ghebrehiwet, B.; Yin, W., "Tobacco and e-cigarette products initiate Kupffer Cell inflammatory responses,"*Molecular Immunology* [Epub ahead of print], June 11, 2015.

Salem, M. L. (2005). Immunomodulatory and therapeutic properties of the *Nigella sativa* L. seed. Int. Immunopharmacol.; 5: 1749-1770.

Sangi, S., Ahmed, S. P., Channa, M. A., Ashfaq, M., Mastoi, S. M. (2008). A new and novel treatment of opioid dependence: *Nigella sativa* 500 mg. *J. Ayub Med. Coll*. Abbottabad; 20: 118-124.

Schwartz, R. D., Kellar, K. J. (1983). Nicotinic cholinergic receptor binding sites in the brain: regulation in vivo. Science; 220: 214–216.

Seamans, J. K. Yang, C. R. (2004). The principal features and mechanisms of dopamine modulation in the prefrontal cortex, Prog. *Neurobiol*.; 74: 1–58.

Shram, M. J. and Le, A. D. (2010). Adolescent male Wistar rats are more responsive than adult rats to the conditioned rewarding effects of intravenously administered nicotine in the place conditioning procedure. *Behav. Brain Res*.; 206, 240-244.

Sifat, A. E., Vaidya, B., Kaisar, M. A., Cucullo, L., Abbruscato, T. J. (2018). Nicotine and electronic cigarette (E-Cig) exposure decreases brain glucose utilization in ischemic stroke. *J. Neurochem*.; 147:204–21.

Singh, T., Arrazola, R. A., Corey, C. G. (2016). Tobacco use among middle and high school students–United States, 2011–2015. MMWR Morb. Mortal Wkly Rep. 65(14): 361–367.

Sun, M., & Zigman, S. (1978). An improved spectrophotometric assay for superoxide dismutase based on epinephrine autoxidation. *Analytical biochemistry*, 90(1), 81–89. https://doi.org/10.1016/0003-2697(78)90010-6

Sussan, T.E.; Gajghate, S.; Thimmulappa, R.K.; Ma, J.; Kim, J.H.; Sudini, K.; Consolini, N.; Cormier, S.A.; Lomnicki, S.; Hasan, F.; Pekosz, A.; Biswal, S., "Exposure to electronic cigarettes impairs pulmonary anti-bacterial and anti-viral defenses in a mouse model," *PLOS ONE*, February 4, 2015.

Tapper, A. R., McKinney, S. L., Marks, M. J., Lester, H. A. (2007). Nicotine responses in hypersensitive and knockout alpha 4 mice account for tolerance to both hypothermia and locomotor suppression in wildtype mice. *Physiol. Genomic*s; 31: 422–428.

Torres, O. V., Tejeda, H. A., Natividad, L. A. and O'Dell, L. E. (2008). Enhanced vulnerability to the rewarding effects of nicotine during the adolescent period of development. Pharmacol. *Biochem. Behav*.90, 658-663.

Tzschentke, T. M. (1998). Measuring reward with the conditioned place preference paradigm: a comprehensive review of drug effects, recent progress and new issues. Prog. *Neurobiol*.; 56, 613-672.

Valavanidis A, Vlachogianni T, Fiotakis K. Tobacco smoke: involvement of reactive oxygen species and stable free radicals

in mechanisms of oxidative damage, carcinogenesis and synergistic effects with other repairable particles. Int J Environ Res Public Health. 2009; 6 (2):445-462.doi:10.3390/ijerph6020445.

van Dooran, R., Leijdekkers, C. M., & Henderson, P. T. (1978). Synergistic effects of phorone on the hepatotoxicity of bromobenzene and paracetamol in mice. *Toxicology*, 11(3), 225–233. https://doi.org/10.1016/s0300-483x(78)91389-6.

Vizi, E.S., Palkovits, M., Lendvai, B., Baranyi, M., Kovacs, K.J. Zelles, T. (2004). DistiNCV temperature-dependent dopamine-releasing effect of drugs of abuse in the olfactory bulb, *Neurochem. Int.*; 45: 63–71.

Weaver, S. R., Huang, J., Pechacek, T. F., Heath, J. W., Ashley, D. L., Eriksen, M. P. (2015). Are electronic nicotine delivery systems helping cigarette smokers quit? Evidence from a prospective cohort study of U.S. adult smokers, 2015–2016. *PLOS ONE* 13(7):e0198047.

World Health Organization (2013). Report on the global tobacco epidemic. WHO Press, World Health Organization, Geneva, Switzerland.

Zambrano, C. A., Salamander, R.M., Collins, A. C., Grady, S. R., Marks, M. J. (2012). Regulation of the distribution and fuNCVion of [(125)I] epibatidine binding sites by chronic nicotine in mouse embryonic neuronal cultures. *J. Pharmacol. Exp. Ther.*; 342: 245–254.

Zoli, M., Lena, C., Picciotto, M. R., Changeux, J. P. (1998). Identification of four classes of brain nicotinic receptors using beta2 mutant mice. *J. Neurosci*. 18:4461–4472.

Niger. J. Physiol. Sci. 38 (December 2023): 187 – 193
www.njps.physiologicalsociety.com

Niger. J. Physiol. Sci.

Full length Research Article

Quercetin Exerts Anticonvulsant Effect through Mitigation of Neuroinflammatory Response in Pentylenetetrazole-induced Seizure in Mice

Adeoluwa, O.A.[1], Adeoluwa, G.O.[1], Adeniyi, F.R.[2], Oni, J.O.[1], Akinluyi, E.T.[1], Olojede, S.O.[3] and Bakre, A.G.[4]

[1] *Department of Pharmacology and Therapeutics, College of Medicine and Health Sciences, Afe Babalola University, Ado Ekiti.*

[2] *Department of Pharmacology and Toxicology, College of Pharmacy, Afe Babalola University, Ado Ekiti.*

[3] *Department of Human Biology, Faculty of Medicine and Health Sciences, Walter Sisulu University, Nelson Mandela Drive, Mthatha, South Africa.*

[4]*Department of Pharmacology and Therapeutics, College of Medicine, University of Ibadan. Ibadan, Nigeria*

Summary: Epilepsy is a chronic disease of the brain characterized by seizures. The currently available anticonvulsants only treat symptoms with serious adverse drug reactions. Therefore, there is need for new therapeutic intervention that will prevent epileptogenesis with greater therapeutic success. Quercetin (QT) is a flavonoid with known neuroprotective and anti-inflammatory properties. The study aimed to investigate its effects against pentylenetetrazole (PTZ)-induced seizures. Animals were divided into four groups (n = 10). Group 1(control) only received vehicle (10 mL/kg), group 2 received vehicle, groups 3 and 4 received QT 12.5 mg/kg and 25 mg/kg respectively. Sixty minutes after treatments, animals in groups 2 to 4 were injected with sub-convulsive dose of pentylenetetrazole (35 mg/kg, i.p.) on every alternate day (48±2h) for 21 days. The mice were observed for 30 minutes after each PTZ injection for seizure activity. Brain samples were collected for biochemical assays. Administration of PTZ caused significant increase in the intensity of seizures, neuronal degeneration and level of proinflammatory cytokines in animals compared to control. These behavioural alterations were attenuated significantly by QT (12.5 and 25 mg/kg). The PTZ-induced increase in IL-12, TNF-α and IFN-ɣ were significantly reduced by pre-treatment with the QT (12.5 and 25 mg/kg, p.o). Quercetin also reduced neuronal loss compared to control. Quercetin attenuates seizures in kindled mice and reduces neuroinflammation and neurodegeneration. This neuroprotective effect may be attributed to its ability to inhibit inflammatory mediators in the brain.

Keywords*: Epilepsy, neuroinflammation, kindling, neurodegeneration, epileptogenesis*

**Authors for correspondence: ag.bakre@mail.ui.edu.ng , Tel: +234-8081062365*

Manuscript received- March, 2023; Accepted- July, 2023

DOI: https://doi.org/10.54548/njps.v38i2.7

INTRODUCTION

Epilepsy is a neurological condition with a prevalence of more than 65 million people worldwide (Pearson-Smith and Patel, 2017). Hallmarks of epilepsy include recurrent seizures (Sankaraneni and Lachhwani, 2015), spontaneous, abnormal and extreme neuronal firing in the central nervous system (Muke *et al*., 2018). Refractoriness to available neuroleptics is one of the significant challenges affecting the effective management of epilepsy (de Souza *et al*., 2019). In addition, an associated cognitive impairment following prolonged administration of these neuroleptics has been reported in 50% of epileptic patients (Mehla *et al*., 2010). The current neuroleptics only focus on reducing the symptoms of epilepsy (Muke *et al*., 2018) without necessarily preventing the onset of epileptic seizures. It is important to develop novel therapeutic agents that will delay epileptogenesis and prolong the latency of epileptic attacks (Muke *et al*., 2018, Samokhina and Samokhin, 2018).

The mechanisms underpinning the pathophysiology of epilepsy are very complex and multifactorial. Increasing knowledge emanating from clinical and experimental studies has suggested and given credence to inflammatory processes as a crucial underlying factor in epilepsy pathology (Riazi *et al*., 2010, Choi *et al*., 2009, Vezzani *et al*., 2011, Vezzani and Baram, 2007). Previous studies have shown the antiepileptic property of steroids and anti-inflammatory agents in some drug-resistant epilepsies (Tavakoli *et al*., 2023, Wheless *et al*., 2007, Wirrell *et al*., 2005, Riikonen, 2004). Similarly, a high level of inflammatory mediators has been demonstrated in febrile convulsion (Dinarello, 2004). The inflammatory hypothesis is further reinforced by the high incidence of epilepsies in an autoimmune system in some patients suffering from

seizures (Dalmau *et al*., 2008, Vincent and Bien, 2008, Bien *et al*., 2007).

Evidence has emerged that inflammation might be a causative factor and the aftermath of epilepsy (Vezzani *et al*., 2011). Numerous inflammatory markers were detected in the brain tissue of patients suffering from refractory epilepsy (Vezzani *et al*., 2011). The occurrence of neuroinflammation in epilepsy that was not associated with immune dysfunction indicates the role of chronic inflammation in the manifestation of epilepsies (Vezzani *et al*., 2011). Evidence of mediators like pro-inflammatory cytokines and microglial as key players in epilepsy has been documented (Ahmadian *et al*., 2019, Salgado *et al*., 2018, Cerri *et al*., 2017, Gales and Prayson, 2017). In an animal model of seizure, activation of microglia has been reportedly significant in elevating tumour necrosis factor-alpha (TNF-α) levels, interleukin-1 beta (IL-1β) levels and other inflammatory biomarkers (Jeon *et al*., 2008, Chen *et al*., 2004, Thompson *et al*., 2004, Gupta *et al*., 2003). Past studies have documented elevated nitric oxide levels concerning pentylenetetrazole (PTZ) kindling in laboratory animals (Ahmadian *et al*., 2019, Haj-Mirzaian *et al*., 2019, Amiri *et al*., 2016, Watanabe *et al*., 2013).

The PTZ kindling model is a chronic epilepsy model, which involves continuous administration of low doses of a convulsant resulting in seizures (Dehkordi *et al*., 2023, Dhir, 2012, McNamara, 1984). It mimics clinical epilepsy and the various psychiatric and neurological changes and symptoms associated with this neurological disorder (Kaur *et al*., 2016). It helps scientists study the pathophysiology and molecular pathways related to the onset and duration of epileptic seizures, which are very important when screening new potential antiepileptic drugs (Shimada and Yamagata, 2018). The three phases of this model involve the pre-kindling phase, the kindling phase and the post-kindling phase (Samokhina and Samokhin, 2018). Continuous administration of PTZ (20 to 40 mg/kg, i.p.) can trigger seizures in laboratory animals such as rats and mice (Dhir, 2012). The PTZ acts by blocking and suppressing gamma amino butyric acid (GABA) mediated neurotransmission at GABAA receptors at alpha 1, 2, 3 and 5 (Samokhina and Samokhin, 2018). The experimental animal population can record various phases of convulsions like myoclonic seizures, straub's tail, clonus, tonic-clonic jerks, and death. Furthermore, the kindling model provides an avenue for researchers to study cognitive deficits associated with epilepsy (Pourmotabbed *et al*., 2011). This model mentioned above is a chronic epilepsy model which can result in neuronal loss and degeneration in the CA1, CA3 and dentate gyrus of the hippocampus with the amygdala and entorhinal cortex (Mehla *et al*., 2010), subsequently resulting in memory impairment.

Phytochemicals and some herbal products with anti-inflammatory properties have been able to ameliorate epileptic symptoms and seizures in recent times (Ahmadian *et al*., 2019, Shimada *et al*., 2014). Quercetin is a flavonoid that possesses neuroprotective properties (Nassiri-Asl *et al*., 2016, Chakraborty *et al*., 2014). The antioxidant and anti-inflammatory effects of quercetin may serve as prime targets in preventing neurodegeneration in epilepsy. Several studies have documented quercetin's anti-inflammatory and antioxidant properties (Li *et al*., 2016b, Li *et al*., 2016a, Zheng *et al*., 2016). Studies have shown an antiseizure effect of quercetin-containing extracts in animal models of epilepsy (Can and Özkay, 2012, Guo *et al*., 2011, Manigauha and Patel, 2010). Although, effect of quercetin against picrotoxin and PTZ-induced convulsion has been demonstrated in several studies, antiepileptic property of quercetin against PTZ-induced seizures and neurodegeneration in kindled mice has not been investigated. Therefore, we evaluated the neuroprotective potential of quercetin against seizures and neurodegeneration in mice using the pentylenetetrazole kindling model.

MATERIALS AND METHODS

Experimental animals: Forty male mice weighing between (22-25g) were purchased from the Central Animal House. The animals were kept in a standard environment with unlimited access to a standard rodent pellet diet and water ad libitum. They were kept in a room temperature-controlled environment with 12hr/12hr (light/dark) cycle, 40-70% relative humidity, with water and standard rodent chow ad libitum. Ethical approval was sought from the Animal Care and Use Research Ethics Committee for the experimental procedures. It was carried out in line with the NIH's care and animal use guidelines.

Drugs and Chemicals: Pentylenetetrazole (Sigma Aldrich), quercetin (Sigma Aldrich), silver nitrate, (Sigma Aldrich) potassium dichromate (Sigma Aldrich).

PTZ-induced kindling model: Kindling was induced using a well-established method (Taiwe *et al*., 2016, Kiasalari *et al*., 2013). In brief, a sub-convulsive dose of PTZ (35 mg/kg, i.p.) was administered every alternate day, and seizure behaviours were monitored for 30 minutes after each PTZ injection. Subsequently, the animals were monitored for 30 min after PTZ administration for seizure activity and scored using a scoring scale of 0 to 6: stage 0: no response; stage 1: hyperactivity, vibrissae twitching; stage 2: head nodding, head clonus and myoclonic jerk; stage 3: unilateral forelimb clonus; stage 4: rearing with bilateral forelimb clonus; stage 5: generalised tonic-clonic seizure with loss of writing reflex, stage 6: lethality (Malhotra and Gupta, 1997, Racine, 1972). The number of myoclonic jerks, the duration and the latencies to myoclonic jerks, generalised tonic-clonic seizures and lethality were recorded. The animals were considered to be kindled after exhibiting at least three consecutive maximum seizures stages.

Experimental procedure: The neuroprotective effect of quercetin on pentylenetetrazole-induced epileptogenesis was evaluated using a known method (Taiwe *et al*., 2016, Kiasalari *et al*., 2013). The animals were randomly divided into four (4) groups of 10 each. Animals in group 1, served as normal control, received vehicle (10 mL/kg, p.o.), group 2 were given vehicle which served as negative control. Mice in groups 3 and 4 were treated with the selected doses of quercetin (12.5 mg/kg and 25 mg/kg, p.o.). Sixty minutes after treatments, animals in groups 2 to 4 were given pentylenetetrazole (35 mg/kg, i.p.) on every alternate day (48± 2 h) for 21 days (total of 10 PTZ injection). The mice were monitored for 30 minutes after each PTZ administration. Several grades of seizures were scored using

a scoring scale according to Racine (1972) as modified by Malhotra and Gupta (1997). The total number of myoclonic seizures, the duration and the latencies of myoclonic seizures, tonic-clonic seizures and lethality were noted.

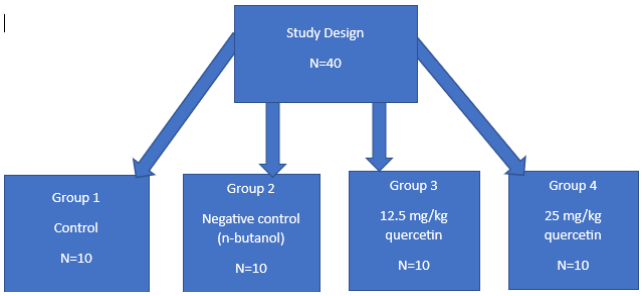

Figure A:
This figure depicts the study design which entails the grouping, total number of animals and agents administered.

Preparation of brain tissues for biochemical studies: After behavioural studies on day 22, mice in respective groups were euthanised with cervical dislocation, and the brain samples were harvested immediately, weighed and cleaned with cold 0.90% saline. Afterwards, the hippocampus was dissected out and homogenised with phosphate buffer (0.1M, PH 7.4) and centrifuged at 10,000 rpm at 4o C for 10 minutes. Thereafter, the supernatant was separated for the various biochemical tests.

Measurement of brain levels of pro-inflammatory cytokines with ELISA techniques: The ELISA technique is a widely used method for measuring the levels of specific proteins or molecules in a sample. In this case, the levels of interferon-gamma (IFN-ɣ), interleukin-12 and tumour necrosis factor-α (TNF- α) were measured in brain tissue samples according to the respective manufacturers' instructions. To quantify the concentration of the cytokines in the brain tissue samples, a standard curve was first generated using known concentrations of the cytokines and their respective optical densities (OD) values obtained at 450nm. The concentrations of cytokines in the brain tissue samples were then extrapolated from this standard curve based on their OD values. These concentrations were expressed as pg/mL.

Golgi Staining Procedure: On the last day of treatment, animals were perfused and their brains fixed with 10% formo-saline. The brain tissues were later stained using Golgi staining techniques.
Brain samples were fixed in 4% paraformaldehyde for 1 day (24 hours). The tissue blocks were thereafter immersed in 3% potassium dichromate for 7 days in darkness. Solution was changed daily. The tissues were later immersed into 2% silver nitrate solution for 72 hours at room temperature in darkness. Before putting tissue blocks to a solution containing silver nitrate. The excess solution was absorbed by using an absorbent paper. The silver nitrate solution was changed several times until brown precipitate stopped appearing. The various brain sections were cut into distilled water using a vibratome which is 60 µm thick. They were mounted on foist plus slides and dried under normal room temperature for 10 minutes. Dehydration through 95% alcohol then 100% alcohol was ensured. Finally, the section was cleared in xylene, covered with slide and snapped.

Statistical analysis: Values were expressed as mean ± SD. All data were analyzed using one-way analysis of variance (ANOVA). The Tukey's post hoc test was carried out in order to spot inter-group differences, the comparison groups being the normal and negative controls. The statistical differences were considered at $p < 0.05$.

RESULTS

Effect of Quercetin on PTZ-induced kindling behaviour in mice: Seizure grades were analysed to know the possible anti-epileptogenic effect of quercetin in the PTZ-induced kindling model. The PTZ-treated group exhibited a significant ($P< 0.05$) increase in seizure intensity from 2nd injection to 9th injection compared to the control. However, quercetin at both doses significantly ($P<0.05$) reduced seizure intensity (stage) compared to the saline+PTZ group in 5th, 6th, 7th, 8th and 9th injections.

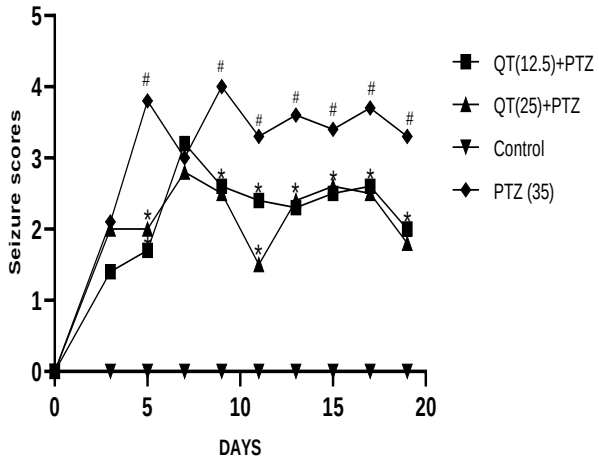

Figure 1:
Effect of quercetin pretreatment (QT 12.5 or 25 mg/kg p.o.) on the mean kindling score as assessed every other day from day1 to day15 of the study. #p < 0.05 in relation to vehicle + saline-treated group. *p < 0.05 in relation to vehicle + PTZ-treated group (group 2) (ANOVA followed by Tukey's test). Group 1: Control (vehicle); group 2: vehicle + PTZ (35 mg/kg); group 3: QT (12.5) + PTZ; group 4: QT (25) + PTZ

Effect of Quercetin on PTZ-induced central IL-12 production: The one-way ANOVA test showed significance elevation [$F (3, 20) = 20.20$, $P = 0.0001$] in brain level of IL-12 between the treated groups. Post hoc analysis further reveal that PTZ significantly ($P< 0.05$) elevated IL-12 level (Fig.c2) compared to the control (VEH). However, pretreatment with Q (12.5 mg/kg and 25 mg/kg, p.o.) significantly decreased hippocampal IL-12 levels in comparison with the PTZ-treated group (VEH + PTZ) (Fig 2).

Effect of quercetin on PTZ-induced central IFN-ɣ production: The one-way ANOVA test showed a significant difference [$F (3, 20) = 9.858$, $P=0.0003$] in the brain level of IFN-ɣ between the treated groups. Post hoc analysis further reveals that PTZ (30 mg/kg i.p.)

significantly (P< 0.05) increased IFN-ɣ level (Fig.3) compared to the control (VEH). However, pretreatment with Q (12.5 mg/kg and 25 mg/kg, p.o.) significantly decreased IFN-ɣ level in relation to the PTZ-treated group (VEH+PTZ) (Fig. 3).

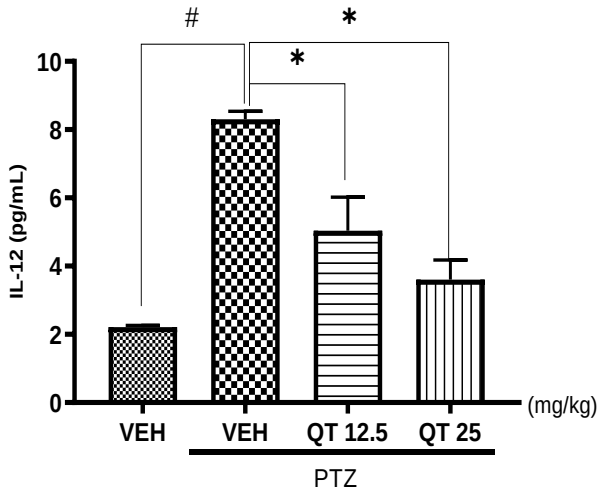

Figure 2:
Effect of quercetin on the brain level of IL-12 in rats subjected to the PTZ model of epilepsy. Data represent mean ± SD (n=6). #p < 0.05 when compared with control group (VEH); ⁎p < 0.05, when compared with PTZ control group (VEH + PTZ); one-way ANOVA with Tukey's multiple comparison

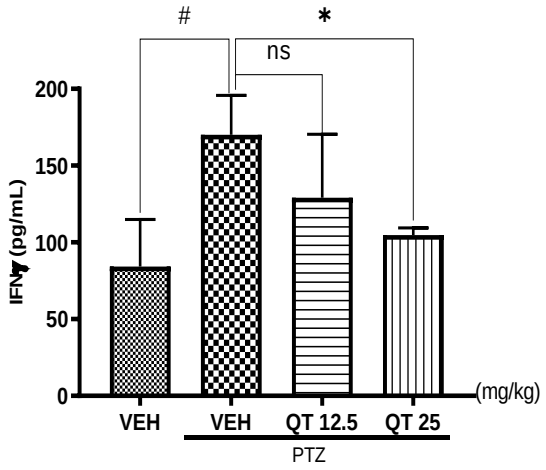

Figure 3:
Effect of quercetin on the brain level of IFN-γ in mice subjected to PTZ model of epilepsy. Data represent mean ± SD (n= 6). # p < 0.05 when compared with control group (VEH); ⁎p < 0.05, when compared with PTZ control group (VEH + PTZ); one-way ANOVA followed by Tukey's multiple comparison.

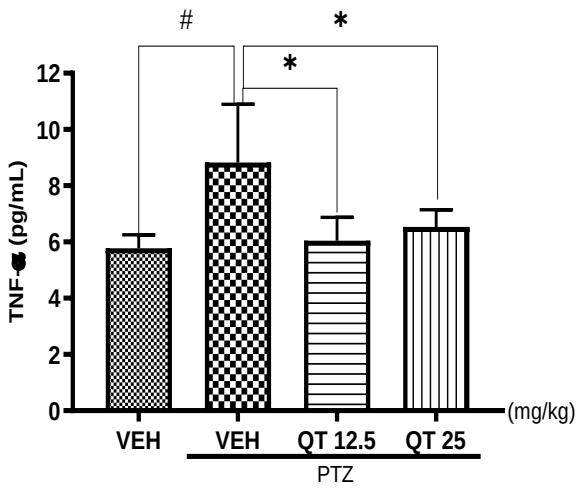

Figure 4:
Effect of quercetin on the brain level of TNF-α in mice subjected to the PTZ model of epilepsy. Data represent mean ± SD (n=5). #p < 0.05 in comparison with the control group (VEH); ⁎p < 0.05, when compared with PTZ control group (VEH + PTZ); one-way ANOVA followed by Tukey's multiple comparison.

Neuroprotective effect of the extract on PTZ-induced neuronal damage: Histology of the hippocampus CA1 revealed evident neurodegeneration of dendrite and neuronal cells in the groups exposed to PTZ. Well-defined pyramidal neurons given rise to a single apical dendrite with many terminal branches and well-arborized basal dendrites were observed in the CA1 of the control animals. The pyramidal cells and dendrites were significantly depleted in the group exposed to the PTZ group compared to the control. However, this depletion was significantly reduced by the treatment with quercetin at 12.5 mg/kg and 25 mg/kg (Plate 1) compared to the group treated with PTZ.

DISCUSSION

Epilepsy is a neurological condition affecting about 30 million people worldwide, out of which 30% of patients no longer respond to conventional medical treatment (Meng and Yao, 2020, Singh and Trevick, 2016, Laxer *et al*., 2014). Some of the features of this neurological disorder include recurrent seizures, an imbalance between inhibitory and excitatory neurotransmitters, and neuronal damage, amongst others (Rana and Musto, 2018). Recent and emerging evidence has linked the pathogenesis of epilepsy with neuroinflammation, which is connected with elevated pro-inflammatory cytokine levels, microglial activation and neurodegeneration (Rana and Musto, 2018).

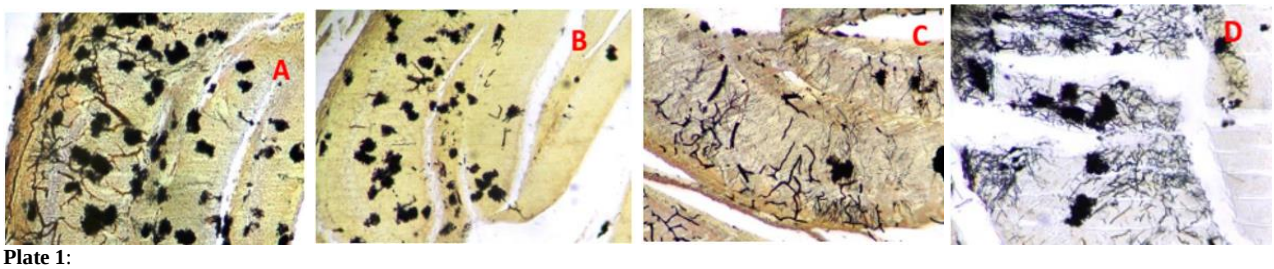

Plate 1:
Photomicrograph of a brain section stained by Golgi cox techniques showing CA1 of the PTZ-treated animals. The control group (A) shows the presence of moderate neuronal processes, while the PTZ group (B) shows depleted neuronal processes. Treatment with QT 12.5 mg/kg (C) and QT 25 mg/kg (D) prevents neuronal loss and shows the presence of mild neuronal processes. Magnification: (X100).

In this study, PTZ kindling epilepsy method was employed to evaluate the neuroprotective property of quercetin in a kindled mouse. Kindling is a chronic epilepsy model, which involves the monotonous administration of sub-convulsive doses of a convulsant resulting in seizures (Dhir, 2012, McNamara, 1984). This model has demonstrated face and construct validities in replicating and mimicking clinical epilepsy and the various psychiatric and neurological changes and symptoms associated with seizure disorders. It makes it possible to study the underlying molecular mechanisms involved in the pathogenesis of epilepsy (Shimada and Yamagata, 2018). Continuous and alternate administration of PTZ induces kindling in laboratory animals, such as rats and mice (Dhir, 2012), by blocking and suppressing GABA-mediated neurotransmission at GABAA receptors (Samokhina and Samokhin, 2018). This chronic model of epilepsy has resulted in neuronal loss and degeneration in the CA1, CA3 and dentate gyrus of the hippocampus and the amygdala (Mehla *et al*., 2010), resulting in memory impairment. Hence, it provides an avenue to study cognitive deficits associated with epilepsy (Pourmotabbed *et al*., 2011) and neuronal decline and morphological changes in the hippocampus and dentate gyrus (Samokhina and Samokhin, 2018).

The findings of this study show that repetitive administration of PTZ sub-convulsive dose consistently elevated the severity of seizures and myoclonic jerks in the PTZ-kindled mice. Conversely, treatment with quercetin significantly reduced the severity of PTZ-induced seizures and myoclonic jerks in mice. While the PTZ induced seizures have been attributed to inhibition of GABA and activation of NMDA (N-methyl-D-aspartate) receptors increasing calcium ion influx into the neurons (Akyuz *et al*., 2021) quercetin on the other hand has been reported to modulates excessive glutamate neurotransmission by acting as an NMDA antagonist, thus blocking the influx of calcium ions into the neurons and preventing abnormal neuronal excitability (Choudhary *et al*., 2011, Subash and Subramanian, 2009). In addition, flavonoids have been shown to modulate GABAA chloride ion channels because of their similar structures with benzodiazepines (Nieoczym *et al*., 2014, Choudhary *et al*., 2011). In managing temporal lobe epilepsy, GABAA receptors are crucial targets (Schipper *et al*., 2016). Therefore, the modulatory action of quercetin as a flavonoid at this receptive site may also account for its antiepileptic effect observed in this study.

There is emerging evidence of an inflammatory undertone in epilepsy pathophysiology. The high incidence of seizures in autoimmune disorders underscores the significance of inflammation in the pathophysiology of epilepsy (Dalmau *et al*., 2008, Vincent and Bien, 2008, Bien *et al*., 2007). In an animal model of seizure, chemoconvulsants like PTZ and kainic acid have been reported to increase and up-regulate pro-inflammatory cytokine via activation of microglia in the brain (Semple *et al*., 2020, Rawat *et al*., 2019, Jeon *et al*., 2008). Consistently, in this study, chronic administration of PTZ has markedly elevated the IL-12, IF-gamma and TNF-alpha levels in the brain of PTZ-treated mice. Epilepsy has been associated with increased interferon-gamma levels (Lach *et al*., 2022). Similarly, inflammatory biomarkers have reportedly been high in febrile convulsion (Dinarello, 2004). From our findings, treatment with quercetin, however, significantly reduced PTZ-induced pro-inflammatory cytokines (i.e. IL-12, TNF-α, IF-gamma). As an anti-inflammatory agent, quercetin has dramatically suppressed the levels of interleukin-12 and interferon-gamma in the brain (Akyuz *et al*., 2021). Previous studies have shown the antiepileptic property of steroids and anti-inflammatory agents in some drug-resistant epilepsies (Wheless *et al*., 2007, Wirrell *et al*., 2005, Riikonen, 2004). The TNF-alpha is a pro-inflammatory cytokine implicated in epileptogenesis, which up-regulates glutamate microglial release by increasing Alpha-amino-3-hydroxy-5-methyl-4-isoxazole propionic acid (AMPA) receptors, thus amplifying glutaminergic excitatory neurotransmission (Rana and Musto, 2018, Galic *et al*., 2012, Takeuchi *et al*., 2006). In addition, TNF alpha downregulates GABA inhibitory neurotransmission, thus triggering abnormal neuronal excitability and epileptogenesis (Rana and Musto, 2018, Stellwagen *et al*., 2005). In addition, TNF-alpha levels were elevated in PTZ-treated animals. In the study, we observed that treatment with quercetin significantly reduced the level of TNF alpha compared to the group of animals that were exposed to PTZ alone.

Furthermore, PTZ triggered the neurodegeneration of dendrites and neuronal cells in the hippocampus CA1 region and dentate gyrus of mice that were exposed to PTZ alone. Quercetin reversed the depletion of dendrites and pyramidal cells in the hippocampus CA1 region and dentate gyrus of mice. This neuroprotective mechanism of quercetin may be attributed to its antioxidant property, ability to downregulate inflammatory mediators and reduce oxidative stress (Wu *et al*., 2020, Rishitha and Muthuraman, 2018), thus protecting the brain from neurodegeneration (Sefil *et al*., 2014).

In conclusion, quercetin was able to suppress PTZ-induced seizures and significantly declined interferon-gamma and interleukin 12 brain levels. In addition, quercetin was able to reverse PTZ-induced neurodegeneration due to its anti-inflammatory, antioxidant and neuroprotective properties of quercetin. Nevertheless, a thorough understanding of the molecular patterns surrounding quercetin's antiepileptic and neuroprotective effects is vital for developing new therapeutic remedies that can ameliorate epilepsy.

Acknowledgements

The authors appreciate the technical support from the technical unit of Department of Pharmacology and Therapeutics, Afe Babalola University Ado Ekiti

REFERENCES

Ahmadian, S. R., Ghasemi-Kasman, M., Pouramir, M. & Sadeghi, F. (2019): Arbutin attenuates cognitive impairment and inflammatory response in pentylenetetrazol-induced kindling model of epilepsy. *Neuropharmacology*, 146, 117-127.

Akyuz, E., Paudel, Y. N., Polat, A. K., Dundar, H. E. & Angelopoulou, E. (2021): Enlightening the neuroprotective effect of quercetin in epilepsy: From mechanism to therapeutic opportunities. *Epilepsy & Behavior*, 115, 107701.

Amiri, S., Haj-Mirzaian, A., Amini-Khoei, H., Shirzadian, A., Rahimi-Balaei, M., Razmi, A., Bergen, H., Rastegar, M., Kordjazy, N. & Haj-Mirzaian, A. (2016): Lithium attenuates the proconvulsant effect of adolescent social isolation stress via involvement of the nitrergic system. *Epilepsy & Behavior*, 61, 6-13.

Bien, C., Urbach, H., Schramm, J., Soeder, B., Becker, A., Voltz, R., Vincent, A. & Elger, C. (2007): Limbic encephalitis as a

precipitating event in adult-onset temporal lobe epilepsy. *Neurology*, 69, 1236-1244.

Can, Ö. D. & Özkay, Ü. D. (2012): Effects of Hypericum montbretti extract on the central nervous system and involvement of GABA (A)/benzodiazepine receptors in its pharmacological activity. *Phytotherapy Research*, 26, 1695-1700.

Cerri, C., Caleo, M. & Bozzi, Y. (2017): Chemokines as new inflammatory players in the pathogenesis of epilepsy. *Epilepsy Research*, 136, 77-83.

Chakraborty, J., Singh, R., Dutta, D., Naskar, A., Rajamma, U. & Mohanakumar, K. P. (2014): Quercetin improves behavioral deficiencies, restores astrocytes and microglia, and reduces serotonin metabolism in 3-nitropropionic acid-induced rat model of Huntington's disease. *CNS neuroscience & therapeutics*, 20, 10-19.

Chen, Z., Duan, R.-S., Concha, Q. H., Wu, Q., Mix, E., Winblad, B., Ljunggren, H.-G. & Zhu, J. 2004. IL-12p35 deficiency alleviates kainic acid-induced hippocampal neurodegeneration in C57BL/6 mice. *Neurobiology of disease*, 17, 171-178.

Choi, J., Nordli, D. R., Alden, T. D., Dipatri, A., Laux, L., Kelley, K., Rosenow, J., Schuele, S. U., Rajaram, V. & Koh, S. 2009. Cellular injury and neuroinflammation in children with chronic intractable epilepsy. *Journal of neuroinflammation*, 6, 1-14.

Choudhary, N., Bijjem, K. R. V. & Kalia, A. N. 2011. Antiepileptic potential of flavonoids fraction from the leaves of Anisomeles malabarica. *Journal of Ethnopharmacology*, 135, 238-242.

Dalmau, J., Gleichman, A. J., Hughes, E. G., Rossi, J. E., Peng, X., Lai, M., Dessain, S. K., Rosenfeld, M. R., Balice-Gordon, R. & Lynch, D. R. 2008. Anti-NMDA-receptor encephalitis: case series and analysis of the effects of antibodies. *The Lancet Neurology*, 7, 1091-1098.

De Souza, A. G., Chaves Filho, A. J. M., Oliveira, J. V. S., De Souza, D. A. A., Lopes, I. S., De Carvalho, M. A. J., De Lima, K. A., Sousa, F. C. F., Vasconcelos, S. M. M. & Macedo, D. 2019. Prevention of pentylenetetrazole-induced kindling and behavioral comorbidities in mice by levetiracetam combined with the GLP-1 agonist liraglutide: involvement of brain antioxidant and BDNF upregulating properties. Biomedicine & Pharmacotherapy, 109, 429-439.

Dehkordi, H. T., Bijad, E., Saghaei, E., Korrani, M. S. & Amini-Khoei, H. 2023. Chronic stress but not acute stress decreases the seizure threshold in PTZ-induced seizure in mice: role of inflammatory response and oxidative stress. Naunyn-Schmiedeberg's Archives of Pharmacology, 396, 973-982.

Dhir, A. 2012. Pentylenetetrazol (PTZ) kindling model of epilepsy. *Current protocols in neuroscience*, 58, 9.37. 1-9.37. 12.

Dinarello, C. A. 2004. Infection, fever, and exogenous and endogenous pyrogens: some concepts have changed. *Journal of endotoxin research*, 10, 201-222.

Gales, J. M. & Prayson, R. A. 2017. Chronic inflammation in refractory hippocampal sclerosis-related temporal lobe epilepsy. *Annals of Diagnostic Pathology*, 30, 12-16.

Galic, M. A., Riazi, K. & Pittman, Q. J. 2012. Cytokines and brain excitability. *Frontiers in neuroendocrinology*, 33, 116-125.

Guo, J., Xue, C., Duan, J.-A., Qian, D., Tang, Y. & You, Y. 2011. Anticonvulsant, antidepressant-like activity of Abelmoschus manihot ethanol extract and its potential active components in vivo. *Phytomedicine*, 18, 1250-1254.

Gupta, Y., Kumar, M. V. & Srivastava, A. 2003. Effect of Centella asiatica on pentylenetetrazole-induced kindling, cognition and oxidative stress in rats. Pharmacology Biochemistry and Behavior, 74, 579-585.

Haj-Mirzaian, A., Ramezanzadeh, K., Tafazolimoghadam, A., Kazemi, K., Nikbakhsh, R., Nikbakhsh, R., Amini-Khoei, H., Afshari, K., Haddadi, N.-S. & Shakiba, S. 2019. Protective effect of minocycline on LPS-induced mitochondrial dysfunction and decreased seizure threshold through nitric oxide pathway. *European journal of pharmacology*, 858, 172446.

Jeon, G. S., Park, S. K., Park, S. W., Kim, D. W., Chung, C. K. & Cho, S. S. 2008. Glial expression of interleukin-18 and its receptor after excitotoxic damage in the mouse hippocampus. *Neurochemical research*, 33, 179-184.

Kaur, D., Pahwa, P. & Goel, R. K. 2016. Protective effect of nerolidol against pentylenetetrazol-induced kindling, oxidative stress and associated behavioral comorbidities in mice. *Neurochemical research*, 41, 2859-2867.

Kiasalari, Z., Khalili, M., Roghani, M., Heidari, H. & Azizi, Y. 2013. Antiepileptic and antioxidant effect of hydroalcoholic extract of ferula assa foetida gum on pentylentetrazole-induced kindling in male mice. *Basic and clinical neuroscience*, 4, 299.

Lach, P., Klus, W., Zajdel, K., Szeleszczuk, A., Komorowska, E., Burda, K. & Kurowski, P. 2022. Neuroinflammation in Epilepsy—Diagnostics and Therapeutic Perspectives. Current Pharmacology Reports, 8, 31-35.

Laxer, K. D., Trinka, E., Hirsch, L. J., Cendes, F., Langfitt, J., Delanty, N., Resnick, T. & Benbadis, S. R. 2014. The consequences of refractory epilepsy and its treatment. *Epilepsy & behavior*, 37, 59-70.

Li, Yao, Han, Yang, J., Chaudhry, M. T., Wang, S., Liu, H. & Yin, Y. 2016a. Quercetin, inflammation and immunity. *Nutrients*, 8, 167.

Li, X., Wang, H., Gao, Y., Li, L., Tang, C., Wen, G., Zhou, Y., Zhou, M., Mao, L. & Fan, Y. 2016b. Protective effects of quercetin on mitochondrial biogenesis in experimental traumatic brain injury via the Nrf2 signaling pathway. *PloS one*, 11, e0164237.

Malhotra, J. & Gupta, Y. K. 1997. Effect of adenosine receptor modulation on pentylenetetrazole-induced seizures in rats. *British journal of pharmacology*, 120, 282-288.

Manigauha, A. & Patel, S. 2010. Pentylenetetrazole induced convulsion in RATS. *International journal of pharma and bio sciences*, 1, 2.

Mcnamara, J. O. 1984. Kindling: an animal model of complex partial epilepsy. *Annals of Neurology: Official Journal of the American Neurological Association and the Child Neurology Society*, 16, S72-S76.

Mehla, J., Reeta, K., Gupta, P. & Gupta, Y. K. 2010. Protective effect of curcumin against seizures and cognitive impairment in a pentylenetetrazole-kindled epileptic rat model. *Life sciences*, 87, 596-603.

Meng, F. & Yao, L. 2020. The role of inflammation in epileptogenesis. *Acta Epileptologica*, 2, 1-19.

Muke, S., Kaikini, A., Peshattiwar, V., Bagle, S., Dighe, V. & Sathaye, S. 2018. Neuroprotective effect of coumarin nasal formulation: kindling model assessment of epilepsy. *Frontiers in pharmacology*, 9, 992.

Nassiri-Asl, M., Hajiali, F., Taghiloo, M., Abbasi, E., Mohseni, F. & Yousefi, F. 2016. Comparison between the effects of quercetin on seizure threshold in acute and chronic seizure models. *Toxicology and industrial health*, 32, 936-944.

Nieoczym, D., Socała, K., Raszewski, G. & Wlaź, P. 2014. Effect of quercetin and rutin in some acute seizure models in mice. *Progress in Neuro-Psychopharmacology and Biological Psychiatry*, 54, 50-58.

Pearson-Smith, J. N. & Patel, M. 2017. Metabolic dysfunction and oxidative stress in epilepsy. *International Journal of Molecular Sciences*, 18, 2365.

Pourmotabbed, A., Nedaei, S., Cheraghi, M., Moradian, S., Touhidi, A., Aeinfar, M., Seyfi, Z. & Pourmotabbed, T. 2011. Effect of prenatal pentylenetetrazol-induced kindling on learning and memory of male offspring. *Neuroscience*, 172, 205-211.

Racine, R. J. 1972. Modification of seizure activity by electrical stimulation: II. Motor seizure. *Electroencephalography and clinical neurophysiology*, 32, 281-294.

Rana, A. & Musto, A. E. 2018. The role of inflammation in the development of epilepsy. *Journal of neuroinflammation*, 15, 1-12.

Rawat, C., Kukal, S., Dahiya, U. R. & Kukreti, R. 2019. Cyclooxygenase-2 (COX-2) inhibitors: future therapeutic strategies for epilepsy management. *Journal of neuroinflammation*, 16, 1-15.

RIAZI, K., GALIC, M. A. & PITTMAN, Q. J. 2010. Contributions of peripheral inflammation to seizure susceptibility: cytokines and brain excitability. *Epilepsy research*, 89, 34-42.

Riikonen, R. 2004. Topical review: infantile spasms: therapy and outcome. *Journal of child neurology*, 19, 401-404.

Rishitha, N. & Muthuraman, A. 2018. Therapeutic evaluation of solid lipid nanoparticle of quercetin in pentylenetetrazole induced cognitive impairment of zebrafish. *Life sciences*, 199, 80-87.

Salgado, P. R. R., Da Fonsêca, D. V., De Melo, C. G. F., Leite, F. C., Alves, A. F., Ferreira, P. B., Piuvezam, M. R., De Sousa, D. P. & De Almeida, R. N. 2018. Comparison of behavioral, neuroprotective, and proinflammatory cytokine modulating effects exercised by (+)-cis-EC and (−)-cis-EC stereoisomers in a PTZ-induced kindling test in mice. *Fundamental & Clinical Pharmacology*, 32, 507-515.

Samokhina, E. & Samokhin, A. 2018. Neuropathological profile of the pentylenetetrazol (PTZ) kindling model. *International Journal of Neuroscience*, 128, 1086-1096.

Sankaraneni, R. & Lachhwani, D. 2015. Antiepileptic drugs—a review. *Pediatric annals*, 44, e36-e42.

Schipper, S., Aalbers, M., Rijkers, K., Swijsen, A., Rigo, J., Hoogland, G. & Vles, J. 2016. Tonic GABAA receptors as potential target for the treatment of temporal lobe epilepsy. *Molecular neurobiology*, 53, 5252-5265.

Sefil, F., Kahraman, I., Dokuyucu, R., Gokce, H., Ozturk, A., Tutuk, O., Aydin, M., Ozkan, U. & Pinar, N. 2014. Ameliorating effect of quercetin on acute pentylenetetrazole induced seizures in rats. *International Journal of Clinical and Experimental Medicine*, 7, 2471.

Semple, B. D., Dill, L. K. & O'brien, T. J. 2020. Immune challenges and seizures: how do early life insults influence epileptogenesis? *Frontiers in Pharmacology*, 11, 2.

Shimada, T., Takemiya, T., Sugiura, H. & Yamagata, K. 2014. Role of inflammatory mediators in the pathogenesis of epilepsy. *Mediators of inflammation*, 2014.

Shimada, T. & Yamagata, K. 2018. Pentylenetetrazole-induced kindling mouse model. JoVE (Journal of Visualized Experiments), e56573.

Singh, A. & Trevick, S. 2016. The epidemiology of global epilepsy. *Neurologic clinics*, 34, 837-847.

Stellwagen, D., Beattie, E. C., Seo, J. Y. & Malenka, R. C. 2005. Differential regulation of AMPA receptor and GABA receptor trafficking by tumor necrosis factor-α. *Journal of Neuroscience*, 25, 3219-3228.

Subash, S. & Subramanian, P. 2009. Morin a flavonoid exerts antioxidant potential in chronic hyperammonemic rats: a biochemical and histopathological study. *Molecular and cellular biochemistry*, 327, 153-161.

Taiwe, G. S., Tchoya, T. B., Menanga, J. R., Dabole, B. & De Waard, M. 2016. Anticonvulsant activity of an active fraction extracted from Crinum jagus L.(Amaryllidaceae), and its possible effects on fully kindled seizures, depression-like behaviour and oxidative stress in experimental rodent models. *Journal of ethnopharmacology*, 194, 421-433.

Takeuchi, H., Jin, S., Wang, J., Zhang, G., Kawanokuchi, J., Kuno, R., Sonobe, Y., Mizuno, T. & Suzumura, A. 2006. Tumor necrosis factor-α induces neurotoxicity via glutamate release from hemichannels of activated microglia in an autocrine manner. *Journal of Biological Chemistry*, 281, 21362-21368.

Tavakoli, Z., Dehkordi, H. T., Lorigooini, Z., Rahimi-Madiseh, M., Korani, M. S. & Amini-Khoei, H. 2023. Anticonvulsant effect of quercetin in pentylenetetrazole (PTZ)-induced seizures in male mice: The role of anti-neuroinflammatory and anti-oxidative stress. *International Immunopharmacology*, 116, 109772.

Thompson, C., Gary, D., Mattson, M., Mackenzie, A. & Robertson, G. S. 2004. Kainic acid-induced naip expression in the hippocampus is blocked in mice lacking TNF receptors. *Molecular brain research*, 123, 126-131.

Vezzani, A. & Baram, T. Z. 2007. New roles for interleukin-1 Beta in the mechanisms of epilepsy. *Epilepsy currents*, 7, 45-50.

Vezzani, A., French, J., Bartfai, T. & Baram, T. Z. 2011. The role of inflammation in epilepsy. *Nature reviews neurology*, 7, 31-40.

Vincent, A. & Bien, C. G. 2008. Anti-NMDA-receptor encephalitis: a cause of psychiatric, seizure, and movement disorders in young adults. *The Lancet Neurology*, 7, 1074-1075.

Watanabe, M., Miyai, A., Danjo, S., Nakamura, Y. & Itoh, K. 2013. The threshold of pentylenetetrazole-induced convulsive seizures, but not that of nonconvulsive seizures, is controlled by the nitric oxide levels in murine brains. *Experimental neurology*, 247, 645-652.

Wheless, J. W., Clarke, D. F., Arzimanoglou, A. & Carpenter, D. 2007. Treatment of pediatric epilepsy: European expert opinion, 2007. *Epileptic disorders*, 9, 353-412.

Wirrell, E., Farrell, K. & Whiting, S. 2005. The epileptic encephalopathies of infancy and childhood. *Canadian journal of neurological sciences*, 32, 409-418.

Wu, D., Zheng, Z., Fan, S., Wen, X., Han, X., Wang, S., Wang, Y., Zhang, Z., Shan, Q. & Li, M. 2020. Ameliorating effect of quercetin on epilepsy by inhibition of inflammation in glial cells. *Experimental and Therapeutic Medicine*, 20, 854-859.

Zheng, J., Wu, J., Chen, J., Liu, J., Lu, Y., Huang, C., Hu, G., Wang, X. & Zeng, Y. 2016. Therapeutic effects of quercetin on early inflammation in hypertriglyceridemia-related acute pancreatitis and its mechanism. P*ancreatology*, 16, 200-210.

Niger. J. Physiol. Sci. 38 (December 2023): 195 – 200
www.njps.physiologicalsociety.com

Niger. J. Physiol. Sci.

Full length Research Article

Effect of Acute Caffeine Exposure on Blood Glucose and Hepatic Glycogen Content in Normal and Thyroidectomized Male Wistar Rats

***Shittu S.T., Ogiogio H.A., Isehunwa G.O. and Alada A.R.A**

Endocrinology and Metabolism Unit, Department of Physiology, University of Ibadan. Ibadan, Nigeria

Summary: Acute caffeine exposure had been shown to induce hyperglycemia however; the influence of thyroid hormones on the caffeine-induced hyperglycemia is yet to be established. The present study was therefore designed to investigate the effect of caffeine exposure on blood glucose and hepatic glycogen content in thyroidectomized rats. Sixty adult male Wistar rats were randomly divided into 10 groups as I-X (n=6). Rats in groups I, III, V, VII and IX were given normal saline, caffeine, prazosin + caffeine, propranolol +caffeine, combined prazosin+ propranolol+caffeine injections respectively while rats in groups II, IV, VI, VIII and X were thyroidectomized and treated in similar manner as the normal rats respectively. Surgical removal of the thyroid gland was done in the thyroidectomised groups while sham-operation was done in Normal group to serve as control. After healing and following an overnight fast, the rats were anaesthetized and the femoral vein and carotid artery were cannulated for drug administration and blood glucose measurement respectively. After stabilization, following basal measurements, rats from each group were injected normal saline or caffeine (6mg/kg) while another sets were pre-treated prazosin (0.2 mg/kg), propanolol (0.5 mg/kg) or their combination before caffeine administration. Blood glucose was then monitored for 60 minutes post-injection of caffeine at 5 minutes interval. Liver samples were collected at the end of the observation period for glycogen content determination. Caffeine caused significant increased blood glucose levels in both normal and thyroidectomized rats which were up to 210% and 180% respectively at the peak of their responses. Liver glycogen content of the thyroidectomized rats (3.11 ± 0.20 mg/100g tissue weight) was significantly higher than the normal rats (1.91 ± 0.43 mg/100g tissue weight). These glycogen contents were significantly reduced by caffeine in both normal (0.25 ± 0.04 mg/100g tissue weight) and thyroidectomized rats (1.65 ± 0.16 mg/100g tissue weight) when compared with their controls. The caffeine effects on blood glucose and hepatic glycogen content were abolished by pretreatment with propanolol or a combination of prazosin and propanolol pretreatment in both normal and thyroidectomized rats but pretreatment with prazosin caused only significant reduction in hyperglycemic response to caffeine. The findings of this study suggest that caffeine-induced hyperglycemia in both normal and thyroidectomized rats are mediated through both alpha and beta adrenoceptors.

Keywords*: Caffeine, Hyperglycemia, Hepatic glycogen, Hypothyroid, Rat*

**Authors for correspondence: st.shittu@ui.edu.ng , Tel: +2348052644680*

Manuscript received- September 2023; Accepted: November 2023

DOI: https://doi.org/10.54548/njps.v38i2.8

INTRODUCTION

Caffeine is a mildly psycho-active commonly consumed substance with an average daily intake of approximately 300 mg from dietary sources such as coffee, tea, soft drinks, chocolate and energy drinks (Shi *et al*., 2016). It is also contained in kola nut, a common masticatory in West Africa (Salahdeen *et al*., 2015). Consumption above 600 mg per day may be addictive and negatively impact the body (Czarniecka-Skubina *et al*., 2021). In fact, consumption of coffee, the major source of caffeine in excess of 5 cups per day has been shown to be a risk factor for several diseases and mortality (Grosso *et al*., 2016; Park *et al*., 2017; Loftfield *et al*., 2018; Abe *et al*., 2019).

Acute exposure to caffeine increased blood glucose, hampered insulin sensitivity, induced adrenaline and cortisol stimulated hepatic glucose production and reduced glucose uptake and utilization by peripheral tissues (Dekker *et al*., 2007; Salahdeen and Alada, 2009; Alagbonsi *et al*., 2016; Shi *et al*., 2016; Reis *et al*., 2018). Physiologically, increased blood glucose is channeled into increased glucose utilization and storage as glycogen. Glycogen, a multi-branched polysaccharide of glucose is stored primarily in the liver to modulate blood glucose between prandial states; it is stored during hyperglycemia and mobilized during hypoglycemia through the activities of glycogen synthase and glycogen phosphorylase, respectively (Han *et al*., 2016). These enzymes, involved in glycogen metabolism have been shown to be influenced by hormones of the thyroid gland (Chu *et al*., 1985; Bollen and Stalmans, 1988).

Thyroid hormones regulate energy metabolism and metabolic processes essential for normal growth and development therefore, their status correlates with body weight and energy expenditure, thus hyperthyroidism is associated with hypermetabolic state characterized by increased basal energy expenditure while hypothyroidism is characterized by declined resting energy expenditure (Mullur *et al*., 2014). Basically, they influence key metabolic pathways that regulate energy storage and expenditure. For instance, they promote insulin secretion and glucose uptake in the gastrointestinal tract, liver, skeletal muscles, and adipose tissue with differences in the manifestation of their effect across the different tissues (Nishi, 2018) therefore their absence may inhibit glucose uptake by these tissues.

Data on the effect of acute caffeine-induced high blood glucose on hepatic glycogen content are lacking and the likely impact of thyroid hormone on the acute effect is yet to be elucidated. The present study was therefore designed to investigate the effect of acute caffeine exposure on hepatic glycogen content in thyroidectomized male Wistar rats. The involvement of the adrenergic receptor was also examined.

MATERIALS AND METHODS

Adult male Wistar rats, fasted for 12 hours were used for this study. They were anesthetized by intraperitoneal injection of 50 mg/kg Sodium thiopental (Roche®, Germany) and firmly secured on a dissecting board to exposed the carotid artery and femoral vein. Cannulas, previously flushed with heparinized saline (100 IU/mL), were inserted into these blood vessels for blood sampling and drug administration, respectively. To ensure unobstructed airflow, the trachea was intubated, and sodium heparin, 300 IU per/kg body weight was administered intravenously to prevent blood clotting. Following the surgical procedures, a stabilization period of approximately 30 minutes to one hour was observed. The drugs of interest (caffeine 6mg/kg, prazosin 0.2mg/kg, propranolol 0.5mg/kg) were injected through the femoral vein, while blood samples were collected from the carotid artery for glucose measurements in each group.

Group I (Control): These rats were given a bolus injection of normal saline through the femoral vein, and blood samples were collected from the carotid artery at specific time intervals of 5min, 10min, 15min, 30min, 45min, and 60min post injection for glucose measurement.
Group II (Control-Thyroidectomized): Similar to Group I, these rats underwent thyroidectomy and received a bolus injection of normal saline. Blood samples were collected as in Group I.
Group III (Caffeine): Rats in this group were given a bolus injection of caffeine dissolved in normal saline. Blood samples were collected as in Groups I and II.
Group IV (Caffeine - thyroidectomized): Similar to Group III, these rats underwent thyroidectomy and received a bolus injection of caffeine. Blood samples were collected as in Groups I and II.
Group V (Prazosin + Caffeine): Rats in this group were first injected with prazosin dissolved in acidified water, followed by a basal blood glucose measurement. Then, they received a bolus injection of caffeine. Blood samples were collected as in Groups I and II.
Group VI (Prazosin + Caffeine - thyroidectomized): Similar to Group V, these rats underwent thyroidectomy and received prazosin followed by caffeine. Blood samples were collected as in Groups I and II.
Group VII (Propranolol + Caffeine): Rats in this group were first injected with propranolol dissolved in normal saline, followed by a basal blood glucose measurement. Then, they received a bolus injection of caffeine. Blood samples were collected as in Groups I and II.
Group VIII (Propranolol + Caffeine - thyroidectomized): Similar to Group VII, these rats underwent thyroidectomy and received propranolol followed by caffeine. Blood samples were collected as in Groups I and II.
Group IX (Prazosin + Propranolol + Caffeine): Rats in this group were first injected with prazosin and propranolol, followed by a basal blood glucose measurement. Then, they received a bolus injection of caffeine. Blood samples were collected as in Groups I and II.
Group X (Prazosin + Propranolol + Caffeine - thyroidectomized): Similar to Group IX, these rats underwent thyroidectomy and received prazosin, propranolol, and caffeine. Blood samples were collected as in Groups I and II.
In each group, the basal blood glucose levels were measured before the respective injections, and subsequent blood samples were collected at 5min, 10min, 15min, 30min, 45min, and 60min post injection of drugs to assess the effects of the given treatments on blood glucose levels.

Procedure for thyroidectomy: Total thyroidectomy was carried out as described by Jin and Sugitani (2021). Briefly, anaesthetized [100 mg/kg Ketamine, i.p. (Ketanir®, Aculife Healthcare Pvt Ltd, India) and 5 mg/kg Xylazine, i.m. (Xylased®, Bioveta, Czech Republic)] rat was firmly secured on a dissecting board, the neck regions was shaved and a longitudinal incision (2.0-2.5 cm) of the neck skin and subcutaneous connective tissue was made. The sternohyoid muscle of the trachea was bluntly separated along the mid line to expose the white trachea and the thyroid glands, which appeared reddish-brown and were attached to the thyroid cartilage on both sides. By ligating the superior thyroid arteries and cutting the thyroid isthmus, one side of the thyroid gland was carefully separated from the trachea, allowing visualization of the recurrent laryngeal nerve running between them. The nerve was cautiously stripped, and one side of the thyroid gland and the isthmus were resected. The same procedure was then repeated on the other side until all thyroid tissue below the thyroid cartilage was removed. Throughout the surgery, measures were taken to prevent bleeding, and any bleeding that occurred was promptly addressed using sterile cotton swabs or gauze. After confirming no further bleeding, the clamp in the neck was removed, and the sternohyoid muscle of the trachea was reset. The incision was sutured layer by layer using catgut, a type of absorbable suture. The site of the suture was covered with penicillin (DBT fortified Procaine Penicillin®, Azhui Chengshi Pharmaceutical Co. Ltd, China) for disinfection and the animals were kept in a warm and well illuminated environment until recovery.

Blood glucose measurement: The blood glucose level was determined using an ACCU-CHEK glucometer ® which is based on the glucose-oxidase method (Trinder, 1969). Test strips were inserted into the glucometer, and small blood sample (approximately 0.05 ml) was applied to the test spot. Within seconds, the glucometer displayed the blood glucose value. Previous studies have shown a high correlation between this method and standard laboratory methods for blood glucose measurement.

Determination of liver glycogen content: After blood glucose monitoring, the liver was quickly removed from each animal 60 minutes after injection under anesthesia. Adherent tissues and blood were removed, and the liver was weighed. A separate one-gram sample of the liver was taken to determine its glycogen content using the anthrone reagents method (Seifter *et al.*, 1950; Jermyn, 1975).

Isolation and purification of glycogen: 1 g of the liver was placed in pre-heated Erlnmeyer flasks containing 10 ml of 30% KOH solution. The liver was digested by heating the flasks for 20 min over light flame with occasional shaking until the tissues dissolved. The solution was allowed to cool. Then, 4 ml of the aliquot from the flasks was taken and placed in a 15 ml centrifuge tube. 5 ml of 95% ethanol was added to the sample, mixed and centrifuged for 5 min; it was then decanted and drained for 5 min. The glycogen precipitated from each sample was dissolved in 0.5 ml distilled water and mixed thoroughly. This was reprecipitated with 5 ml of 95% ethanol and recovered by centrifugation. The centrifugation was repeated four times until a white precipitate was obtained. The final glycogen precipitate was dissolved in 0.5 ml of distilled water. 0.5 ml aliquot was taken from the unknown glycogen solution obtained from above. Then, 0.5 ml of concentrated HCl, followed by 0.5 ml formic acid (88%) and 4 ml of anthrone reagent were added in a stepwise manner. The anthrone reagent was added slowly and mixed thoroughly. 0.5 ml of distilled water was treated as above and used as a blank. Several dilutions of the glycogen standard (0.2 mg/ml) were prepared. The dilutions used were 0.1, 0.2, 0.3, 0.4 ml of standard glycogen solution with enough distilled water to make 0.5 ml. These dilutions of glycogen standard were then treated as above. A standard curve was prepared from this.

All the tubes containing the solutions were heated in boiling water for ten minutes and allowed to cool. A portion of the contents from each tube was poured into a cuvette, bubbles were allowed to disperse and the absorbance was read. The absorbance was read at 630 nm against the blank. Calculation of glycogen was done using Equation 1:

Mg glycogen/100g fresh liver =
Mg glycogen/ml × 10/4 × 2/0.5 × 100/total liver weight

Statistical analysis:
All values were Mean ± S.E.M of the variables measured. Values between two groups were compared using student t-test while analysis of variance (ANOVA) was used to compare mean values in multiple groups. P-values≤0.05was taken as statistical significant.

RESULTS

Effect of Thyroidectomy on serum thyroid hormones in male Wistar rats: The effect of thyroidectomy on circulating thyroid hormone is shown in figure 1, significant reductions were observed in both triiodothyronine (24.45 ± 1.26 Vs 36.55 ± 1.43 pg/ml) and thyroxine (49.28 ± 2.63 Vs 107.6 ± 2.62 pg/ml) in the thyroidectomized rats when compared with the normal rats.

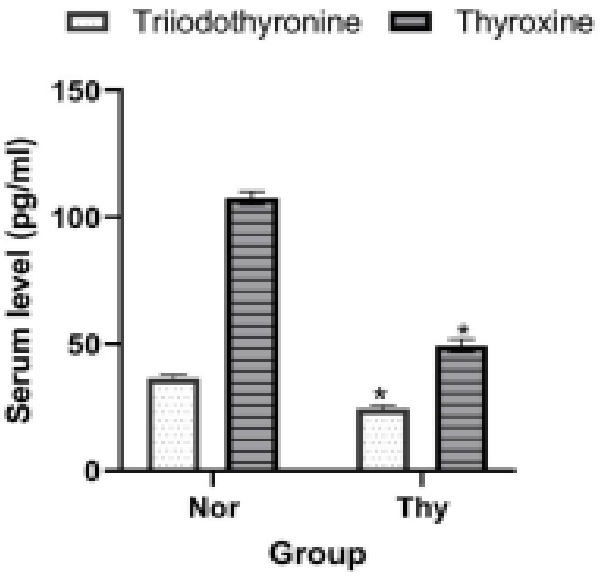

Figure 1:
Effect of thyroidectomy on serum triiodothyronine and thyroxine level in male Wistar rats. *P<0.05 Vs Normal. Nor – Normal, Thy -thyroidectomized

Effect of caffeine on blood glucose in normal and thyroidectomized male Wistar rats: Caffeine caused a significant increase in the blood glucose of both the normal and thyroidectomized rats which was sustained throughout the 60 minutes observation period. The increased blood glucose produced by caffeine in the normal and thyroidectomized rats was however significantly different, for instance, at the peak of their responses, caffeine caused 210 % increase in blood glucose in normal rats while it caused 180 % increase in the thyroidectomized rats (figure 2).

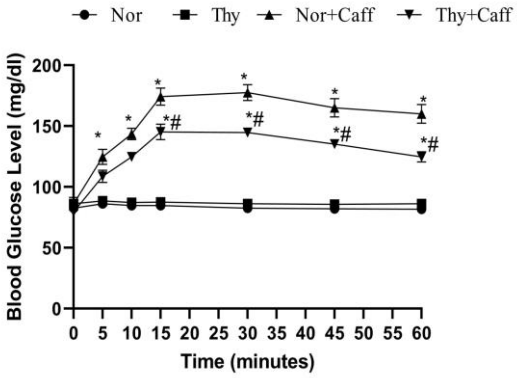

Figure 2:
Effect of caffeine on blood glucose level in normal and thyroidectomized male Wistar rats. *P<0.05 Vs Normal, #P<0.05 Vs Thyroidectomized. Nor – Normal, Thy – thyroidectomized, Nor+Caff – Normal+Caffeine, Thy+Caff – Thyroidectomised+ Caffeine

Effect of adrenergic blockers on caffeine-induced high blood glucose in normal and thyroidectomized male Wistar rats: As shown in figure 3, pretreatment with alpha or beta adrenergic blocker caused significant reduction in the increased blood glucose produced by caffeine in normal (fig 3A) and thyroidectomized (fig 3B) rats. The effect was however abolished when the rats were pretreated with a combination of the 2 adrenergic receptor blockers.

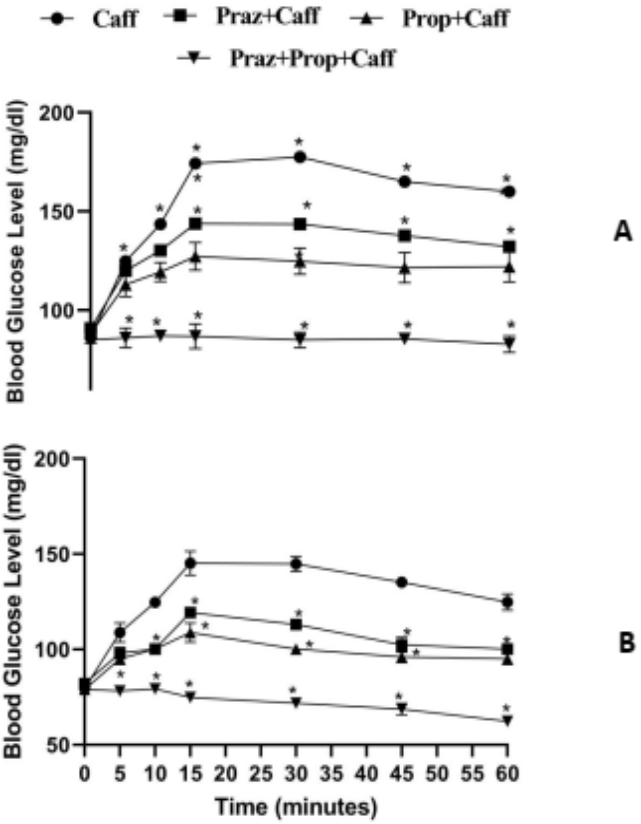

Figure 3:
Effect of adrenergic blockers on caffeine-induced increase blood glucose in (A) normal and (B) thyroidectomized rats. *P<0.05 Vs Caffeine. Caff – Caffeine,
Praz+Caff –Prazosin + Caffeine,
Prop+Caff –Propanolol+Caffeine,
Praz+Prop+Caff – Prazosin+ Propanolol+Caffeine

Effect of caffeine on liver glycogen content in normal and thyroidectomized male Wistar rats: Liver glycogen content of the thyroidectomized rats (3.11 ± 0.20 mg/100g tissue weight) was significantly higher than the normal rats (1.91 ± 0.43 mg/100g tissue weight). These glycogen contents were significantly reduced by caffeine in both normal (0.25 ± 0.04 mg/100g tissue weight) and thyroidectomized rats (1.65 ± 0.16 mg/100g tissue weight) when compared with their respective controls. While pretreatment with prazosin had no effect on the caffeine-induced glycogen depletion, the effect was abolished by propanolol and a combination of prazosin and propanolol, figure 4.

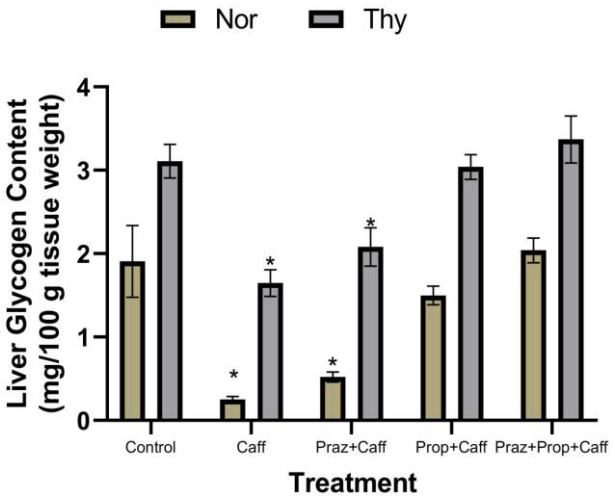

Figure 4:
Effect of caffeine on liver glycogen contents in normal and thyroidectomized male Wistar rats. *P<0.05 Vs Control.

DISCUSSION

The role of thyroid hormones on the effect of acute caffeine exposure on blood glucose and hepatic glycogen was examined. Thyroidectomy caused significant decrease in circulating thyroxine and triiodothyronine level in this study. These decreased hormonal levels are consistence with the levels reported in the method adopted in this study (Jin and Sugitani *et al*., 2021). Caffeine caused significant increased blood glucose level in normal and thyroidectomized rats of this study. This effect is in consonance with the well documented effect of acute caffeine exposure (Oyebola and Alada, 1993; Dekker *et al*., 2007; Salahdeen and Alada, 2009; Alagbonsi *et al*., 2016; Shi *et al*., 2016; Reis *et al*., 2018) on blood glucose in normal rats. Caffeine increases blood glucose through its stimulation of adrenal gland release of adrenaline (Battram *et al*., 2005), hence studies have linked acute caffeine consumption, increased plasma adrenaline and decreased insulin sensitivity (Dekker *et al*., 2007). Caffeine acts directly on the adrenal medulla by stimulating the caffeine-sensitive calcium ion store (Usachev *et al*., 1993) which is coupled with exocytotic release of stored adrenaline by the chromaffin cells of the adrenal medulla (García *et al*., 2006). The increased adrenaline mediates increase blood glucose by promoting hepatic glycogenolysis and gluconeogenesis while it inhibits insulin-dependent glucose disposal (Sherwin and Saccà, 1984). Several studies have documented that intracellular calcium mobilization is dependent on thyroid hormone (Dho *et al*., 1989; Marino *et al*., 2006) and thyroidectomy had been shown to suppress intracellular calcium release (Amadi *et al*., 2005), it conceivable that caffeine-mediated calcium release which is associated with increased adrenaline release will be hindered in the thyroidectomized rats, it is therefore not surprising that caffeine-elicited increase blood glucose was reduced from 210 % to 180 % in the thyroidectomized rats of this study.

The lack of total abolishment of the caffeine-induced increased blood glucose in the thyroidectomized rats of the current study may be linked with the interaction of caffeine

with adenosine receptor, caffeine is a potent non-selective adenosine receptor antagonist and exerts most of its biological activities by blocking all types of adenosine receptors (Ribeiro and Sebastião, 2010). Agonist of adenosine receptors have been shown to decrease blood glucose and their blockade increases blood glucose (Alagbonsi *et al*., 2016) therefore, caffeine may utilize the adenosine receptor blockade pathway independently of its direct stimulation of adrenaline release to increase blood glucose level. Earlier reports have shown that adenosine receptor expression is greatly increased in hypothyroid rats (Baños *et al*., 2002) thus, their blood glucose lowering effect may be effectively blocked by caffeine administration in the thyroidectomized rats hence providing additional pathway for caffeine induction of high blood glucose level in the thyroidectomized rats.

The significant depletion in hepatic glycogen content induced by caffeine in normal and thyroidectomized rats in this study is consistent with the effect of caffeine on hepatic glycogen content reported by Martin *et al*. (2004). Although, the effect of caffeine on hepatic glycogen is conflicting, some studies have reported that it inhibits glycogenolysis by competitive binding of glycogen phosphorylase a (Ercan-Fang and Nuttall, 1997; Tsitsanou *et al*., 2000) while others reported that it potentiates glycogenolysis secondary to its stimulation of adrenaline release (Knapik *et al*., 1983; García *et al*., 2006). These conflicting reports appear to be settled by the findings of Jarrar and Obeid (2014) that the time of caffeine administration determines if it will be glycogenolytic or glycogen-sparing. Administration of caffeine to fasted animals 1 hour before meal ingestion caused significant glycogenolysis while co-administration with meal or 1 hour after meal shifted the effect to glycogen-sparing (Jarrar and Obeid, 2014), the glycogenolytic effect of caffeine observed in the current study is in tandem with their former observation given that caffeine was administered to fasted animals. In addition to the glycogenolytic effect of adrenaline secondary to caffeine stimulation, the antagonistic effects of caffeine on adenosine receptors could synergistically activate glycogenolysis (Davis *et al*., 2003). Hence, the observed glycogen depletion in the thyroidectomized rats of this study may not be surprising given that blockade of adenosine receptors by caffeine stimulates glycogen depletion (Davis *et al*., 2003) and hypothyroidism in rats is associated with increased expression of adenosine receptor (Baños *et al*., 2002) thereby providing more binding sites to be blocked in the thyroidectomized rats. It is worth noting that, glycogen content of the thyroidectomized rats was significantly higher than the normal rats, this aligns with the association of hypothyroidism with decreased gluconeogenesis and glycogenolysis resulting in increased hepatic glycogen content (Storm *et al*., 1984; Chakrabarti *et al*., 2007) as well as reduction in glycogen phosphorylase activity secondary to reduced responsiveness to adrenergic stimulation in the thyroidectomized rats (Chu *et al*., 1985).

The abolishment of the caffeine-induced increased blood glucose and hepatic glycogen depletion observed in this study underscores the role of adrenergic receptors in mediating the caffeine effect and the postulation that induction of adrenaline release is a primary mechanism by which caffeine mediates its effect on glucose metabolism. In conclusion, caffeine elicits hyperglycemic and glycogenolytic effects in both normal and thyroidectomized rats through mechanism that involves adrenergic stimulation.

REFERENCES

Abe S.K., Saito E., Sawada N., Tsugane S., Ito H., Lin Y., Tamakoshi A., Sado J., Kitamura Y., Sugawara Y., et al. (2019). Coffee consumption and mortality in Japanese men and women: A pooled analysis of eight population-based cohort studies in Japan (Japan Cohort Consortium). Preventive Medicine, 123:270–277

Alagbonsi, A.I., Salman, T.M., Salahdeen, H.M. and Alada, A.A. (2016).

Effects of adenosine and caffeine on blood glucose levels in rats. Niger J

Exp Clin Biosci 4:35-41.

Amadi, K., Sabo, M.A,, Adelaiye, A.B. and Sagay, A.S. (2005). Dependence of calcium on thyroid hormone for the regulation of cellular functions. Nigerian Journal of Physiological Sciences. 20(1-2):95-100.

Baños, G., Martínez, F., Grimaldo, J. I. and Franco, M. (2002). Adenosine participates in regulation of smooth muscle relaxation in aortas from rats with experimental hypothyroidism. Canadian Journal of Physiology and Pharmacology, 80(6): 507-514.

Battram, D.S., Graham, T.E., Richter, E.A. and Dela, F. (2005). The effect of caffeine on glucose kinetics in humans – influence of adrenaline. Journal of Physiology, 569, 347–355.

Bollen, M. and Stalmans, W. (1988). The effect of the thyroid status on the activation of glycogen synthase in liver cells. Endocrinology, 122(6):2915-9.

Chakrabarti, S., Guria, S., Samanta, I. and Das, M. (2007). Thyroid dysfunction modulates glucoregulatory mechanism in rat. Indian Journal of Experimental Biology, 45, 549-553

Chu, D.T., Shikamat, H., Khatra, B.S. and Exton, J.H. (1985). Effects of Altered Thyroid Status on & Adrenergic Actions on Skeletal Muscle Glycogen Metabolism. Journal of Biological Chemistry, 260(18), 9994-1000.

Czarniecka-Skubina, E., Pielak, M., Sałek, P., Korzeniowska-Ginter, R. and Owczarek, T. (2021). Consumer Choices and Habits Related to Coffee Consumption by Poles. International Journal of Environmental Research and Public Health, 18(8):3948.

Davis, J.M., Zhao, Z., Stock, H.S., Mehl, K.A., Buggy, J. and Hand, G.A. (2003). Central nervous system effects of caffeine and adenosine on fatigue. American Journal of Physiology Regulation Integration and Comparative physiology, 284, R399-R404.

Dekker, M., Gusba, J., Robinson, L., and Graham, T (2007). Glucose homeostasis remains altered by acute caffeine ingestion following 2 weeks of daily caffeine consumption in previously non-caffeine-consuming males. British Journal of Nutrition, 98(3), 556-562.

Dho, S., Ansah, T.A. and Case, R.M (1989). Influence of thyroid status on Ca2+ mobilization and amylase secretion in rat pancreatic acini. Cell Calcium, 10(8), 551-560.

Ercan-Fang, N, and Nuttall, F.Q. (1997). The effect of caffeine and caffeine analogs on rat liver phosphorylase-a activity. Journal of Pharmacology, 280:1312–8.

García, A.G., García-De-Diego, A.M., Gandía, L., Borges, R., and García-Sancho, J. (2006). Calcium signaling and exocytosis in adrenal chromaffin cells. Physiological Review, 86(4):1093-131.

Grosso, G., Micek, A., Godos, J., Sciacca, S., Pajak, A., Martínez-González, M.A., Giovannucci, E.L. and Galvano, F. (2016). Coffee con-sumption and risk of all-cause, cardiovascular, and cancer mortality in smokers and non-smokers: A dose-response

me-ta-analysis. European Journal of Epidemiology, 31:1191–1205.

Han, H.S., Kang, G., Kim, J., Choi, B. and Koo, S. (2016). Regulation of glucose metabolism from a liver-centric perspective. Experimental and Molecular Medicine, 48, e218.

Jarrar, S.F. and Obeid, O.A. (2014).Timing of caffeine ingestion alters postprandial metabolism in rats. Nutrition, 30(1): 107-111.

Jermyn, M.A. (1975). Increasing the sensitivity of the anthrone method for carbohydrate. Analytical Biochemistry 68, 322-335.

Jin, S. and Sugitani, I. (2021). TSH Suppression was induced in rat model after total thyroidectomy. Journal of Nippon Medical School 88: 311-318

Knapik, J.J., Jones, B.H., Toner, M.M., Daniels, W.L. and Evans, W.J. (1983) Influence of caffeine on serum substrate changes during running in trained and untrained individuals. Biochemistry of Exercise, 13:514–519.

Loftfield, E., Cornelis, M.C., Caporaso, N., Yu, K., Sinha, R., Freedman N. (2018). Association of coffee drinking with mortality by genetic variation in caffeine metabolism: Findings from the UK biobank. JAMA Internal Medicine, 178:1086–1097.

Marino, F., Guasti, L., Cosentino, M., De Piazza, D., Simoni, C., Bianchi, V., Piantanida, E., Saporiti, F., Cimpanelli, M.G., Crespi, C., Vanoli, P., De Palma, D., Klersy, C., Frigo, G.M., Bartalena, L., Venco, A., Lecchini, S. (2006). Thyroid hormone and thyrotropin regulate intracellular free calcium concentrations in human polymorphonuclear leukocytes: In vivo and in vitro studies 2006 International Journal of Immunopathology and Pharmacology, 19(1), 149-160.

Martin, J.V., Nolan, B., Wagner, G.C. and Fisher, H. (2004). Effects of dietary caffeine and alcohol on Liver carbohydrate and fat metabolism in rats. Medical Science Monitor, 10(12):BR455-61.

Mullur, R., Liu, Y.Y. and Brent, G.A. (2014). Thyroid hormone regulation of metabolism. Physiol Rev. 94(2):355-382.

Nishi, M. (2018). Diabetes mellitus and thyroid diseases. Diabetol International, 9:108–12.

Park, S.Y., Freedman, N.D., Haiman, C.A., Le Marchand, L., Wilkens, L.R., Setiawan, V.W. (2017) Association of coffee consumption with total and cause-specific mortality among nonwhite populations. Annals of Internal Medicine, 167:228–235.

Reis, C.E.G., Dórea, J.G., da Costa, T.H.M. (2018). Effects of coffee consumption on glucose metabolism: A systematic review of clinical trials. Journal of Traditional Complement Medicine, 9(3):184-191.

Ribeiro, J.A. and Sebastião, A.M. (2010). Caffeine and adenosine. Journal of Alzheimers Disease, 20 (1):S3-15.

Salahdeen, H.M. and Alada, A.R.A. (2009). Role of adrenergic receptors in the caffeine induced increase in glucose uptake by the canine hindlimb. Niger J Physiol Sci 24 (2):141 7

Salahdeen, H.M., Omoaghe, A.O., Isehunwa, G.O., Murtala, B.A., and Alada, A.R.A. (2015). Gas chromatography mass spectrometry (GC-MS) analysis of ethanolic extracts of kolanut (Cola nitida) (vent) and its toxicity studies in rats. Journal of Medicinal Plants Research, 9, 56-70.

Seifter, S., Dayton, S., Novic, B. and Muntwryler, E. 1950). The estimation of glycogen with anthrone reagent. Archives of Biochemistry 25,191-199

Sherwin, R.S. and Saccà, L. (1984). Effect of epinephrine on glucose metabolism in humans: contribution of the liver. American Journal of Physiological, 247(2 Pt 1):E157-65.

Shi, X., Xue, W., Liang, S. et al (2016). Acute caffeine ingestion reduces insulin sensitivity in healthy subjects: a systematic review and meta-analysis. Nutrition Journal, 15, 103.

Storm, H., Van Hardeveld, C. and Kassenaar, A. (1984). The influence of hypothyroidism on the adrenergic stimulation of glycogenolysis in perfused rat liver, Biochimica Biophysica Acta, 798-350.

Tsitsanou, K.E., Skamnaki, V.T. and Oikonomakos, N.G. (2000). Structural basis of the synergistic inhibition of glycogen phosphorylase a by caffeine and a potential antidiabetic drug. Archives of Biochemistry and Biophysics, 384:245–54.

Usachev, Y., Shmigol, A., Pronchuk, N., Kostyuk, P. and Verkhratsky, A. (1993). Caffeine-induced calcium release from internal stores in cultured rat sensory neurons. Neuroscience, 57(3):845-59.

Niger. J. Physiol. Sci. 38 (December 2023): 201– 209
www.njps.physiologicalsociety.com

Niger. J. Physiol. Sci.

Full length Research Article

Evaluation of Testicular Function and Structural Changes of Wistar Rats Following Antiretroviral Exposure: Protective Role of *Cyperus esculentus*

***Ogedengbe, O.O.[1,3], Bature, A.[3], Fafure, A.A.[3], Kehinde, S.O.[3], Adekeye, A.O.[3], Akintayo, C.O.[4], Ajiboye, B.O.[2]. and Adeeyo, O.A.[1]**

[1]Department of Anatomy, Faculty of Basic Medical Sciences, Federal University Oye-Ekiti, Ekiti State, Nigeria
[2]Department of Biochemistry, Faculty of Science, Federal University Oye-Ekiti, Oye-Ekiti, Ekiti State, Nigeria
Departments of [3]Anatomy and [4]Physiology, College of Medicine and Health Sciences, Afe Babalola University, Ado Ekiti, Ekiti State, Nigeria

Summary: This study examined the ability of *C. esculentus* plants to mitigate testicular dysfunction, which is thought to be a probable side effect of antiretroviral toxicity. Adult Wistar male rats weighing 90–110 g were divided into six groups and administered the prescribed treatments. In addition to testicular histology and stereological parameters, testosterone levels, follicle-stimulating hormone levels, antioxidant markers, malondialdehyde (MDA), superoxide dismutase (SOD), and glutathione levels were also evaluated. The adverse consequences of highly active antiretroviral therapy (HAART) include considerable reduction of germ cells, expansion of the tubular lumen, enlargement of interstitial spaces, and alarmingly low cell counts. Compared to the other treatment groups, MDA levels dramatically increased, whereas GSH and antioxidant enzyme (SOD) levels significantly decreased. Testicular architecture was largely conserved after treatment with C. esculentus, with a notable increase in the cellular densities of germinal and interstitial cells and a notable decrease in the tubular lumen. Vacuolation, architectural malformations, and hypoplastic changes were reduced. Significant improvements were also observed in *C. esculentus* in terms of elevated antioxidant SOD and GSH levels and decreased MDA levels. *C. esculentus* reduced architectural distortions and testicular dysfunction caused by HAART, and improved testicular morphology. Further exploration of these pathways is required.

Keywords*: Cyperus Esculentus, highly active antiretroviral therapy, testicular dysfunction, antioxidants, Testosterone, Follicle-stimulating hormone*

**Author for correspondence: oluwatosin.ogedengbe@fuoye.edu.ng , Tel: +2348163422223*

Manuscript received- September, 2023; Accepted: November, 2023

DOI: https://doi.org/10.54548/njps.v38i2.9

INTRODUCTION

The quality of life of those with HIV/AIDS has significantly improved with increased life expectancy, thanks to the discovery and considerable advancement in the use of highly active antiretroviral medication during the last four decades (Achila *et al*., 2022). Highly Active Antiretroviral Therapy (HAART), which has been widely adopted, has altered the treatment and progression of HIV infection, with the consequences of chronic HIV infection and HAART playing an increasingly significant role in morbidity and mortality (Naidu *et al*., 2021). HAART, however, necessitates ongoing administration, which has been linked to negative consequences, such as the emergence of drug resistance, unfavorable drug interactions, and systemic drug toxicity (Olojede *et al*., 2021).

HAART has been proven to be useful in treating retroviral diseases, particularly HIV/AIDS, but it has also been documented to cause infertility, which ultimately leads to a decrease in reproductive ability (Ogedengbe *et al*., 2018c). This is due to the relatively strong permeability of the gonads to many antiretroviral medications that constitute HAART (Trezza and Kashuba, 2014). HAART can have a direct effect on the cells responsible for producing sperm, leading to decreased production or complete infertility in some cases. HAART has been hypothesized to cause topological alterations in sperm cells, resulting in mitochondrial damage, decreased sperm motility, and reduced fertility (Ogedengbe *et al*., 2018a). Such changes in sperm cells may also increase the risk of offspring inheriting genetic mutations from their parents (Haas and Tarr, 2015). Therefore, it is important to monitor the effect of HAART on male fertility. Understanding the effects of HAART on male fertility could provide valuable insights into the implications of this therapy for reproductive health.

Natural medicinal plants are increasingly being used globally for treating illnesses because of their perceived efficacy and low incidence of complications (Sharif *et al*.,

2020). *Cyperus Esculentus* (tiger nut) has been shown to have preventive effects on testicular weight and spermatogenesis (Achoribo and Ong, 2017, Adelakun *et al*., 2021). *C. esculentus* treatment improves testicular weight, sperm concentration, motility, viability, and progression in rats and mice, while reducing abnormal sperm morphology (Atoigwe-Ogeyemhe *et al*., 2018). Its anti-inflammatory, antioxidant, and antimicrobial properties make it a promising herbal remedy for male reproductive issues and for oxidative stress reduction, potentially reducing chronic diseases.

Based on quantitative analysis, *C. esculentus* is known to possess potent phytochemicals that support its strong antioxidant effects, including alkaloids, flavonoids, saponins, tannins, phenols, and glycosides (Nwosu *et al*., 2022). Furthermore, *C. esculentus* increases testosterone and gonadotropin levels in rats (Al-Shaikh *et al*., 2013). This suggests that *C. esculentus* may be useful as a natural supplement for men with low testosterone levels. Additionally, *C. esculentus* has been found to be a potential alternative to sildenafil citrate as a treatment for erectile dysfunction (ED) (Singh *et al*., 2018, Olabiyi *et al*., 2018). Studies suggest that *C. esculentus* help improve libido and sexual performance in men (Malviya *et al*., 2016, Masuku *et al*., 2020). *C. esculentus* are also high in vitamin E, which is important for maintaining hormonal balance and may therefore be beneficial for male reproductive health (Bazine and Arslanoğlu, 2020). Unfortunately, HAART delivery to anatomical sanctuary spots and HIV latent storage sites has not yet exploited the unique properties of C. esculentus. Therefore, this study aimed to assess the therapeutic role of *C. esculentus* against HAART-induced testicular dysfunction.

MATERIALS AND METHODS

Animals and treatments: The present study involved 30 male Wistar rats weighing 90-110 g, housed at the University of Afe Babalola's Animal House in Ado-Ekiti, Nigeria. All animal treatments were performed in accordance with the standards for handling and treating laboratory animals (Albus, 2012). The Animal Ethics Board approved the study protocol, which was assigned the protocol number AB/EC/15/03/007. The animals were subjected to a 12-hour cycle of light and darkness, fed and watered continuously, and allowed to acclimate for a period of two weeks. Zidovex LN, a HAART medication combining zidovudine, lamivudine, and nevirapine (Huff, 2003), was purchased from the Federal Teaching Hospital in Ido-Ekiti, Nigeria. The dosage for animals was estimated using the therapeutic equivalent dose for humans in a rat model (Ogedengbe *et al*., 2018b).

Plant Material: Dried tiger nuts (C. esculentus) were obtained from the Ado-Ekiti market in Southwest Nigeria and validated by the Plant Science Department of Afe Babalola University. Following drying, the samples were finely milled into a powder.The powder were extracted over three days in water. Chemical studies were conducted using aqueous extraction techniques to identify active plant components (Udefa *et al*., 2020). Crude aqueous extraction was performed on air-dried plant powder before evaporation at a low pressure. Constant weight was achieved by evaporating the extracted fraction in a vacuum oven at 40°C. Paste extracts (500 and 1000 mg/kg) were administered after reconstitution with distilled water.

Qualitative phytochemical screening qualitative phytochemical screening: Using the techniques of Sofowora (1993) and Evans (2002), dried extracts were evaluated for the amounts of steroids, flavonoids, saponins, alkaloids, tannins, reducing sugar, terpenoids, glycosides, as well as cardiac glycosides.

Quantitative phytochemical analyses quantitative phytochemical analyses: The dried extracts were quantified for steroids, alkaloids, phenols, tannins, and glycosides content. The Harborne method was used to determine the alkaloids, whereas other phytochemicals were measured spectrophotometrically (Harbone, 1973).

Experimental design: Following an arbitrary distribution of six groups (A–F) of five rats each, animals received the following treatments:
Group A-Control was orally administered distilled water
Group B-Treatment involved administering a HAART cocktail containing zidovex LN, which was diluted in 100 milliliters of distilled water to equal animal doses of 1.35, 0.68, and 0.92 mg/kg body weight, respectively. The equivalent doses of zidovudine, lamivudine, and nevirapine were 600 mg/day, 300 mg/day, and 400 mg/day, respectively(Ogedengbe *et al*., 2018a, Kehinde *et al*., 2021).
Group C- treated with HAART+ 500mg/kg/bw C. esculentus,
Group D- treated with HAART+1000mg/kg/bw C. esculentus,
Group E- treated with 500mg/kg/bw *C. esculentus* (Udefa *et al*., 2020)
Group F- treated with 1000mg/kg/bw *C. esculentus* (Udefa *et al*., 2020)
Daily oral delivery was used for all treatments. The animals were euthanized via cervical dislocation a day after the final dosage following eight weeks of treatment.

Body weight determination: Prior to starting the therapy, weekly, and finally on the last day of the trial, the animals were weighed. An electric scale was used to measure body weight in the morning from 8:00 to 10:00. (HX-T electronic weighing balance; HX-302 T, China).

Sample collection: Day 57 saw cervical dislocation and slaughter of the animals. Through cardiac puncture, 3 milliliters (mL) of blood was extracted from the heart and placed in simple tubes to clot for two hours. After centrifugation, the supernatant (serum) was collected for biochemical analysis after 15 minutes at 1000 g (Kehinde *et al*., 2021).

Body and Testicular weight: The body weight (BW) of the animals was measured every week until they were sacrificed, and testicular weight (TW) was determined using a digital balance (HX-T electronic weighing balance HX-302 T, China). Testicles were measured separately, and the average value was considered as one observation (TW), which was measured in grams (g).

Semen analysis: The caudal epididymis of each animal was removed from the testis, sliced in 0.5 ml of normal saline, mixed properly, and 20 µl of semen, which was needed to fill the capillary, was drawn out and placed into an automated sperm quality analyzer (SQA IIC-P manufactured by Medical Electronic System Ltd., serial no. 2840) to test sperm quality. Semen parameters were measured, and morphology and motility were measured in percentages. Sperm count was determined in millions/ml.

Organ index: The relative weights of the testes were determined using the following formula:

$$\text{Relative organ weight} = \frac{\text{Absolute organ weight}}{\text{Final body weight}} \times 100\%$$

Histological studies: Testicular tissue samples were fixed in 10% neutral-buffered formalin and subjected to histological examination. A rotary microtome (Microm GmbH, serial no. 42861, CAT. no. 02100) was used to produce fine slices with a thickness of 5 µm. Hematoxylin and eosin (H&E) staining is generally used to analyze tissue structures (Schulte *et al*., 2020). The slides were analyzed by a histopathologist who was blinded to the research protocol.

Morphometry: Weibel (2020) point-counting approach was to determine testicular interstitium (I), lumina (L), and germinal epithelium (GE) volumes. Six fields from four testicular sections were randomly selected for analysis using an Olympus microscope (CX 22RFS1, SN 2M82873, with a cameroscope at a magnification of 400 ×). A 10 mm grid with 180 test points per image was overlayed onto 5 m haematoxylin and eosin-stained tissue sections. The number of point crossings on the grid (PN) that covered each tissue component and the total number of points on the grid (PT) were divided to obtain the volume density (Vd) of each tissue component (Bielli *et al*., 2001).

$$Vd = PN/PT$$

One hundred (100) was multiplied by the Vd values for GE, L, and I, and the results are presented as percentages (%). Each testicular component's absolute volume (AV) was calculated using a modified version of Howard and Reed (2004) methodology. This was calculated by dividing the relevant volume density by testicular weight (TW). Values are expressed in mL.

Serum analysis of Testosterone and Follicle Stimulating (FSH) Hormonal levels: Blood was drawn from the heart, coagulated for two hours, and centrifuged for five minutes at 3000 rpm. Hormone levels in the recovered supernatant (serum) were measured. Testosterone and FSH levels were examined using ELISA kits with catalogue numbers TE187S and FS232F (Calbiotech Inc., 1935 Cordell Ct., El Cajon, CA 92020), following the manufacturer's instructions.

Measurement of serum malondialdehyde (MDA) concentration in the testis: The method of Albro *et al*. (1986) was used to determine the malondialdehyde (MDA) concentration in the serum. Serum (0.1 mL of serum was mixed for 15 min in a water bath with 2 mL of a 1:1:1 combination of tert-butyl alcohol (TBA), trichloroacetic acid (TCA), and hydrochloric acid (HCl) (TBA 0.37%, 0.25N HCl, and 15% TCA). After cooling and centrifuging the mixture, the clear supernatant was measured at 535 nm against a reference blank.

Measurement of serum reduced glutathione (GSH) concentration in the testis: With a few minor modifications, the measurement was performed using serum samples in accordance with the procedure outlined by Sedlak and Lindsay (1968). The concept was based on the precipitation of proteins using a tungstate/sulfuric acid solution and the formation of a yellow color following the reaction with 5, 5′-dith-iobis-2-nitrobenzoic acid (DTNB). In comparison to the control, the absorbance was measured at 412 nm for 30–60 s. Using a standard GSH curve, the concentration of glutathione (GSH) were calculated.

Measurement of serum superoxide dismutase (SOD) concentration in the testis: The method of Berwal and Ram (2018) was used to measure the superoxide dismutase (SOD). Microsome dilution was achieved by diluting 0.1 mL serum (1:10) in 0.9 mL of distilled water. To make an aliquot, 2.5 ml of 0.05M carbonate buffer were mixed with 0.2 ml of diluted microsome. The procedure was initiated by the addition of 0.3 ml of 0.3 mM adrenaline. The reference mixtures used were 2.5 ml of 0.05 M carbonate buffer, 0.3 ml of 0.3 mM adrenaline, and 0.2 ml distilled water. The absorbance was measured at a wavelength of 480 nm from 30 to 150 s.

Statistical analysis: GraphPad Prism version 5.00 for Windows was used to analyze morphometric data using conventional parametric tests. The findings are shown as mean ± standard error of the mean (GraphPad Software, San Diego, CA, USA) after one-way analysis of variance (ANOVA) and Tukey's multiple comparison test was conducted. Statistical significance was set at $p < 0.05$.

RESULTS

Phytochemical Analysis: A qualitative analysis of the aqueous extraction of *Cyperus Esculentus* showed the presence of saponins, steroids, cardiac glycosides, and terpenoids. Quantitative analysis also showed the presence of phenols, tannins, cardiac glycosides, steroids, and alkaloids, and their respective amounts, with steroids and alkaloids having higher values than the other phytochemicals present (Table 1).

Table 1:
Quantitative and qualitative phytochemical analyses of aqueous extraction of *Cyperus Esculentus*.

Phytochemical	Status	Phytochemical	Quantity (%)
Alkaloid	+	Phenol (%)	0.542
Tannin	+	Tannin (mg/100g)	2.762
Flavonoid	-	Cardiac glycosides (%	0.945
Glycoside	-	Steroid (%)	28.76
Reducing sugars	-	Alkaloid (%)	10.00
Saponin	+		
Steroid	+		
Cardiac Glycosid	+		
Terpenoids	+		

(Key: + = present; − = not present).

Organ-body weight changes: The following groups were compared: B, C, D, E, and F versus A; C and D vs. B; E vs. C; and F vs. D. All groups showed insignificant increases in body weight, with Group D presenting the greatest weight difference, while Group A showed the smallest. For both testicular weight (TW) and relative organ weight (TW/BW X100), there were no significant differences ($p > 0.05$) observed (Table 2).

Changes in sperm counts: Compared to the control group A, group B (HAART) showed a significant ($p < 0.05$) decrease in sperm counts (Table 3).

Changes in sperm motility

Progressive motility: Compared to control group A, group B showed a significant reduction ($p < 0.001$) in progressive motility. Adjuvant treatment with *C. esculentus* significantly increased this parameter in groups C ($p < 0.05$) and D ($p < 0.001$) compared with that in group B (Table 3).

Non-progressive motility: Significant increases in non-progressive motility were recorded in groups B ($p < 0.001$) and C ($p < 0.05$), in contrast to group A (the control group). Additionally, co-administration of *C. esculentus* significantly lowered non-progressive sperm motility compared to HAART group B in groups C ($p < 0.01$) and D ($p < 0.001$) (Table 3).

Immotile sperms: HAART-treated group B had the highest number of immotile sperms, whereas group A had the lowest, with no significant difference ($p < 0.05$) observed between the groups (Table 3).

Changes in germinal epithelium (GE)

Volume density: Group B had a significantly reduced GE volume density ($p < 0.05$) compared with the control group. Group D also showed a significant increase ($p < 0.05$) in this parameter following adjuvant therapy with C. esculentus, in contrast to Group B (Table 4).

Absolute volume: Adjuvant co-treatment with *C. esculentus* substantially enhanced ($p < 0.05$) the absolute volume in group D, as opposed to HAART group B.

Table 2:
Body weight, testicular weight, relative testicular weight

Groups	Initial BW (g)	Final BW (g)	Weight diff (g)	Difference %	TW (g)	(TW/BW)X100
A	144.4 ± 4.5	207.7 ± 7.0	63.3	43.8	2.3 ± 0.22	1.10
B	147.2 ± 4.1	216.3 ± 11.4	69.1	46.9	2.7 ± 0.06	1.23
C	146.8 ± 7.6	209.0 ± 4.5	62.2	42.4	2.5 ± 0.07	1.20
D	142.2 ± 7.0	227.5 ± 5.7	85.3	60.0	2.8 ± 0.11	1.22
E	149.0 ± 5.7	226.8 ± 5.6	77.8	52.2	2.9 ± 0.09	1.21
F	145.6 ± 6.7	225.9 ± 8.0	80.3	55.3	2.6 ± 0.18	1.10

The recorded data are shown as mean ± standard error of mean (SEM) (all values compared were $p > 0.05$). A: Control; B (HAART); C (HAART + 500 mg/kg C. esculentus); D (HAART + 1000 mg/kg C. esculentus); E (500 mg/kg C. esculentus); F (1000 mg/kg C. esculentus).

Table 3:
Seminal fluid analysis: epididymal sperm count and motility

Groups	Sperm Count (10^6/ml)	Sperm motility (%)		
		Progressive	Non-Progressive	Immotile
A	44 ± 4.8	47 ± 6.3	14 ± 2.3	14 ± 1.4
B	23 ± 1.3[a]	21 ± 3.6[b]	57 ± 3.4[e]	38 ± 4.8
C	35 ± 2.5	42 ± 2.6[c]	34 ± 2.7[f,g]	30 ± 3.8
D	34 ± 1.5	58 ± 3.1[d]	21 ± 3.8[h]	19 ± 8.3
E	33 ± 1.3	48 ± 3.5	21 ± 2.4	21 ± 2.4
F	35 ± 3.5	55 ± 4.1	23 ± 2.2	18 ± 7.2

The recorded data are displayed as mean ± standard error of mean (SEM) (all values compared were $p > 0.05$). A: Control; B (HAART); C (HAART + 500 mg/kg C. esculentus); D (HAART + 1000 mg/kg C. esculentus); E (500 mg/kg C. esculentus); F (1000 mg/kg C. esculentus).
The following groups were compared: B, C, D, E, and F versus A; C and D vs. B; E vs. C; and F vs. D.
[a]($p<0.05$) B vs A; [b]($p<0.01$) B vs A; [c]($p<0.05$) C vs B; [d]($p<0.001$) D vs B; [e]($p<0.001$) B vs A, [f]($p<0.05$) C vs A, [g]($p<0.01$) C vs B, [h]($p<0.001$) D vs B

Table 4:
Volume density and absolute volume stereological measurements of germinal epithelium, lumen, and interstitium

	Germinal epithelium		Lumen		Interstitium	
Groups	Vd (%)	Av (ml)	Vd (%)	Av (ml)	Vd (%)	Av (ml)
A	66 ± 2.2	1.5 ± 0.05	23 ± 2.2	0.5 ± 0.06	12 ± 0.3	0.3 ± 0.01
B	29 ± 9.2[a]	0.8 ± 0.25	50 ± 2.2[d]	1.4 ± 0.06[f]	15 ± 2.0	0.4 ± 0.05
C	47 ± 1.9	1.2 ± 0.01	27 ± 0.9[e]	0.7 ± .003[g]	18 ± 0.6	0.5 ± 0.01[i]
D	62 ± 2.2[b]	1.7 ± 0.06[c]	27 ± 0.6[e]	0.8 ± 0.02[g]	9.7±1.5[h]	0.3 ± 0.04[j]
E	60 ± 5.0	1.7 ± 0.15	22 ± 4.5	0.6 ± 0.13	10 ± 1.4[h]	0.3 ± 0.04
F	66 ± 5.0	1.7 ± 0.13	19 ± 0.9	0.5 ± 0.02	14 ± 0.9	0.4 ± 0.02

The recorded data are displayed as mean ± standard error of mean (SEM) (all values compared were $p > 0.05$). A: Control; B (HAART); C (HAART + 500 mg/kg C. esculentus); D (HAART + 1000 mg/kg C. esculentus); E (500 mg/kg C. esculentus); F (1000 mg/kg C. esculentus).
The following groups were compared: B, C, D, E, and F versus A; C and D vs. B; E vs. C; and F vs. D
[a]($p<0.05$) B vs A; [b]($p<0.05$) D vs B; [c]($p<0.05$) D vs B; [d]($p<0.01$) B vs A; [e]($p<0.01$) C & D vs B; [f]($p<0.001$) B vs A; [g]($p<0.01$) C & D vs B; [h]($p<0.05$) D & E vs C; [i]($p<0.05$) C vs A; [j]($p<0.05$) D vs C

Changes in Lumen (L)

Volume density: Compared to control group A, there was a significant increase in luminal density in group B ($p < 0.01$). Comparing groups C and D to HAART group B, adjuvant co-treatment with *C. esculentus* considerably ($p < 0.01$) lowered this parameter (Table 4).

Absolute volume: When comparing group B to Control group A, there was a significant ($p < 0.001$) increase in group B's absolute lumen volume. Comparing groups C and D to group B, co-treatment with *C. esculentus* significantly decreased this parameter ($p < 0.01$).

Changes in Insterstitium (I)

Volume density: When compared to group C, the interstitial volume densities of groups D and E decreased significantly ($p < 0.05$) (Table 4).

Absolute volume: In contrast to group A, group C exhibited a statistically significant increase ($p < 0.05$) in this parameter, whereas group D showed a statistically significant decrease ($p < 0.05$) in comparison to group C.

Histopathological examination of testicular tissue:
The testicular cross-sections of groups A, E, and F showed well-preserved cytoarchitecture and minimal **histological** alterations. Seminiferous tubules were occupied by different spermatogenic stages, these groups also have typical basement membranes and interstitial gaps. Cellular infiltration was not observed (Fig. 1A, E, & F).
Seminiferous tubules in HAART-treated groups B and C showed a significant loss of germ cells, enlarged tubular lumen, widening interstitial gaps, and hypocellularity. However, with adjuvant *C. esculentus* co-treatment, groups C and D exhibited notable enhancement with increasing germinal and interstitial cell density and a reduction in the tubular lumen. Architectural deformities, hypoplastic alterations, and vacuolations were also minimized (Fig 1 B, C & D).

Changes in serum testosterone and FSH hormonal levels: Figures 2A and B display the mean and standard error with 95% confidence intervals.

Testosterone: The mean testosterone levels of groups E (61.87 ± 0.82 ng/mL) and F (55.48 ± 7.55 ng/mL) increased significantly ($p < 0.05$) when compared to the Control-group A (15.38 ± 4.2 ng/mL) (Fig. 2A). Meanwhile, when compared to *C. esculentus* alone in Group E (61.87 ± 0.82 ng/mL), HAART co-treatment with *C. esculentus* in Group C (12.44 ± 0.36 ng/mL) considerably ($p < 0.05$) reduced this parameter. For groups B and D, the mean testosterone levels are (40.38 ± 11.45 ng/mL) and (35.57 ± 14.30 ng/mL), respectively (Fig. 2A).

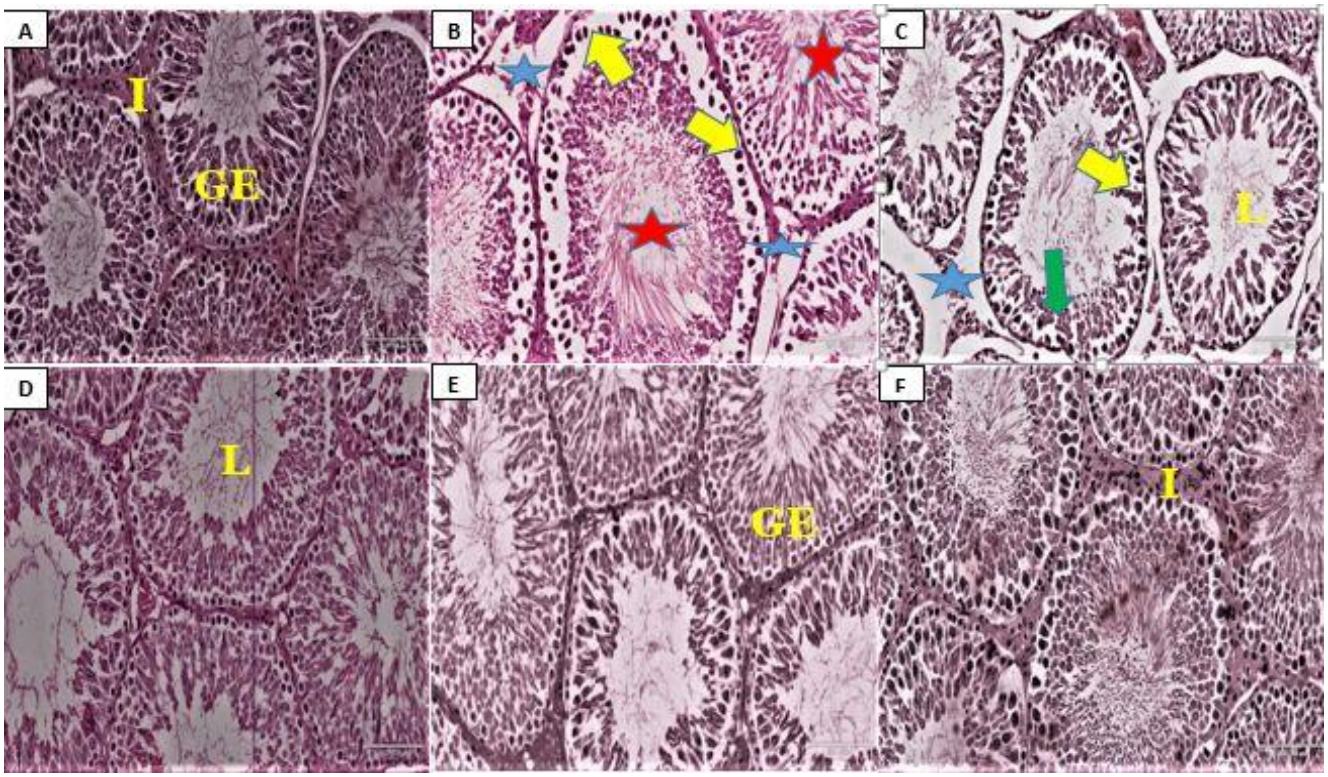

Plate 1:
Photomicrograph of testicular histological sections of groups A-F (H and E). Testicular sections from the control animals 'A revealed a germinal epithelium (GE) with well-preserved cytoarchitecture and normal cellular composition. Leydig cell-filled interstitial (I) spaces were prevalent. Immotile spermatozoa were observed in the lumen (L) (H&E × 100). Group 'B' revealed substantial loss of germ cells (yellow arrow), lumen widening (red star), and an enlarged and broadened hypocellular interstitium (blue star), (H&E X 100). In group C, the cellular densities of the germinal epithelium (green arrow) and interstitium improved significantly. Group D similarly demonstrated increased cellular density of germinal epithelium with an expanded interstitium and some hypocellularity (yellow star). Groups E and F were comparable to the control group (H&E staining, × 100).

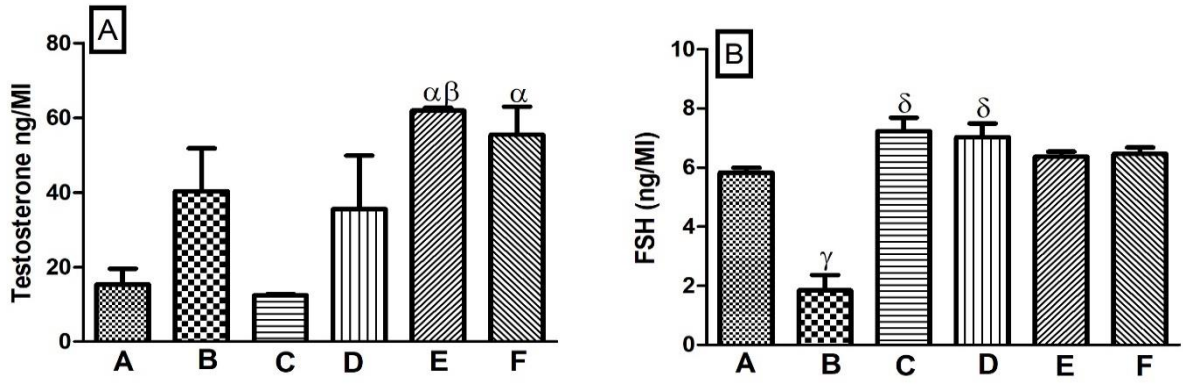

Figure 1:
Effect of *C. esculentus* and HAART treatment on serum testosterone (A) and serum follicle-stimulating hormone (B). The values were all compared at $p < 0.05$, and are shown as the mean ± SEM.; A Control; B (HAART), C (HAART + 500 mg/kg/bw *C. esculentus*), D(HAART + 1000 mg/kg/bw *C. esculentus*), E(500 mg/kg/bw *C. esculentus*), F(1000 mg/kg/bw *C. esculentus*).
The following groups were compared: B, C, D, E, and F versus A; C and D vs. B; E vs. C; and F vs. D.
For serum testosterone: $^{\alpha}(p < 0.05)$ E&F vs A; $^{\beta}(p < 0.05)$ E vs C
For serum FSH: $^{\gamma}(p < 0.001)$ B vs A; $^{\delta}(p < 0.001)$ C & D vs B

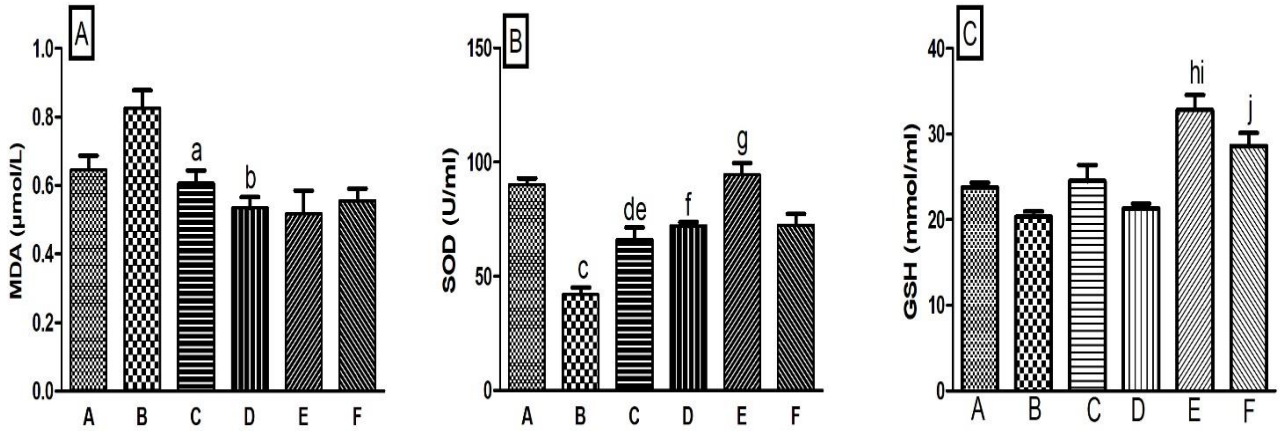

Figure 2:
Effect of *C. esculentus* and HAART treatments on the Serum (A) malondialdehyde (MDA) (B) Superoxide dismutase (SOD) (C) Reduced glutathione (GSH)
The values were all compared at $p < 0.05$, and are shown as the mean ± SEM; A Control; B (HAART), C (HAART + 500 mg/kg/bw *C. esculentus*), D(HAART + 1000 mg/kg/bw *C. esculentus*), E(500 mg/kg/bw *C. esculentus*), F(1000 mg/kg/bw *C. esculentus*).
The following groups were compared: B, C, D, E, and F versus A; C and D vs. B; E vs. C; and F vs. D.
For MDA: $^{a}(p < 0.05)$ C vs B; $^{b}(p < 0.01)$ D vs B
For SOD: $^{c}(p < 0.01)$ B vs A, $^{d}(p < 0.05)$ C vs A; $^{e}(p < 0.05)$ C vs B; $^{f}(p < 0.01)$ D vs B; $^{g}(p < 0.01)$ E vs C
For GSH: $^{h}(p < 0.01)$ E vs A; $^{i}(p < 0.01)$ E vs C; $^{j}(p < 0.01)$ F vs D

FSH: Group B receiving HAART had a mean serum FSH level of 1.8 ± 0.52 ng/mL, which was significantly lower ($p < 0.001$) than the control group A (5.80 ± 0.17 ng/mL). Furthermore, adjuvant *C. esculentus* treatment in groups C (7.2 ± 0.46 ng/mL) and D (7.0 ± 0.46 ng/mL) significantly increased ($p < 0.001$) this parameter as compared to HAART group B respectively. Groups E and F have mean serum FSH levels of (6.4 ± 0.16 ng/mL) and (6.5 ± 0.22 ng/mL), respectively (Fig. 2B).

Malondialdehyde: As shown in fig 3A, adjuvant co-treatment of *C. esculentus* with HAART in groups C ($p < 0.05$) and D ($p < 0.01$) significantly decreased MDA concentration compared to HAART group B. The mean MDA concentrations in groups A, B, C, D, E, and F were 0.65 ± 0.04 mol/L, 0.83 ± 0.05 mol/L, 0.61 ± 0.44 mol/L, 0.53 ± 0.03 mol/L, 0.52 ± 0.07 mol/L, and 0.56 ± 0.03 mol/L, respectively (Fig 3A).

Superoxide dismutase: The mean superoxide dismutase enzyme activity is shown in Figure 3B. SOD levels in HAART group B (42 ± 3.1 U/ml) were significantly lower ($p < 0.001$) than those in control group A (90 ± 2.9 U/ml). Meanwhile, compared to group A, this parameter increased significantly ($p < 0.05$) in group C (66 ± 5.3 U/ml). Compared to the HAART alone group B, the SOD levels in groups C ($p < 0.05$) and D ($p < 0.01$) increased to varying degrees. This parameter was significantly higher ($p< 0.01$) in Group E than in Group C. Groups D, E, and F had mean SOD levels of (72 ± 1.6 U/ml), (95 ± 5.1 U/ml), and (72 ± 4.8 U/ml), respectively (Fig 3B).

Reduced glutathione: *C. esculentus* treatment increased GSH concentrations in group E (33 ± 1.8 mmol/ml) significantly ($p < 0.01$) when compared to Control groups A (24 ± 0.6 mmol/ml) and C (25 ± 1.9 mmol/ml), respectively. This parameter increased significantly ($p < 0.01$) in Group F (29 ± 1.6 mmol/ml) compared to Group D (21 ± 0.6 mmol/ml). B's mean GSH concentration is (20 ± 0.6 mmol/ml).

DISCUSSION

When compared to their antiretroviral therapy-naive peers, HAART treated patients typically experience testicular dysfunction, which is characterized by a decline in sperm motility, count, viability, and volume of seminal fluid (Ogedengbe *et al*., 2018c, Savasi *et al*., 2019). Findings of the present study suggest that antiretroviral medications have a detrimental impact on testicular functional indicators, since HAART-treated rats showed a significant decrease in sperm count, progressive sperm motility, and an increase in the percentage of immobile spermatozoa. The risk of reduced fertility in the testes is thought to be associated with high levels of gonad permeability to antiretroviral medications (Adana *et al*., 2018). Our results also corroborate previous studies that found a favorable correlation between the reduction in sperm functional characteristics and the use of HAART (Akhigbe *et al*., 2021, Ogunlade *et al*., 2022).

Meanwhile, adjuvant *C. esculentus* co-treatment with HAART (groups C and D) resulted in considerably better semen quality (progressive and non-progressive motilities) than HAART alone (group B). These observations and the stereological data (volume density and absolute volume) showed a positive association. Sperm cells require mitochondrial energy metabolism, which can be impaired by toxicants owing to their limited glycolysis capacity. This process is crucial for motility, metabolism, and other functions (Costa *et al*., 2023). It is likely that disruption of mitochondrial energy metabolism may significantly affect sperm cell function and fertility, leading to testicular dysfunction and infertility, as seen in this protocol, thus emphasizing the importance of this crucial process in sperm cells (Ogedengbe *et al*., 2018c).

Reactive oxygen species (ROS) are byproducts of energy metabolism and regulate normal physiological activities. Excessive levels of ROS can compromise the body's ability to detoxify and fight free radicals, leading to oxidative stress and cell damage (Deluao *et al*., 2022). Free radicals induce lipid peroxidation, causing cell damage and death. Antiretroviral drugs can increase ROS generation, causing testicular imbalance, oxidative stress damage, and lower spermatogenic indices, thereby negatively affecting male fertility (Akhigbe *et al*., 2021; Ogunlade *et al*., 2022).

The amount of oxidative stress in the body is gauged by measuring malondialdehyde (MDA), a result of lipid peroxidation. Oxidative stress, which increases the susceptibility of cellular organelles to malfunctions, may be caused by high MDA levels in the body (Olojede *et al*., 2021). This can be accomplished by inhibiting the lipid metabolic pathways. Our findings, which were similar to those of previous studies, revealed higher levels of testicular MDA following HAART treatment, indicating testicular lipid peroxidation (Ogedengbe *et al*., 2018b, Kehinde *et al*., 2021). In support of the vulnerability of testes to oxidative damage, we hypothesized that the HAART Group B could be dependent on a high concentration of polyunsaturated fatty acids, which are easily damaged by free radicals, coupled with lower cytoplasmic levels of scavenging enzymes (Lenzi *et al*., 2000). Additionally, the high sensitivity of sperm cells to mitochondrial activity renders them more vulnerable to the damage caused by oxidative stress (Hussain *et al*., 2023). Thus, disturbance in the cell energy supply may result in immobilization of sperm and axonemal damage, which are required for motility (Mohlala *et al*., 2023).

Our findings also showed that the MDA levels of the *C. esculentus* and HAART co-treatment groups were significantly lower than those of the HAART alone group. *C. esculentus* maintain its capacity as a potent antioxidant with pharmacokinetic effects that may mitigate HAART oxidative stress damage, while enhancing sperm motility, viability, and morphology. Its low levels of polyunsaturated fatty acids, tocopherol, and phytosterol contribute to its high oxidative stability and inhibition of membrane lipid peroxidation (Nwangwa *et al*., 2020), thus mitigating the effects of HAART, as reflected in our study.

Biomarkers that have been found to be essential indicators of oxidative stress severity include glutathione and superoxide dismutase (Sahiner *et al*., 2018). In this experiment, an alteration in the antioxidant defense system may be shown by the lower concentrations of testicular antioxidant enzymes (GSH and SOD) in the HAART alone group. The increased GSH and SOD levels in the C. esculentus-treated groups provided additional evidence in favor of the plant's alleged antioxidative properties. These traits are essential for a successful conception.

Mitochondrial DNA denaturation experiments were not performed to uncover deficits in energy-generating pathways and structural abnormalities. Instead, we used ROS level as a universal indicator of oxidative stress. However, this study showed that *C. esculentus* may have a protective function by efficiently preventing pro-oxidants from inactivating antioxidant enzymes, which would lessen the structural abnormalities that have been reported in the mitigation of HAART effects on testicular parameters in Groups C and D. Therefore, *C. esculentus* appears to be a viable therapeutic agent for HAART-induced infertility.

Both the HAART alone and co-treatment groups C and D in the current investigation demonstrated notable spermatogenic cell degeneration according to histological findings and stereological assessments. Along with having a broader lumen and larger hypocellular interstitium, these groups also exhibited a lower volume density and absolute volume of the germinal epithelium. The decrease in seminiferous epithelial layers may be caused by inhibitory mechanisms against Spermatogonium B, which extends the G-1 phase of the spermatogenic cycle (Jedlinska-Krakowska *et al*., 2006). Mutations in mitochondria may also promote apoptosis and necrotic cell death, decreasing the number of germ cells that can progress to the next stages of spermatogenic development (Vera *et al*., 2004, Bisht *et al*., 2017). Our findings support prior investigations, indicating that HAART induction causes extensive necrosis and disruption of spermatogenesis in germinal cells, as evidenced by reduced seminiferous tubular diameter, hypocellular interstitium, and enlarged lumen (Ogedengbe

et al., 2018b, Owembabazi *et al*., 2023). The capacity of *C. esculentus* to attenuate histological alterations and loss of germ cells as a result of its concurrent use with HAART is reflected in testicular sections of groups C and D, which show some normalcy, as portrayed by the volume densities and absolute volumes of the germinal epithelium. This, in turn, improves the efficacy and viability of sperm, consequently protecting the seminiferous epithelium.

Follicle-stimulating hormone is regarded as a physiological signal to gain access to Sertoli cell activity. According to Jensen *et al*. (1997), it is also known that its effect on Sertoli cells increases the testis's capacity for sperm production. Contrary to its independent effects on spermatogenesis, testosterone works in conjunction with FSH to promote normal sperm production (Simoni and Santi, 2020). Thus, both testosterone and FSH must operate optimally during spermatogenesis (Oduwole *et al*., 2021). Comparing *C. esculentus* groups E and F to Control and HAART co-treatment group C, there were notable significant increases in testosterone levels. Additionally, increased FSH levels were observed in adjuvant *C. esculentus* co-treatment groups C and D compared to the HAART-only group B. These findings support the beneficial effects of *C. esculentus* and the detrimental effects of HAART on testosterone levels and Sertoli cell functions.

In conclusion, HAART has extended the life expectancy of AIDS patients but has detrimental consequences on usage persistence, affecting architecture, function, and semen indices. The antioxidant properties of *C. esculentus* reduced these effects and promoted spermatogenesis. Further investigations are required to quantify these effects.

Acknowledgements

Afe Babalola University's College of Medicine and Health Sciences is acknowledged for their assistance with the principal author. Afe Babalola University's Anatomy Department is recognized for its technical assistance and laboratory examination of the histological samples.

Authors Contributions

OOO conceived, designed, analyzed, supervised the experiment, and drafted the manuscript. BA and FAA were involved in methodology and project administration. AAO and ACO provided technical support for this study. KSO, ABO, and AOA provided material support and reviewed the manuscript.

REFERENCES

Achila, O. O., Abrhaley, F., Kesete, Y., Tesfaldet, F., Alazar, F., Fisshaye, L., Gebremeskel, L., Mehari, R. & Andemichael, D. 2022. Dyslipidemia and associated risk factors among HIV/AIDS patients on HAART in Asmara, Eritrea. *PloS one*, 17, e0270838.

Achoribo, E. S. & Ong, M. T. 2017. Tiger Nut (*Cyperus Esculentus*): Source of Natural Anticancer Drug? Brief Review of Existing Literature. *Euromediterranean Biomedical Journal*, 12,(19), 091-094.

Adana, M., Akang, E., Peter, A., Jegede, A., Naidu, E., Tiloke, C., Chuturgoon, A. & Azu, O. 2018. Naringenin attenuates highly active antiretroviral therapy-induced sperm DNA fragmentations and testicular toxicity in Sprague-Dawley rats. *Andrology*, 6, 166-175.

Adelakun, S. A., Akintunde, O. W. & Ogunlade, B. 2021. Fluoride-induced testicular degeneration and sperm quality deteriorations: Salutary role of *Cyperus Esculentus* tubers (tiger nut) extract in animal model. *Revista Internacional de Andrología*, 19, 201-212.

Akhigbe, R., Hamed, M. & Aremu, A. 2021. HAART exacerbates testicular damage and impaired spermatogenesis in anti-Koch-treated rats via dysregulation of lactate transport and glutathione content. *Reproductive Toxicology*, 103, 96-107.

Al-Shaikh, M. N., Wahab, T. A., Kareem, S. A. & Hamoudi, S. R. 2013. Protective effect of chufa tubers (*Cyperus Esculentus*) on induction of sperm abnormalities in mice treated with lead acetate. *Int J Drug Dev Res*, 5, 99-102.

Albro, P. W., Corbett, J. T. & Schroeder, J. L. 1986. Application of the thiobarbiturate assay to the measurement of lipid peroxidation products in microsomes. *Journal of Biochemical and Biophysical Methods*, 13, 185-194.

Albus, U. 2012. Guide for the Care and Use of Laboratory Animals (8th edn). SAGE Publications Sage UK: London, England.

Atoigwe-Ogeyemhe, B. E., Odigie, E. B. & Achukwu, P. U. 2018. Aqueous Extract of *Cyperus Esculentus* L.(Cyperaceae) Enhances Libido and Spermatogenesis in Male Wistar Rats: doi. org/10.26538/tjnpr/v2i11. 2. *Tropical Journal of Natural Product Research (TJNPR)*, 2, 471-475.

Bazine, T. & Arslanoğlu, F. 2020. Tiger nut (*Cyperus Esculentus*); morphology, products, uses and health benefits. Black Sea Journal of Agriculture, 3, 324-328.

Berwal, M. & Ram, C. 2018. Superoxide dismutase: A stable biochemical marker for abiotic stress tolerance in higher plants. *Abiotic and biotic stress in plants*, 1-10.

Bielli, A., Katz, H., Pedrana, G., Gastel, M. A. T., Moraña, A., Castrillejo, A., Lundeheim, N., Forsberg, M. & Rodriguez-Martinez, H. 2001. Nutritional management during fetal and postnatal life, and the influence on testicular stereology and Sertoli cell numbers in Corriedale ram lambs. *Small Ruminant Research*, 40, 63-71.

Bisht, S., Faiq, M., Tolahunase, M. & Dada, R. 2017. Oxidative stress and male infertility. *Nature Reviews Urology*, 14, 470-485.

Costa, J., Braga, P. C., Rebelo, I., Oliveira, P. F. & Alves, M. G. 2023. Mitochondria Quality Control and Male Fertility. *Biology*, 12, 827.

Evans, W. 2002. Trease and Evans Pharmacognosy. 15th edtion. Edinburgh, Saunders, 249.

Haas, D. W. & Tarr, P. E. 2015. Perspectives on pharmacogenomics of antiretroviral medications and HIV-associated comorbidities. Current Opinion in HIV and AIDS, 10, 116-122.

Harbone, J. 1973. Methods of Plant Analysis Chapter II In: Phytochemical methods: A guide to modern techniques of plant analysis Toppan Company Ltd. Japan, 1, 4-5.

Howard, V. & Reed, M. 2004. Unbiased stereology: three-dimensional measurement in microscopy, Garland Science.

Huff, B. 2003. Showdown at the X4 Corral. GMHC Treatment Issues: the Gay Men's Health Crisis Newsletter of Experimental AIDS Therapies, 17, 1-5.

Hussain, T., Kandeel, M., Metwally, E., Murtaza, G., Kalhoro, D. H., Yin, Y., Tan, B., Chughtai, M. I., Yaseen, A. & Afzal, A. 2023. Unraveling the harmful effect of oxidative stress on male fertility: A mechanistic insight. *Frontiers in Endocrinology*, 14.

Jedlinska-Krakowska, M., Bomba, G., Jakubowski, K., Rotkiewicz, T., Jana, B. & Penkowski, A. 2006. Impact of oxidative stress and supplementation with vitamins E and C on testes morphology in rats. *Journal of Reproduction and Development*, 52, 203-209.

Jensen, T. K., Andersson, A.-M., Hjollund, N. H. I., Scheike, T., Kolstad, H., Giwercman, A., Henriksen, T. B., Ernst, E., Bonde, J. P. & Olsen, J. 1997. Inhibin B as a serum marker of spermatogenesis: correlation to differences in sperm concentration and follicle-stimulating hormone levels. A study of 349 Danish men. The *Journal of Clinical Endocrinology & Metabolism*, 82, 4059-4063.

Kehinde, S. O., Ogedengbe, O. O., Linus, E. A., Erinomo, O. O., Ajumobi, K. O., Naidu, E. C. S. & Azu, O. O. 2021. Histomorphological study of the effects of aqueous extract of

Curcuma longa on highly active antiretroviral therapy-induced testicular toxicity. *Andrologia*, 53, e13952.

Lenzi, A., Gandini, L., Picardo, M., Tramer, F., Sandri, G. & Panfili, E. 2000. Lipoperoxidation damage of spermatozoa polyunsaturated fatty acids (PUFA): scavenger mechanisms and possible scavenger therapies. *Frontiers in Bioscience-Landmark*, 5, 1-15.

Malviya, N., Malviya, S., Jain, S. & Vyas, S. 2016. A review of the potential of medicinal plants in the management and treatment of male sexual dysfunction. *Andrologia*, 48, 880-893.

Masuku, N. P., Unuofin, J. O. & Lebelo, S. L. 2020. Promising role of medicinal plants in the regulation and management of male erectile dysfunction. *Biomedicine & Pharmacotherapy*, 130, 110555.

Mohlala, K., Offor, U., Monageng, E., Takalani, N. B. & Opuwari, C. S. 2023. Overview of the Effects of Moringa oleifera Leaf Extract on Oxidative Stress and Male Infertility: A Review. *Applied Sciences*, 13, 4387.

Naidu, E. C. S., Olojede, S. O., Lawal, S. K., Rennie, C. O. & Azu, O. O. 2021. Nanoparticle delivery system, highly active antiretroviral therapy, and testicular morphology: The role of stereology. *Pharmacology Research & Perspectives*, 9, e00776.

Nwangwa, J. N., Udefa, A. L., Amama, E. A., Inah, I. O., Ibrahim, H. J., Iheduru, S. C., Okorie, N. E., Ogar, J. A., Madaki, F. N. & Owai, P. O. 2020. *Cyperus Esculentus* L.(tigernut) mitigates high salt diet-associated testicular toxicity in Wistar rats by targeting testicular steroidogenesis, oxidative stress and inflammation. *Andrologia*, 52, e13780.

Nwosu, L. C., Edo, G. I. & Özgör, E. 2022. The phytochemical, proximate, pharmacological, GC-MS analysis of *Cyperus Esculentus* (Tiger nut): A fully validated approach in health, food and nutrition. *Food Bioscience*, 46, 101551.

Oduwole, O. O., Huhtaniemi, I. T. & Misrahi, M. 2021. The roles of luteinizing hormone, follicle-stimulating hormone and testosterone in spermatogenesis and folliculogenesis revisited. *International journal of molecular sciences*, 22, 12735.

Ogedengbe, O., Jegede, A., Onanuga, I., Offor, U., Peter, A., Akang, E., Naidu, E. & Azu, O. 2018a. Adjuvant potential of virgin coconut oil extract on antiretroviral therapy-induced testicular toxicity: An ultrastructural study. *Andrologia*, 50, e12930.

Ogedengbe, O., Naidu, E., Akang, E., Offor, U., Onanuga, I., Peter, A., Jegede, A. & Azu, O. 2018b. Virgin coconut oil extract mitigates testicular-induced toxicity of alcohol use in antiretroviral therapy. *Andrology*, 6, 616-626.

Ogedengbe, O. O., Naidu, E. & Azu, O. O. 2018c. Antiretroviral therapy and alcohol interactions: X-raying testicular and seminal parameters under the HAART era. *European journal of drug metabolism and pharmacokinetics*, 43, 121-135.

Ogunlade, B., Jeje, S., Adelakun, S. & Akingbade, G. 2022. Moringa oleifera restored semen quality, hormonal profile, and testicular morphology against Highly Active Antiretroviral Therapy-induced toxicity in adult male Wistar rats. *JBRA Assisted Reproduction*, 26, 3.

Olabiyi, A. A., Carvalho, F. B., Bottari, N. B., Lopes, T. F., Da Costa, P., Stefanelo, N., Morsch, V. M., Akindahunsi, A. A., Oboh, G. & Schetinger, M. R. 2018. Dietary supplementation of tiger nut alters biochemical parameters relevant to erectile function in L-NAME treated rats. Food Research International, 109, 358-367.

Olojede, S. O., Lawal, S. K., Dare, A., Moodley, R., Rennie, C. O., Naidu, E. C. & Azu, O. O. 2021. Highly active antiretroviral therapy conjugated silver nanoparticle ameliorates testicular injury in type-2 diabetic rats. Heliyon, 7, e08580.

Owembabazi, E., Nkomozepi, P. & Mbajiorgu, E. F. 2023. Impact of Concurrent Exposure of Diabetic Male Sprague Dawley Rats to Alcohol and Combination Antiretroviral Therapy (cART) on Reproductive Capacity. *Applied Sciences*, 13, 5096.

Sahiner, U. M., Birben, E., Erzurum, S., Sackesen, C. & Kalayci, Ö. 2018. Oxidative stress in asthma: Part of the puzzle. *Pediatric Allergy and Immunology*, 29, 789-800.

Savasi, V., Parisi, F., Oneta, M., Laoreti, A., Parrilla, B., Duca, P. & Cetin, I. 2019. Effects of highly active antiretroviral therapy on semen parameters of a cohort of 770 HIV-1 infected men. *PLoS One*, 14, e0212194.

Schulte, B. A., Harley, R. A. & Spicer, S. S. 1990. Carbohydrate histochemistry. In: Gil J (ed) *Models of lung disease*: microscopy and structural methods. Lung biology in health and disease series. Marcel Dekker, New York, pp 147–159

Sedlak, J. & Lindsay, R. H. 1968. Estimation of total, protein-bound, and nonprotein sulfhydryl groups in tissue with Ellman's reagent. *Analytical biochemistry*, 25, 192-205.

Sharif, H., Akash, M. S. H., Rehman, K., Irshad, K. & Imran, I. 2020. Pathophysiology of atherosclerosis: Association of risk factors and treatment strategies using plant-based bioactive compounds. *Journal of Food Biochemistry*, 44, e13449.

Simoni, M. & Santi, D. 2020. FSH treatment of male idiopathic infertility: Time for a paradigm change. Andrology, 8, 535-544.

Singh, R., Gupta, A. K. & Kaka, K. 2018. Traditional medicinal plants as scientifically proven Aphrodisiacs. *International Journal of Health and Biological Sciences*, 1, 29-36.

Sofowora, A. 1993. Medicinal plants and traditional medicine in Africa. Spectrum Books Limited. Ibadan, Nigeria, 1-153.

Trezza, C. R. & Kashuba, A. D. 2014. Pharmacokinetics of antiretrovirals in genital secretions and anatomic sites of HIV transmission: implications for HIV prevention. *Clinical pharmacokinetics*, 53, 611-624.

Udefa, A. L., Amama, E. A., Archibong, E. A., Nwangwa, J. N., Adama, S., Inyang, V. U., Inyaka, G. U.-U., Aju, G. J., Okpa, S. & Inah, I. O. 2020. Antioxidant, anti-inflammatory and anti-apoptotic effects of hydro-ethanolic extract of *Cyperus Esculentus* L.(tigernut) on lead acetate-induced testicular dysfunction in Wistar rats. *Biomedicine & pharmacotherapy*, 129, 110491.

Vera, Y., Diaz-Romero, M., Rodriguez, S., Lue, Y., Wang, C., Swerdloff, R. S. & Sinha Hikim, A. P. 2004. Mitochondria-dependent pathway is involved in heat-induced male germ cell death: lessons from mutant mice. *Biology of reproduction*, 70, 1534-1540.

Weibel, E. R. 1990. Morphometry: Stereological theory and practical methods. In: Models of Lung Disease—Microscopy and Structural Methods. Ed. Gil, J. Marcel Dekker. New York. 47, pp. 199–247.

Niger. J. Physiol. Sci. 38 (December 2023): 211 – 221
www.njps.physiologicalsociety.com

Niger. J. Physiol. Sci.

Full length Research Article

Gestational Administration of Aqueous Leaf Extract of *Jatropha tanjorensis* Alleviates Postpartum-like Behaviours in Experimental Rats

Antai, A.B., *Ukoh, I.E., Bisong, S.A., Edet, E.A. and Johnny, M.I.
Department of Physiology, Faculty of Basic Medical Sciences, University of Calabar, , P.M.B. 1115, Calabar, Cross River State, Nigeria

Summary: This study examines the effect of gestational administration of aqueous leaf extract of *Jatropha tanjorensis* (JT) on postpartum-like behavioural outcomes to delineate its possibility as a prophylactic, therapeutic agent in the treatment of postpartum symptoms. Inseminated female rats (120-150g) were grouped into two-control and JT group (n=10). Control received 20 ml/kg of distilled water and JT group received 500 mg/kg of JT orally once daily for 21 days in gestation. Non-pregnant rats were excluded from the study. Parameters assessed at postpartum include antidepressant-like (force swim test, FST; tail suspension-test, TST), locomotor (open field test, OFT), anxiolytic-like (elevated plus maze, EPM; light-dark box, LDB), learning and memory (T-maze; novel object recognition task, NORT), social (nest score) and analgesic-like (hot plate test, HPT; tail flick test, TFT) behaviours. JT increased ($P<0.05$) mobility and latency to immobility durations in FST and TST; open arm entry ($P<0.001$) and duration ($P<0.01$) in EPM and light box duration ($P<0.05$) in LDB; locomotion and exploration, but reduced anxiety-like levels in EPM, LDB and OFT. It increased nest score ($P<0.05$); mean retraction time ($P<0.01$) of TFT. JT showed positive score for short and long term memory in NORT and improved percentage alternation in T-maze though not significant compared to control. In conclusion, the aqueous extract has a therapeutic effect that reduces postpartum-like depression and anxiety, and improves locomotor activity. JT can be a preventive and adjuvant therapeutic option for pregnant women.

Keywords*: Jatropha, postpartum disorder, Emotionality, Pain, Gestation*

**Authors for correspondence: ukohrichard@yahoo.com , Tel: +2348064355375*

Manuscript received- December 2022; Accepted- July 2023

DOI: https://doi.org/10.54548/njps.v38i2.10

INTRODUCTION

In females, pregnancy, delivery, and postpartum period are uniquely characterized by extremely varying behavioural changes. However, in a large subset of mothers, these phases also represent a risk period for the development of postpartum disorders such as postpartum depression (PPD), anxiety (PPA) and cognitive deficits (Zhang *et al*., 2021). PPD and PPA have many negative consequences on maternal health (Ali *et al*., 2013), which include biological and psychological factors, risky behaviours and mother-child interactions (Slomian *et al*., 2019; Field, 2017). Cognitive decline was also reported to have consequence on mother-child interactions (Postma *et al*., 2014; Albin-Brooks *et al*., 2017). It is estimated that mothers display about 10-20% PPA and over 25% PPD (Cárdenas *et al*., 2020), and over 80% cognitive decline (Qiu *et al*., 2021). The main predictor for postpartum disorders is an antenatal episode of the illness (Grant *et al*., 2008; Topiwala *et al*., 2012). However, postpartum hyperalgesia due to acute pain after delivery was shown to increase the development of postpartum disorder (Eisenach *et al*., 2008; Lim *et al*., 2018). Evidence from animal and clinical studies indicated that pain sensation could change from acute pain caused by tissue damage to a complex and multifaceted pain syndrome (Maldonado and De Jesus, 2021; Quesada *et al*., 2021). However, these symptoms in postpartum women are often overlooked, leading to lower diagnosis rates and even lower treatment rates (Zhang *et al*., 2021).

Jatropha tanjorensis is a perennial herb normally grown in Southern Nigeria commonly called 'Hospital too far' (Oyewole *et al*., 2012). Phytochemical screening of JT leaf revealed that it contains bioactive constituents such as alkaloids, flavonoids, tannins, cardiac glycosides, anthraquinones and saponins (Iroanya *et al*., 2018). Cook and Samman, (1996) reported that flavonoids due to their high antioxidant capacity have health-promoting properties and help reduce the risk of diseases. Bribi *et al*., (2017) and Contreras *et al*., (2017) in their separate studies observed that alkaloid exert antioxidant and analgesic activities, while Feng *et al*., (2006) reported anti-inflammatory and anxiolytic activities of plant alkaloids. Albuquerque *et al*., (2005) reported that tannins are known to heal wounds and inflamed mucous membranes, while Wagner and Elmadfa, (2003) reported that they possesses antioxidant properties. Madubuike, *et al*., (2015) reported that the leaf extract of JT

possesses antioxidant and anti-diabetic properties. Iroanya *et al*., (2018) reported that JT improve haematological indices which revealed an enhancement of bone marrow function. Falodun *et al*., (2013) reported that JT increases the amount of iron available for erythropoiesis, increase packed cell volume and hemoglobin concentration in rats and recommended the extracts usage in physiological conditions like pregnancy and during menstruation. Nindaratnasari, (2017) reported JT usage to ease baby delivering process.

Despite the well documented multi-dimensional usage of *Jatropha tanjorensis*, there is no report on the behavioural effects of the plant extract on maternal health. Hence, this study describes the effect of gestational administration of an aqueous leaf extract from JT on several postpartum-like behavioural outcomes to delineate the possibility of using JT as a prophylactic, therapeutic agent in the treatment of postpartum symptoms. This paper could be the first or one of the first few studies examining the effect of JT on neurological aspects of postpartum responses in rats. One of the strengths of this paper is the extensive behavioural assessments showing several measures of neuropsychiatric, social, nociceptive, and cognitive responses. However, the paper lacks important underlying molecular explanations of the behavioural outcomes. A look at HPA/HPG/oxytocin levels might improve the robustness of the data.

MATERIALS AND METHODS

Preparation of Extract: The leaves of *Jatropha tanjorensis* were harvested from the botanical garden of the University of Calabar, Nigeria. A voucher specimen has been kept in the botanical garden (Herb/Bot/UCC/182). They were prepared as described by Agarwal *et al*., (2007). The leaves was thoroughly washed with clean water and air-dried at room temperature for two days, then further dried in an oven at 40°C for 24 hours. The crispy leaves were then ground into fine powder and preserved in moisture-free, airtight laboratory containers for further use. The powdered plant material (100 g) was macerated with water (1000 ml) in ratio of 1g of the powdered plant to 10ml of water and was agitated intermittently for 48 hours, filtered into a clean glass jar. Filtration was done using a Whatman No 1 filter paper to separate the filtrate from the residue. The filter paper was folded into four portions and put in the funnel and placed into 1,000ml beaker, the filtrate containing the extract was carefully poured into the funnel which filtered into the beaker through the filter paper. After obtaining the filtrate, it was then poured into an evaporating dish which was thereafter dried on a thermostatically controlled water bath at 42 0C. The drying was monitored until it turned into a paste form. The yield of the aqueous extract of JT weighed 73g. The extraction method closely represents how the leaves might be consumed locally. Hence the results have a tendency for a more direct application.

Determination of LD_{50}: The LD_{50} was determined by the method of Lorke, (1983) using 12 female albino Wistar rats which comprised of two phases. In the first phase the rats were divided into 3 groups of 3 rats each and were treated with the aqueous leaf extract of JT at doses of 10, 100 and1000mg/kg body weight orally. In the second phase 3 rats were divided into 3 groups of 1 rat each and were treated with the aqueous leaf extract of JT at doses of 1000, 1600, 2900, and 5000mg/kg body weight orally. In both phases the animals were observed for 24h for signs of toxicity as well as mortality. There was no toxicity and mortality recorded even at the highest dose of 5000mg/kg. Therefore, in this study the extract dosage of 500mg/kg was considered safe for pregnant rats.

Experimental animals: Thirty albino rats (20 females and 10 males) weighing between 120 -150g were obtained from the College of Medical Sciences animal house of University Calabar, Cross River State, Nigeria. The animals were kept under standard laboratory conditions and housed in well ventilated plastic cages at room temperature and relative humidity with light and dark cycles (12hr/12hr). The animals were acclimatized for one week and were provided standard rat pellet (Pfizer feed PLC, Lagos, Nigeria) and water ad libitum.

Ethical consideration: Ethical approval was obtained from the University of Calabar College Ethical Committee on the use of experimental animals with protocol number (093PHY3321).

Experimental design: In the model of natural pregnancy, rats were caged at a ratio of 1 male to 2 females, and the appearance of vaginal plug was considered day 1 of gestation (Zhang *et al*., 2021). The inseminated female rats were randomly assigned into two groups. Group 1 served as control (n=10) which received 20 ml/kg of distilled water (vehicle) orally, while Group 2 served as JT treated (n=10) and received 500mg/kg of JT orally for 21 days throughout gestation. After two weeks of observation, the number of inseminated female rat not pregnant rats was excluded from the study. The pregnant rats for control (n=7) and for JT (n=9).

Neurobehavioural assessments of postpartum rats:

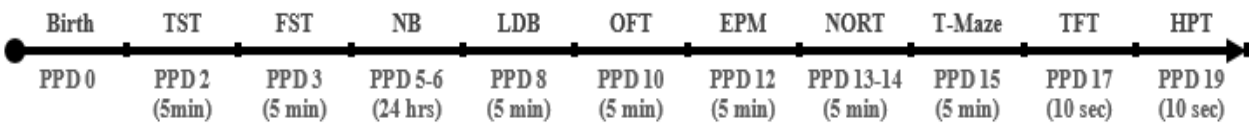

Plate 1:
Experimental design for neurobehavioural studies and durations. Tail suspension test (TST), Force swim test (FST), Nesting behaviour (NB), Light dark box (LDB), Open field test (OFT), Elevated plus maze (EPM), Novel object recognition task (NORT), Tail flick test (TFT), Hot plate test (HPT), Postpartum day (PPD)

Assessment for anti-depressant activity

Force swim test: A transparent container of diameter 15 cm, height 25 cm and with a water depth of 20 cm was allowed to sit overnight to maintain a temperature at 30°C ± 1°C. At this depth of water, rat was unable to touch the bottom or the side walls of the container with their paws or tail. On PPD 3 each dam was allowed to swim in the transparent container for 5 min and the behavioural score was recorded using a stopwatch. After the test session, the dam was scooped up from the transparent container with a plastic container and placed in a holding cage filled with paper towel to dry before being returned to their home cages. After each trial, the water was changed. Behaviour scored include latency to immobility, mobility, immobility and frequency of defecation (Englisch *et al*., 2009).

Tail suspension test (TST): A tail suspension box made of wood with dimensions (55 height x 60 width x 11.5 cm depth) was used. The compartment width and depth was sufficiently sized so that the dam couldn't make contact with the walls. On PPD 2, each dam was suspended by hanging by the tail using adhesive tape and its body hung down in the air. TST is based on the assumption that the animal will try to escape the stressful situation. After a certain time, the animal ceases to struggle and immobility occurs; longer immobility phases are sign of depressive behaviour. Test was carried out in a lit room with minimal background noise for a period of 5 min. Behavioural Score include mobility, immobility and latency to immobility (Englisch *et al*., 2009).

Assessment of locomotion and emotionality

The open field test: The OFT apparatus is a white painted plywood (72 X 72 cm) with blue lines drawn on the floor to divide it into 18 x 18 cm squares. A central square (18 x 18 cm) is drawn in the middle of the open field. On PPD 10 each dam was placed in the center of the apparatus and allowed to explore the area for 5 min. Behaviours Scored include line crossing, center square entry (CSE), rearing, stretch attend postures (SAP), grooming and freezing. Each dam was then given a score for total locomotor activity and emotionality that was calculated as the sum of line crosses and number of rears (Bisong *et al*., 2010). The apparatus was cleaned with 70 % ethanol after each trial.

Assessment of anti-anxiety activity

Elevated plus-maze test: The EPM apparatus consists of two open arms (30 × 5 cm), and two closed arms (30 × 5 × 15 cm), elevated 25 cm above floor level. The arms are connected to a central square (5 × 5cm) where the dam is placed. The edges, 4 mm high, surrounds the open arms, reducing the chances of rats falling from the apparatus. On PPD 12, each dam was individually placed in the center square of the apparatus and allowed to freely explore the apparatus for 5 min. The dam behavior was recorded for the test period of 5 min and then analyzed. After each dam, the entire maze was cleaned with 70% ethanol. Behaviour scored include, open arm entry, closed arm entry, head dips, SAP, grooming, rearing, urination and defecation (Sutulovic *et al*., 2021).

Light/dark transition box: The apparatus is made of a rectangular box (45 x 27 x 27 cm), partitioned into two unequal compartments. The box has two compartments, a light and a dark one. The dark chamber is smaller and often is the compartment considered as safe by the mice. The small compartment (18 x 27 cm) was painted black and the larger compartment (27 x 27 cm) was painted white. These compartments were connected by a door (7.5 x 7.5 cm) located at floor level in the center of the wall between the two compartments. The floor was divided into 9 x 9 cm squares and covered with plexiglas. Both compartments were covered with lids of clear plexiglas. A 60-watt table lamp located 40 cm above the center of the white compartment provided bright illumination of white light. On PPD 8, each dam was placed in the center of the white compartment facing the door and allowed to explore the apparatus for 5 min. The dam's behaviour was recorded by a digital camera set up high above the plexiglass. After each dam, the entire apparatus was cleaned with 70% ethanol. Behaviours scored include transitions, line crosses, rearing, SAP, grooming, dark box and light box duration (Bisong *et al*., 2017).

Assessment of learning and memory

Novel object recognition test: The NORT assesses rodent's ability to recognize a familiar object over a variable length of time; this ability has been coined recognition memory (Ajiwhen and Bisong, 2013). The NORT modified by Shimoda *et al*., (2021) was used to test cognitive memory. On PPD 13, there is an initial habituation to the apparatus prior to the NORT for 5 min, and then two trials in the NORT, an acquisition trial (trial 1) and a retention trial (trial 2). These two trials are separated by a inter-trial interval of 15 min (short-term) and 24 hours (long-term). Each dam is placed in an arena and allowed to investigate two identical objects for 5 min. After the retention period, trial 2 is completed where dam is presented with a familiar object (one of the objects from trial 1) and a novel object (not present in trial 1). It was cleaned with 70 % ethanol before the next dam was put on the apparatus. Behaviours scored during the NORT include: discrimination Index which is the time spent between the novel and familiar objects (Shimoda *et al*., 2021).

$$\text{Discrimination Index} = \frac{\text{Novel object exploration time} - \text{Familiar object exploration time}}{\text{Novel object exploration time} + \text{Familiar object exploration time}}$$

Habituation Index: Total time spent in exploring the two objects during the familiarization phase and the test phase (Antunes and Biala, 2012).

T-maze spontaneous alternation test: The T-maze is an elevated or enclosed apparatus in the form of a 'T' placed horizontally. It is made of wood painted black and consist of three arms, the starting arm which is the base of the T-maze measuring 50 x 16 cm and two goal arms (left and right) measuring 50 x 10 cm with a wooden door cut to fit at the entrance, which give animal two environment to explore. The wall height of the enclosed T-maze is 30 cm. On PPD 15, each dam was placed on the maze and allowed

to explore the maze for 5 min. This maze was used for 2-trials and the maze was cleaned with 70% ethanol before the next rat was put on the apparatus. Prior to Trial 1, the left and right arm doors of the maze was open and the rat was placed at the base of the Maze, and a stopwatch was used to record the time it took the animal to explore the goal arms. When all four paws of dam enter one arm, the arm door is closed for 2 min and arm entry is recorded as right (R) or left (L). Trial 2 was done after 15 min, the same procedure was followed as Trial 1.

Spontaneous alternation behaviour (SAB) is based on the fact that rodents prefer to visit the less recently visited arm, thus implicating that it will need to recall which was the last arm visited. The percentage alternation was calculated as reported by Sivakumar *et al*., (2017).

Percentage alternation:

$$\frac{\text{The number of correct choices X 100}}{\text{Total sets performed}}$$

Assessment of social behaviour

Nesting: On PPD 5 cotton wool was provided as nesting material. Five gram (5g) of the nesting material was placed in the home cage and examined after 24 hours for nest building behaviour. Nest scoring include: (a) Nestlet not noticeably touched (90% or more intact), (b) Nestlet partially torn (50-90% intact), (c) Less than 50% of nestlet remains intact, but not gathered into a nest site but spread throughout cage, (d) More than 90% of the nestlet is torn into a flat nest (e) More than 90% of the nestlet is torn, nest is fairly even (Deacon, 2006).

Assessment of pain sensation

Hot Plate Test: On PPD 19, each dam was dropped gently on the hot-plate (Hotplate analgesia meter Columbus instruments OHIO-43204 USA) set at 55±1°C. The reaction time was recorded using a stopwatch as the interval between placement of the animals on the hot plate and the first time it licked its fore-paws (Yam *et al*., 2020).

Tail flick test:: This experiment was conducted according to the modified method adopted by Sanchez-Mateo *et al*., (2006) using hot water bath. On PPD 17, the terminal 2 cm of the rat tail in each group was immersed in hot water contained in a 500 ml beaker maintained at 55±1°C. A thermometer was placed inside the water to monitor the temperature (Sanchez-Mateo *et al*., 2006). The time in seconds to clearly withdraw the tail out of the water was taken as the reaction time, with a cut-off time of immersion at 10 sec (Sudipta *et al*., 2013).

Statistical Analysis:

Data were expressed as Mean ± Standard Error of Mean (SEM). Sample size for each treatment group is stated in respective table or figures. Data were first examined for normality using Shapiro-Wilk normality test, with $p>0.05$ the null hypothesis was accepted signifying normal distribution of the data. Normally distributed data were analyzed with independent Student's t-test for comparison between means of the two groups. A difference between means was considered significant at $p < 0.05$. The statistical software used include SPSS version 20 and graphpad prism version 8.

RESULTS

Acute toxicity study: The median lethal dose (LD50) value of the aqueous leaf extract of JT leaves in rat was found to be greater than 5000 mg/kg body weight, orally. There was no toxicity and mortality recorded even at the highest dose of 5000mg/kg.

Neurobehavioural observation

Antidepressant-like activity of JT in dams: In FST, The mean latency to immobility for control and JT treated dams are 70.61 ± 7.59 and 103.88 ± 10.31 respectively. Latency to immobility was significantly ($P<0.05$) higher in the JT group when compared to the control (Figure 1).

The mean duration of immobility for control and JT treated dams are 64.89 ± 7.23 and 45.61 ± 4.99 respectively. Duration of immobility was significantly ($P<0.05$) reduced in the JT group when compared to the control (Figure 2).

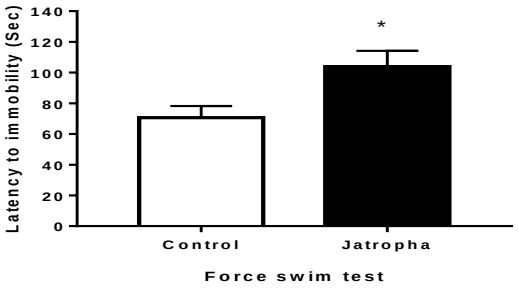

Figure. 1:
Comparison of latency to immobility in FST between experimental groups
Values are mean ± SEM, n= control (7); Jatropha (9)
*p<0.05 vs control

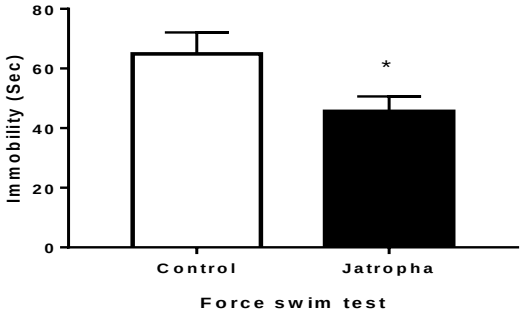

Figure. 2:
Comparison of Immobility in FST between experimental groups
Values are mean ± SEM, n= control (7); Jatropha (9) *p<0.05 vs control

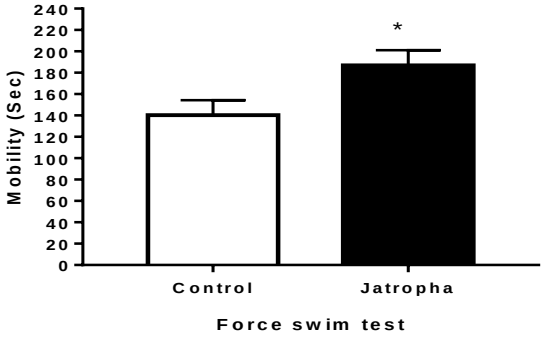

Figure. 3:
Comparison of mobility in FST between experimental groups Values are mean ± SEM, n= control (7); Jatropha (9)
*p<0.05 vs control

The mean duration of mobility for control and JT treated dams are 140.22 ± 14.13 and 186.80 ± 14.31 respectively. Duration of mobility was significantly (P<0.05) higher in the JT group when compared to the control (Figure 3).
The mean frequency of defecation for control and JT treated dams are 7.29 ± 0.81 and 3.22 ± 0.55 respectively. Frequency of defecation was significantly (P<0.01) higher in the control when compared to the JT group (Figure 4). In TST, the mean latency to immobility for control and JT treated dams are 48.47 ± 6.29 and 75.84 ± 7.83 respectively. Latency to immobility was significantly (P<0.05) higher in the JT group when compared to the control (Figure 5). The mean duration of immobility for control and JT treated dams are 97.03 ± 6.81 and 34.09 ± 2.59 respectively. Duration of immobility was significantly (P<0.001) higher in the control when compared to JT group (Figure 6). The mean duration of mobility for control and JT treated dams are 154.93 ± 8.96 and 190.62 ± 9.24 respectively. Duration of mobility was significantly (P<0.05) higher in the control when compared to JT group (Figure 7).

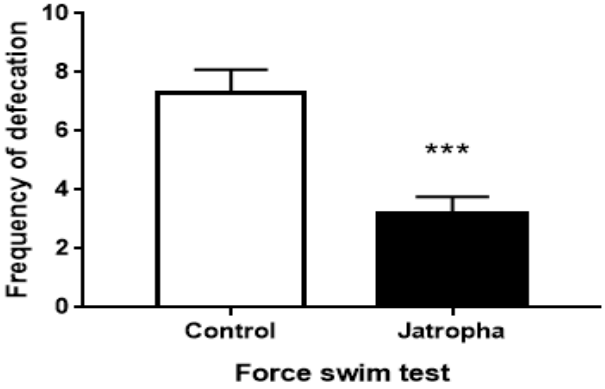

Figure. 4:
Comparison of frequency of defecation in FST between experimental groups
Values are mean ± SEM, n= control (7); Jatropha (9)
***p<0.001 vs control

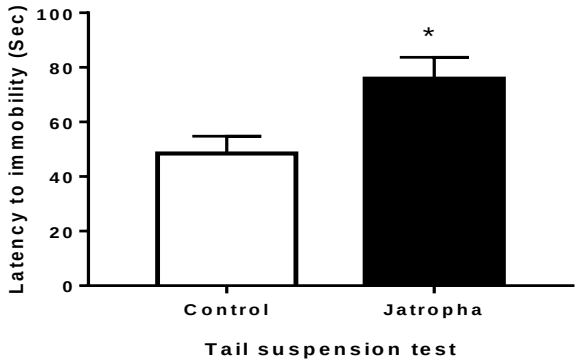

Figure. 5:
Comparison of latency to immobility in TST between experimentalgroups
Values are mean ± SEM, n= control (7); Jatropha (9)
*p<0.05 vs control.

Anxiolytic-like activity of JT in dams: Table 1 shows the effects aqueous leaf extract of JT in dams subjected to anxiolytic-like activity in EPM. Results obtained indicate that administration of JT caused a significant (P<0.05) decrease in the frequency of head dip, urination, defecation, grooming and it duration compared to control. The frequency of SAP and close arm frequency were significantly (P<0.01) lower in the JT group compared to control. The close arm duration was significantly (P<0.001) lower in the JT group compared to control. The frequency of entry into the open arm (P<0.001) and open arm duration (P<0.01) were significantly higher in the JT group compared to control.

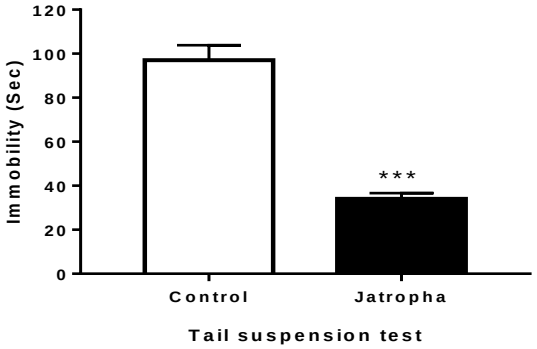

Figure. 6:
Comparison of immobility in TST between experimental groups
Values are mean ± SEM, n= control (7); Jatropha (9)
***p<0.001 vs control

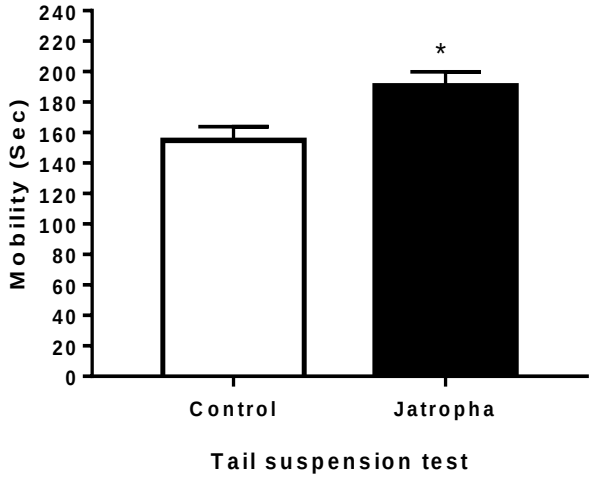

Figure. 7:
Comparison of mobility in TST between experimental groups
Values are mean ± SEM, n= control (7); Jatropha (9)
*p<0.05 vs control

Table 1:
Comparison of EPM activities in JT dams

Parameters	Control	Jatropha
Head dipping	7.86 ± 1.5	3.44 ± 1.06*
Rearing	11.29 ± 1.41	17.56 ± 2.06*
Stretch attend posture	7.43 ± 0.97	3.33 ± 0.58**
Grooming frequency	3.57 ± 0.97	1.00 ± 0.44*
Grooming duration	45.72 ± 15.91	6.01 ± 2.47*
Open arm frequency	0.86 ± 0.26	2.78 ± 0.32***
Open arm duration	15.50 ± 7.31	162.58 ± 30.73**
Close arm frequency	2.00 ± 0.22	1.22 ± 0.15**
Close arm duration	284.46 ± 7.31	99.72 ± 31.36***
Urination	3.00 ± 0.82	0.33 ± 0.24*
Defecation	2.29 ± 0.57	0.78 ± 0.22*

Values are Mean ± SEM, n= control (7); Jatropha (9) * P<0.05, ** P<0.01, *** P<0.001 significantly different compared to control.

Table 2 shows the summary of behaviours scored in the LDB test following treatment with the aqueous leaf-extract of JT. The frequency of line crossing, rearing, transitioning in the light and dark chamber, as well as duration in the light box were significantly (P<0.05) higher in the JT group compared to control. The frequency of SAP and duration in the dark box were significantly (P<0.05) lower in the JT group compared to control. The duration of grooming was significantly (P<0.01) lower in the JT group compared to control.

Table 2:
LDB test of dams treated with JT

Parameters	Control	Jatropha
Line crossing	57.29 ± 7.10	74.67 ± 3.82*
Rearing	18.86 ± 4.07	30.0 ± 1.82*
Transition frequency	6.57 ± 1.2	10.89 ± 1.02*
SAP	2.71 ± 0.29	1.44 ± 0.41*
Grooming	38.34 ± 7.07	14.57 ± 3.25**
Light box duration	60.30 ± 13.07	150.16 ± 32.90*
Dark box duration	215.62 ± 19.38	106.59 ± 35.85*
Urination	4.86 ± 0.74	2.00 ± 0.76*
Defecation	4.57 ± 0.81	2.00 ± 0.65*

Values are Mean ± SEM, n= control (7); Jatropha (9) * P<0.05, ** P<0.01 significantly different compared to control.

Table 3:
OFT of dams treated with JT

Parameters	Control	Jatropha
Line crossing	63.14 ± 8.05	108.44 ± 11.50**
Rearing	21.57 ± 3.75	40.89 ± 4.51**
SAP	3.00 ± 1.02	0.44 ± 0.29*
Grooming frequency	3.71 ± 0.89	3.44 ± 0.94^{NS}
Grooming duration	32.23 ± 9.41	25.72 ± 7.46^{NS}
Freezing frequency	4.71 ± 0.64	2.11 ± 0.56**
Freezing duration	72.73 ± 10.74	32.24 ± 12.92*
CSE frequency	1.43 ± 0.48	4.33 ± 1.12*
CSE duration	9.90 ± 4.73	45.91 ± 13.19*
Urination	4.86 ± 1.18	2.00 ± 0.62*
Defecation	3.71 ± 0.78	1.56 ± 0.50*

Values are Mean ± SEM, n= control (7); Jatropha (9) * P<0.05, ** P<0.01 significantly different compared to control. NS= Not significant

Locomotor activity and emotionality using open field maze: The frequency of line crossing, rearing (P<0.01), CSE and duration were significantly (P<0.05) higher in the JT group compared to control, while the frequency of SAP, urination, defecation and duration of freezing were significantly (P<0.05) lower in the JT group compared to control. The freezing frequency was significantly (P<0.01) lower in the JT group compared to control, as shown in Table 3.

Social behaviour: Observations of nest building for control and JT treated group are: 2.71 ± 0.47 and 4.11 ± 0.26 respectively. Nest building increased significantly (P<0.05) in the JT group compared to the control (Figure 8).

Cognitive function: Results for NORT showed the mean index of habituation for short term memory (STM) of control and treated dams as 5.63 ± 2.85 and 3.11 ± 3.26 respectively. There was no significant differences among group (Figure 9).

The mean index of habituation for long term memory (LTM) of control and treated dams are -2.28 ± 2.85 and 1.06 ± 5.86 respectively. There was no significant differences among group (Figure 10). The mean index of discrimination for STM of control and treated dams are -0.005 ± 0.12 and 0.26 ± 0.17 respectively. There was no significant differences among group (Figure 11). The mean index of discrimination for LTM of control and treated dams are 0.02 ± 0.21 and 0.19 ± 0.21 respectively. There was no significant difference among group (Figure 12).

T -Maze test results for STM showed the percentage alternation for control and treated dams as 42.86 ± 20.20 and 77.78 ± 14.70 respectively. There was no significant difference among group (Figure 13).

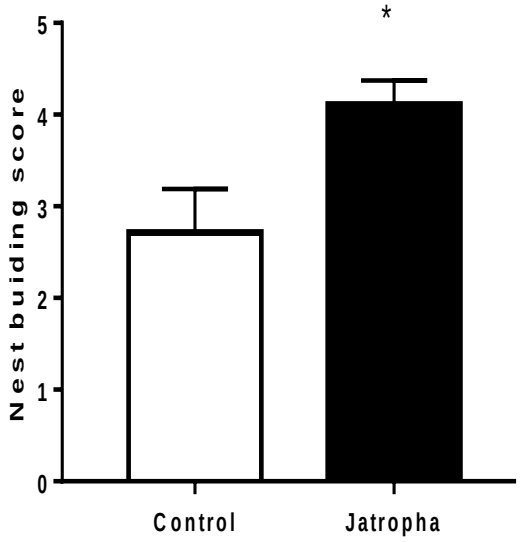

Figure. 8:
Comparison of nest building score between experimental group
Values are mean ± SEM, n= control (7); Jatropha
*p<0.05 vs control

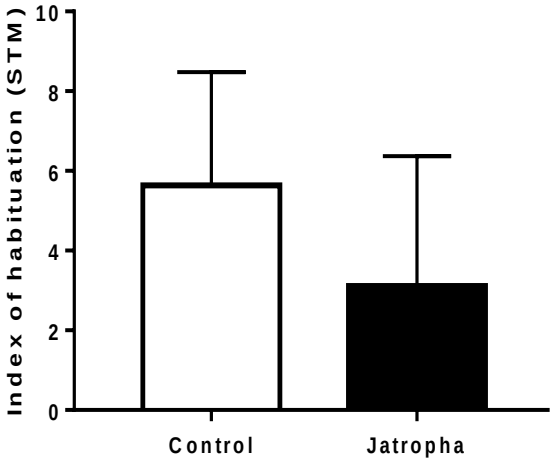

Figure 9:
Comparison of Index of habituation (STM) in NORT between experimental groups.
Values are mean ± SEM, n= control (7); Jatropha (9)

Pain sensation: The mean retraction time of HPT for control and JT treated dams are 11.03 ± 1.40 and 11.79 ±

2.20 respectively. There was no significant differences between the groups (Figure 14).

The mean retraction time of TFT test for control and treated dams are 6.19 ± 0.83 and 9.78 ± 0.82 respectively. There was significant ($P<0.01$) increase in the retraction time of the JT dams compared to the control (Figure 15).

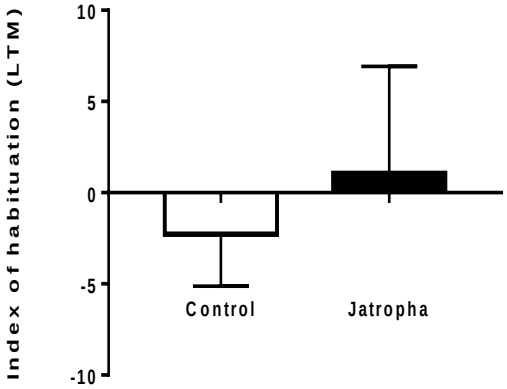

Figure 10:
Comparison of Index of habituation (LTM) in NORT between experimental groups.
Values are mean ± SEM, n= control (7); Jatropha (9)

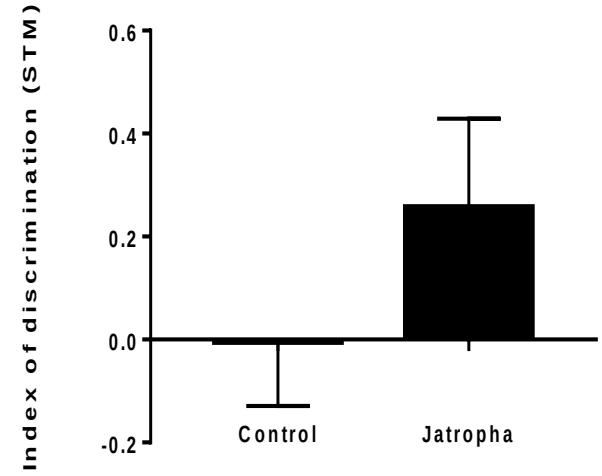

Figure 11:
Comparison of Index of discrimination (STM) in NORT between experimental groups.
Values are mean ± SEM, n= control (7); Jatropha (9)

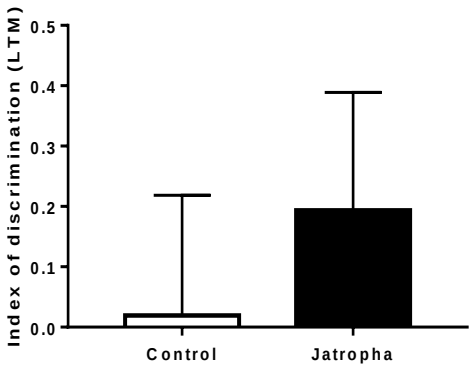

Figure 12:
Comparison of Index of discrimination (LTM) in NORT between experimental groups.
Values are mean ± SEM, n= control (7); Jatropha (9)

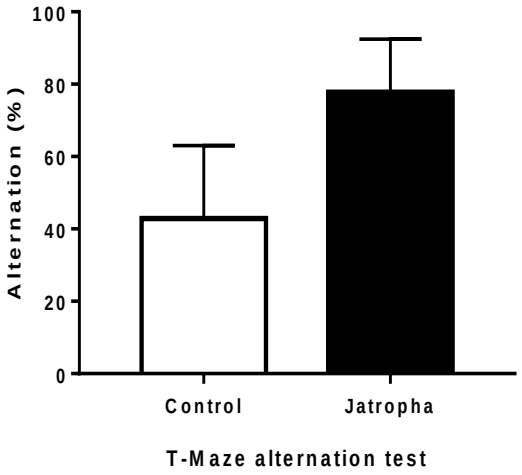

Figure 13:
Comparison of percentage alternation between experimental groups.
Values are mean ± SEM, n= control (7); Jatropha (9)

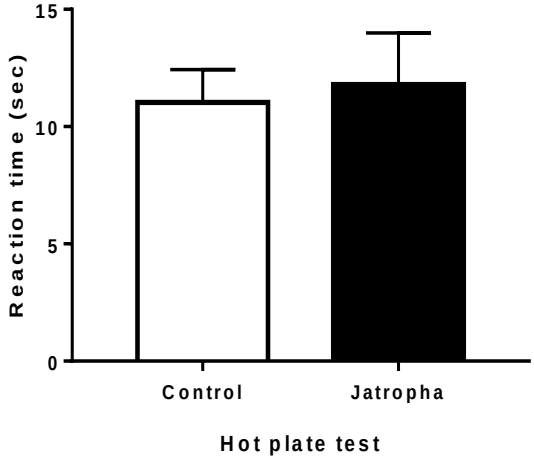

Figure 14:
Comparison of reaction time in HPT between experimental groups.
Values are mean ± SEM, n= control (7); Jatropha (9)

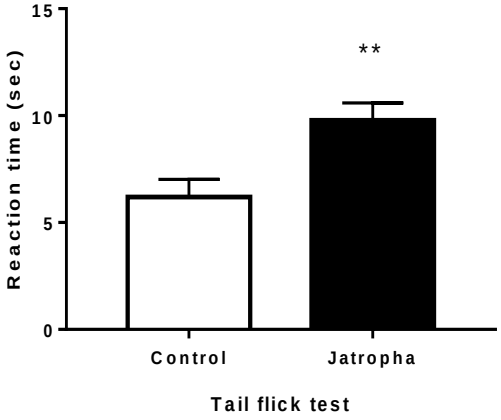

Figure 15:

Comparison of reaction time in TFT between experimental groups
Values are mean ± SEM, n= control (7); Jatropha (9)
**- Significant at p< 0.01 versus control

DISCUSSION

The occurrence of postpartum disorders after childbirth is well known during postpartum, but the treatment options for these symptoms during this special period remain limited (Zhang *et al*., 2021). In the present study, we reported that gestational administration of aqueous leaf extract of JT significantly contributed to the alleviation of postpartum-like behaviour in rats. Antidepressant-like profile was observed in JT treated dams; this is evidenced by the increased duration of latency to immobility and mobility, as well as decrease duration of immobility in both the FST and TST. Immobility has been considered to reflect behavioural despair similar to that seen in human depression, and antidepressant medications are able to reduce the immobility time in rodents (Vanzella *et al*., 2012), whereas latency to the first immobility is a measure of active stress coping (Everton *et al*., 2018). It is very likely that JT contains active principles that could lessen postpartum-like depression. Some studies have reported similar antidepressant-like potential of Hypericum perforatum (Vieira *et al*., 2013), methanol root bark extract of Securinega virosa (Shehu *et al*., 2017) and folic acid (Zhang *et al*., 2021) at postpartum in rodent.

The results of EPM and LDB showed that JT-treated dams exhibited a preference for the open arm of the EPM and the light arm of the LDB. This behaviour is considered an anxiolytic-like profile (Habr *et al*., 2011, La-Vu *et al*., 2020). Habr *et al*., (2011) reported that dams exhibited decreased time spent in the open arms of the EPM. Nic Dhonnchadha *et al*., (2003) reported that dams with less anxiety-like level tend to venture more into the open arm of the EPM and the light arm of the LDB. According to Kraeuter *et al*., (2019), the avoidance of the open arm in EPM is an indicative of anxiety-like activity, while less anxiety-like animals tend to explore the environment more. The JT-treated dams made higher transitions between the brightly illuminated area and the dark arm of the LDB. Miller *et al*., (2011) reported that rodents exhibiting higher anxiety-like levels make fewer transitions between chambers in the LDB. Similarly, anxiolytic-like potential of Hypericum perforatum (Vieira *et al*., 2013) and folic acid (Zhang *et al*., 2021) at postpartum in rodent was reported.
Studies have conclusively linked results from OFT with other measures of anxiety in rodent models (Seibenhener and Wooten 2015)). Miller *et al*., (2011) reported that convergence of results among multiple behavioural paradigms would increase assurance about the most relevant influences on postpartum anxiety-like behaviour. Studies comparing locomotor activities between dams and virgin rats in OFT reported that dams exhibited decreased locomotion (Silva *et al*., 1997), while Habr *et al*., (2011) observed decreased locomotion and rearing frequency in dams suggesting increased anxiety-like and emotionality behaviour. The aqueous leaf extract of JT increased locomotor activity by increasing the frequency of line crossings and rearing in LDB and OFT as well as rearing frequency in EPM. Locomotor activity is considered as an index of alertness (Yadav *et al*., 2008). The high frequency of such behaviours indicates increased locomotion and exploration, and refers to a lower anxiety-like level (Zimcikovaa *et al*., 2017). Increase in line crosses, rearing and transition frequency in both LDB and OFT observed in JT is an indication of CNS stimulant properties (Harquin *et al*., 2012).

Several well-known antidepressants was reported to decrease locomotor activity (Shehu *et al*., 2017). Contrary to this study, the aqueous leaf extract of JT not only reduces postpartum-like depression, it as well increase locomotor activity. La-Vu *et al*., (2020) reported that rodents in all paradigms demonstrating an increase in SAP, defecation, and urination indicate greater anxiety-like behaviour. Results from EPM, OFT and LDB showed a reduction in these behaviours, FST also showed reduced defecation frequency signifying that JT was able to reduce anxiety-like behaviour. SAP is a good identifier for exploratory and anxiety-like conflict behaviour in rodent and can be used to evaluate the effects of medications at reducing these internal conflicts (Holly *et al*., 2016). JT was effective in reducing this conflict in dams. Defecation is a parameter that indicates an increase in emotionality (Habr *et al*., 2011), JT improved emotionality by reducing the frequency of defecation.

Holmes *et al*., (2003) reported that increase grooming and head dip in EPM and grooming in LDB specify increased anxiety-like levels. JT treated dams reduced these behaviours in EPM and LDB but did not reduce grooming in OFT. Silva *et al*., (1997) reported that an increase in anxiety may lead to a freezing that ultimately leads to a reduction in OFT locomotion activity. In this study the frequency and duration of freezing was significantly reduced. This may be due to the effect of JT in lessening postpartum-like anxiety thereby increasing locomotor activity.

In this study, JT treated dams showed increased CSE and the duration of time spent in the central square. Brown *et al*., (2004) reported that high frequency/duration of these behaviours indicates high exploratory behaviour and low anxiety-like levels.

The percentage alternations was not significantly different in the JT group compared to control. The result index of discrimination in NORT can vary between +1 and -1, where a positive score indicates more time spent with the novel object, a negative score indicates more time spent with the familiar object, and a zero score indicates a null preference (Burke *et al*., 2010). Index of discrimination for STM in NORT showed a positive score in JT group compared to negative in control suggesting better cognitive function. Index of discrimination for LTM was not significant in JT group compared to control. Investigation of STM during index of habituation did not differ significantly, while LTM showed a positive score in JT group compared to control. This index and T-Maze percentage alternation however did not differ between control and JT group indicating no change in retention and hence memory.

Nest building is a common behavior in rodents, at the same time it is a kind of maternal behavior and a social behavior, associated with maintaining body temperature. The treated dam had a higher nesting score which means they showed higher interaction and building of nest.

The index of pain is measured via the escape behavior, withdrawal reflexes, licking behaviors and vocalization of these rodents which becomes the substitute for human pain

experiences in animal models (Negus *et al*., 2006). JT altered latency to painful thermal stimulus TFT. The extension of the latency time in the TFT is related to the central analgesic effect of administered drugs (Negus *et al*., 2006). Thus, this study suggest that the extracts may modulate central nociceptive pathways.

In conclusion, the result shows that aqueous leaf extract of JT has a therapeutic effect that reduces postpartum-like depression and anxiety, and possess CNS stimulant effect with improve locomotor activity in dams. This may be developed as a preventive and adjuvant therapeutic option for pregnant women.

Acknowledgement

Authors hereby acknowledge William Sunday William, Chidi Erengwa Chiozoadighi, Ugi Emmanuel and God-knows Edith for their kind assistance in the laboratory.

REFERENCES

Agarwal, S.P., Rajesh, K., Ritesh, K., Khalid, M.D. and Roop, K.K. (2007). Shilajit: a review. Phytother Res; 21(5): 401-5.

Ajiwhen, I.O. and Bisong, S.A. (2013). Effect of ethanolic extract of Carpolobia lutea G. Don

(polygalaceae) root on learning and memory in CD1 mice. Niger J Physiol Sci; 28, 141–145.

Albin-Brooks, C., Nealer, C., Sabihi, S., Haim, A. and Leuner, B. (2017). The influence of offspring, parity, and oxytocin on cognitive flexibility during the postpartum period. Horm Behav; 89, 130–136.

Albuquerque, U.P., Monteiro, J.M. and Araujo, E.L. (2005): Taninos: Uma abordagem da quimica a ecologia. Qwim Nova; 28, 892-896.

Ali, N.S., Mahmud, S., Khan, A. and Ali, B.S. (2013). Impact of postpartum anxiety and depression on child's mental development from two peri-urban communities of Karachi, Pakistan: a quasi-experimental study. BMC Psychiatry; 13(1): 274.

Antunes, M. and Biala, G. (2012). The novel object recognition memory: neurobiology, test procedure, and its modifications. Cogn Process; 13(2): 93-110.

Bisong, S.A., Brown R. and Osim, E.E. (2010). Comparative effects of Rauwolfia vomitoria and chlorpromazine on locomotor behaviour and anxiety in mice. Journal of Ethnopharmacology; 132: 334–339.

Bisong, S.A., Okon. U.A, Chukwu, J.A.O., Sanya, O.A., Akinnuga, M.A. and Unirere, G.N. (2017). Long term consumption of coconut oil diet increased anxiety related behaviour in CD1 mice. Journal of Complementary and Alternative Medical Research; 2(1):1-13.

Bribi, N., Belmouhoub, M.B. and Maiza, F. (2017). Analgesic and anti-inflammatory activities of ethanolic extract of fumaria capreolata. Phytothérapie; 15(4): 211-216.

Brown, R.E., Gunn, R.K., Schellinck, H.M., Wong A.A. and O'Leary, T.P. (2004). MPD: Brown1 Mouse phenome database web site. The Jackson Laboratory; Bar Harbor, Maine USA: Anxiety, exploratory behavior, and motor activity in 14 inbred strains of mice.

Cárdenas, E.F., Kujawa, A. and Humphreys, K.L. (2020). Neurobiological changes during the peripartum period: implications for health and behavior. Social Cognitive and Affective Neuroscience; 1097–1110.

Contreras, M.D., Bribi, N., Gomez-Caravaca, A. and Antonio, J.G. (2017). Alkaloids profiling of fumaria capreolata by analytical platforms based on the hyphenation of gas chromatography and liquid chromatography with quadrupole-time-of-flight mass spectrometry. International Journal of Analytical Chemistry; 5178729: 1-16.

Cook, N.C. and Samman, S. (1996). "Review: flavonoids-chemistry, metabolism, cardio-protective effects and dietary sources," Journal of Nutritional Biochemistry; 7(2): 66–76.

Deacon, R.M.J. (2006). Assessing nest building in mice. Nat Protoc; 1: 1117–1119.

Eisenach, J.C., Pan, P.H., Smiley, R., Lavand'homme, P., Landau, R. and Houle, T.T. (2008). Severity of acute pain after childbirth, but not type of delivery, predicts persistent pain and postpartum depression. Pain; 140:87–94.

Englisch, S., Knopf, U., Scharnholz, B., Kuwilsky, A., Deuschle, M. and Zink M. (2009). Duloxetine for major depressive episodes in the course of psychotic disorders: an observational clinical trial. Journal of Psychopharmacology; 23(8): 875-882.

Éverton, R.Q.S., Cristiane, S.F.M., Enéas, A.F.J., Ademar, S.M., Bruno, G.P. and José G.S.M. (2018). Linalool-rich essential oils from the Amazon display antidepressant-type effect in rodents. J Ethnopharmacol; 212: 43-49.

Falodun, A., Udu-Cosi, A.A., Erharuyi, O., Imiege, V., Falodun, J.E., Agbolanhor, O. and Hamann, M. T. (2013). *Jatropha tanjorensis* – Review of Phytochemistry, Pharmacology and Pharmacotherapy. Journal of Pharmaceutical and Allied Sciences; 10(3): 1955-1964.

Feng, Z., Norio, N. and Teruaki A. (2006). Pharmacokinetics of berberine and its main metabolites in conventional and pseudo germ-free rats determined by liquid chromatography/ion trap mass spectrometry. Drug Metabolism and Disposition; (34): 2064–2072.

Field, T. (2017). "Postpartum anxiety prevalence, predictors and effects on child development: a review," Journal of Psychiatry and Psychiatric Disorders; 1(2): 86–102.

Grant, K.A., McMahon, C. and Austin, M.P. (2008). Maternal anxiety during the transition to parenthood: a prospective study. Journal of Affective Disorders; 108: 101–111

Habr, S.F., Bernardi, M.M., Conceição, I.M. Freitas, T.A. and Felicio, L.F. (2011). Open field behavior and intra-nucleus accumbens dopamine release in vivo in virgin and lactating rats. Psychology and Neuroscience; 4(1): 115 – 121.

Harquin, S.F., David, E.T., Armand, A.B. and Lucian, H. (2012). Anxiolytic and Antidepressant-Like Effects of the Aqueous Extract of Alafia multiflora Stem Barks in Rodents. Advances in Pharmacological Sciences; 1-8.

Holly, K.S., Orndorff, C.O. and Murray, T.A. (2016). MATSAP: An automated analysis of stretch-attend posture in rodent behavioral experiments. Scientific Reports; 6:31286

Holmes, A., Kinney, J.W., Wrenn, C.C., Li, Q., Yang, R.J. and Ma, L. (2003). Galanin GAL-RI receptor null mutant mice display increased anxiety-like behaviour specific to the elevated plus maze. Neuropsychopharmacol; 28(6): 1031-1044.

Iroanya, O.O., Egwuatu, T.F., Chukwudozie, O.F., Tolupo, D. and Adesanya, A. (2018). Hepato-nephroprotective, hematopoietic and anti-spermatogenic effect of the ethanolic extract of *Jatropha tanjorensis* using Male albino rats. European Journal of Biomedical and Pharmaceutical Sciences; 5(7): 121-130.

Kraeuter A.K., Guest, P.C. and Sarnyai, Z. (2019). The Elevated Plus Maze Test for Measuring Anxiety-Like Behavior in Rodents: Techniques and Protocols. Methods in molecular Biology; 1916:69-74.

La-Vu, M., Tobias, B.C., Schuette, P.J. and Adhikari, A. (2020). To Approach or Avoid: An Introductory Overview of the Study of Anxiety Using Rodent Assays. Frontiers in Behavioral Neuroscience; 14:145.

Lim, G., Farrell, L.M., Facco, F.L., Gold, M.S. and Wasan, A.D. (2018). Labor analgesia as a predictor for reduced postpartum depression scores: a retrospective observational study. Anesth Analg; 126:1598–605.

Lorke, D. (1983). A new approach to tropical acute toxicity testing. Archiv Toxicol; 53: 275-287.

Madubuike, K.G., Yusuf, N.O. and Ibekwe, A. M. (2015). Hepatoprotective activity of methanolic extract of *Jatropha tanjorensis* in carbon tetrachloride– induced hepatotoxicity. Archives of Applied Science Research; 7(5): 45-48.

Maldonado, R.J. and De Jesus, O. (2001). Hyperesthesia. StatPearls [internet]. Treasure Island (FL). StatPearls publishing.

Miller, S.M, Piasecki, C.C and Lonstein, J.S. (2011) Use of the light-dark box to compare the anxiety-related behavior of virgin and postpartum female rats. Pharmacol Biochem Behav; 100(1): 130-137.

Negus, S.S., Vanderah, T.W. Brandt, M.R., Bilsky, E.J. Becerra, L. and Borsook, D. (2006). Preclinical assessment of candidate analgesic drugs: Recent advances and future challenges. Journal of Pharmacology and. Experimental Therapeutics; 319: 507–514

Nic Dhonnchadha, B.A., Bourin, M. and Hascoet, M. (2003). Anxiolytic-like effects of 5-HT2 ligands on three mouse models of anxiety. Behav Brain Res; 140, 1-2, 203–214.

Nindaratnasari, (2017). 15 Top Benefits of Jatropha Leaves. DrHealthBenefits.com

Oyewole, I.O., Magaji, Z.J. and Awoyinka, O.A. (2012). Biochemical and toxicological studies of aqueous extract of Tethonia diversifolia (Hemsel) leaves in Wistar albino rats. Journal of Medicinal Plants Research; 1: 30-33.

Postma, I.R., de Groot, J.C., Aukes, A.M., Aarnoudse, J.G. and Zeeman, G.G. (2014). Cerebral white matter lesions and perceived cognitive dysfunction: the role of pregnancy. American Journal of Obstetrics and Gynecology; 211: 257.e1–257.e5.

Qiu, T., Wen, H., Liu, Z., Pan, X. and Zeng, T. (2021). Investigation Regarding Early Cognitive Function of Women in the Postpartum Period and the Analysis of Influencing Factors. Scientific and Medical Research; 14:3747-3754.

Quesada, C., Kostenko, A., Ho, I., *et al*. (2021). Human surrogate models of central sensitization: a critical review and practical guide. European Journal of Pain; 25:1389–428.

Sanchez-Mateo, C.C., Bonkanka, C.X., Hernandez-Perez, M. and Rabanal, R.M. (2006). Evaluation of analgesic and topical anti-inflammatory effects of Hypericum reflexum L. J. Ethnopharmacol; 107: 1-6.

Seibenhener, M.L., and Wooten, M.C. (2015). Use of the Open Field Maze to Measure Locomotor and Anxiety-like Behavior in Mice. J Vis Exp; e52434

Shehu, A., Magaji, M.G., Sanni, B. and Abdu-Aguye, S.N. (2017). Antidepressant Activity of Methanol Root Bark Extract of Securinega Virosa (Ex Willd) Bail in Albino Mice. Bayero Journal of Pure and Applied Sciences; 10(2): 277-282

Shimoda, S., Ozawa, T., Ichitani, Y. and Yamada, K. (2021). Long-term associative memory in rats: Effects of familiarization period in object-place-context recognition test. PLoS ONE; 16(7): e0254570

Silva, M.R.P., Bernardi, M.M., Nasello, A.G. and Felicio, L.F. (1997). Influence of lactation on motor activity and elevated plus maze behavior. Brazalian Journal of Medicinal and Biological Research; 30:241-244.

Sivakumar, G., Vidyadhara, D.J., Shivananda, K.N., Rajesh, T., Mohandas-Rao, K.G. and Rai, K.S. (2017). Prophylactic Choline Supplementation Attenuates Vascular Cognitive Impairment in Rodent Model of Ischemic Stroke. Indian J Physiol Pharmacol; 61(3): 246-255.

Slomian, J., Honvo, G., Emonts, P., Reginster, J.Y. and Bruyere, O. (2019). "Consequences of maternal postpartum depression: A systematic review of maternal and infant outcomes," Women's Health; 15: 1–55.

Sudipta, S., Tanmoy, G., Tanushree, S. and Tapan, K.M (2013). "Evaluation of Analgesic and Anti-Inflammatory Activity of Chloroform and Methanol Extracts of Centella asiatica Linn", International Scholarly Research Notices; 6.

Sutulovic N, Grubac Z, Suvakov S, *et al*. (2021). Experimental Chronic Prostatitis/Chronic Pelvic Pain Syndrome Increases Anxiety-Like Behavior: The Role of Brain Oxidative Stress, Serum Corticosterone, and Hippocampal Parvalbumin-Positive Interneurons. Oxidative Med. Cell. Longevity; 17.

Topiwala, A., Hothi, G. and Ebmeier, K.P. (2012). Identifying patients at risk of perinatal mood disorders. Practitioner; 256: 15–18, 12.

Vanzella, C., Bianchetti, P., Sbaraini, S., Vanzin, S.I., Melecchi, M.S., Caramão, E.B. and Siqueira, I.R. (2012). Antidepressant-like effects of methanol extract of Hibiscus tiliaceus flowers in mice. Biomedical Central Complementary and Alternative Medicine; 12:41

Vieira, V.A., Camposa, L.V., Silva L.R., Guerraa, M.O., Peters, V.M. and Sá, R.S. (2013). Evaluation of postpartum behaviour in rats treated with Hypericum perforatum during gestation. Revista Brasileira Farmacognosia; 23: 796-801

Yadav, A.V. Kawale, L.A. and Nade, V.S. (2008). "Effect of Morus alba L. (mulberry) leaves on anxiety in mice," Indian J Pharmacol; 40, (1), 32–36.

Yam, M.F., Loh, Y.C., Oo, C.W. and Basir, R. (2020). Overview of Neurological Mechanism of Pain Profile Used for Animal "Pain-Like" Behavioral Study with Proposed Analgesic Pathways. Int J Mol Sci; 21, 4355.

Zhang Q, Huang Q, Yao L, *et al*. (2021). Gestational Folic Acid Administration Alleviated Maternal Postpartum Emotional and Cognitive Dysfunction in Mice. Front Pharmacol; 12:701009.

Zimcikovaa, E., Simkob, J., Karesovac, J., Kremlacekd, J. and Malakova, J. (2017). Behavioral effects of antiepileptic drugs in rats: Are the effects on mood and behavior detectable in open-field test? Seizure; 52:35–40.

Niger. J. Physiol. Sci. 38 (December 2023): 223 – 227
www.njps.physiologicalsociety.com

Niger. J. Physiol. Sci.

Research Article

Antidepressant-Like Effects of *Cinnamomum verum* on Open-Space Forced Swim-Induced Depression in Mice

Hanafi, A.A., *Yusha'u, Y., Benjamin, J., Muhammad, U.A., Idris, B., Adams, E.D., Idris, A.O., Eneji, F.O., Haruna, I.I., and Imam, A.I.

Department of Human Physiology, Faculty of Basic Medical Sciences, College of Medical Sciences, Ahmadu Bello University, Zaria-Nigeria

Summary: Depression is a mental disorder characterized by depressive episodes, such as low mood, low self-esteem, feeling of guilt, and poor concentration. Depression has a high comorbidity with cognitive impairments. Studies have shown that cinnamon has anti-inflammatory antiviral, antihypertensive, antioxidant and anti-diabetic potentials. Therefore, the aim of the research was to assess the antidepressant effect of cinnamon on open-space forced swim-induced depression in mice. Twenty-five (25) Swiss albino mice were grouped into five groups (n=5). Group I: control (negative control) exposed to open-space forced swim test (OSFST) without any treatment, Groups II, III and IV received graded doses of Cinnamon 12.5, 25, and 50 mg/kg, group 5 (positive control) received fluoxetine 20 mg/kg orally. The animals were subjected to OSFST, Open Field Test (Line Crossing) and Novel Object Recognition Test (NORT). Administration of cinnamon showed decreased immobility time (behavioural despair) in OSFST compared to control and fluoxetine groups ($p < 0.05$). However, no statistically significant effect was observed in line crossing (locomotor activity) and the discrimination ratio of NORT (non-spatial short-term memory) between cinnamon administered groups and the control group. In conclusion, cinnamon has shown antidepressant-like effect in open-space forced swim-induced depression in mice.

Keywords*: Cinnamon, Depression, Cognitive impairment, Immobility time, Behavioural despair*

**Address for correspondence*: yusufshau@gmail.com, *Tel: +234-8100872166*

Manuscript received- January, 2023; Accepted: July, 2023

DOI: https://doi.org/10.54548/njps.v38i2.11

INTRODUCTION

Depression is a common mental disorder, characterized by persistent sadness and also loss of interest in pleasurable activities that the individual once enjoyed as well as behavioural despair (WHO,2017; Yusha'u *et al.*., 2017). It also affects sleep and appetite together with extreme fatigue (Calheiros *et al.*., 2016; Yusha'u *et al.*., 2021). One in four people in the world is affected by mental disorders or neurological disorders at some point in their lives (Simplice *et al.*., 2014). Almost 450 million people currently suffer from such conditions, this makes mental disorders to be among the leading cause of ill-health and disability worldwide (Simplice *et al.*., 2014). In Africa, about 29.19 million people suffer from depression, with over 7 million in Nigeria (Gbadamosi *et al.*., 2022). Furthermore, a comorbid condition associated with depression is anxiety, together, these two are debilitating conditions that greatly impair psychological, social, and emotional wellbeing (Kalin, 2020).

Depression often leads to cognitive impairment due to a reduced level of neurotransmitters like acetylcholine and increased levels of cytokines such as interleukin (IL)-1, IL-6 and tumour necrosis factor alpha (TNF-α) that control mood in the brain (Mustapha *et al.*., 2021). It was found that prolonged therapy with some antidepressants like SSRI's may be associated with cognitive side effects in adult subjects with MDD (Bortolato *et al.*., 2016). Several oxidative disturbances in depression have been reported in clinical and preclinical studies, including lipid peroxidation, decrease catalase (CAT) and superoxide dismutase (SOD) activities which were often associated with serotonergic and noradrenergic systems dysfunctions (Calheiros *et al.*., 2016). In depressed patients peripheral blood sample, increase in granulocytes and macrophage have been reported which was associated with the increase in pro-inflammatory cytokines levels commonly seen in depressed patients (Dowlati *et al.*., 2010).

Cinnamomum verum (Cinnamon) the eternal tree of tropical medicine, belongs to the Lauraceae family. Cinnamon is one of the most important spices used daily by people all over the world is commonly found in cooking ingredients worldwide and is believed to provide health benefits. Cinnamon contains various chemical compounds like flavonoid and terpenoid that work as an antidepressant via influencing BDNF synthesis and secretions, and exerting anti-inflammatory and anti-oxidant effects (Jana *et al.*., 2013). The most common and effective class of antidepressants used is the selective serotonin reuptake inhibitors (SSRI's) which include fluoxetine, paroxetine and

citalopram. They replaced the tricyclic antidepressants class due to less toxicity and other side effects(Khawam, 2006; Brent, 2016;). However, side effects reduce compliance to SSRI's usage; some of these side effects include ideation of suicide, anxiety, insomnia, erectile dysfunction and nightmares (Yaseen and Mohammed, 2020). Scientific reports showed that cinnamon extract has neuro-protective, hepato-protective, cardio-protective, gastro-protective, and anti-inflammatory properties due to its phenolic acid and flavonoid compounds (Santos and Guilherme, 2018; Prabhashini *et al.*., 2019).

Cinnamaldehyde is the major component of cinnamon amongst other components. Cinnamaldehyde metabolism in the body produces sodium benzoate (NaB) metabolite, where NaB is thought to be able to increase BDNF expression in rat (Jana *et al.*., 2013). Proanthocyanidin is proved to be protective against depression and anxiety, where it has antidepressant activity by increasing BDNF expression in the hippocampus and frontal cortex of chronically stressed mice (Martinowich and Lu, 2008). Hence, the aim of this study is to assess the effects of aqueous bark extract of cinnamon on depression and non-spatial short-term memory in mice.

MATERIALS AND METHODS

Drugs and Reagents: *Cinnamomum verum* was purchased from Arabian-Syrian Company, South City Plaza, Selangor, Darul-Ehsan, Malaysia. Fluoxetine was purchased from VS International Private Limited Plot Number 17 and 18, Golden Indl estate Somnath Road, Dabhel, Daman-396215, India. Marketed by Fidson Healthcare Private Limited Company, 268, Ikorodu Road, Obanikoro, Lagos-Nigeria. NAFDAC registration number: 04-8881.

Aqueous bark extraction of Cinnamomum verum: The aqueous bark extract of *Cinnamomum verum* was prepared according to the method of Abdeen *et al.*. (2018), with some modifications. Cinnamon bark 500 g was grinded to powder form to reduce its size. The powder form of cinnamon bark was dissolved in 3 litres of water for 24 hours to avoid fermentation. The dissolved *Cinnamomum verum* bark was then filtered and the residue was removed. The water content was evaporated so as to get the solid aqueous form of cinnamon.

Experimental Design; Twenty-five (25) healthy Swiss albino mice (18-26 g) of both sexes aged 6-8 weeks were purchased from the Animal House, Department of Human Physiology, Faculty of Basic Medical Sciences, Ahmadu Bello University (A.B.U) Zaria-Nigeria. They were housed in plastic cages containing sawdust bedding and fed with pellets made from grower's mash, maize offal as binder and water ad libitum. Ethical clearance was obtained from Ahmadu Bello University Committee on Animal Use and Care with Approval Number: ABUCAUC/2021/008. The animals were grouped into five groups. Each group consisting of five mice (n=5). Daily administration of aqueous bark extract of cinnamon was carried for 2 weeks via oral route. Group I were exposed to OSFST without any treatment (Negative control). Groups II, III and IV were administered graded doses of aqueous bark extract of cinnamon 12.5 mg/kg, 25 mg/kg and 50 mg/kg respectively (Parisa *et al.*., 2020), While Group V, were treated with fluoxetine 20 mg/kg (Positive control) (Hu *et al.*., 2016).

Neurobehavioural Assays

Open-space forced swim test: The open space forced swim test was conducted as described in Figure 1 (Yusha'u *et al.*., 2021)

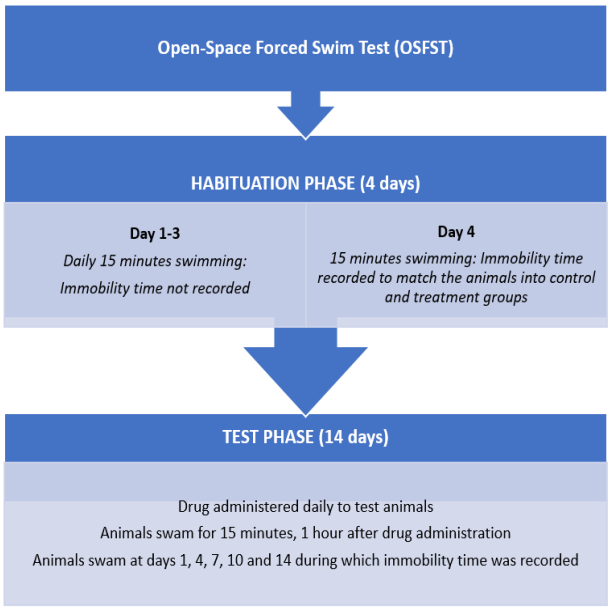

Figure 1:
Schedule for open-space forced swim test (Yusha'u *et al.*., 2021)

Determination of Line crossing using open field test: Line crossing (an index of locomotor activity) occurs when the mouse crosses one of the grid lines which separate the squares in the open field with all four limbs (Bagewadi *et al.*., 2015). This is a parameter observed by conducting the open field test with an open field test apparatus (50-L × 50-W × 30-H cm). The floor of the apparatus is compartmentalized into 5 × 5 = 25 square areas (10 cm square × 25) and central 4 × 4 = 16 square areas are considered as the central part. Before the testing phase, the mouse was placed at the centre of the floor space and allowed to acclimatize to the surrounding area for 2 minutes. Thereafter, mice were placed into the apparatus from the left-hand corner and allowed to move freely to explore the open field arena (test session) individually for 5 min (Bagewadi *et al.*., 2015).

Measurement of non-spatial short-term memory using novel object recognition test: The novel object recognition test (NORT) apparatus is used in the assessment of non-spatial short-term memory. The apparatus is a rectangular arena that is made up of opaque plastic and measures 42 cm × 52 cm. The walls are 40 cm high. It involves two phases: training and testing (Zhang *et al.*., 2012). The mouse is placed in the arena for 5 minutes, where it encountered two identical sample objects (testing phase). At the end of the training phase, the mouse was placed back in its home cage for a 5minutes delay (±15 seconds) and the NORT apparatus with the objects wiped with 70% ethanol to avoid olfactory cue. For the testing phase, animals were returned to the arena for 3 minutes where one of the familiar objects was replaced with a novel object. Successful novel object

recognition is indexed by greater exploration of the novel object compared to the familiar object. The discrimination ratio was calculated as the total time spent exploring the recently seen object (novel object) divided by the time exploring both objects sampled at the test (familiar objects) (Thur *et al.*., 2014).

Statistical analysis: Results were expressed as Mean ± SEM. All analysis were done using one way analysis of variance (ANOVA), except data for OSFST which was analysed by two-way repeated measures ANOVA and time spent on familiar and novel objects in NORT analysed by independent sample T-test. Where significance, Tukey's post-hoc test was conducted for multiple comparison using GraphPad prism version 8.0.2. for windows. Values of $p < 0.05$ were considered statistically significant.

RESULTS

Depression analysis using open space forced swim test: Two-way repeated measures ANOVA was conducted to access the effects of treatments and time on immobility time as a depression index. There was no statistically significant effect of time on the different treatment groups [F (3.004, 60.07) =2, p = 0.05]. There was interaction between the treatments and time [F (16,80) = 8.05, $p < 0.001$]. Similarly, significant effects were observed between treatment groups [F (4,20) = 21.0, $p < 0.001$]. At day 1, the immobility time was decreased in CN 50 mg/kg group when compared with untreated negative control group. At day 4, the immobility time was decreased in CN 12.5 mg/kg and fluoxetine group when compared with the negative control group. At day 14 all the treatment groups had less immobility time when compared with the negative control group.

Assessment of locomotor activity with open field test: As shown in Figure 3, one-way ANOVA revealed no statistically significant ($p > 0.05$) difference in frequency of line crossing (an index of locomotor activity) between all the treatment groups when compared with the OSFST untreated negative control group.

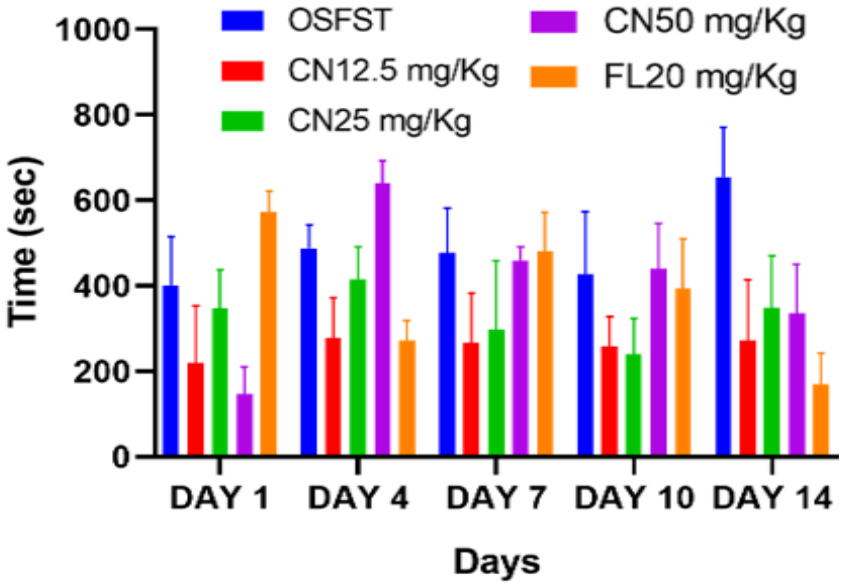

Figure 2: Effects of aqueous bark extract of cinnamon on depression in mice exposed to open-space forced swim test. Results expressed as mean ± SEM, (n=5), * showed statistically significant difference compared to control. # Showed statistically significant different when compared with fluoxetine, CN= Cinnamon, Flu= fluoxetine.

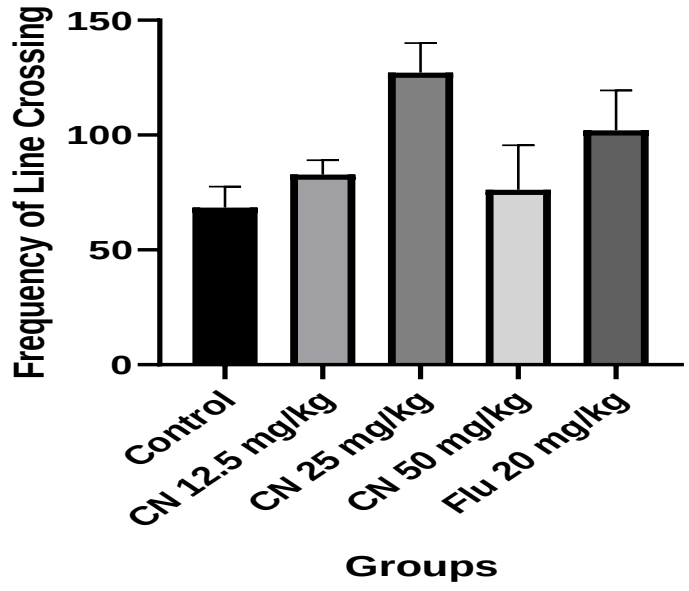

Figure 3: Effects of aqueous bark extract of cinnamon on locomotor activity in mice exposed to open-space forced swim test using open field test. Results presented as mean SEM: The mean difference was not statistically significant different $p > 0.5$ (n=5), using one-way ANOVA, Graph pad prism version 8.0.2, CN: Cinnamon, Flu: Fluoxetine.

Table 1:
Effects of aqueous bark extract of cinnamon on time spent on familiar and novel objects using novel object recognition task in mice subjected to open-space forced swim test

Groups	Time Spent on Familiar Object (Seconds) Mean ± SEM	Time Spent on Novel Object (Seconds) Mean ± SEM	P-value	t-value
Control	2.8 ± 0.97	4.0 ± 1.38	0.497	0.712
CN 12.5 mg/kg	5.8 ± 2.44	3.2 ± 0.73	0.337	1.021
CN 25 mg/kg	5.2 ± 2.44	9.0 ± 1.70	0.237	1.278
CN 50 mg/kg	2.0 ± 2.00	3.6 ± 1.47	0.537	0.645
Flu 20 mg/kg	2.4 ± 0.51	3.0 ± 0.71	0.511	0.688

Results presented as mean ± SEM, (n=5) using independent sample t-test, Graph pad prism version 8.0.2. CN: Cinnamon, Flu: Fluoxetine, OSFST: Open-Space Forced Swim Test

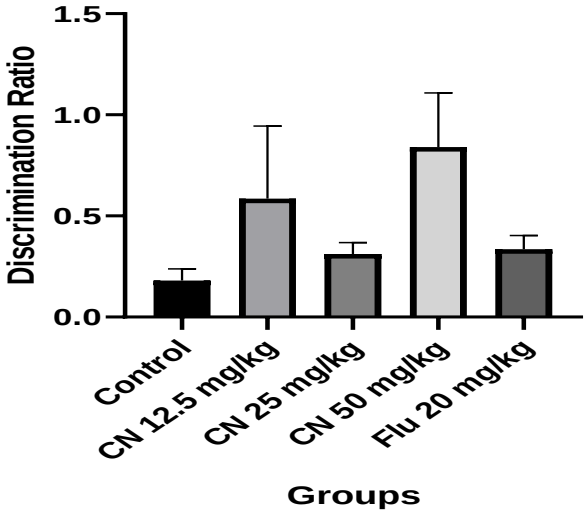

Figure 4:
Effect of aqueous bark extract of cinnamon on discrimination ratio in mice exposed to open-space forced swim test using novel object recognition task.
Results presented as mean ± SEM, (n=5), the mean difference is not statistically significant compared to the control group using one-way ANOVA, Graph pad prism version 8.0.2, CN: Cinnamon, Flu: Fluoxetine.

Assessment of non-spatial short-term memory: The discrimination ratio (an index of short-term memory) did not differ significantly ($p > 0.05$) between the treatment groups and the untreated OSFST group as revealed by one-way ANOVA (Figure 4). Similarly, as shown in Table 1, independent sample T-test showed no statistically significant ($p > 0.05$) difference between time spent on the novel object when compared with the familiar object of the NORT in all the treatment groups as well as the OSFST negative control group.

DISCUSSION

Depression is a common mental disorder, characterized by persistent sadness and also loss of interest in pleasurable activities that the individual once enjoyed as well as behavioural despair (WHO,2017; Yusha'u *et al.*., 2017). This study observed a decreased in immobility time (an index of depression) in OSFST induced-depressed mice treated with CN 12.5 mg/kg, CN 50 mg/kg and Flu 20 mg/kg in swimming days 1, 4, 7 and 14 when compared with control. The findings of this study is in conformity with the study of Parisa *et al.*., (2020) that stated cinnamon possessed the potential to reduce the duration of immobility and potentially reduce symptoms of depression. The main compound contained in cinnamon is cinnamaldehyde, which is a phenol group. Phenols have anti-inflammatory effects, which are believed to be able to inhibit the inflammatory cascade that forms the basis of the pathogenesis of depressive disorders (Partan *et al.*., 2018). Furthermore, Sohrabi *et al.*. (2017) conducted a depressive-like behaviour test using cinnamon essential oil. They observed significant improvements in the immobility time during forced swim test (FST) and tail suspension test (TST).

The study also showed no difference in frequency of line crossing (an index of locomotor activity) between all the treatment groups when compared with the OSFST untreated negative control group. The locomotor activity was used to screen out antidepressants from psychotonics or psychostimulants. Antidepressants do not significantly improve line crossing in OFT while psychotonics or psychostimulants like amphetamine does so. This is in conformity with the study of Yusha'u *et al.*. (2021) and previous report of Cryan *et al.*. (2005) who reported that psychotonics are clinically ineffective antidepressants. They show anti-immobility effects in the TST but increase locomotor activity. Psychostimulants are a broad class of sympathomimetic drugs (Wood *et al.*., 2014). Psychostimulants are the most used psychotropic substances over the world. A psychostimulant can be defined as a psychotropic substance with the capacity to stimulate central nervous system. It causes excitation and elevated mood, as well as increased alertness and arousal. Its global effect is to speed up signals into the brain. Some examples of psychostimulants include amphetamine, cocaine, nicotine, caffeine (Favrod-coune & Broers, 2010).

The result of discrimination ratio showed that cinnamon and fluoxetine did not differ significantly with the OSFST only group. Contrary to (Kawatra and Rajagopalan, 2015; Kelestemur *et al.*., 2016) findings which states that cinnamon also exerts strong brain protective and pro-cognitive effects in various models of neurodegeneration. In addition, according to Modi *et al.*. (2016), oral administration of cinnamon and sodium benzoate (NaB) increased memory consolidation-induced activation of cAMP- response element binding protein (CREB) and expression of plasticity-related molecules in vivo in the hippocampus of poor learning mice and improved their memory and learning almost to the level observed in untreated good learning ones.

In conclusion aqueous bark extract of cinnamon shows an antidepressant-like effect on depressed mice exposed to OSFST but did not significantly affect non-spatial short-term memory and locomotor activity of the mice subjected to NORT and OFT respectively. However, there is need for further research on the effect of cinnamon on the brain biomarkers of depression and cognition.

REFERENCES

Abdeen, A., Abdelkader, A., Abdo, M., Wareth, G., Aboubakr, M., Aleya, L., and Abdel-Daim, M. (2018). Protective effect of cinnamon against acetaminophen-mediated cellular damage and apoptosis in renal tissue. *Environmental Science and Pollution Research*, 26(1): 240-249. https://doi.org/10.1007/s11356-018-3553-2

Bagewadi, H. G., Ak, A. K., & Shivaramegowda, R. M. (2015). An Experimental Study to Evaluate the Effect of Memantine in Animal Models of Anxiety in Swiss Albino Mice. 2–6. https://doi.org/10.7860/JCDR/2015/13233.6287

Bortolato, B., Miskowiak, K. W., Köhler, C. A., Maes, M., Fernandes, B. S., Berk, M., & Carvalho, A. F. (2016). Cognitive remission : a novel objective for the treatment of major depression ? *BMC Medicine*, 1–18. https://doi.org/10.1186/s12916-016-0560-3

Brent, D. A. (2016). A n t i d e p re s s a n t s a n d Suicidality. *Psychiatric Clinics of NA*, 39(3), 503–512. https://doi.org/10.1016/j.psc.2016.04.002

Calheiros, M., Silva, C., Nádia, C., Sousa, S. De, Xavier, P., Gomes, L., Valente, G., Oliveira, D., Yvelize, F., Araújo, R., Coelho, N., Calheiros, J., Silva, G., Kalyne, L., Moreira, A., Macêdo, D., Maria, S., & Vasconcelos, M. (2016). Progress in Neuro-Psychopharmacology & Biological Psychiatry Evidence for protective effect of lipoic acid and desvenlafaxine on oxidative stress in a model depression in mice. *Progress in Neuropsychopharmacology & Biological Psychiatry*, 64,142–148. https://doi.org/10.1016/j.pnpbp.2015.08.002

Dowlati, Y., Herrmann, N., Swardfager, W., Liu, H., Sham, L., Reim, E. K., & Lanctôt, K. L. (2010). A Meta-Analysis of Cytokines in Major Depression. BPS, 67(5), 446–457. https://doi.org/10.1016/j.biopsych.2009.09.033

Favrod-coune, T., & Broers, B. (2010). The Health Effect of Psychostimulants: A Literature Review. 2333–2361. https://doi.org/10.3390/ph3072333

Hu, B., Doods, H., Treede, R., & Ceci, A. (2016). Neuroscience Letters Duloxetine and 8-OH-DPAT , but not fluoxetine , reduce depression-like behaviour in an animal model of chronic neuropathic pain. *Neuroscience Letters,* 619, 162–167. https://doi.org/10.1016/j.neulet.2016.03.019

Jana, A., Modi, K. K., Roy, A., Anderson, J. A., & Breemen, R. B. Van. (2013). Up-Regulation of Neurotrophic Factors by Cinnamon and its Metabolite Sodium Benzoate : Therapeutic Implications for Neurodegenerative Disorders. 739–755. https://doi.org/10.1007/s11481-013-9447-7

Kalin, N. H. (2020). The Critical Relationship Between Anxiety and Depression. May, 365–367. https://doi.org/10.1176/appi.ajp.2020.20030305

Kawatra, P., & Rajagopalan, R. (2015). Cinnamon : Mystic powers of a minute ingredient. 7, 1–6. https://doi.org/10.4103/0974-8490.157990

Kelestemur, T., Yulug, B., Burak, A., & Caglar, M. (2016). Neuroscience Letters Targeting different pathophysiological events after traumatic brain injury in mice : Role of melatonin and memantine. *Neuroscience Letters*, 612, 92–97. https://doi.org/10.1016/j.neulet.2015.11.043

Khawam, E. A. (2006). Side effects of antidepressants : An overview. 73(4).

Martinowich, K., & Lu, B. (2008). Interaction between BDNF and Serotonin : Role in Mood Disorders. 73–83. https://doi.org/10.1038/sj.npp.1301571

Mustapha, S., Oshafu, M. Y., Adam, U. M., Yusha'u, Y., & Daku, A. B. (2021). Influence of Antidepressant Medication on Short Term Memory in Chronic Mild Stress Mouse Model of Depression. 12(1), 22–28.

Parisa, N., Tamzil, N. S., Arroyantri, B., & Maritska, Z. (2020). Antidepresant effects of Cinnamon (*Cinnamomum burmannii*) extract in depressed induced rats using 3-minutes Tail Suspension method Antidepresant effects of Cinnamon (Cinnamomum burmannii) extract in depressed induced rats using 3-minutes Tail Suspension method. August 2019. https://doi.org/10.32539/bsm.v3i3.91

Partan, R. U. M. I., Hidayat, R., Saleh, M. G. S. I., Parisa, N., & Tanzil, N. I. A. S. (2018). Effect Of Supplementation Kayu Manis (Cinnamomum Burmannii) Extract In Neuronal Cell Death Protection In Wistar Rats Lir-Psychotic On Haloperidol Therapy. 11(2).

Santos, H. O., & Guilherme, A. R. (2018). Clinical Nutrition ESPEN To what extent does cinnamon administration improve the glycemic and lipid pro fi les ? Clinical Nutrition ESPEN, 1–9. https://doi.org/10.1016/j.clnesp.2018.07.011

Simplice, F. H., Emery, T. D., Abaissou, N., & Hervé, H. (2014). Enhancing Spatial Memory : Anxiolytic and Antidepressant Effects of Tapinanthus dodoneifolius (DC) Danser in Mice. 2014.

Thur, K. E., Nelson, A. J. D., & Cassaday, H. J. (2014). Ro 04-6790-induced cognitive enhancement : No effect in trace conditioning and novel object recognition procedures in adult male Wistar rats Pharmacology , Biochemistry and Behavior Ro 04-6790-induced cognitive enhancement : No effect in trace conditioning and novel object recognition procedures in adult male Wistar rats. November. https://doi.org/10.1016/j.pbb.2014.10.006

Wood, S., Sage, J. R., Shuman, T., & Anagnostaras, S. G. (2014). Psychostimulants and Cognition : A Continuum of Behavioral and Cognitive Activation. 15261(January), 193–221.

Yusha'u, Y., Muhammed, U. A., Nze, M., Egwuma, J. M., Igomu, O. J., and Abdulkadir, M. (2017). Modulatory Role of Rutin Supplement on Open Space Forced Swim Test Murine Model of Depression. 32(December), 201–205.

Yusha'u, Y, Mustapha, S., Umar, A. H., Imam, M. I., & Umar, B. (2021). Alpha-lipoic acid attenuates depressive symptoms in mice exposed to chronic unpredictable mild stress . 9(July), 58–68.

Yusha'u, Yusuf, Adam, U. M., Wahab, A. A., Ibrahim, M., & Saleh, A. (2021). OPEN ACCESS | RESEARCH NOTES Alpha-lipoic acid enhances short-term spatial memory of mice in open-space forced swim-induced depression mouse model.

Zhang, R., Xue, G., Wang, S., Zhang, L., Shi, C., & Xie, X. (2012). Novel Object Recognition as a Facile Behavior Test for Evaluating Drug Effects in A ␣ PP / PS1 Alzheimer ' s Disease Mouse Model. 31, 801–812. https://doi.org/10.3233/JAD-2012-120151.

Niger. J. Physiol. Sci. 38 (December 2023): 229 – 237
www.njps.physiologicalsociety.com

Niger. J. Physiol. Sci.

Full length Research Article

Methanolic Leaf Extracts of *Ricinus communis* Ameliorated Cardiovascular Dysfunction in Dichlorvos-exposed Rats

***Saka W.A., Moronkeji F.M., Akano F.M. and Adeshina O.S.**

Department of Physiology, Faculty of Basic Medical Science, Ladoke Akintola University of Technology, Ogbomoso, Oyo State, Nigeria

Summary: Cardiovascular diseases are the leading causes of death globally resulting in 17-19 million death every year. The search for an effective medicine to manage cardiovascular disorder without any side effect has led to the use of traditional based medicine. 75% of the world's population has been reported to depend on traditional medicine as their basic form of health care and this has resulted to the use of herbal medicine in the treatment and management of metabolic diseases. The study evaluated the effect of methanolic extract of *Ricinus communis* on DDVP-induced cardiotoxicity in male Wistar rats. Thirty-two (32) male Wistar rats were randomly divided into four groups of eight (8) rats each. Group A served as control rats, received 10mL/Kg of dimethyl sulfoxide (DMSO) and distilled water solution (vehicle) for six weeks. Group B served as DDVP-induced rats and were exposed to DDVP (15 minutes daily) for 3 weeks without any treatment. Group C rats received DDVP as in group B and then administered 300mg/kg of *R. communis* extract for 42days. While Group D rats were administered 300mg/kg of *R. communis* extract daily, for 6 weeks in addition to normal feed and water. Exposure to DDVP caused significant cardiac dysfunction evidence by alteration in cardiovascular variables and electrocardiac function, compromised lipid profile and reduced antioxidant enzymes. However, treatment with methanolic extract of *Ricinus communis* improved antioxidant defense system, attenuate hemodynamic impairment and left ventricular dysfunction, as well as inhibit lipid peroxidation and prevent hyperlipidemia in rats. In addition, histopathology observation showed that *Ricinus communis* extract was able to regenerate the myocardial injury caused by exposure to dichlorvos. In conclusion, *Ricinus communis* exhibited cardioprotective properties and may be a potential remedy for cardiovascular diseases with low risk of toxicity.

Keywords*: Cadiovascular diseases, Ricinus communis, cardiovascular variable, electrocardiac function, dichlorvos (DDVP)*

**Authors for correspondence: wsaka@lautech.edu.ng , Tel: +234-8063101718*

Manuscript received- May, 2023; Accepted- September, 2023

DOI: https://doi.org/10.54548/njps.v38i2.12

INTRODUCTION

Cardiovascular diseases (CVD) currently stand as the predominant cause of disability and mortality worldwide (WHO, 2017). In 2015, approximately 17 million deaths were attributed to cardiovascular diseases, accounting for 30% of the total global mortality (WHO, 2017). Among these deaths, 7.2 million resulted from heart attacks, and 5.7 million were due to stroke (Forreira, 2020). Notably, about 80% of these fatalities occurred in low and middle-income countries, affecting both men and women almost equally (Leone, 2015). Estimations suggest that if the current trend persists, by 2030, around 23.6 million people will succumb to cardiovascular diseases, primarily from heart attacks and strokes (Forreira, 2020). This positions cardiovascular diseases among the most prevalent non-communicable diseases (WHO, 2017).

Cardiovascular diseases encompass a broad spectrum of conditions that impact the cardiac muscles and/or vascular systems. This category includes coronary heart disease (heart attacks), cerebrospinal disease, hypertension, rheumatoid heart disease, peripheral artery disease, and heart failure (Forreira, 2020). Recognized potential risk factors for CVD comprise tobacco use, physical inactivity, elevated Low-Density Lipoprotein (LDL) Cholesterol, diabetes, and a constellation of interconnected metabolic risk factors (Cannon, 2007). The Framingham Heart Study, initiated in 1961, pioneered the concept of risk factors, establishing connections between high cholesterol, hypertension, tobacco usage, and diabetes mellitus with future cardiovascular diseases (Mahmood *et al*., 2014). Additionally, environmental toxic substances, including pesticides like dichlorvos, may influence novel risk pathways such as inflammation and oxidative stress (Anna, 2010). Consequently, ecological toxicants should be considered significant risk factors for cardiovascular disease (Mostafalou *et al*., 2013).

Dimethyl 2,2-dichlorovinyl phosphate, commonly abbreviated as DDVP, is an organophosphate (OP) insecticide and pesticide that exerts its toxic effects on humans and animals by inhibiting the enzyme acetylcholinesterase (USEPA, 2007). Due to its chemical properties, the most likely route of exposure to dichlorvos in human is through the inhalation of air contaminated with

it. Another reported route of exposure is through skin contact (with soil or surfaces contaminated with dichlorvos) or oral exposure by ingesting DDVP-contaminated food (USPH, 1995). Reported side effects resulting from acute exposure to DDVP are palpitations, nausea, vomiting, diarrhea, headache, fatigue, drowsiness, eye irritations and at very high concentrations, convulsions and coma (Saka *et al*., 2022a). Tests involving acute exposure of rats, mice, and rabbits have demonstrated that dichlorvos has high to extreme acute toxicity through oral, dermal, or inhalation exposure (WHO, 1992). Evidence from previous studies has revealed that organophosphates (OP) poisonings lead to cardiovascular abnormalities, such as alterations in the normal conducting activity and capacity of the heart, and ventricular arrhythmias expressed in electrocardiography (ECG) (Mostafalou and Abdollahi, 2013; Karki *et al*., 2004). Other risk effects of exposure to OP include neurotoxicity (Henshaw and Iwara, 2018), carcinogenicity (Greim *et al*., 2015), mutagenicity (Bhinder and Chaudhry, 2013), hepatotoxicity, and nephrotoxicity (Soboleve *et al*., 2021; Saka *et al*., 2022a).

The utilization of medicinal plants in traditional healing dates back to the origin of humanity (Ameh and Eze, 2010). Approximately two-thirds of the global population, primarily in developing countries, is estimated to depend on traditional medicine as their primary healthcare approach (Oladeji, 2016). The practice of traditional medicine remains prevalent in treating diseases in the African continent, attributed to the socio-cultural and socio-economic lifestyle of Africans, the lack of adequate basic healthcare facilities, and a shortage of qualified medical personnel (Singh *et al*., 2015). However, since the advent of civilization, medicinal plants have been an essential aspect of life (Singh *et al*., 2015). Globally, it is estimated that over 80,000 plant species have been utilized as medicinal plants. The significance of medicinal plants lies in their availability, relevance, acceptability, minimal side effects, and affordability.

Ricinus communis L. (*R. communis*), commonly known as the castor plant, is an erect, rapidly growing shrub characterized by dark red stems and can reach a height of about 6 meters. It is found across various continents worldwide, including the Arabian Peninsula, and has been cultivated for at least 6000 years (Scarpa and Guerci, 1982). The plant is often referred to as the castor oil plant due to the abundant oil that can be extracted from it (Chan *et al*., 2010). Many researchers believe it originated from Tropical Africa, and in Saudi Arabia, it is commonly known as Kherwa (Scarpa and Guerci, 1982). In Nigeria, it is called Laara or Ilarum/Iru by the Yorubas, Ogili Ugba or Ogili Isi by the Igbos, and Cika-gidaa by the Hausas (Toplak, 2005). *Ricinus communis* leaves have a historical therapeutic use spanning 4000 years, predominantly in herbal medicine for treating various diseases, disorders, and infections. All parts of *Ricinus communis* , including leaves, roots, bark, and various components, have been employed for medicinal purposes. The plant has been used as a laxative for over 2500 years in Greece and Rome (Scarpa and Guerci, 1982). Furthermore, *Ricinus communis* is utilized in the treatment of tumors and various diseases. Phytochemicals found in the castor plant include steroids, saponins, alkaloids, terpenoids, flavonoids, coenzyme Q10, vitamins A and E, and glycosides (Waseem *et al*., 2018). The combined effects of vitamin C and vitamin E have been observed to have a positive impact on carotid atherosclerosis (Shargorodsky *et al*., 2010). *Ricinus communis* has been reported to possess numerous medicinal properties (Waseem *et al*., 2018). However, there is paucity of information on the metabolic effect of *Ricinus communis* leaves extract on cardiovascular function and heart tissue disease. Hence, the medicinal properties of methanolic extract of the leaf on cardiovascular function parameters in DDVP-induced rats were investigated in this study.

MATERIALS AND METHODS

Animals: Thirty-two (32) male Wistar rats were used in this study. The animals were obtained from Animal House of the Department of Physiology, Ladoke Akintola University of Technology (LAUTECH), Ogbomoso. The animals ranged from 200 – 250g. They were acclimatized for 2 weeks under suitable environmental conditions (standard conditions of 12 hours light and dark cycles) and housed in plastic cages at the Animal House. They were fed with standard grower's mash rat pellets *ad libitum*, with care to avoid any unnecessary stress and cages kept clean and odor-free at all times.

Ethical Review: This study was approved by the Ethics Review Committee of the Faculty of Basic Medical Sciences, LAUTECH, Ogbomoso, with Ethic Number: FBMS/AEC/P/074/22.

Treatments

Group A: Control groups: rats were administered 10mls/kg of (DMSO and distill water, prepared at 1:19mls respectively) daily, for a period of 6 weeks.

Group B: DDVP-exposed group: rats were exposed to 1ml of concentrated DDVP for 15 minutes daily via inhalation, for a period of 3 weeks.

Group C: DDVP+ 300mg/kg of *R.communis*: exposed to DDVP as in B above and were concomitantly administered with 300mg/kg solution of *R. communis* extract dissolved in DMSO and distilled water (as prepared for group 1 rats above) for 42days.

Group D: Extract Only: rats were administered 300mg/kg of *R. communis* extract dissolved in DMSO and distilled water (as prepared for group 1 rats above) daily, for 6 weeks.

Collection, extraction and preparation of methanolic extract': Fresh *Ricinus communis* leaves were plucked from a farm in Aduin area of Ogbomoso town, Oyo state, Nigeria. The castor plants were identified by Dr. (Mrs) Ogundola, a botanist in the Department of Pure and Applied Biology, LAUTECH, Ogbomoso, Oyo State. The leaves were thoroughly washed with running tap water 2-3times and then finally washed with distilled water and shade-dried for seven days, then dried in an oven below 50^{o}C and powdered using electric grinder and stored in air tight containers for later use. A standard dose of 300mg/kg was administered to the rats in groups III and IV for 42days.

Drugs and Chemicals: The trade name of the local pesticide used for this study is **Sniper^{TM}.** DDVP, containing 1000g/liter of 2,3-dichlorovinyl dimethyl phosphate (DDVP); manufactured by (Forward (Beinaj)

Hepu Pesticide Co. Limited, China, for Saro Agrosciences Limited, Oyo State, Nigeria) was used. The pesticide, which contains dichlorvos as the active ingredient, was purchased from New Waso market, Ogbomoso, Oyo State. Other chemicals used in this study include 96.4% methanol, Dimethyl sulfoxide (DMSO), formalin, distilled water and chloroform.

Exposure to DDVP: Animals in Group II and III were exposed to 98.54g/m^3 of DDVP via inhalation, as modified by Saka *et al*. (2022a). In addition, 1ml of the pesticide was soaked in cotton wool and placed in a desiccator. The rat was also placed inside the desiccator and allowed to inhale the dichlorvos for 15 minutes daily for 21 days to induce cardiotoxicity. The medium follows the diffusion principle.

Blood Collection and Preparation of Tissues homogenate: After 6 weeks of experimental procedure, the animals were taken to the Department of Veterinary Medicine of University of Ibadan, Oyo State, Nigeria, where the blood pressure and ECG were measured. The animals were later fasted overnight few days after getting back to Ogbomoso. After overnight fast, the animals were anesthetized via chloroform inhalation using a desiccator, blood sample was collected via cardiac puncture into lithium heparinized bottles, centrifuged, and plasma obtained for estimation of lipid profile. The heart tissues were excised, weighed and fixed in 10% buffered formalin inside plain sample bottles for histopathological study. The supernatant obtained from homogenized tissues was assayed for the assessment of oxidative stress markers (GPx, CAT, MDA and SOD)

Phytochemical screening of methanolic extract of *Ricinus communis* : Qualitative phytochemical analysis of *Ricinus communis* extract using methanol was performed and reported as previously documented by Nortjie *et al*. (2022) and Saka *et al*. (2022).

Saponins: 5ml of the extract was boiled in 20ml of distilled water in a water bath and filtered. Approximately 10ml of the filtrate was mixed with 5ml of distilled water and shaken vigorously to obtain a stable, persistent foam. The resulting foam was then mixed with three drops of olive oil and shaken vigorously. The formation of emulsion indicated the presence of saponin

Alkaloids: 1ml of the extract was stirred with 5ml of 1% (v/v) aqueous HCl on a steam bath and filtered when hot. Distilled water was added to the residue, and then 1ml of the filtrate was treated with a few drops of Mayer's reagent, Wagner's reagent, and Dragendoff's reagent. Alkaloids were confirmed by forming a yellow color with Mayer's reagent, red precipitate with Dragendoff's reagent, and reddish-brown precipitate with Wagner's reagent.

Terpenoids: 5ml of the extract was added to 2ml of chloroform. 3ml of concentrated H_2SO_4 was then carefully added to form a layer. Reddish-brown discoloration of the interfaced was observed, indicating the presence of terpenoid.

Steroids: 2ml of acetic anhydride was mixed with 2ml of the extract, followed by the addition of 2ml of concentrated H_2SO_4. A color change confirmed the presence of steroids from violet to blue or green.

Glycosides: 5ml of the extract was mixed with 2ml of glacial acetic acid containing one drop of ferric chloride solution. This was then underplayed with 1ml of concentrated sulphuric acid. The presence of glycoside was confirmed by forming a violet-green ring below the brown circle.

Flavonoids: One milliliter (1ml) of 10% (w/v) NaOH was added to 3ml of the extract. The formation of yellow color confirmed the presence of flavonoids.

Tannins: One millimeter (1ml) of the extract was boiled with 20ml of distilled water in a test tube and filtered. Three drops of 0.1% ferric chloride were added to the filtrate. The formation of green color confirmed the presence of tannin.

Anthraquinones: Five millimeters (5ml) of the seed oil was mixed with 10ml of benzene and filtered. Five millimeters (5ml) of 10% NH3 solution was added to the filtrate. The presence of anthraquinones was established by developing red color in the ammoniacal (lower) phase

Test for saponins: Extract was mixed with 5 ml of distilled water in a test tube and then it was shaken vigorously, formation of stable foam indicated the presence of Saponins.

Test for Phenol: Extract was mixed with 3-4 drops of ferric chloride solution. Bluish black or blue green color indicated positive test for phenol.

Test for amino acids (Ninhydrin test): Extract was boiled with 2 ml of 0.2% Solution of Ninhydrin. Violet color indicated the presence of amino acids.

Test for Carbohydrates (Benedict's test): 2 ml of Benedict's reagent was added to the extract and heated on boiling Water bath for 2 minutes, reddish brown precipitate indicated the presence of Carbohydrates.

Blood Pressure (BP) & Heart Rate (HR): Blood pressure and heart rates of the animals were taken using the tail cuff method (as designed by Rogers (2000) at the Department of Veterinary Medicine, University of Ibadan. Blood pressure readings were taken with a computerized system that automatically performs rapid, simultaneous, multiple measurements of cardiac parameters (CODA). It involves the use of a tail-cuff placed on the tail of the rat to occlude blood flow and at all-cuff incorporating the volume pressure recording (VPR) sensor placed distal to the occlusion cuff to measure BP parameters. As the occlusion cuff is slowly deflated the VPR cuff measures the physiological characteristics of the returning systolic blood flow resulting in values for systolic and diastolic BP, mean BP, heart pulse rate, tail blood volume and flow.

Waveform acquisition is described below: Mouse tails were passed through cuffs (13mm long, with a 9mm diameter) and immobilized by adhesive tape in a V-shaped block between a light source above and a photoresistor below the tail. Evaluated photoelectrically, blood flow in the

tails produces oscillating waveforms that are digitally sampled 200times per second per channel. The waveforms displayed on the monitor are computer analyzed before and during a programmable routine of cuff inflation and deflation. Tail-cuff BP is defined as the cuff inflation pressure at which the waveform amplitude falls below a programmable percentage of its original amplitude for a specified number, of waveform cycles. Adjustment of these parameters allows BPs to be determined without interference from background noise.

Mean Arterial Blood Pressure (MAP): The mean arterial blood pressure was calculated using the mathematical relation of:

$$MABP = DBP + \frac{(SBP - DBP)}{3}$$

Where *MABP = Mean Arterial Blood Pressure*
DBP = Diastolic Blood Pressure
SBP = Systolic Blood Pressure

Pulse Pressure (PP)
Pulse pressure was calculated using the following formula:

$$PP = SBP - DBP$$

Where *PP= Pulse Pressure*
SBP= Systolic blood pressure (mmHg)
DBP=Diastolic blood pressure (mmHg).
It refers to the force that the heart generates each time a contraction occurs.

Rate Pressure Product (RPP): The Rate Pressure Product was calculated using the following formula:

$$RPP = \frac{HR \times SBP}{100}$$

Where *RPP = Rate Pressure Product*
HR= Heart Rate (bpm)
SBP= Systolic Blood Pressure (mmHg).

Electrocardiogram (ECG): Electrocardiography readings were taken using EdanVE-1010 machine, a PC-based diagnostic tool intended to acquire, process and store electrocardiograph (ECG) signals from pets such as rats undergoing resting test. After the BP analysis, the rats were sedated with ketamine (50mg/kg) and xylazine (0.75mg/kg) administered subcutaneously, there after gel was applied to the four limbs and chest of the rats. Five veterinary ECG leads, one for chest (V) and four for the limbs (RA, LA, RL, LL), with each lead attached to an atraumatic alligator lip electrode were then connected to the gels pot and the cardiogram was recorded for 60s with the custom-made software accompanying the system.

Determination of Lipid Profile: Total cholesterol, triglyceride, and HDL cholesterol were determined using Randox Commercial Kits. The chylomicrons' very-low-density lipoprotein (VLDL) and low-density lipoprotein (LDL) serum are precipitated by phosphotungstic acid and magnesium ions. Therefore, LDL was calculated from the results of Total cholesterol, Triglyceride, and High-density lipoprotein (Saka *et al.,* 2022).

Determination of Oxidative stress marker: The activity of superoxide dismutase (SOD) in the heart was determined by the method of Misra and Fridovich (1972) and modified by Kakkar *et al*. (1984). GPx activity was estimated using calorimetric method (Saka *et al.,* 2020). The level of lipid peroxidation as malondialdehyde (MDA) and Catalase (CAT) activity were determined based on the principle of Varshney and Kale (1990) and Aebi (1974), respectively.

Histopathology of the Excised Organs: The fixed organs were analyzed at the Histopathology Laboratory of the University College Hospital, Ibadan following standard protocol (Abiona *et al.,* 2019). Photomicrography, H & E were done in accordance to the principle of (Avwioro, 2010).

RESULTS

Phytochemical screening of methanolic-extract of *Ricinus communis* : Table 1 shows the findings of the qualitative phytochemical studies. *Ricinus communis* extract was found to contain alkaloid, tannin, saponin, flavonoids, phenol, terpenoids, carbohydrate and glycosides.

Table 1:
Phytochemical screening of methanolic-extract of *Ricinus communis*

Phytochemical test	Results
Alkaloid	+
Tannin	+
Saponin	+
Flavonoids	+
Phenol	+
Terpenoids/Isoprenoids	+
Amino acids	-
Carbohydrate	+
Glycoside	+

+: Present; - :Absent

Estimation of cardiovascular variables: The effects of dichlorvos and methanolic extract of *Ricinus communis* leaf on cardiovascular variable is summarized in Table 2. Administration of Dichlorvos induced extensive cardiovascular dysfunction evident by significant increase ($P< 0.05$) in systolic blood pressure (SBP), diastolic blood pressure (DBP), pulse pressure (PP), mean arterial pressure (MAP), blood volume, rate pressure product (RPP) as well as heart rate (HR) in rats exposed to DDVP when compared to control group. However, treatment with *Ricinus communis* extract in pathogenic rats significantly reduced SBP, blood volume, RPP, HR with a non-significant difference in DBP, PP and MAP when compared to DDVP-exposed rats. Also, *Ricinus communis* treated rats has significantly decreased cardiovascular variables when compared to DDVP-exposed rats at $p<0.05$.

Estimation of electro-cardiac function

Effects of Methanolic extract of *Ricinus communis* leaf on Electrocardiogram (ECG) in male Wistar rats exposed to DDVP: The result (Table 3) revealed an alteration in electro-cardiac function evident by significant increase ($p\leq 0.05$) in P-duration, QRS Complex, QT interval, corrected QT interval, R-Amplitude with a non-significant difference in PR-Interval in DDVP-exposed rats

when compared to control group. However, administration of methanolic leaf extract of *Ricinus communis* significantly decreased PR-Interval, QRS-complex and QTC-Interval with a corresponding non-significant difference in P-Duration, QT-Interval and R-Amplitude when compared with DDVP-exposed rats. Electro-cardiac function in *Ricinus communis* leaf extract recorded a normal range as compared to control rats.

Estimation of lipid profile: The effects of dichlorvos and methanolic extract of *Ricinus communis* on lipid profile such as cholesterol (CHOL), Triglyceride (TAG), High density lipoprotein (HDL) and low density lipoprotein (LDL) is summarized in Table 4. Exposure of rats to DDVP caused abnormalities in lipoprotein metabolism as shown by increase in CHOL ($p<0.05$), LDL ($p<0.05$), TAG ($p>0.05$) with a corresponding decrease in HDL ($p<0.05$) when compared with control rats. However, treatment with methanolic extract of *Ricinus communis* decreases elevated level of CHOL ($p<0.05$), LDL ($p>0.05$), TAG ($P>0.05$) with significant increase in HDL ($p<0.05$) when compared with DDVP-exposed rats. Also, administration of *Ricinus communis* methanolic leaf extract revealed a significantly normal lipid profile as compared to DDVP-exposed rats.

Estimation of oxidative stress: The effect of DDVP and *Ricinus communis* on oxidative stress marker such as glutathione peroxidase (GPx), malondialdehyde (MDA), superoxide peroxidase (SOD) and Catalase (CAT) were assessed and summarized in table 5. Administration of DDVP induced oxidative damage to rats evident by generation of free radicals (significant increase in MDA concentration) and suppression of antioxidant enzymes (significant decrease in GPx, SOD and CAT activities) as compared to control rats ($p<0.05$).

Table 2:
Effects of Methanolic extract of *Ricinus communis* leaf on cardiovascular variable in DDVP-exposed rats

Parameters	I	II	III	IV
Systolic blood pressure (mmHg)	116.0 ± 2.10	146.5 ± 2.39[a]	132.2 ± 2.51[a,b]	123.0 ± 1.32[b,c]
Diastolic blood pressure (mmHg)	83.33 ± 2.06	93.67 ± 1.05[a]	93.00 ± 1.63[a]	86.50 ± 1.78[b]
Pulse Pressure (mmHg)	32.67 + 1.73	52.83 ± 2.14[a]	39.17 ± 1.54[a]	32.00 ± 1.51[b,c]
Mean arterial blood pressure (MAP) (mmHg)	94.22 ± 1.91	111.3 ± 1.28[a]	106.1 ± 1.83[a]	101.7 ± 0.72[a,b]
Blood volume (ml/kg)	65.51 ± 7.20	116.9 ± 3.14[a]	67.06 ± 3.54[b]	87.09 ± 7.08[b]
Rate Pressure Product	31.76 ± 1.70	41.62 ± 0.61[a]	34.17 ± 0.89[b]	27.81 ± 2.30[b,c]
Heart Rate (HR) (bpm)	291.7 ± 0.88	351.3 ± 2.91[a]	286.0 ± 3.00[b]	238.3 ± 2.19[a,b,c]

Values are expressed in Mean ± SEM (n=8)
Groups with different superscript(s) are significantly different at p≤0.05.
[a]Represent significant difference when compared with Group I. [b]Represent significant when compared with Group II. [c] Represent significant difference when compared with Group III.
Group I = Control; Group II = DDVP-exposed rats; Group III = DDVP + 300mg/kg of Ricinus communis ; Group IV: Ricinus communis only

Table 3:
Effects of Methanolic extract of *Ricinus communis* leaf on Electrocardiac-function in DDVP-exposed rats

Parameters	I	II	III	IV
P-Duration (ms)	35.33 ± 3.38	43.33 ± 4.67[a]	40.67 ± 3.48	35.00 ± 5.13[a]
PR-Interval (ms)	44.00 ± 2.08	55.33 ± 0.33	45.67 ± 2.33[b]	41.67 ± 0.88[c]
QRS Complex (ms)	16.33 ± 0.88	35.00 ± 0.58[a]	18.00 ± 0.58[b]	23.33 ± 1.76[a,b,c]
QT-Interval (ms)	124.00 ± 2.33	100.7 ± 2.85[a]	86.33 ± 5.36[a]	113.0 ± 3.61[c]
QTC Interval (ms)	262.7 ± 1.86	218.0 ± 9.07[a]	165.0 ± 5.69[a,b]	231.7 ± 6.01[a,c]
R-Amplitude (mV)	0.329 ± 0.02	0.528 ± 0.02[a]	0.474 ± 0.03	0.449 ± 0.02[b,c]

Values are expressed in Mean ± SEM (n=8)
Groups with different superscript(s) are significantly different at p≤0.05.
[a]Represent significant difference when compared with Group I. [b]Represent significant when compared with Group II. [c] Represent significant difference when compared with Group III.
Group I = Control; Group II = DDVP-exposed rats; Group III = DDVP + 300mg/kg of *Ricinus communis* ; Group IV: *Ricinus communis* only

Table 4:
Effects of Methanolic extract of *Ricinus communis* leaf on lipid profile in DDVP-exposed rats

Parameters	**I**	**II**	**III**	**IV**
CHO (mg/dL)	47.68 ± 1.03	66.67 ± 4.05[a]	60.55 ± 3.37[a,b]	46.33 ± 1.57[b,c]
TAG (mg/dL)	60.38 ± 3.55	62.53 ± 0.60	61.07 ± 2.19	48.96 ± 1.27[a,b,c]
HDL (mg/dL)	13.68 ± 0.61	10.37 ± 0.56[a]	12.59 ± 0.87[b]	14.57 ± 0.37[b,c]
LDL (mg/dL)	22.05 ± 2.59	37.43 ± 1.69[a]	36.21 ± 1.93[a]	22.49 ± 1.97[b,c]

Values are expressed in Mean ± SEM (n=8)
Groups with different superscript(s) are significantly different at p≤0.05.
[a]Represent significant difference when compared with Group I. [b]Represent significant when compared with Group II. [c] Represent significant difference when compared with Group III.
Group I = Control; Group II = DDVP-exposed rats; Group III = DDVP + 300mg/kg of *Ricinus communis* ; Group IV: *Ricinus communis* only.

Table 5:

Effects of Methanolic extract of *Ricinus communis* leaf on oxidative stress marker in DDVP-exposed rats

Parameters	I	II	III	IV
GPx (µg/mL)	0.11 ± 0.01	0.05± 0.01[a]	0.07± 0.02[a,b]	0.09± 0.00[b]
SOD (U/mL)	5.66 ± 0.36	2.07 ± 0.42[a]	5.23 ± 0.25[b]	4.57 ± 0.2150[b]
CAT (mU/g)	0.52 ± 0.01	0.24 ± 0.15[a]	0.51 ± 0.03[b]	0.76 ± 0.01[a,b,c]
MDA (nmol/mL)	15.77 ± 1.00	24.05 ± 1.37[a]	17.26 ± 0.52[b]	14.47 ± 1.59[b]

Values are expressed in Mean ± SEM (n=8)
Groups with different superscript(s) are significantly different at p≤0.05.
[a]Represent significant difference when compared with Group I. [b]Represent significant when compared with Group II. [c] Represent significant difference when compared with Group III.
Group I = Control; Group II = DDVP-exposed rats; Group III = DDVP + 300mg/kg of *Ricinus communis* ; Group IV: *Ricinus communis* only

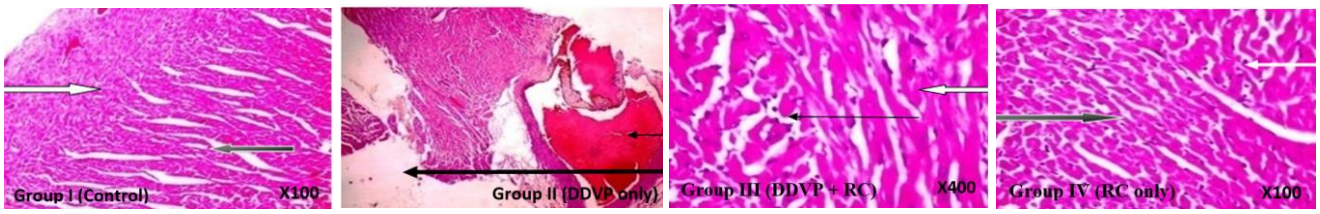

Plate 1:
Photomicrographs of heart section of normal control rats (Group I) depicts normal myocytes, epicardial layer (white arrow) and normal myocardial layer seen (black arrow), no pathological lesion seen but a photomicrograph of heart section of Group II induced with dichlorvos revealed normal epicardial layer (slender arrow) and marked fat degeneration and necrosis of the myocardial layer seen (black arrow), emblic myocytes vessels and valves (slender arrow). A photomicrograph of heart section of Group III treated with 300mg/kg of *Ricinus communis* methanolic extract after administration of dichlorvos showed normal epicardial layer (white arrow) and the mild infiltration of inflammatory cells of myocardial layer (slender arrow). Administration of methanolic extract of *Ricnius communis* extract to rats (Group IV) revealed a normal myocyte, epicardial layer (white arrow) and normal myocardial layer seen (black arrow) with no pathology.

However, treatment with methanolic extract of *Ricinus communis* significantly increases GPx, SOD, CAT and decreases MDA concentration when compared with DDVP-exposed rats. Also, administration of *Ricinus communis* extract to rats significant improved antioxidant enzymes and reduced peroxidation of lipid when compared to DDVP-exposed rats at $p<0.05$

DISCUSSION

The frequent utilization of pesticides and insecticides has heightened human exposure to environmental pollutants, potentially leading to both acute and chronic adverse health effects. The synthetic chemicals present in pesticides may contribute to long-term environmental repercussions. Within homes, individuals are exposed to insecticides, the toxicity profiles of which have not been thoroughly investigated. Dichlorvos (DDVP), a highly hazardous chemical classified by the WHO as (Class Ib) (WHO, 1992), accumulates in humans and induces toxic effects in various organs of the body (Tsitsimpikoua *et al*., 2013). Despite the wealth of knowledge regarding cardiovascular diseases (CVDs), their prevalence continues to escalate. Cardiovascular disease (CVD) remains the foremost cause of premature deaths globally (Kumar *et al*., 2010). Consequently, there is an immediate need for new, safe, effective, and relatively affordable drug candidates.

In the present study, dichlorvos induced cardiovascular dysfunction evidenced by significant alterations in cardiovascular variables such as increased arterial blood pressure (both systolic and diastolic pressure), mean arterial pressure (MAP), pulse pressure (PP), volume, rate pressure product (RPP), and heart rate. These findings align with a prior report by Saka *et al*. (2020). The ability of DDVP to induce changes in cardiovascular variables may stem from its stimulation of adrenergic responses or dysfunction in left ventricular contraction. Rats exposed to DDVP exhibited a substantial increase in arterial blood pressure (DBP, SBP, and MAP), contrary to the findings of Jun *et al*. (2018). However, administration of the methanolic extract of *Ricinus communis* restored DDVP-induced alterations in cardiovascular variables.

This study has also disclosed that *Ricinus communis* leaves possess a significant capacity to reduce systolic and diastolic blood pressure, pulse pressure, mean arterial blood pressure, and rate pressure product induced by exposure to DDVP. The blood pressure regulatory activity of *Ricinus communis* could be attributed to the presence of phytochemicals such as tannins and saponins embedded in the extract. Tannins exert physiological effects such as accelerating blood clotting, reducing blood pressure, decreasing serum lipid levels, inducing liver necrosis, and modulating immune responses, as reported by Chung *et al*. (1998). Saponins also aid in controlling cardiovascular disease and cholesterol in humans (Oladeji, 2016). Additionally, it has been revealed that *Ricinus communis* leaves extract exhibits a significant antioxidant capacity on cardiac tissues. Therefore, *Ricinus communis* is effective and possesses sufficient potency in the management of high blood pressure, which could otherwise lead to conditions like cardiac failure, stroke, and other cardiovascular diseases or potentially result in death. Thus, this finding suggests that R.communis may be a potential remedy for cardiovascular diseases with low risk of toxicity.

Electrocardiac function parameters, including P-duration, PR-interval, QRS-complex, QT-interval, QTC-Interval, and R-Amplitude, were evaluated in this study. Administration of DDVP to rats resulted in abnormal electrocardiac function evidenced by a significant increase in P-duration, QRS-complex, QT-Interval, QTC interval, R-Amplitude, and a non-significant difference in PR-Interval compared to control rats (as shown in Table 3). P-duration reflects the depolarization of the atrium of the heart, while PR-Interval represents the time of conduction of electric signals through the atrial and atrioventricular (AV) node. Therefore, the observed prolongation in P-wave and PR-Interval duration in DDVP-exposed rats indicates an increased risk of atrial fibrillation, myocardial fibrosis, and even death in the study population (Cheng *et al*., 2009). QRS-Complex duration corresponds to conduction through the ventricular myocardium and serves as a predictor of sudden cardiac death (Kurl *et al*., 2012). The widening of QRS-complex duration observed in DDVP-exposed rats indicates impairment in hemodynamic performance and mitral regurgitation (Kass *et al*., 1999). QT-Interval and corrected QT Interval signify the electrical activity of the ventricles, while R-Amplitude measures the heart rate. The observed fluctuations in QT-interval, corrected QT Interval, and increased R-Amplitude in DDVP-exposed rats suggest that DDVP predisposes rats to ventricular arrhythmia (torsades de pointes) and attendant seizures (Trinkley *et al*., 2013). This possibly contributes to the observed DDVP-induced increase in systolic blood pressure (SBP), diastolic blood pressure (DBP), heart rate (HR) and pulse pressure, as seen in this study. However, treatment with the methanolic extract of *Ricinus communis* significantly ameliorated the deviations in electrocardiac parameters compared to dichlorvos-induced rats. This reveals the cardioprotective effect of the extract, which aligns with the findings of Charan *et al*. (2009).

The alteration in the lipid profile observed in DDVP-exposed rats as demonstrated in this study, is characterized by a significant increase in serum total cholesterol (TC), triglyceride (TG), and low-density lipoprotein (LDL) levels, accompanied by a corresponding reduction in high-density lipoprotein (HDL) levels. These changes in the lipid profile of DDVP-exposed rats indicate abnormalities in lipoprotein metabolism. Lipoproteins play roles in various metabolic processes, such as immune reactions, coagulation, and tissue repair. Oxidative alteration of lipoproteins, particularly LDL, along with the suppression of lipoprotein antioxidants, especially Vitamin E, has been associated with the accumulation of cholesterol and an increased susceptibility to atherosclerosis (Olayinka *et al*., 2011). Elevated levels of TG, TC, and LDL, along with a concurrent decrease in HDL, generally signify an increased risk of cardiovascular disease. However, treatment with the methanolic extract caused a significant increase in HDL, coupled with a corresponding decrease in LDL, serum cholesterol, and TG. The leaf extract of *Ricinus communis* demonstrated hypolipidemic activity by significantly reducing triglycerides, cholesterol, LDL, and increasing HDL in rats' plasma, suggesting the herb's potential as a remedy for hyperlipidaemia and cardiovascular diseases (Kwiterovich, 2000). This aligns with the ethnobotanical use of the leaf extract as a natural remedy against cardiovascular disease in the West Africa Sub-Region. The present results support previous findings by Oyewole *et al*. (2016), who reported the modulatory effect of *Ricinus communis* leaf extract on cadmium-chloride-induced hyperlipidaemia and pancytopaenia in rats. The hypolipidaemic and blood-boosting activities of the leaf can be attributed to its phytochemical constituents present in the extract, as reported earlier (Oyewole *et al*., 2010; Kensa and Syhed, 2011). Some of these phytochemicals have been reported to have positive physiological actions on haematopoiesis and lipid metabolism in animals and humans (Brown, 1996).

Oxidative stress which has been described as an imbalance between pro-oxidants and antioxidants is a major contributor to cardiac injury. It is widely accepted that antioxidant enzymes play a crucial role in defending against prooxidants, protecting cellular integrity, and preventing the pathogenesis of various degenerative diseases (Saka *et al*., 2022b). In situations of oxidative stress, disturbances in the normal redox state within cells can lead to an overwhelming effect on the enzymatic antioxidant enzymes, notably SOD, CAT, GST, and GPx, due to the excessive production of free radicals. Oxidative stress has been implicated in various conditions, including inflammatory diseases, alcoholism, smoking-related disorders, ischemic diseases, and more (Lobo *et al*., 2010; Dailiah *et al*., 2012; Prabu *et al*., 2013). The overall decrease observed in the status of enzymatic antioxidants in the heart homogenates of dichlorvos-exposed rats in the present study indicates a net suppression of the total antioxidant capacity in the tissue. This finding aligns with other reports (Ahmed *et al*., 2015; Saka *et al*., 2020; 2021). Treatment with methanolic extract of *Ricinus communis* ameliorated this effect, highlighting the antioxidant potential of the extract, as reported by Waseem *et al*. (2018). This result suggests that the plant extract contains bioactive constituents capable of donating hydrogen ions to free radicals, thereby scavenging them and preventing their potential to induce cellular damage. This affirms the protective influence of *Ricinus communis* extract on oxidative stress induced by dichlorvos exposure.
Lipid peroxidation, a crucial pathogenic event in myocardial necrosis, serves as a sensitive marker of oxidative stress induced by DDVP. The elevated level of MDA, a product of lipid peroxidation, reflects the extent of damage to cardiac tissues (Khalil *et al*., 2015). Malondialdehyde levels are commonly utilized as markers of oxidative stress (Maddock and Pariante, 2001). In this study, there was an observed increase in MDA levels in the DDVP-treated group. The findings presented in this study indicate that the methanolic extract of *Ricinus communis* could mitigate the elevation of DDVP-induced MDA content. The reduction in MDA levels in heart tissues might be attributed to the enhanced activities of antioxidant enzymes like SOD and GPx. It is plausible that the free radicals induced by DDVP were effectively neutralized and/or scavenged by the extract, resulting in the cardioprotective effect of the extract. Histopathological findings also revealed that exposure to DDVP altered the histoarchitecture of heart tissue, evidenced by marked fat degeneration and necrosis of the myocardial layer, embolic vessels, and valves in the myocytes compared to control rats. However, treatment with the methanolic extract of *Ricinus communis* resulted in a normal epicardial layer and mild infiltration of inflammatory cells in the myocardium.

In conclusion, *Ricinus communis* positively modulates cardiovascular dysfunctions, as evidenced by its attenuation of abnormal cardiovascular function, cardiac electrical activity, and lipid profile caused by DDVP in rats. The findings also indicate that the methanolic extract of *Ricinus communis* can mitigate DDVP-induced oxidative stress. Consequently, this study suggests that *Ricinus communis* alleviates cardiovascular dysfunction either through the reduction of cardiac oxidative stress or its hypolipidaemic effect. Therefore, the study infers that the leaf of *Ricinus communis* may serve as a potential remedy for cardiovascular diseases with a low risk of toxicity.

REFERENCES

Abiona O.O, Anifowose A.J., Awojide S.H., Adebisi O.C., Adesina B.T. and Ipinmoroti M.O. (2019). Histopathological biomarking changes in the internal organ of Tilapia (Oreochomis niloticus) and Cat fish (Clarias gariepinus) exposed to heavy metal contamination from Dandaru pond, Ibadan, Nigeria, *Journal of Taibah University for Science*, 13:1, 903-911.

Aebi H. (1974). Catalase. In: Bergmeyer HU, editor, Methods of enzymatic analysis. Verlag Chemie, Weinheim, Germany; 1974; 673-678p. 29.

Ahmed, D., Khan, M. and Saeed, R. (2015). Comparative analysis of phenolics, flavonoids, and antioxidant and antibacterial potential of methanolic, hexanic and aqueous extracts from Adiantum caudatum leaves. *Antioxidants*. 4(2): 394-409.

Ameh, G.I. and Eze C.S. (2010). Phytochemical and Ethnobotanical Evaluation of the leaves of Talium triangulare (Jacq) Wild. *Nig. J. Biotech*. Vol. 21(2010) 50-54. ISSN: 018917131.

Anna L.H. (2010). Role of oxidative stress in organophosphate insecticide toxicity – Short review. *Pesticide Biochemistry and Physiology*. 98(2):145-50.

Armstrong, M., Kerndt, C.C., Moore, R.A. (2021). Physiology, Baroreceptors. Ini Satatpearls. Treasure Island (FL): StatPearls Publishing; 2022 Jan.

Avwioro, O.G. (2010). Histochemistry and tissue pathology, principle and techniques, Claverianum press, Nigeria.

Bhinder, P. and Chaudhry, A. (2013). Mutagenicity Assessment of organophosphates using polymerase chain reaction-restriction fragment length polymorphism assay. *Toxicol Int*. 20(3): 254 – 260.

Brown D.J. (1996). Herbal prescriptions for better health. Rocklin, CA: Prima Publishing. 139-44.

Cannon, C.P. (2007). Cardiovascular disease and modifiable cardio-metabolic risk factors. *Clin Cornerstone*.8(3): 11-28.

Chan AP, Crabtree J, Zhao Q, Lorenzi H, Orvis J, Puiu D, *et al*. (2010). Draft genome sequence of the oilseed species *Ricinus communis* . *Nat Biotechnol* 28(9): 951-956.

Charan SK, Arora S, Goyal S, Kishore K, Ray R, Chandra NT, *et al*. (2009) Cardioprotective effects of benazepril, an angiotensin converting enzyme inhibitor, in an ischaemia-reperfusion model of myocardial infarction in rats. *J Renin Angiotensin Aldosterone Syst* 10: 201-9.

Cheng S., Keyes M.J., Larson M.G., McCabe E.L., Newton-Cheh C., Levy D *et al*. (2009). Long term outcomes in individuals with prolonged PR interval or first degree atrioventricular block, JAMA, Catterall WA 301: 2571-2577

Chung J.W., Kim N., Kang J., Park S.H., Kim W.J, Ko Y., Bae H.J. (2015). Blood pressure variability and development of early neurological deterioration following acute ischemic stroke. *Journal of Hypertension*. 33(10) 2099-2106.

Chung, K. T. (1998). Tannins and Human Health. *Crit Rev Food Sci Nutr*. 38(6):421-64.

Dailey Roopha P and Padmalatha C (2012). Effect of an herbal preparation on heavy metal (cadmium) induced antioxidant system in female Wistar rats. *J Med Toxicol*. 8:101 117. 42.

Forreira, J.P. (2020) Cardiovascular and non-cardiovascular death distinction: the utility of troponin beyond N-terminal pro-B-type natriuretic peptide. Findings from the BIOSTAT-CHF study. *European Journal of Heart Failure*, 22(1), pp. 81-89.

Greim, H., Saltmiras, D., Mostert, V., Strupp, C. (2015). Evaluation of carcinogenic potential of the herbicide glyphosate, drawing on tumor incidence data from fourteen chronic/carcinogenity rodent studies *Crit Rev. Toxicol*. 2015 Mar; 45(3): 185-208.

Henshaw U.O. and Iwara A.I. (2018). Dichlorvos toxicity: A public health perspective. *Interdiscip Toxicol*. 2018 Aug 11(2): 129-137.

Jun Liu, Liang Chen, Huihe Lu (2018). Cardioprotective effect of salvianolic acid B against isoproterenol-induced inflammation and histological changes in a cardiotoxicity rat model. *Tropical Journal of Pharmaceutical Research* 17 (11): 2189-2197.

Kakkar P., Das B. and Viswanathan P.N. (1984). A modified spectrophotometric assay of superoxide dismutase. *Indian J Biochem Biophys.* 21:130-132.

Karki P., Ansari J.A., Bhandary S., Koirala S, (2004) Cardiac and electrocardio-graphical manifestations of acute organophosphate poisoning. *Singapore Med J* 45: 385-389.

Kass DA, Chen CH, Curry C. *et al*. (1999): Improved left ventricular mechanics from acute VDD pacing in patients with dilated cardiomyopathy and ventricular conduction delay. *Circulation*. 99:1567-1573.

Kensa V.M. and Syhed Y.S. (2011). Phytochemical screening and antibacterial activity on *Ricinus communis* L. *Plant Sciences Feed*. 1 (9): 167-173.

Khalil, M.I., Ahmmed, I., Ahmed, R., Tanvir, E.M., Afroz, R., Paul, S. *et al*. (2015).'Amelioration of isoproterenol-induced oxidative damage in rat myocardium by *Withania somnifera* leaf extract' *Biomedical Research International* 24159, 1–10.

Kumar SV, Fareedullah M, Sudhakar Y, Venkateswarlu B, Kumar EA (2010). Current review on organophosphorus poisoning. *Arch Appl Sci Res* 4: 199-215.

Kurl S, Makikallio TH, Rautaharju P, Kiviniemi V, Laukkanen JA. (2012). Duration of QRS complex in resting electrocardiogram is a predictor of sudden cardiac death in men. *Circulation* 125:2588-2594

Kwiterovich P.O. (2000). The metabolic pathways of high-density lipoprotein, low-densitylipoprotein, and triglycerides: a current review. *The American Journal of Cardiology.* 12: 5-10. 2000.

Leone A. (2015) Preventive measures to fight cardiovascular death disease: Current Results and future perspectives. *J cardiol curr Res* 3(4): 00110.

Lobo V, Patil A, Phatak A, *et al* (2010). Free radicals, antioxidants, and functional foods impact human health. *Pharmacogn Rev*. 4:118 126.

Maddock, C. & Pariante, C.M. (2001). 'How does stress affect you? An overview of stress, immunity, depression, and disease', Epidemiologia Psychiatria Sociale 10(3), 153–162. https://doi.org/10.1017/S1121189X00005285.

Mahmood S.S., Ley D., Vasan R.S., Wang T.J. (2014). The Framinghan Heart study and the epidemiology of

cardiovascular disease: a historical perspective. *Lancet.* Mar 15:383(9921). 999-1008.

Misra H.P. and Fridovich I. (1972). The role of superoxide anion in the autoxidation of epinephrine and a simple assay for superoxide dismutase. *J Biol Chem*. 247(10):3170–3175.

Mostafalou S., Abdollahi M. (2013). Pesticides and human chronic diseases: Evidence, mechanisms, and perspectives. *Toxicology and Applied Pharmacology*. 268:157–77.

Nortjie, E., Basitere, M., Moyo, D., Nyamukamba, P. (2022). Extraction Methods, Quantitative and Qualitative Phytochemical Screening of Medicinal Plants for Antimicrobial Textiles: A Review. Plants.

Oladele O. (2016). The characteristics and Roles of Medicinal Plants; Some Important Medicinal Plants in Nigeria. Nat Prod. *Ind J*. 12(3):102.

Olayinka ET, Ore A, and Akinnawo OO (2011). Protective role of ethanolic extract of Sorghum bicolor leaf sheath against cadmium induced oxidative stress in rats. *Int J Pharm Biomed Res*. 2:254 260.

Oyewole O.I, Owoseni A.A. and Faboro E.O. (2010). Studies on medicinal and Toxicological properties of Cajanus cajan, *Ricinus communis* and Thymus vulgaris. *Journal of Medicinal Plant Research.* 4(19): 2004-2008.

Oyewole O.I, Shoremi M.O., and Oladele J.O (2016). "Modulatory Effects of *Ricinus communis* Leaf Extract on Cadmium Chloride-Induced Hyperlipidemia and Pancytopenia in Rats." *American Journal of Biomedical Research*, vol. 4, no. 2 (2016): 38-41. doi: 10.12691/ajbr-4-2-2.

Prabu SM, Muthumani M, Shagirtha K (2013). Quercetin potentially attenuate cadmium-induced oxidative stressmediated cardiotoxicity and dyslipidemia in rats. *Eur Rev Med Pharmacol Sci.* 17:582 595.

Roger V.L. (2007). Epidemiology of myocardial infarction. *Med Clin N Am.* 91(4):537–552.

Saka W. A., Adeshina O. S., Yusuf M. G., Omole A. I (2022a). Hepatoprotective and Renoprotective effect of Moringa oleifera Seed Oil on Dichlorvos-induced Toxicity in Male Wistar rats. *Niger. J. Physiol. Sci*. 37: 119 – 126.

Saka W.A, Kehinde B.D, Akintola A.O, Akwu B.P, Ibikunle G.J, Owolabi G.O, Adeshina O.S. and Folorunso K.P (2022b). Cardiotoxic effects of car paint fumes exposure on cardiac tissues of male wistar rats. *J Bio Med Open Access*; 3(2):126.

Saka WA, Akhigbe RE, Abidoye AO, Dare OS, and Adekunle AO (2021). Suppression of uric acid generation and blockade of glutathione dysregulation by L-arginine ameliorates dichlorvos-induced oxidative hepatorenal damage in rats. *Biomedicine and Pharmacotherapy*; 138: 111443.

Saka, W.A., Ayoade, T.E., Akhigbe, T.M. and Akhigbe, R.E. (2020). Moringa oleifera seed oil partially abrogates 2,3-dichlorovinyl dimethyl phosphate (Dichlorvos)-induced cardiac injury in rats: evidence of role of oxidative stress. *J Basic Clin Physiol Pharmacol*:20190313.

Scarpa A. and Guerci A. (1982). "Various uses of the castor oil plant (*Ricinus communis* L.). Review :*Journal OS Ethnopharmacology*. Vol. 5, No 2, pp. 117-137.

Shargorodsky M, O Debby, Z Mattas, R Zimlichman (2010) Effect of long term treatment of antioxidants (vitamin C, vitamin E, coenzyme Q and selenium) on arterial compliance, humoral factor and inflammatory markers in patients with multiple cardiovascular risk factors. *Nutrition and metabolism* 7: 55-63.

Singh A, Uppal G. A. (2015). Review on Carissa Caranadas phytochemistry, Ethnopharmacology and micropropagation as conservation strategy. *Asian Journal of Pharmaceutical and Clinical Research.* 63(3): 367-375.

Soboleve, V.E; Sokolava, M.O; Jenkins, R.O.; Goncharou, N.V (2021). Nephrotic Effects of Paraoxon in three rat models of acute intoxication. *Int. J. Mol. Sci*; 22, 13625.

Toplak Galle K. Domestic medicinal plants. Zagreb: Mozaic book; 2005. pp. 60–1.

Trinkley KE, Page RN, Lien H,Yamonouye K, Tisade JE. QT interval prolongation and the risk of torsades de pointers:essentials for clinicians. *Curr Med Res Opin* 2013; 29:1719-26

Tsitsimpikou, C., Tzatzarakis, M., Fragkiadaki, P., Kovatsi, L., Stivaktakis, P., Kalogeraki, A., Kouretas, D. & Tsatsakis, A.M (2013). Histopathological lesions, oxidative stress and genotoxic effects in liver and kidneys following long term exposure of rabbits to diazinon and propoxur. *Toxicology*., 10; 307:109-14.

U.S. Public Health Service (USPHS) (1995). Hazardous Substance Data Bank. Washington, DC. Pp5-9.

USEPA: United States Environmental Protection Agency. Dichlorvos TEACH Chemical summary U.S EPA. *Toxicity and exposure assessment for children*; 2007. pp. 1–13.

Varshney R and Kale R.K.(1990). Effect of calmodulin antagonists on radiation-induced lipid peroxidation in microsomes. *Int J Biol*. 158:733–741.

Waseem M, Abdul I, Nahid HH, Jamal SM, Saleh AK, Kulvinder SS, Roop SB (2018). Therapeutic role of *Ricinus communis* L. and its bioactive compounds in disease prevention and treatment. *Asian Pacific Journal of Tropical Medicine* 11(3) March 2018.

WHO: World Health Organization. (1992). International Programme on chemical safety. WHO recommended classification of pesticide by hazards and guidelines to classification 1994–1995, UNEP/ILO/WHO.

World Health Organization (2017). Cardiovascular Diseases (CVDs) (World Health Organization). Available: https://www.who.int/news-room/factsheets/ detail/cardiovascular-diseases-(CVDs) [Accessed 26-06-2019.

Niger. J. Physiol. Sci. 38 (December 2023): 239 – 246
www.njps.physiologicalsociety.com

Niger. J. Physiol. Sci.

Full length Research Article

Immunohistochemical and Morphological Changes Associated with Hepatic Damage in Lead Acetate-Induced Toxicity and Mitigatory Properties of Naringin in Cockerel Chicks

Esan O.[a], Ajibade T.O.[b]*, Ebirim C.G.[c], Adetona M.O.[d], Oyagabemi A.A.[c], Omobowale T.O.[a], Oladele O.A.[a], Adedapo A.A.[e], Oguntibeju O.[f], Yakubu M.A.[g], Nwulia E.[h]

Departments of [a]Veterinary Medicine, [b]Veterinary Physiology and Biochemistry, [e]Veterinary Pharmacology and Toxicology, Faculty of Veterinary Medicine, University of Ibadan, Nigeria
[c]Pan African University, Institute of Earth and Life Sciences Institute, Nigeria
[d]Department of Anatomy, Faculty of Basic Medical Sciences, University of Ibadan, Nigeria
[f]Phytomedicine and Phytochemistry Group, Department of Biomedical Sciences, Faculty of Health and Wellness Sciences, Cape Peninsula University of Technology, Bellville 7535, South Africa
[g]Department of Environmental & Interdisciplinary Sciences, College of Science, Engineering & Technology, COPHS, Texas Southern University, Houston, TX, USA.
[h]Howard University, College of Medicine, Department of Psychiatry and Behavioral Sciences, Howard University Hospital, 2041 Georgia Avenue, Washington, DC 20060, USA.

Summary: Lead (Pb) toxicity constitutes a major health hazard to both humans and animals especially in the developing countries. It is a ubiquitous environmental contaminant found in the air essentially because of unregulated mining and other industrial activities. Lead can be found naturally in the soil thus, contaminating crops for human and animal food, as well as run-off water and air pollution. Intensively and extensively reared domestic chickens are exposed to contamination via inhalation and ingestion of contaminated food materials. Naringin, a product from citrus plant has been described to possess excellent metal chelating ability. Naringin is rich in flavonoid with attendant antioxidant, anti-autophagy, anti-inflammatory, hepatoprotective and cardio-nephroprotective properties. This study was conducted to investigate the hepatoprotective and modulation of oxidative stress in commercial cockerel chickens by Naringin. Thirty-six commercial cockerel chickens were randomly assigned into six groups A-F of six birds each viz: Group A served as control group while groups B, C, and D received Lead acetate at 300 ppm via drinking water continuously till the end of the experiment. In addition, groups C and D were treated with Naringin at 80 mg/kg and 160mg/kg, respectively, via oral gavage for 8 weeks. Groups E and F were administered naringin only at 80mg/kg and 160mg/kg respectively for eight weeks. Pb toxicity induced degenerative changes in the histological sections as well as, higher expression of hepatic caspase 3 as shown by immunohistochemistry. There was increased oxidative stress markers (H_2O_2, MDA) and depletion of the antioxidant defense system markers SOD, GPx, GSH, and GST. It concluded that Co- treatment with Naringin ameliorated oxidative stress, enhanced antioxidant defense system, reduced the expression of hepatic caspase 3 thus, offering protection against lead acetate-induced derangements in the liver of commercial cockerel chickens.

Keywords*: Lead acetate, Naringin, Oxidative stress, Immunohistochemistry*

**Authors for correspondence: toajibade@gmail.com, Tel: +234-9071842142*
Manuscript received- October 2022; Accepted: June 2023
DOI: https://doi.org/10.54548/njps.v38i2.13

INTRODUCTION

Lead (Pb) has been described as a toxic heavy metal causing significant health problems worldwide (WHO, 2021). It is found majorly as naturally occurring metal within the Earth's crust either in trace or large quantities as influenced by human activities such as mining and other industrial activities (Teerasarntipan, 2020). Also, Pb is one of the most frequently found metal in the environment considering its extensive industrial uses that include manufacture of different range of batteries, additives in paints, use in fuel to increase the octane ratings, ammunitions, and manufacture of radiation protection materials (Babalola and Areola, 2010).

Exposure to Pb in humans has been estimated to account for almost a million deaths as well as, loss of about 21.7 million years of healthy life worldwide with the highest burden in developing countries (IHME, 2019). IHME (2019) showed that lead exposure was ostensibly responsible for approximately 62.5% of the global burden

of developmental cognitive disability of unknown aetiology in children as well as 8.2% of global hypertensive heart disease in adults. Major sources of environmental Pb contamination to the avian species is through anthropogenic activities, polluted air carrying lead dust, water runoffs from mining sites, contaminated feed ingredients and erosions (De Francisco *et al*., 2003). Pb contamination is usually transferred to food animals through direct or indirect exposures and is mostly through the deposition of contaminants in soil and aquatic environment from emissions and human activities (Hossain *et al*., 2014). A low concentration of 1.0 mg/kg has been found to significantly cause problems in growth and reduction of blood δ-aminolaevulinic acid dehydratase enzyme (Hossain *et al*., 2014).

By affecting the central and peripheral nervous system, hematopoietic system, cardiovascular system, kidneys, liver, and reproductive system, Pb has been discovered to trigger a variety of physiological, biochemical, and behavioral dysfunctions in animals and humans. Toxicity studies is closely correlated with the route and duration of exposure, level of intake, absorption rate, and efficiency of excretion (Fakunle *et al*., 2013; Matovic *et al*., 2015).
Pb is a non-redox metal, and the principal mechanism of toxicity is via the induction of oxidative stress through the activities of reactive oxygen species (ROS) as well as, the depletion of the antioxidant defense system in various tissues (Matovic *et al*., 2015; Oyagbemi *et al*., 2015). Free radicals and ROS generated have been reported to precipitate lipid peroxidation and depletion of antioxidant status, by altering cellular membrane integrity and fatty acid composition (Oyagbemi *et al*., 2015; Omobowale *et al*., 2016). Pb toxicity has been shown to result in activation of Nuclear Factor Kappa β (NF-Kβ) that is a master regulator of pro-inflammatory cytokines (Omobowale *et al*., 2016; Vallverdú-Coll *et al*., 2019).

Pb can be absorbed into the bloodstream through either the respiratory or gastrointestinal tracts depending on the route of exposure and is eventually re-distributed into the bones and soft tissues, with significant amounts in the bones, liver, and kidneys (Oyagbemi *et al*., 2014). Pb affects the immune system of avian species causing imbalances between Th1 and Th2-type responses mounted by the separate classes of T-lymphocytes, leading to a depression of the Th1 responses associated with cell mediated immunity (Vallverdú-Coll *et al*., 2019).

A major cardinal step in disease prevention and management is neutralization of free radicals' activities/ROS by antioxidants deactivation or stabilization of these free radicals/ROS to prevent them from causing significant damage to biological systems (Munazza and Muhammad, 2018).

Naringin is a naturally occurring flavonoid glycoside that has a wide range of bioactive activities such as anti-inflammatory, free radical scavenging, antioxidant and immunomodulatory effect on animal and human health (Venkateswara *et al*., 2017). Flavonoids are important components of the human diet. Though not considered as nutrients, they are major class of plant secondary metabolites that serve a range of functions including antioxidant activities and other various health benefits (Venkateswara *et al*., 2017). Naringin is rapidly transformed into naringenin by the action of enzymes such as α-rhamnosidase and β-glucosidase and has been reported to have protective effect against radiation induced chromosomes damage in mouse bone marrow and influence the propagation reactions of free radicals and their formation by inhibiting the enzymes involved and by chelating transition metals (Cavia-Saiz *et al*., 2010).

Naringin has been shown to have neuroprotective properties and has been demonstrated to have an impact on iron-induced oxidative stress as well as chelate certain metals, such as nickel (Golechha *et al*., 2010; Ganesh and Tiyagura, 2011; Kulasekaran *et al*., 2011). In their studies, Ozkaya *et al*., (2016) and Wang *et al*., (2012) found that naringin and naringenin could lower oxidative damage in the liver and functioned as Pb chelating agents. Naringin used as a dietary supplement in poultry improved the quality, oxidative stability and nutritional value of broiler meat (Goliomytis *et al*.,2015; Hager-Theodoride *et al*., 2021) in their investigation.

MATERIALS AND METHODS

Chemicals/Reagents: Lead acetate trihydrate ($(C_2H_3O_2)2Pb.3H_2O$), Naringin, oxidized glutathione (GSSG), and thiobarbituric acid (TBA) were purchased from Sigma (St. Louis, MO, USA). Biotinylated secondary antibody and caspase 3 monoclonal antibody was purchased from Elabscience Biotechnology, China.

Animal housing and Experimental design: Thirty-six-day old cockerel chicks were reared together for six weeks before randomly distributed into six groups (A-F) of six chickens per group. Group A served as the control, Group B was administered (Pb; 300 ppm) only, Group C was administered (Pb and 80 mg/kg Naringin), Group D was administered (Pb and 160 mg/kg Naringin), Group E was administered (80 mg/kg Naringin) only and Group F was administered (160 mg/kg Naringin) only. The dosage of Pb administered was selected based on the previous study of Amini *et al*. (2021). The chickens were fed starter chick feed and later growers mash from Top® Feeds Limited, Ibadan as often as required, and water was made available *ad libitum*. Pb and NAR were co-administered via drinking water and oral gavage respectively for eight weeks. Ethical approval was sought and granted by the university of Ibadan animal care and use research committee with the approval number UI-ACUREC/ 021-0421/16.

Sample Collection and Preparation: Twenty-four hours after the last administration, chickens were euthanized by quick cervical dislocation. The whole liver was rapidly dissected out on ice, rinsed with distilled water, blotted with filter paper, and weighed for the determination of organ weight as well as relative organ weight respectively for biochemical assay. Subsequently, about 2 g each of the liver sample was collected inside universal bottle and frozen until biochemical assays while, samples for histology were fixed in 10% formalin.

Preparation of hepatic post-mitochondrial fractions: The harvested liver samples were chopped into bits and homogenized in homogenizing buffer (0.1M phosphate buffer, pH 7.4) using a Teflon® homogenizer. The

homogenate was centrifuged at 10,000 × g rpm for 10 minutes with a cold centrifuge at −4°C to obtain post-mitochondrial fractions (PMFs). The supernatants obtained (PMFs) obtained were used for biochemical assays.

Biochemical Assays

Determination of antioxidant defense system: Superoxide dismutase (SOD) was determined according to Misra and Fridovich's method with slight modification by Oyagbemi *et al*., (2015). Additionally, the glutathione peroxidase (GPx) activity was determined in accordance with Beutler *et al*., (1963), glutathione S-transferase (GST) activity was calculated using Habig *et al*. (1974) method using 1-chloro-2,4-dinitrobenzene as substrate, and reduced glutathione (GSH) content was calculated using Ellman method (1959).

Determination of markers of oxidative stress: The method outlined by Wolf's (1994) was used to measure the formation of hydrogen peroxide (H_2O_2) while Malondialdehyde (MDA), a product of lipid peroxidation was determined using the technique outlined by Varshney and Kale (1990).

Determination of serum Total protein: Serum total protein was determined by Biuret's method as described by Gornal *et al.,* (1949).

Histopathology: Hepatic tissues were fixed in 10% formalin embedded in paraffin wax, and sections of 5-6 mm in thickness were made and thereafter stained with Hematoxylin and Eosin (H&E) as previously described by Drury and Walington, (1976).

Immunohistochemistry: Caspase 3 Monoclonal Antibody in the liver was assayed using an immunohistochemistry procedure as described by Oyagbemi *et al*. (2019) with a small modification using a 2-step plus Poly-HRP Anti Mouse/Rabbit IgG Detection System with DAB solution (Catalog number: E-IR-R217 from Elabscience Biotechnology®, China). The liver samples were embedded in paraffin, fixed with 10% paraformaldehyde, and sectioned at a thickness of 5 m. The slides were therefore dewaxed for 2 minutes in a 100% solution of xylene before being hydrated for 2 minutes in each of three distinct concentrations of ethanol (100%, 90%, and 80%). Thereafter, the slides were rinsed and immersed for 5 minutes in a PBS buffer tank. A citrate buffer solution containing 2.1 g of citric acid monohydrate and 14.75 g of trisodium citrate dehydrate, adjusted to pH 6.0, was used to perform the antigen retrieval in a microwave oven. Endogenous peroxide (H_2O_2 block) was done in accordance with the kit's instructions (E-IR-217C) from the manufacturer. The sections were covered with drops of H_2O_2 before being incubated in a humidifying chamber at room temperature for 10 minutes. The slides were rinsed before placing once more in the PBS tank for five minutes at room temperature. To prevent nonspecific binding, goat serum (E-1R-R217A) was applied to the slides, which were then incubated for 30 min at room temperature in a humidifying chamber. Following incubation, the tissues were probed with primary antibodies, specifically Caspase 3 Monoclonal Antibody, and incubated for 2 hr at room temperature in a humidifying chamber. Thereafter, the slides were rinsed with PBS and secondary antibody labelled (E-1R-R217B) was added, and the slides were incubated in humidifying chamber at room temperature for 20 min. The slides were then rinsed and submerged for five minutes in a PBS tank. Finally, a few drops of the substrate diaminobenzidine (DAB) were added after it had been prepared by mixing 50µL of DAB concentrate (E-1R-R217D) with 1 mL of DAB solution (E-1R-R217E) in the dark for 10 seconds. The reaction was stopped with deionized water, and slides were submerged in hematoxylin for 3 seconds prior to rinsing with PBS. The slides were immersed for two minutes each in 70%, 80%, 90%, 100%, and 100% ethanol, followed by 100% xylene. Slides were taken out, given enough time to dry, and then a DPX mountant and cover slip was used. Sections were examined using a digital camera and a Leica software application package version 3.4 light microscope (Leica LAS-EZ®).

Statistical analysis

The Student's t-test was used to evaluate the test of significance between the groups. All values were expressed as mean ± standard deviation. Additionally, the One-Way Analysis of Variance (ANOVA) using GraphPad Prism 5.0's Turkey's post-hoc test was performed, with p-Values less than 0.05 regarded as statistically significant.

RESULTS

Antioxidant defense status and oxidative stress markers: There was significant increase in the valves of makers of oxidative stress, H_2O_2 and MDA, when compared with the control (Group A) and this was ameliorated in both groups treated with different doses of naringin as indicated in figures 1 and 2 respectively.

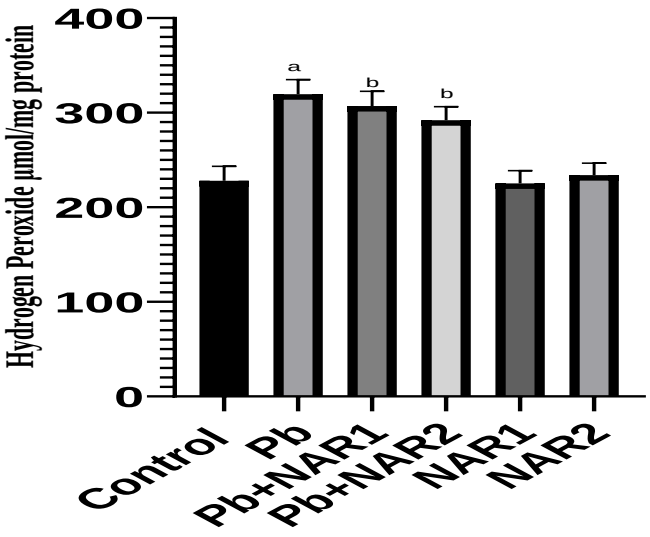

Figure 1:
Effect of Lead toxicity and Naringin on hepatic hydrogen peroxide (H_2O_2) generation. A (Control), Pb (Lead acetate; 300 ppm), Pb+Nar1 (Lead acetate + Naringin 80 mg/kg), Pb+Nar2 (Lead acetate + Naringin 160 mg/kg), Nar1 (Naringin 80 mg/kg), Nar2 (Naringin 160 mg/kg). Notes: Superscript (a) indicates significant difference at $p<0.05$ when compared with Control. Superscript (b) indicates significant difference when compared with Pb.

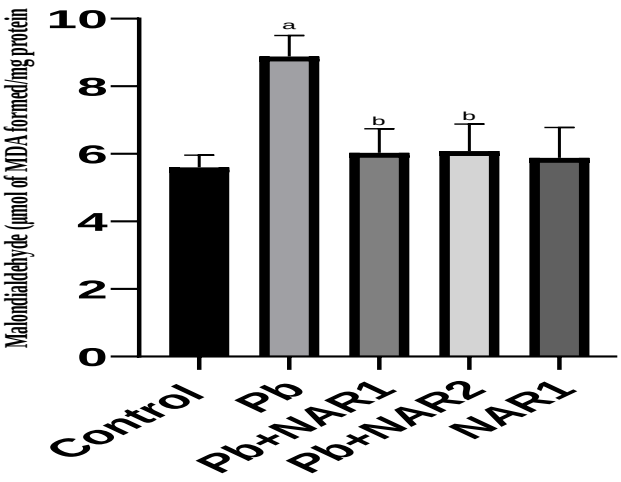

Figure 2:
Effect of Lead toxicity and Naringin on hepatic Malondialdehyde (MDA) content. A (Control), Pb (Lead acetate; 300 ppm), Pb+Nar1 (Lead acetate + Naringin 80 mg/kg), Pb+Nar2 (Lead acetate + Naringin 160 mg/kg), Nar1 (Naringin 80 mg/kg), Nar2 (Naringin 160 mg/kg). Notes: Superscript (a) indicates significant difference at $p<0.05$ when compared with Control. Superscript (b) indicates significant difference when compared with Pb.

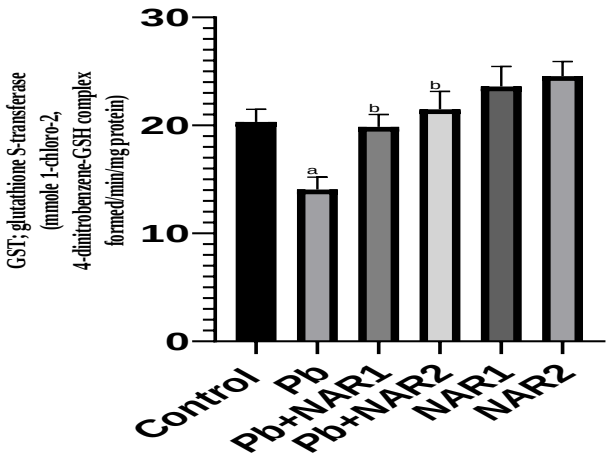

Figure 4:
Effect of Lead toxicity and Naringin on hepatic Glutathione S-transferase (GST) activity. A (Control), Pb (Lead acetate; 300 ppm), Pb+Nar1 (Lead acetate + Naringin 80 mg/kg), Pb+Nar2 (Lead acetate + Naringin 160 mg/kg), Nar1 (Naringin 80 mg/kg), Nar2 (Naringin 160 mg/kg). Notes: Superscript (a) indicates significant difference at $p<0.05$ when compared with Control. Superscript (b) indicates significant difference when compared with Pb.

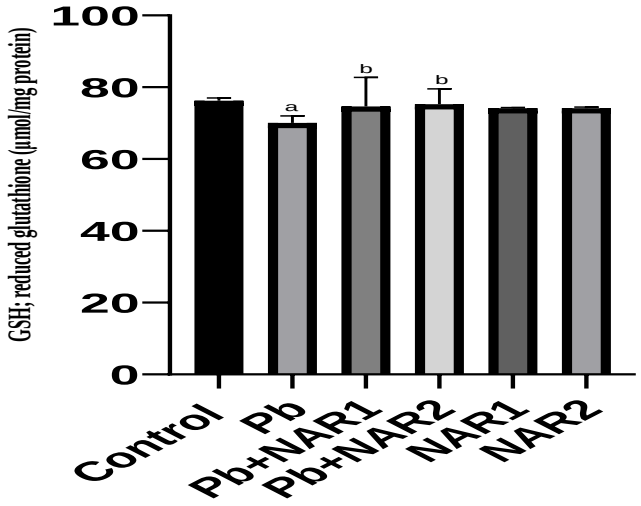

Figure 3:
Effect of Lead toxicity and Naringin on hepatic reduced glutathione(GSH) content. A (Control), Pb (Lead acetate; 300 ppm), Pb+Nar1 (Lead acetate + Naringin 80 mg/kg), Pb+Nar2 (Lead acetate + Naringin 160 mg/kg), Nar1 (Naringin 80 mg/kg), Nar2 (Naringin 160 mg/kg). Notes: Superscript (a) indicates significant difference at $p<0.05$ when compared with Control. Superscript (b) indicates significant difference when compared with Pb.

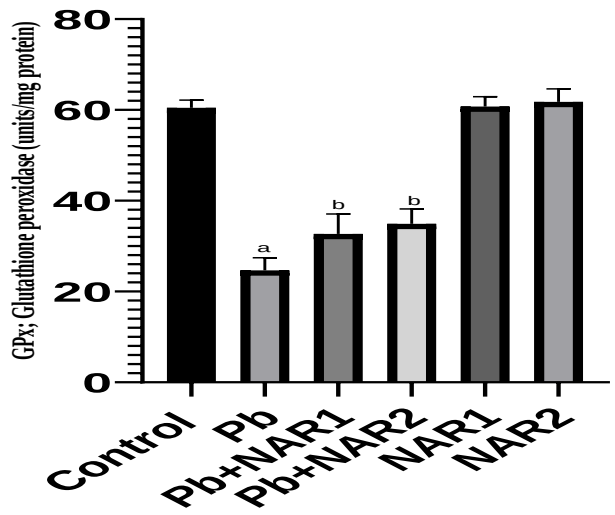

Figure 5:
Effect of Lead toxicity and Naringin on hepatic Glutathione peroxidase (GPx) activity. A (Control), Pb (Lead acetate; 300 ppm), Pb+Nar1 (Lead acetate + Naringin 80 mg/kg), Pb+Nar2 (Lead acetate + Naringin 160 mg/kg), Nar1 (Naringin 80 mg/kg), Nar2 (Naringin 160 mg/kg). Notes: Superscript (a) indicates significant difference at $p<0.05$ when compared with Control. Superscript (b) indicates significant difference when compared with Pb.

There were remarkable significant ($p<0.05$) reductions in the activities of GSH (Figure 3), GST (Figure 4), GPx (Figure 5), and SOD (Figure 6) in the Pb intoxicated chicks when compared to the control across all the experimental groups. Co-administration of Pb and two different doses of naringin however produced significant improvement in the activities of the hepatic antioxidant defence system relative to the Pb alone with the group with the higher dose of naringin (160mg/kg) showing optimum valves in the experimental birds.

Histology: At X40 magnification, group A which served as the control had no observable lesion while severe locally extensive hepatocellular necrosis and inflammation were observed in the group treated with Pb only (Group B) as shown in Figure 7. There was moderate centrilobular hepatocellular degeneration in group C while Group D showed centrilobular plate atrophy and bridging fibrosis (Figure 7). Groups E and F that were administered naringin at 80mg/kg and 160mg/kg respectively had no observable lesions.

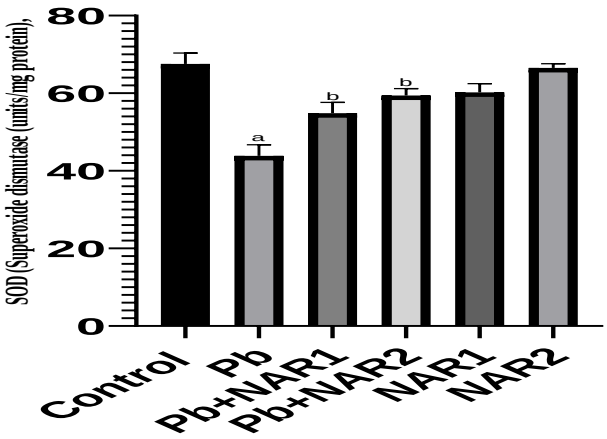

Figure 6:
Effect of Lead toxicity and Naringin on hepatic superoxide dismutase (SOD) activity. A (Control), Pb (Lead acetate; 300 ppm), Pb+Nar1 (Lead acetate + Naringin 80 mg/kg), Pb+Nar2 (Lead acetate + Naringin 160 mg/kg), Nar1 (Naringin 80 mg/kg), Nar2 (Naringin 160 mg/kg). Notes: Superscript (a) indicates significant difference at $p<0.05$ when compared with Control. Superscript (b) indicates significant difference when compared with Pb.

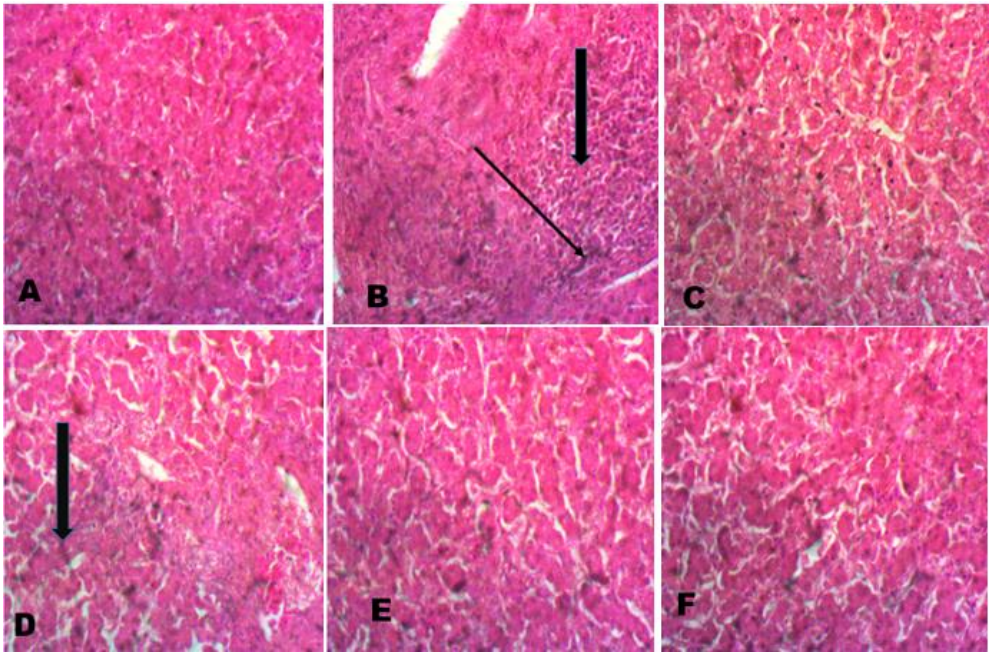

Plate 1.
The Histology of the Liver.
A (Control), B (Lead acetate, 300 ppm), C (Lead acetate, 300 ppm + Naringin 80 mg/kg), D (Lead acetate, 300 ppm + Naringin 160 mg/kg), E (Naringin 80 mg/kg), F (Naringin 160 mg/kg).

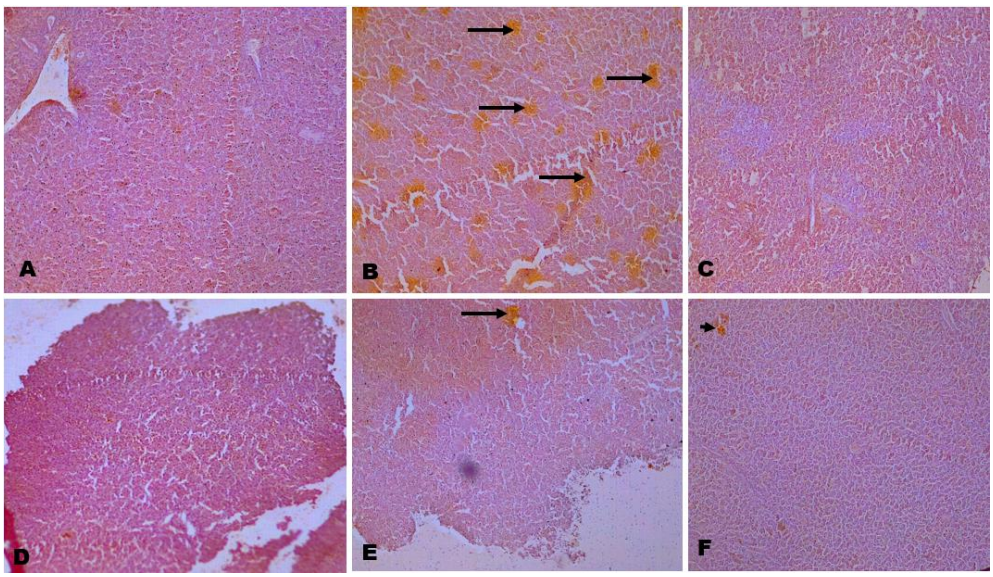

Plate 2.
The immunohistochemistry of liver caspase 3. A (Control), B (Lead acetate; 600 ppm), C (Lead acetate + *Naringin 8*0 mg/kg), D (Lead acetate + Naringin 80 mg/kg), E (Naringin 80 mg/kg), F (Naringin 100 mg/kg). Slides stained with high definition Heamtoxylin. (Magnification x 100)

Immunohistochemistry: The immune localization of Caspase 3 in the hepatocytes revealed higher expressions in the Pb exposed group when compared to the control and groups co-treated with naringin (Figure 8). The reduction in the expressions of Caspase 3 is indicative of amelioration of apoptosis and hepatoprotective effects of naringin against Pb acetate toxicity as shown by the reduction in the expression of caspase 3 in the groups treated with naringin and groups administered naringin only thus.

DISCUSSION

According to several studies (Herring *et al*., 2018, González *et al*., 2019, Moncls *et al*., 2020, Descalzo *et al*., 2021), Pb poisoning continues to be one of the most serious public health issues, especially in underdeveloped nations. Pb exposure has a variety of detrimental impacts on the body's systems, but the most notable is increased oxidative stress, which is crucial for the development of disease (Amini *et al*., 2019). In soft tissues, the chicken liver was found to have the second highest Pb content after the kidney. The liver, which has been regarded as the greatest Pb store of soft tissues in animals, oversees detoxifying a variety of compounds (Wang *et al.,* 2021).

The Pathogenesis and pathophysiology of Pb-induced toxicity have been linked to the production of free radicals that generate oxidative stress and deplete the antioxidant defense system (Nasiruddin *et al*., 2020; Gadde *et al.,* 2021). According to our research, the birds in the Pb- induced toxicity group showed a noticeably higher level of hydrogen peroxide (H_2O_2) production, lipid peroxidation product (MDA) content, and oxidative stress in the liver of the experimental birds. Our results are consistent with earlier findings that showed Pb poisoning caused a significant rise in oxidative stress, inflammation, and apoptosis (Gagan *et al.,* 2012; Omobowale *et al.,* 2014; Oyagbemi *et al*., 2015; Matovic *et al*., 2015; Omobowale *et al*., 2016).

Furthermore, we found that Pb intoxication resulted in considerable reductions in reduced glutathione (GSH) levels as well as in the activities of glutathione S-transferase (GST), superoxide dismutase (SOD), and glutathione peroxidase (GPx). But, naringin co-administration enhanced the antioxidant defense system and reduced the oxidative stress markers described above. Therefore, these results are consistent with the conclusion of other studies on the antioxidant capabilities of naringin (Baranowska *et al*., 2021; Deng *et al*., 2022).

Compared to the control and treatment groups, there was a significant decrease in serum total protein in Pb-intoxicated birds. Naringin treatment considerably increased the serum total protein concentration as shown by the findings of this study. As observed by Moussa and Bashandy (2008), a decrease in serum total protein has been linked to kidney and cardiac failure. Additionally, in this study, birds exposed to Pb alone showed higher MPO activity when compared to the control and groups given naringin. MPO, however, has been described as a novel sign of oxidative stress, kidney damage, inflammation, and a diagnostic marker of cardiomyopathy including cardiac arrest and heart attack (Khan *et al.,* 2018; Veltman *et al*., 2021; Peng *et al*., 2021; Wei *et al*., 2021; Sandamali *et al*., 2021). The decrease in MPO activity in naringin-treated birds suggested that naringin had anti-inflammatory, hepatoprotective, and cardioprotective effects in Pb-exposed birds.

With numerous pharmacological advantages, such as antioxidant, anti-inflammatory, and anti-apoptotic qualities, naringin is a commonly accessible flavonoid that is found in citrus fruits. In this study, naringin was administered to groups at doses of 80 mg/kg and 160 mg/kg, which significantly increased the levels of enzymatic and non-enzymatic antioxidants, reduced oxidative stress, improved serum NO, and decreased MPO activity. Naringin was also found to have antioxidant, anti-inflammatory, and anti-apoptotic properties.

Exposure to lead has been shown to cause fatty changes in the liver parenchyma, degraded hepatocytes, and nuclear pyknosis, which results in an increase in the number of apoptotic cells in the liver (Ashrafizadeh *et al*., 2018). This was consistent with our observations of severe inflammation and hepatocellular necrosis in the untreated group. Additionally, lead toxicity, as observed by Chi *et al.,* (2017) may result in cellular oedema that causes mitochondria to rupture, vacuolize, and wrinkle. Naringin was co-administered in the treatment groups, and this resulted in varied degrees of improvement for all these pathologies. According to Ashrafizadeh *et al.,* (2018), lead toxicity may be responsible for the development of intracellular inclusions, localized atrophy, and intracytoplasmic calcification in the proximal tubules of rats. According to reports, lead destroys the morphologic structures of hepatocytes by causing cellular disruptions, necrosis, and the infiltration of inflammatory cells in the liver, as was the case in the untreated group (Chi *et al*., 2017). The dilatation of the liver portal vein and the scaffolding of the hepatic lobules and pyknotic regions identified in the degenerating hepatocytes have also been reported in lead intoxication in chickens (Haleagrahara *et al.,* 2010).

In contrast to other groups that received naringin in conjunction with Pb or naringin alone, immunohistochemistry revealed increased expression of Caspase 3 in the liver of Pb-treated birds. The conserved family of proteins known as caspase 3, which is widely expressed, is known for its active proteolytic functions in the execution of apoptosis in cells in response to extrinsic or intrinsic inducers of this method of cell death (Eskandari and Eaves 2022). In multicellular creatures, however, caspase 3 also appears to serve important functions in controlling the development and upkeep of both healthy and pathological cells and tissues, according to mounting data (Sudhakar *et al*., 2008).

Additionally, Walsh *et al*., (2008) reported that caspase 3 is the predominant executioner caspase, although caspase 7 may play multiple roles depending on the substrate. This discovery is consistent with our study's finding that caspase 3 is expressed more abundantly in Pb-induced toxicity. Caspase3, the main enzyme responsible for apoptotic death, makes cell death more effective (Eskandari and Eaves 2022).

As a result, our study has shown that co-administration of a naturally occurring substance with a high flavonoid content, such as naringin, can reverse oxidative stress, reduce the production of free radicals, and significantly improve the antioxidant defense system.

Overall, it can be said that naringin, a metal chelating flavonoid, protects the liver from lead acetate toxicity by acting as an antioxidant and an anti-inflammatory agent, and as a metal chelator. Additionally, co-admiration of naringin with lead reduced the oxidative stress caused by lead and markedly enhanced the antioxidant defense system and serum nitric oxide bioavailability. Therefore, the naringin administration either in chicken feeds or water act as a heavy metal chelator, which could be advantageous to the poultry industries.

Acknowledgements
The African Union, through the Pan African University Institute of Earth and Life Sciences Institute (PAULESI), provided money for this work, and the Cardio-renal Laboratory at the University of Ibadan provided the facilities. The authors are extremely grateful for both.

REFERENCES

Ahmad, A., Dempsey, S.K., Daneva, Z., Azam, M., Li, N., Li, P. and Ritter. J.K. (2018). Role of Nitric Oxide in the Cardiovascular and Renal Systems. Int. J. Mol. Sci. 19:2605

Ajarem, J.S., Hegazy, A.K, Allam, G.A., Allam, A.A, Maodaa, S.N. and Mahmoud A.M. (2021). Effect of Visnagin on Altered Steroidogenesis and Spermatogenesis, and Testicular Injury Induced by the Heavy Metal Lead. Comb. Chem. High Throughput Screen. 24(6):758-766

Amini, N., Sarkaki, A., Mahin, D., Seyyed, A. M., Akram A. and Mohammad B. (2019). Protective effects of naringin and trimetazidine on remote effect of acute renal injury on oxidative stress and myocardial injury through Nrf-2 regulation. Pharmacol. Rep. 71(6):1059-1066.

Ashrafizadeh, M., Rafiei, H. and Ahmadi, Z. (2018). Histological Changes in the Liver and Biochemical Parameters of Chickens Treated with Lead Acetate II. Iran J. Toxicol. 12: 6.

Babalola, O.O. and Areola J.O. (2010). Interactive roles of terpenoid extract from the leaves of neem plant (Azadirachta indica, A. Juss) on lead induced toxicity in pregnant rabbits. J. Med. Plants Res. 4 (12):1102-1107.

Baranowska, M., Koziara, Z., Suliborska, K., Chrzanowski, W., Wormstone, M., Namieśnik, J., and Bartoszek, A. (2021). Interactions between polyphenolic antioxidants quercetin and naringenin dictate the distinctive redox-related chemical and biological behavior of their mixtures. Sci Rep. 11(1): 12282.

Beutler, E., Duron, O. and Kelly, MB (1963) Improved method for determination of blood glutathione reduced. J Lab Clin Med. 61: 882- 888.

Brentnall, M., Rodriguez-Menocal, L., De Guevara, R. L., Cepero, and Boise, L. H. (2013). Caspase-9, caspase-3 and caspase-7 have distinct roles during intrinsic apoptosis. BMC Cell Biol. **14**, 32.

Broseghini-Filho, G.B., Almenara, C.C., Vassallo, D.V. and Padilha A.S. (2016). Blood Pressure Decreases Following Lead Treatment Cessation: Highest NO Bioavailability Involved. Biol. Trace Elem. Res. 170(2): 410-414.

Cavia-Saiz, M., Busto, D.M., Maria, C.P., Natividad, O., Perez-Mateos, M. and Pilar, M. (2010). Antioxidant properties, radical scavenging activity and biomolecule protection capacity of flavonoid naringenin and its glycoside naringin: a comparative study. J. Sci. Food Agric. 90: 1238–1244.

Chi, Q., Liu, T., Sun, Z., Tan, S., Li, S. and Li, S. (2017). Involvement of mitochondrial pathway in environmental metal pollutant lead-induced apoptosis of chicken liver: perspectives from oxidative stress and energy metabolism. Environ. Sci. Pollut. Res.. 2017 24 (36):28121-31.

De Francisco, N., Ruiz, T. J. D. and Agüera, E. I. (2003). Lead and lead toxicity in domestic and free-living birds. Avian Pathology, 32 (1): 3-13.

Deng, M., Jia, X., Dong, L., Liu, L., Huang, F., Chi, J., Ma, Q., Zhao, D., Zhang, M. and Zhang, R. (2021). Structural elucidation of flavonoids from Shatianyu (Citrus grandis L. Osbeck) pulp and screening of key antioxidant components. Food Chem. 366:130605.

Descalzo, E., Camarero, P.R, Sánchez-Barbudo, I.S., Martinez-Haro, M., Ortiz-Santaliestra, M.E., Moreno-Opo, R. and Mateo, R. (2021). Integrating active and passive monitoring to assess sublethal effects and mortality from lead poisoning in birds of prey. Sci. Total. Environ. 750:142260.

Drury, R.A., (1976). Wallington E.A. Carlton's Histopathological Techniques. 4th ed. Oxford University Press, London, pp 139-142

Ellman, G. L. (1959). Tissue sulfhydryl groups. Arch Biochem Biophys. 82(1):70

Eskandari, E. and Eaves, C. J. (2022). Paradoxical roles of caspase-3 in regulating cell survival, proliferation, and tumorigenesis. J. Cell Biol. 221 (6): e202201159.

Fakunle, P.B., Ajibade, A.J., Oyewo, E.B. and Adeyemi, O.H. (2013). A study of some effects of aqueous extract of neem (Azadiractha indica) leaves on the lead acetate induced neurotoxicity in the superior colliculus of adult wistar rats (Rattus norvegicus). Br. J. Pharm. Res. 3(2): 217-231.

Gadde, R. and Betharia, S. (2021). N,N'bis-(2-mercaptoethyl) isophthalamide (NBMI) exerts neuroprotection against lead-induced toxicity in U-87 MG cells. Arch. Toxicol. 95(8): 2643-2657.

Gagan, F., Deepesh, G. and Archana, T. (2012). Toxicity of lead: A review with recent updates. Interdiscip Toxicol. 5(2):47–58.

Ganesh, C.J. and Reddy, T.K. (2011). Alleviation of iron induced oxidative stress by the grapefruit flavanone naringin in vitro. Chemico-Biological Interactions. 190: 121–128.

Golechha, M., Chaudhry, U., Bhatia, J., Daman, S. and Singh D. (2011). Naringin Protects against Kainic Acid-Induced Status Epilepticus in Rats: Evidence for an Antioxidant, Anti-inflammatory and Neuroprotective Intervention. Biol. Pharm. Bull. 34(3) 360—365.

Goliomytis, M., Kartsonas, N., Charismiadou, M.A., Symeon, P.E. and Deligeorgis, S.G. (2015). The Influence of Naringin or Hesperidin Dietary Supplementation on Broiler Meat Quality and Oxidative Stability. PloS one. 10: e0141652.

González, F., Camacho, M., Tiburón, N.P., Peña, M.Z., Rueda, L.R. and Luzardo, O.P. (2019). Suitability of anodic stripping voltammetry for routine analysis of venous blood from raptors. Environ. Toxicol. Chem. 38(4):737-747.

Gornal, A.G., Bardawill J.C. and David M.M. (1949). Determination of serum proteins by means of Biuret reaction. J. Biol. Chem. 177: 751–766.

Habig, W.H., Pabst, M.J. and Jakpoby, W.B. (1974) Glutathione transferase, a first enzymatic step in mercapturic acid formation. J. Biol. Chem. 249, 7130–7139.

Hager-Theodorides, A.L., Massouras, T., Simitzis, P.E., Moschou, K., Zoidis, E., Sfakianaki, E., Politi, K., Charismiadou, M., Goliomytis, M. and Deligeorgis, S. (2021). Hesperidin and Naringin Improve Broiler Meat Fatty Acid Profile and Modulate the Expression of Genes Involved in Fatty Acid β-oxidation and Antioxidant Defense in a Dose Dependent Manner. Foods. 10, 739.

Haleagrahara, N., Jackie, T., Chakravarthi, S., Rao, M. and Kulur, A. (2010). Protective effect of Etlingera elatior (torch ginger) extract on lead acetate-induced hepatotoxicity in rats. The Journal of toxicological sciences. 35(5): 663- 71.

Herring, G., Eagles-Smith, C.A. and Varland, D.E. (2018). Mercury and lead exposure in avian scavengers from the Pacific Northwest suggest risks to California condors: Implications for reintroduction and recovery. Environ Pollut. 243:610-619.

Hossain, M.A., Mostofa, M., Alam, M.N., Sultana, M.R., and Rahman, M.M. (2014). The ameliorating effects of garlic (allium sativum) against lead (pb) intoxication on body weight, dressing percentages, feed consumption and feed

conversion ratio in lead induced broiler chickens. Bangl. J. Vet. Med.12 (1): 1-7.

Khan, A.A., Alsahli, A.M., and Rahmani, A.H. 2018. Myeloperoxidase as an Active Disease Biomarker: Recent Biochemical and Pathological Perspectives. Med. Sci. 6:33

Kucukler, S., Benzer, F., Yildirim, S., Gur, C., Kandemir, F.M., Bengu, A.S., Ayna, A., Caglayan, C. and Dortbudak, M.B. (2021). Protective Effects of Chrysin Against Oxidative Stress and Inflammation Induced by Lead Acetate in Rat Kidneys: A Biochemical and Histopathological Approach. Biol. Trace Elem. Res. 199:1501-1514.

Kulasekaran, G., Dharmalingam, P. and Ganapasam, S. (2011). Neuroprotective effect of naringin, a dietary flavonoid against 3-Nitropropionic acid induced neuronal apoptosis. Neurochem. Inter. 59, 1066–1073.

Long, X., Sun, F., Wang, Z., Liu, T., Gong, J., Kan, X., Zou, Y. and Zhao, X. (2021) Lactobacillus fermentum CQPC08 protects rats from lead-induced oxidative damage by regulating the Keap1/Nrf2/ARE pathway. Food Funct. 12(13):6029-6044

Matović, V., Aleksandra, B., Đukić-Ćosić, D., Zorica, B. (2015). Insight into the oxidative stress induced by lead and/or cadmium in blood, liver and kidneys. Food and Chemical Toxicology. 78:130-40.

Monclús, L., Shore, R.F. and Krone, O. (2020). Lead contamination in raptors in Europe: A systematic review and meta-analysis. Sci. Total Environ. 748:141437.

Moussa, S.A. and Bashandy, S.A. (2008). Biophysical and Biochemical changes in the blood of rats exposed to lead toxicity. Romanian J. Biophys. 18: 123–133.

Munazza, S. and Muhammad, S.A. (2018). Neem (*Azadirachta indica*) And Its Potential for Safeguarding Health, Prevention and Treatment of Diseases. Matrix Sci. Med. 2(1):04-08.

Nasiruddin, R. M., Karim, N., Changlek, S., Atiar, R. M., Tangpong, J., Hajjar, D., Alelwani, W., Makki, A.A. (2020). Thunbergia laurifolia leaf extract partially recovers lead-induced renotoxicity through modulating the cell signaling pathways. Saudi J. Biol. Sci. 27(12):3700-3710.

Omobowale, T.O, Oyagbemi, A.A, Akinleye, S.A, Ola-Davies, O.E, Saba, A. B., Olopade, J.O. and Adedapo, A.A. (2016). Effect of Exposure and Withdrawal on Lead-induced Toxicity and Oxidative Stress in Cardiac Tissues of Rats. Toxicol. Intern. 23(1): 12-17

Omobowale, T.O., Oyagbemi, A.A., Akinrinde, A.S., Saba, A.B., Daramola O.T., Ogunpolu B.S., Olopade J.O. (2014). Failure of recovery from lead induced hepatoxicity and disruption of erythrocyte antioxidant defence system in Wistar rats. Environ. Toxicol. Pharmacol. 37:1202–1211.

Oyagbemi, A.A, Omobowale, T.O., Awoyomi, O.V., Ajibade, T.O., Falayi, O.O., Ogunpolu B.S., Okotie, U.J., Asenuga, E.R., Adejumobi, O.A., Hassan, F.O., Ola-Davies, O.E., Saba, A.B., Adedapo, A.A. and Yakubu, M.A. (2019). Cobalt chloride toxicity elicited hypertension and cardiac complication via induction of oxidative stress and upregulation of COX-2/Bax signaling pathway. Hum. Exp. Toxicol. 38(5): 519-532

Oyagbemi A.A., Omobowale T.O., Akinleye S.A., Adebowale B.S., Blessing S.O., Oluwabusola D. (2014). Lack of Reversal of Oxidative Damage in Renal Tissues of Lead Acetate-Treated Rats. Environ. Toxicol. Environ Toxicol. 30(11):1235-43.

Ozkaya, A., Zafer, S., Uzeyir, D. and Mustafa, O. (2016). Effects of Naringenin on Oxidative Stress and Histopathological Changes in the Liver of Lead Acetate Administered Rats. J Biochem. Mol. Toxicol. 30: 5.

Sandamali, J.A.N., Hewawasam, R.P., Jayatilaka K.A.P.W. and Mudduwa L.K.B. (2021). *Cinnamomum zeylanicum* Blume (*Ceylon cinnamon*) bark extract attenuates doxorubicin induced cardiotoxicity in Wistar rats. Saudi Pharm. J. 29(8):820-832

Sudhakar, C., Jain N. and Swarup G. (2008). Sp1-like sequences mediate human caspase-3 promoter activation by p73 and cisplatin. FEBS J. 275: 2200 –2213

Teerasarntipan, T., Chaiteerakij, R., Prueksapanich, P. and Werawatganon D. (2020). Changes in inflammatory cytokines, antioxidants and liver stiffness after chelation therapy in individuals with chronic lead poisoning. BMC Gastroenterol. **20,** 263 (2020).

Vallverdú-Coll, N., Mateo, R., Mougeot F. and Ortiz-Santaliestra. M.E. (2019). Immunotoxic effects of lead on birds. Sci. Total Environ. 689:505-515.

Varshney, R. and Kale, R.K. (1990). Effect of calmodulin antagonists on radiation induced lipid peroxidation in microsomes. Inter. J. Rad. Biol. 58: 733–743.

Veltman, D., Wu, M., Pokreisz, P., Claus, P., Gillijns, H., Caluwé, E., Vanhaverbeke, M., Gsell, W., Himmelreich, U., Sinnaeve, P.R. and Janssens S.P. (2021). Clec4e-Receptor Signaling in Myocardial Repair After Ischemia-Reperfusion Injury. JACC Basic Transl. Sci. 6(8):631-646.

Venkateswara, R. P., Kiran, S.D.V.S., Rohini, P. and Bhagyasree P. (2017). Flavonoid: A review on Naringenin. J. Pharmacog Phytochem. 6(5): 2778- 2783.

Walsh, J.G., Cullen, S.P., Sheridan, C., Luthi, A.U., Gerner, C. and Martin, S.J. (2008). Executioner caspase-3 and caspase-7 are functionally distinct proteases. Proc. Natl Acad. Sci. USA.105 (35): 12815-12819.

Wang, J., Yang, Z., Lin, L., Zhao, Z., Liu, Z., Liu, X. (2012). Protective effect of naringenin against lead-induced oxidative stress in rats. Biol. Trace Elem. Res. 146: 354–359.

Wang, S., Li, Q., Gao, Y., Zhou Z. and Li, Z. (2021). Influences of lead exposure on its accumulation in organs, meat, eggs and bone during laying period of hens, Poul. Sci. 100: 101249.

Wei, H., Xue, Q., Sun, L. and Lv, J. (2021). BRD4 inhibition protects against myocardial ischemia/reperfusion injury by suppressing inflammation and oxidative stress through PI3K/AKT signaling pathway. J Cardiovasc Pharmacol.

Wolff S.F. (1994). Ferrous ion oxidation in the presence of ferric ion indicator xylenol orange for measurement of hydrogen peroxides. Methods Enzymol. 233:182–189.

Xia, Y. and Zweiler, J.L. (1997). Measurement of myeloperoxidase in leucocyte containing tissue. Anal biochem. 245:93-96.

Niger. J. Physiol. Sci. 38 (December 2023): 247 – 253
www.njps.physiologicalsociety.com

Niger. J. Physiol. Sci.

Full length Research Article

Ameliorative Effects of Coconut Water on Hematological and Lipid Profiles of Phenylhydrazine-treated Rats

***Adeleye G.S.[1], Odesanmi E.O.[2], Ajeigbe K.O.[3], Omayone T.[4], Odetola A.[5], Sobanke A.O.[5]**

Departments of [1]Physiology and [2]Medical Biochemistry, Ekiti State University, Ado Ekiti, Nigeria
[3]Department of Physiology Federal University, Oye Ekiti. Ekiti State, Nigeria
[4]Department of Physiology Federal University of Technology, Akure. Ondo State, Nigeria
[5]Department of Physiology Nnmadi Azikiwe University, Awka.

Summary: Low amounts of haemoglobin, or red blood cells, are the hallmark of the disorder known as anaemia, which typically affects expectant mothers and small children. The nutrient-rich coconut water is thought to hasten hematopoiesis or make red blood cells. Finding out how coconut water affected the lipid profiles and haematological indices of rats under phenylhydrazine anaesthesia was the aim of the study. Six groups of thirty rats were created: one for phenylhydrazine-untreated groups, one for standard control, one for iron therapy, one for ferrous treatment, and one for coconut water treatment (0.5 ml/kg). Using a haematology analyzer, the amounts of erythrocytes, hematocrit, and haemoglobin were determined. The results showed that compared to the control group, the anaemia produced by phenylhydrazine had significantly lower levels of TG and LDL and greater levels of HDL. After being fed anaemia, rats who received 0.5 millilitres per kilogramme of coconut water had greater levels of HDL and lower levels of TG, LDL, and VLDL. The study discovered that coconut water raised erythrocyte and HB levels in rats with induced anaemia, indicating a beneficial impact on haematological parameters. These results imply that coconut water can help treat anaemia, significantly enhancing blood coagulation and reducing cholesterol. To completely comprehend the mechanisms underlying these effects and to ascertain the most appropriate dosage and course of treatment, more research is necessary. The advantages of coconut water as a potential anaemia therapy alternative are highlighted throughout the entire study.

Keywords*: Anaemia, Hematology, Lipid profiles, hematopoiesis, coconut*

**Authors for correspondence: adeguyton@gmail.com , Tel: +234-8060220741*

Manuscript received- January 2023; Accepted- August 2023

DOI: https://doi.org/10.54548/njps.v38i2.14

INTRODUCTION

The most prevalent causes of anaemia are hemoglobinopathies, parasite infections, viral diseases like TB, HIV, and malaria, and dietary deficiencies in folate, vitamins B12, and A. Iron deficiency is one of the most common causes of anaemia. In 2019, anaemia affected 36.5% of pregnant women worldwide, 39.8% of children aged 6 to 59 months and 29.6% of non-pregnant women (WHO, 2021). This substantial percentage requires medical care.

To investigate the mechanism of hemolytic anaemia in rats, phenylhydrazine is utilized (Yeshoda 1942; Berger 1985a). Hemolytic anaemia is brought on by phenylhydrazine, which also causes a variety of cellular changes and the oxidative stress-related death of red blood cells. A model for examining the pathogenesis of hemolytic anaemia, the impact of anaemia on other physiological processes, or the onset of related disorders is provided by PHZ-induced toxic anaemia. The majority of currently prescribed anti-anemic drugs have adverse effects, delaying the development of effective anti-anemic therapies despite significant investments made over the years. Consequently, in recent years, alternative treatments with negligible or no adverse effects have become increasingly popular. When oxidative stress and the predominance of degenerative diseases are present, foods that naturally contain antioxidants can be employed as a method to minimize morbidity and death (Winarsi, 2007; Astuti, 2008). Coconut water is produced from palm plants, typically grown in tropical settings. It is a naturally occurring and highly healthy beverage. Because coconut water contains various nutrients, including vitamins, minerals, antioxidants, amino acids, enzymes, and growth hormones, it offers therapeutic benefits (Bhagya, 2012). Recent research indicates that coconut water is an excellent source of vitamin C and the free-form amino acid L-arginine, which can reduce the risk of lipid peroxidation and heart disease (John Kennedy et al., 2013). The purpose of this study is to look into how coconut water affects the lipid profiles, antioxidant enzymes, and haematological markers of rats that have been exposed to anaemia caused by phenylhydrazine.

MATERIALS AND METHODS

ADAM equipment South Africa) set includes distilled water, formalin, phenyl-hydrazine, a beaker, Micropipettes, a freezer, a timer, and test tubes.

Test Subjects: Wistar rats weighing between 120 and 150 g were used in this study. The animals were purchased from the animal house at Ekiti State University Ado-Ekiti. When the animals arrived, they were randomly assigned to cages. The chambers in which the animals were housed had a temperature of 24±2°C and a relative humidity of 30–70%.

Approach to feeding: Every animal received regular commercial pelleted rat meal and had unrestricted access to water.

Grouping of Animals: The five groups of five animals each were created by randomly assigning the animals to different groups.
Group 1: Normal control (fed a diet that is 100% standard)
Group 2: Positive Control (given an entirely conventional diet and an anaemic environment)
Group 3: Coconut water plus Phenyl Hydrazine
Group 4: Ferrous + Phenylhydrazine
Ferrous+ normal diet is group five.

Phenyl-Hydrazine Administration: The procedure followed Harris and Kugler's (1971) description. All the rats were given subcutaneous injections of 2.5 per cent neutralized phenylhydrazine hydrochloride at a dose of 10 mg/kg body weight in order to induce anaemia, with the exception of the control rats.

Samples Collection: Animals were put to sleep at the conclusion of the experiment (using diethyl ether), and samples of their organs and blood were taken. Through the use of syringe needles to puncture the conspicuous ear vein, three to four millilitres of blood were drawn from each rabbit and placed into bijou bottles, either with or without EDTA (for serum). To prevent coagulation, 1 millilitre of blood was thoroughly mixed with EDTA before being used for haematological testing. When centrifuging the 4 ml of blood for 10 minutes at 1000 rpm, the serum was recovered when the blood had clothed at room temperature. Up until they were utilized in biochemical tests, serum samples were kept at -20°C.

Haematological Test: Full blood count comprising red cell count, Hb, white cell count and differentials, platelets as well as Hb indices were determined from the remaining whole blood that was placed in EDTA test tubes using ABX Micros 60 Haematology Analyzer (Horiba-ABX, Montpellier, France). Thin blood film was prepared and stained using Leishman stain for morphologic assessment of the red blood cells. The stained films were examined under the light microscope using × 40 objectives to select a good area for examination and then a drop of oil placed on the film and examined with the × 100 objective (Adewoyin et al., 2014).

Biochemical Assay

Estimation of Lipid Profiles: The lipid profile parameters were determined using ELITech chemistry reagents kit from ELITech Group Clinical Systems (Paris, France). The cholesterol reagent kit with product code (SL) was used for cholesterol determination, the HDL-C reagent kit with product code (HDL SL 2G) was used for HDL-C determination and LDL-C precipitation and triglycerides reagent kit product code (MONO SL NEW) was used to determine LDL-C and triglycerides. The instrument used was the Mindray B-300 chemistry analyzer manufactured by Shenzhen Mindray Bio-Medical Electronics Company, Limited. The procedures of work and preparation of the working reagents were done as described by the manufacturer (Ge et al.,2015).

Statistics Analysis: All of the data were evaluated as SEM using ONE-WAY ANOVA and n = 5. Using Version 6 of the Graph Pad Prism.

RESULTS

Figure 1a,1b and 1c show the Changes in serum level of lipid profiles in normal control, anemic control, coconut water treated and ferrous treated phenylhydrazine-induced rats. From the results, the rats treated with phenylhydrazine had significantly lower levels of Low density lipoprotein (figure 1a), Triglycerides (figure 1a), Total cholesterol(figure 1b), very low density lipoprotein(figure 1c), and significantly ($P < 0.001$) increased in levels of High density lipoprotein (figure 1b) after consuming coconut water at a dose of 0.5 ml/kg body weight for 14days**.**

Additionally, figure 2a 2b and 2c show the Changes in hematological parameters in normal control, anemic control, coconut water treated and ferrous treated phenylhydrazine-induced rats. From the results, it was observed that the percentage of neutrophil (figure 2a), concentration of hemoglobin (figure 2a), percentage of pack cell volume (figure 2b), percentage of lymphocytes(2b), concentration of reb blood cells(2c) and white blood cells (2c) in subjects treated with coconut water, are significantly (p 0.05) increased compared to the anemic untreated group.

DISCUSSION

Anaemia is characterized by a drop in red blood cell count or an increase in haemoglobin concentration within them, both of which are found to be below normal limits, according to MedlinePlus (2021). Medical care is in high demand due to the illness's widespread prevalence (MedlinePlus, 2021). It has been demonstrated that phenylhydrazine causes hemolytic anaemia by oxidative stress and cellular alterations that result in red blood cell loss (Graf and Graf, 2022). Essential insights into the pathophysiology, effects of anaemia on other physiological processes, and associated disorders can be gained from research on PHZ-induced toxic anaemia (Graf and Graf 2022). In anaemic individuals, there is a favourable correlation between serum cholesterol levels and haemoglobin and hematocrit levels (Osman and Ibrahim, 2021). Moreover, iron-induced free radical damage suggests

that anaemia patients may be more vulnerable to ischemic heart disease (Spence and Hegele, 2002).

The study discovered that rats treated with phenylhydrazine had significantly lower levels of LDL, VLDL, TC, and TG and higher levels of HDL after consuming coconut water at a dose of 0.5 ml/kg body weight per day for 14 days. The results of the present investigation are consistent with those of previous studies by Agbafor et al. (2015), Agbafor et al. (2013), Mohammed (Mohammed & Luka 2013), Sandhya et al. (2006), and John Kennedy et al. (2013).

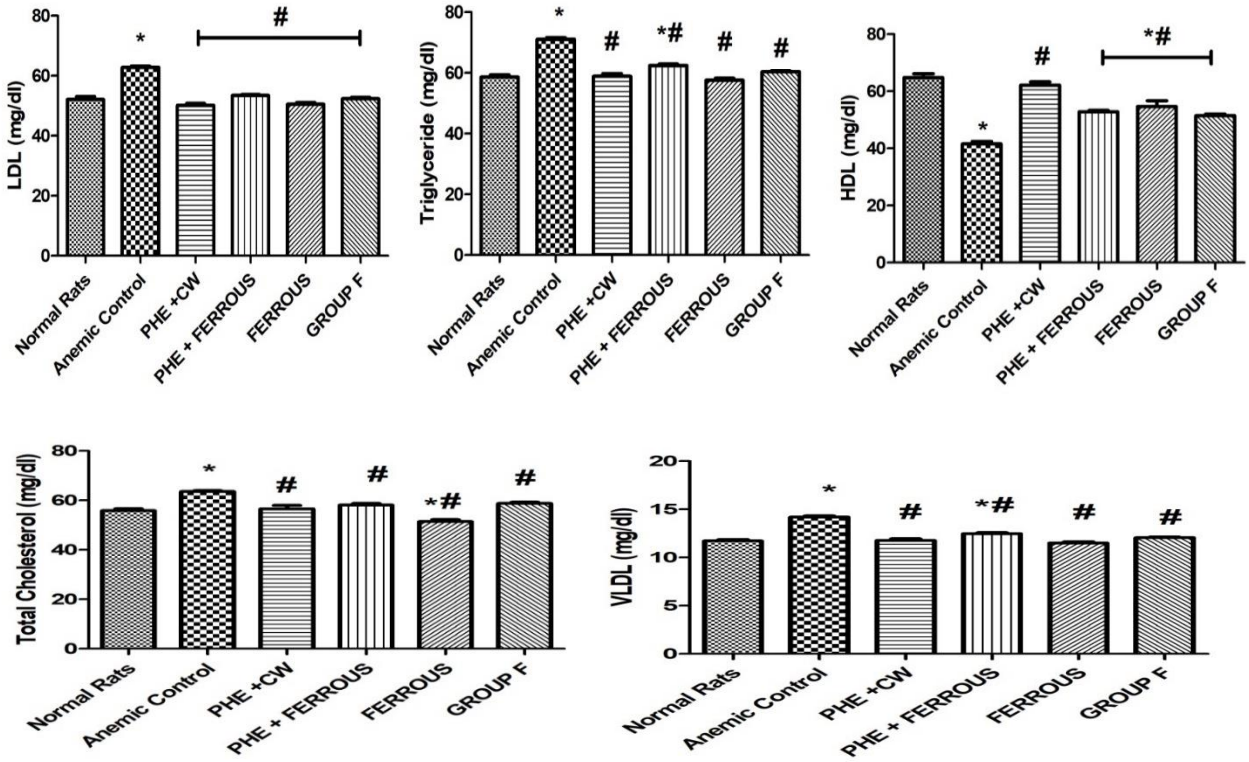

Figure 1:
Effects of coconut water on lipid profiles of phenylhydrazine-induced anemia

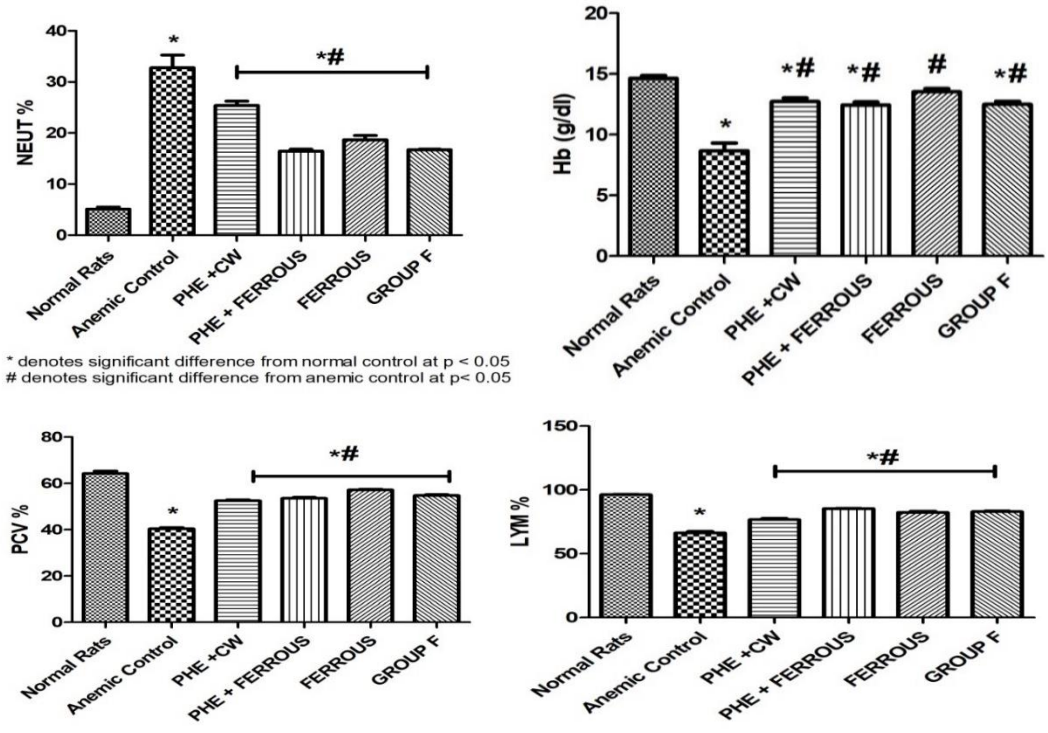

Figure 2a:
Effects of coconut water on hematological indices of phenylhydrazine-induced rats

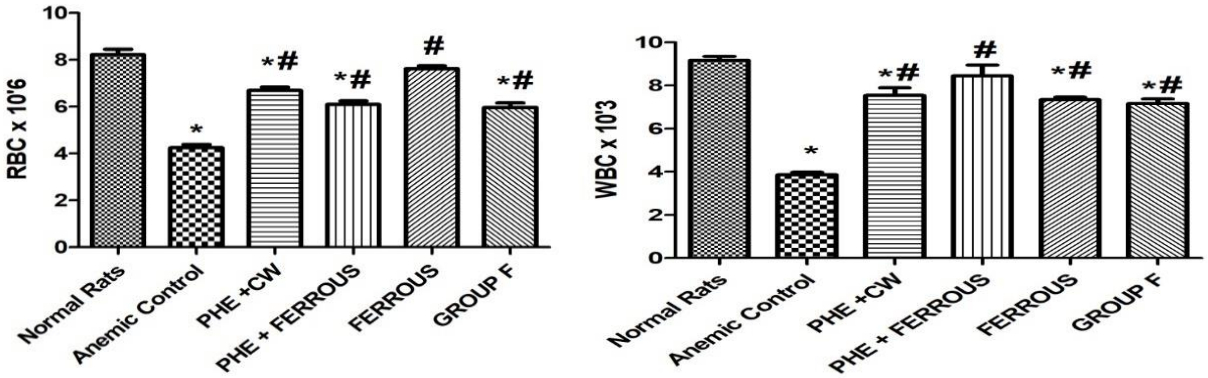

Figure 2b:
Effects of coconut water on hematological indices of phenylhydrazine-induced rats

In coconut water, the free amino acids L arginine, ascorbic acid, calcium, magnesium, and potassium all have physiologically active properties and may have chemoprotective effects. Rats fed a diet high in fat and cholesterol showed similar hypolipidemic responses to coconut water and the cholesterol-lowering medication lovastatin (Reddy & Lakshmi 2014). Additionally, vitamin C from coconut water protects HDL cholesterol and helps with the reverse cholesterol transport process, according to McRae's (2008) research. This study discovered that the anaemic rats given coconut water had a considerably lower TG level than the control group. Triglycerides, a kind of fat in the blood, can also increase the risk of heart disease. Given that studies have shown that vitamin C in coconut water boosts intracellular tetrahydrobiopterin (BH4) and NOS activity, this may be related to the vitamin (Sandhya & Rajamohan, 2008).

The findings of this study demonstrate that giving coconut water at a dose of 0.5 ml/200g reduces TG and LDL levels while raising HDL in rats with hydrazine-induced anaemia. Additionally, after receiving coconut water, the experimental groups' haemoglobin values significantly (p 0.05) increased compared to the anaemic untreated group (PHE). PCV, RBC, HB, and WBC all experienced significant increases in values. When rats were given an ethanol leaf extract of yellow mombin, similar outcomes were observed (Asuquo 2013). However, WBC levels—composed of neutrophils, monocytes, eosinophils, basophils, and lymphocytes—were significantly lower in the anemia-induced group (p 0.05). Indicators of the immune system's response to infection include white blood cells, lymphocytes, and neutrophils; it was discovered that the injection of coconut water significantly decreased these values. Murray (2000) noted that some substances could cause blood cells to synthesize more quickly, indicating that the water may include one or more substances that interact to enhance the production and release of committed stem cells, hematopoietic growth factors, and erythropoietin.
However, the finding that the haematological parameter increased in this study is consistent with the findings of Agbafor et al. (2015), which showed that coconut water elevated the haematological parameter in animals. Ascorbic acid, calcium, magnesium, potassium, and the free amino acid L arginine have all been present in coconut water (Sandhya & Rajamohan, 2006; John Kennedy et al., 2013). These nutrients serve as chemoprotective agents and have a direct impact on the production of bone marrow blood.

In summary, the findings of this investigation suggest that coconut water can prevent anaemia, which could be ascribed to a bioactive component. Furthermore, the coconut water's antioxidant action might be connected to its hematopoietic potential. As a result, the current study backs up the traditional medicine's medicinal use of coconut water to cure anaemia.

REFERENCES

Agbafor, S. O., ELOM, M. E., Ogbanshi, A. O., OKO, A. J., Uraku, V. U. O., Nwankwo, B. A., Ale and OBIUDU K.I.(2015).Antioxidant Property and Cardiovascular Effects of Coconut (Cocosnucifera) Water.*International Journal of Biochemistry Research & Review*. 5(4): 259-263.

Dina, O.A., Adedapo, A.A., Oyinloye, and Saba, A.B. (2003). Haematologocal effect of aqueous extract of Telfairia Occidentalis.; *African journal of biomedical research*, 3: 181-188

Agbor, G.A., Oben, J.E. and Ngogang. J.Y.(2005): Haematinic activity of Hibiscus cannabinus. *Afr. J.Biotechnol*. 4:833–837.

Ajeigbe. K.O., Ndaman, Z.A., Amegor, O.F., Onifade, A.A., Asuk, A.A., Ibironke, G.F and Olaleye, S.B.(2011). Anti-Nociceptive and Anti-Inflammatory Potential of Coconut Water (CocosNucifera L.) In Rats and Mice. *Australian Journal of Basic and Applied Sciences.* 2011; 5(9): 1116-1122

Alleyne, T. (2005). The control of hypertension by use of coconut water and mauby: two tropical food drinks. *West Indian Med J*. 54:3-8. 70. Shah, N.J. 1956.

Amasino, R.M. (2005). Kinetin arrives. The 50th anniversary of a new plant hormone. *Plant Physiol*. 138: 1177–1184.

Amer, J., Goldfarb, A. and Fibach, E. (2004) .Flow cytometric analysis of the oxidative status of normal and thalassemic red blood cells. *Cytometry* 60A:73–80.

Anurag, P. and Rajamohan, T. (2003). Beneficial effect of tender coconut water against isoproterenol induced toxicity on heart mitochondrial activities in rats. *Indian Journal of Biochemistry and Biophysics*. 40:278-80

Anurag, P. and Rajamohan, T.(2011). Antioxidant and Antithrombotic Activity of Tender Coconut water in Axperimental Myocardinal Infarction. *Journal of Food Biochemistry*. 35:1501-7.

Astuti, S.(2008) Isoflavon Kedelai dan Potensinya sebagai Penangkap Radikal Bebas. Jurnal Teknologi Industri dan Hasil Pertanian. 2008;13:126-36

Berger, J. (1985). Experimentally induced toxic-haemolytic anaemia in laboratory rats following phenaetin administraton. *Folia Haematol*. 112:571–579,.

Berger, J. (1985).Age-related sensitivity of rats to induction of anaemia. *Folia Haematol*. 114:408–413.

Berger, J. (1985a).Screening of toxic-haemolytic anaemia in laboratory rats: a model of phenylhydrazineinduced haemolysis. *Haematologia* 18:193– 200.

Berleth, T., Krogan, N.T. and Scarpella, E. (2004). Auxin signals - turning genes on and turning cells around. *Curr. Opin. Plant Bio*. 7: 553–563.

Beutler, E. (2001). Hemolytic anemia due to chemical and physical agents. In Beutler E, Coller BS,Lichtman MA, Kipps TJ, Seligsohn U (eds): Williams Hematology, 6th edition, New York2001, pp. 629–632.

Bhagya, D. Prema, L. and Rajamohan, T. (2012). Therapeutik Effects of Tender Coconut water on Oxidative Stress in fructosa fed Insulin Resistant Hypertensive Rats. *Asian Pasific Journal of Tropical Medicine*. 270-6.

Bialek, L., Michalczuk, L. and Cohen, J.D. (1992).Auxin biosynthesis during seed germination in Phaseolus vulgaris. *Plant Physiol*. 100,: 509–517.

Biswas, S., Bhattacharyya, J. and Dutta,. A.G.(2005).Oxidant induced injury of erythrocyte – role of green tea leaf and ascorbic acid. *Mol. Cell. Biochem*. 276:205–210.

Blakeslee, J.J., Peer, W.A. and Murphy, A.S. (2005).Auxin transport. Curr. Opin. Plant Bio. 8; 494–500.

Brodsky, R.A. and Jones and R.J.(2005). Aplastic anaemia. *Lancet*. 365(9471):1647-56.

Brugnara, C.and Defranceschi, L.(1993). Effect of cell age and phenylhydrazine on the cation- transport properties of rabbit erythrocytes. *J. Cell Physiol*. 154:271–280, 1993.

Burkhard, M.J., Brown, D.E. and McGrath, J.P. et al (2001) Evaluation of the eryhroid regenerative response in two different models of experimentally induced iron deficiency anemia. *Vet. Clin. Pathol*. 30:76–85.

Claro, L.M., Leobart, M.S. and Comar, S.R. (2006).do Nascimento AJ: Effect of vitamins C and E on oxidative processes in human erythrocytes. *Cell Bioch. Funct*. 24:531–535.

Clemens MR, Remmer H, Waller HD: Phenylhydrazine-induced lipid-peroxidation of red-blood-cells invitro and invivo –monitoring by the production of volatile hydrocarbons. *Biochem. Pharmacol*. 33:1715–1718, 1984.

Criswell, K.A., Sulkanen, A.P., Hochbaum, A.F. and Bleavins, M.R(2000).Effects of phenylhydrazine or phlebotomy on peripheral blood, bone marrow and erythropoietin in Wistar rats. *J. Appl. Toxicol*. 20:25–34, 2000.

Damin, S. (2009). Pengantar Kimia: Buku Panduan Kuliah Mahasiswa Kedokteran dan Program Strata I Fakultas Bioeksakta. Jakarta: EGC;.

Datta, K., Soni, J.L. and Datta, I.(1990). An avian model for the study of acute hemolytic anemia in the domestic fowl (Gallus domesticus*). Biomed. Biochim. Acta* 49:607–611.

Debray, C., Vaille, C., Souchard, M. and Roze, C. (1967).Action in vitro of phenylhydrazine and hydrogen peroxide on rat and human red cells. *Pathol. Biol*. 15:1167–1178, 1967.

DeJong, K., Geldwerth, D., Kuypers, F.A(1997) .Oxidative damage does not alter membrane phospholipid asymmetry in human erythrocytes. *Biochemistry* 36:6768–6776.

Delhi, K.L. and Ghosh, S. (2012). Medical laboratory Technology. Procedure Manual for Routine Diagnostic Tests. Vol I (Second edition), 263-266.

Depeint, F., Bruce, W.R., Shangari, N., Mehta, R, O'Brien, P.J. (2006). Mitochondrial function and toxicity: Role of B vitamins on the one-carbon transfer pathways. *Chem. Biol. Interact*, 163: 113– 132. 51.

Dharmasiri, N., Dharmasiri, S., Weijers, D., Lechner, E., Yamada, M., Hobbie, L., Ehrismann, J.S., Jurgens, G. and Estelle. (2005). M. Plant development is regulated by a family of auxin receptor F Box proteins. *Dev. Cell*. 9:109–119.

Dornfest BS, Bush ME, Lapin DM, Adu S, Fulop A, Naughton BA: Phenylhydrazine is a mitogen and activator of lymphoid-cells. *Ann. Clin. Lab. Sci*. 20:353–370, 1990.

Dornfest, B.S., Lapin, D.M., Adu, S. and Naughton, B.A (1992). Dexamethasone suppresses the generation of phenylhydrazine-induced anemia in the rat. Proc. Soc. *Exp. Biol. Med.* 199:491–500.

Edward, B.E., Martin, P.,E., Christine,.J,G., Seidman, S., and Ya-Huei, W. C. (1995). "Calcium- Ion–Sensing Cell-Surface Receptors", *The New England Journal of medicine*. 333: 234-240.

Evans, P, Halliwell, B. 2001.Micronutrients: Oxidant/antioxidant Status. *Br. J. Nutr.* 85: S67– S74.

Ewan, H. and Michael, B.(200) . "Functional properties of whey, whey components, and essential amino acids: mechanisms underlying health benefits for active people (review)", *The Journal of Nutritional Biochemistry*. 14: 251–258.

Ezzati, M., Lopus, A.D., Dogers, A., Vander, H.S. and Murray C.(2002). Selected major risk factors and global and regional burden of disease. *Lancet* 360 : 1347-60

Falconer, E.(1933). Treatment of polycythemia: the reticulocyte response to venesection, phenylhydrazin and radiation. *Ann. Intern. Med*. 7:172–189.

Farapti, S.S and Parlindungan, S.(2013). Effect of tender coconut water on systolic and diastolic blood pressure in prehypertensive women. *Health Science Indones.* 2013; 4 (2): 64-68

Fife, B. (2008).Coconut Water for Health and Healing. USA: Piccadily Books, Ltd.

Fischer, E. (1875) .Über aromatische Hydrazinverbindungen. Ber. Dtsch. Chem. Ges. 8:589– 594, 1875.

Franz,. J. (1971)."Gastric Function", Nutrition Today. 6: 2-11. 66.

Garrett, R.H. and Grisham, G.M. (2005). Biochemistry, 3rd ed.; Thomson Brooks/Cole: Belmont, CA, USA.

Geetha, V., Bhavana, K.P., Chetana, R., Gopala Krishna, A.G. and Suresh Kumar, G.(2016).Studies on the Composition and In-Vitro Antioxidant Activities of Concentrates from Coconut Testa and Tender Coconut Water. *Journal of Food Processing &Technolog.* 7(5):1-5

Giffin, H. and Allen, E.(1928).Experiments with phenylhydrazine. I. Studies on the blood. *Ann. Intern.* Med. 1:655–676, 1928.

Giffin. H., Allen, E.(1933).The control and complete remission of polycythemia vera following the prolonged administration of phenylhydrazine hydrochloride. *Am. J. Med. Sci.* 185:1– 13,

Gilmour, K.M and Perry, S.F(1996).The effects of experimental anaemia on CO2 excretion in vitro in rainbow trout, Oncorhynchus mykiss. *Fish Physiol. Bioch.* 15:83–94, Golab J,

Ginter, E., Bobek, P., Kubec, F., Vozár, J. and Urbanová, D.(1982). Vitamin C in the control of hypercholesterolemia in man. *Int J Vitam Nutr Res Suppl* 1982; 23:137-52.

Goh, Y.I and Koren, G. (2008). Folic acid in pregnancy and fetal outcomes. *J. Obstet. Gynaecol*. 28: 3–13. 57.

Graf, H. and Graf, E. (2022). Phenylhydrazine-Induced Hemolytic Anemia: A Model for the Study of Hemolytic Anemia. Frontiers in Physiology, 13, [online] 661.

Gullapalli, H.S., Avinash, P .T. and Namrata, H. G. (2013).Effect of supplementation of tender coconut water on blood pressure of primary hypertensive subjects. *International Journal of Medical Research &Health Sciences*. 2013; 2(2):172-176

Harper, J.L., Marcel, E.C. and Emmanuel, C. B. (2015). Iron Deficiency Anemia:Practice essentials, Pathophysiology and Etiology.Medscape.

Hedge, B.M.(2011) Coconut for Health & Health. *Indian Coconut Jurnal*. LIV:4-7.

Jakubowska, A. and Kowalczyk, S. (2005). A specific enzyme hydrolyzing 6-O(4-O)-indole-3- ylacetyl-β-d glucose in immature kernels of Zea mays. *J. Plant Physiol*. 162 :207–213

Jean Yong, W.H. (2009) ."The Chemical Composition and Biological Properties of Coconut (Cocos nucifera L.) Water, Molecules. 14: 5144- 5164.

Johnkennedy, N., Joy, D.N., Ndubueze, E.H., Melvina, N., Richard, E. and Vitus, O. (2013).Antioxidant and cardioprotective effect of coconut water against doxorubicin induced cardiomyopathy. J*ournal of Krishna Institute of Medical Sciences University* 2013; 2():37-41

Johnkennedy, N., Joy, D.N., Ndubueze, E.H., Melvina, N., Richard, E. and Vitus, O.(2013). Antioxidant and Cardioprotective Effect of Coconut Water against Doxorubicin Induced Cardiomyopathy. *Journal of Krishna Institute of Medical Sciences University*.2:37-41

Kapur, D., Agarwal, K.N., Sharma, S., Kela, K. and Kaur, I., (2002). Iron status of children aged 9-36 months in an urban slum Integrated Child Development Services project in Delhi. Indian Pediatr. 139:136-44.

Kemendustrian, R.I.(2010) Roadmap Industri Pengolahan Kelapa Direktorat Jenderal Industri Agro. In: Perindustrian K, editor. Jakarta.

Kende, H. and Zeevaart. J. (1997). The five "Classical" plant hormones. *Plant Cell*. 9: 1197–1210.

Ketaren, K.S., Novianry, V.and Hadi, D.P. (2016).Uji efektivitas air kelapa muda (Cocos nucifera L.) terhadap hemoglobin pada tikus putih (Rattus norvegicus) sebagai anti anemia setelah diinduksi siklofosfamid. Skripsi Pendidikan Dokter-Fakultas Kedokteran Universitas Tanjungpura.

Kilbridge, J., Bakea, T.G., Parapia, L.A., Khoury, S.A., Shugaidef, S.W. and Jerwood, D.(1999). Anaemia during pregnancy as a risk factor for iron-deficiency anaemia in infancy: a case- control study in Jordan. *Int. J. Epidemiol* 28:461-8.

Kumar, C.A, Kumar, K.U., Kumari, K.V. and Rao, R.(2013). L-Arginine Mitigates Heavy Metal Inhibited Nitric Oxida Synthase Activity in Tissues of the Albino Rat. *The Bioscan*. 8:937-9.

Lieberman, M., Marks, A.D and Smith, C. (2007). Mark's Essentials of Medical Biochemistry. A Clinical Approach; Lippincott Williams & Wilkins: Baltimore, MD, USA.

Lima, E., Sausa, C., Meneses, L., Ximenes, N., Junior ,M.A.,Vasconcelos, G., Lima, N., Patrocinio, M., Macedo, D., Vasconcelos, S. (2015): A phytochemical and pharmacological review. *Brazilian Journal of Medical and Biological Research*. 48 (11): 953-964

Liu. S .1., Jia, J., Cai, D., Li, S., Zhang, C. and Zhang, Y. (2015). Mitochondria defects are involved in lead-acetate-induced adult hematopoietic stem cell decline. *Toxicol Lett*;3(7):1-8.

Lukose, R.M. (2013).The Chemical Composition of Tender Coconut (Cocos Nucifera L.) Water and Coconut Meat and Their Biological Effect in Human Body. *International Journal of Green and Herbal Chemistry*.2(3):723-9

Ma, Z., Ge, L., Lee, A.S., Yong, J.W., Tan, S.N. and Ong, E.S. (2008). Simultaneous analysis of different classes of phytohormones in coconut (Cocos nucifera L.) water using high-performance liquid chromatography and liquid chromatographytandem mass spectrometry after solid-phase extraction, *Anal. Chim. Acta*. 610: 274–281.

Macalalag, E.V. and Macalalag, A.L. (1987) . young coconut water renoclysis for urinary stone dissolution. *Int Surg*. 72:247.

Malaka, T. and Iryani, M. (2011).The Correlation of Lead in Blood and Haemoglobin Concentration and Hematocrit Value of Toll Booth Workers at Jagorawi. Kesmas. J Kesehat Masy Nas.;6(1):35-41.

Mandal, S.M., Dey, S., Mandal, M., Sarkar, S., MariaNeto, and Franco, O.L.(2009). Identification and structural insights of three novel antimicrobial peptides isolated from green coconut water. *Peptides*. 30:633-637.

Matsui, K.N., Gut, J.W., de Oliveira, P.V. and Tadini, C.C. (2008). Inactivation kinetics of polyphenol oxidase and peroxidase in green coconut water by microwave processing. *Journal of Food Engineering*. 88:169-176. 62..

McRae, M.P. (2008).Vitamin C supplementation lowers serum low-density lipoprotein cholesterol and triglycerides: a meta-analysis of 13 randomized controlled trials. *J Chiropr Med* 2008; 7(2): 48–58.

Medeiros, V.P, and Medeios, A.C. (2012) Therapeutic use of coconut water. *J Surg CI Res*. 3:75- 83

MedlinePlus. (2021). Anaemia. [online] Available at: https://medlineplus.gov/anaemia.html

Miller, C.O., Skoog, F., Von Saltza, M.H. and Strong, F.M. Kinetin. (1955). a cell division factor from deoxyribonucleic acid. J. Am. Chem. Soc. 77: 1392–1393. 43. Werner, T, Motyka, Strnad, V and Schmulling, T. (2001). Regulation of plant growth by cytokinin. P*roc. Natl. Acad. Sci. USA.* 98: 10487–10492.

Mohammed, A., Luka, C.D.(2013). Effect of coconut oil, coconut water and palm kernel oil on some biochemical parameters in albino rats. *IOSR-JPBS* 6(3): 56-59

Muhammad, N.E.(2018). Coconut water vinegar ameliorates recovery of acetaminophen induced liver damage in mice. *BMC Complementary and Alternative Medicine*.18:195

Mulyanti, E. D., Kis, D. and Noor, W(2016). Effectiveness of tender coconut water (cocosnucifera l) againtsparasitemia index and hemoglobin levels in malaria infection. *International Jounal of Pharmaceutical Sciences and Research.* 7(9): 3873-3876

Nancy, C(2000)."Iron metabolism: Iron Deficiency and Iron Overload", *Genomics and Human Genetics*. 1:75-98.

Natasha, S. and Yasmin G.(2010). Inkosi Albert Luthuli Central Hospital. Proceedings of South African Thalassaemia Association.

Osman, E. and Ibrahim, M. (2021). The Correlation between Serum Cholesterol and Hemoglobin Level in Patients with Anemia. *J Cardiovasc Dis Diagn*, 9(2),] 111-114.

Pasricha, S.R, Flecknoe-Brown, S.C. and Allen K.J,(2010). Diagnosis and management of iron deficiency anaemia: a clinical update. *Med J Aust*. 2010 Nov 1; 193(9):525-32.

Prabhakar, R. and Mohana L. (2014) Coconut Water - Properties, Uses, Nutritional Benefits in Health and Wealth and in Health and Disease: A Review. *Journal of Current trends in Clinical Medicine& laboratory biochemistry*.2 (2):6-18

Prathapan, A. And Rajamohan, T,. (2011). Antioxidant And Antithrombotic Activity Of Tender Coconut Water In Experimental Myocardial Infarction. *Journal of Food Biochemistry*. (2011). 35(5):1501-1507

Prema R. (1992). Anaemia in pregnancy. In: Ratnam SS, Bhasker Rao K, Arulkumaran S, editors. Obstetrics and gynaecology for postgraduates, Vol 1. Madras: orient Longman.42-53.

Prema, R. (1989). Nutrition in Pregnancy. In: Gopalan C, Kaur S, editors. Women and nutrition inIndia, Special Publication No. 5. New Delhi: *Nutrition Foundation of India*:153- 93.

Priya, A. (2014).. Coconut Water Uses, Composition and properties : a review. *Fruits*. 2011;67:87-107.

Priya, S.R. and Ramaswamy, L.(2014). Tender Coconut Water-Natures Elixir to Mankind. *International Journal of Recent Scientific Research*. 2014;5(8):1485-90.

Rattan, S.I. (1994). Method and composition for ameliorating the adverse effects of aging. US Pat. 5371089.

Reddy, E.P. and Lakshmi, T.M.(2014). Coconut Water - properties, uses, nutritional benefits in health and

wealth and in health and disease: A Review. JCTCMLB 2014, 2(2):6- 18

Riboli, E and Norat, T. (2003). Epidemiologic evidence of the protective effect of fruit and vegetables on cancer risk, *Am. J. Clin. Nutr*. 78: 559–569.

Robert, H.S, and Friml, J. (2009). Auxin and other signals on the move in plants. *Nat. Chem*. Biol. 5: 325–332.

Robinson, K., Arheart, K., Refsum, H., Brattström, L., Boers, G., Ueland, P., Rubba, P., Palma- Reis, R., Meleady, R., Daly, L., Witteman, J and Graham I. (1998). Low circulating folate and vitamin B6 concentrations: Risk factors for stroke, peripheral vascular disease, and coronary artery disease. *Circulation*. 97: 437–443.

Sandhya and Rajamohan T.(2014) The role of coconut water on nicotine-induced reproductive dysfunction in experimental male rat model. *Food Nutri Sci* 5(): 1121-1130

Sandhya, V.G. and Rajamohan, T. (2006). Beneficial effects of coconut water feeding on lipid metabolism in cholesterol-fed rats. *J Med Food 2006*; 3(): 400-7.

Sandhya, V.G. and Rajamohan, T. (2008). Comparative Evaluation of the Hypolipidemic effect of coconut water and lovastatin in rats fed fat cholesterol enriched died. *Food Chem Toxicol*. 46:3586-92.

Scheinberg, P. and Young, N.S., (2012). How I treat acquired aplastic anemia. Blood. 120(6):1185- 96.

Shenkin, A.(2006). The key role of micronutrients. Clinical Nutr. 25: 1–13. Journal of Current Trends in Clinical Medicine & Laboratory Biochemistry Volume 2, Issue 2, April-June 2014 P 18

Spence, J. D. and Hegele, R. A. (2002). Ischaemic heart disease and anemia. The Lancet, 360(9330), [online] 674-679

Sun, X., Xie, Y., Wu, L., Zhu, W., Hu, J. and Lu R. (2012). Lead acetate reduces the ability of human umbilical cord mesenchymal stem cells to support hematopoiesis in vitro. *Mol Med Rep*.;(6):827-32.

Tkachenko, H. and Kurhalyuk, N. (2011).Role of L-Arginine Against lead Toxicity in Liver of Rats with Different Resistance to Hypoxia. *Pol J Environ Stud*. 20(5):1319-25

Toteja, G.S. and Singh, P., (2004). Micronutrient profile of Indian population. New Delhi: Indian Council of Medical Research. Turner MR, Talbot K; Functional vitamin B12 deficiency. *Pract Neurol*. 2009 Feb;9(1):37-41. U.S. Department of Health & Human Services, https://www.nhlbi.nih.gov/health/healthtopics/topics/anemia/

Tucker, G.A. and Roberts, J.A. (2000). Plant Hormone Protocols; Humana Press Inc.: Totowa, NJ, USA. pp 200

Vishal, D. and Stephen, G. (2008). "Role of copper in human neurological disorders", *Am J Clin Nutr*. 88: 855-858.

White, C.R, Parks, D.A., Patel, R.P, Shelton, J., Tarpey, M.M. and Freeman, B.A.(2004). L- Arginine inhibits xanthine oxidase-dependent endothelial dysfunction in hypercholesterolemia. *FEBS Leff* 561(1-3): 94-8.

WHO (2004). Micronutrient deficiency: Battling iron deficiency anaemia: the challenge. Available from: http://www.who.int/nut/ida.htm, accessed on April 24, 2008

WHO, (2005). Worldwide prevalence of anaemia 1993–2005 : WHO global database on anaemia / Edited by Bruno de Benoist, Erin McLean, Ines Egli and Mary Cogswell.

WHO.(2021).Anaemia in children and women: WHO global anaemia estimates, 2021 edition; WHO geneva, Switzerland.

Zulaikhah, S.T,. ,Danis, P., Bagus, S., Nuri, S. , Brillian, J..M and Alfiza, N.S.(2017). Effect of tender coconut water on blood lipid levels in hight fat diet fed male rats. *Journal of Krishna Institute of Medical Sciences University (JKIMSU). 6 (2): 63-68*

Zulaikhah, S.T. (2017).The role of antioxidant to prevent free radicals in the body. Sains Med J Med Heal.;8(1). 8. Lima EBC, Sousa CNS, Meneses LN, Ximenes NC, Júnior MAS. Cocos nucifera (L.) (Arecaceae): A phytochemical and pharmacological review. *Brazilian J Med Biol Res*. 2015;48(11):953-64.

Zulaikhah, S.T. and Anies, A. S.(2015).Effects of tender coconut water on antioxidant enzymatic superoxida dismutase (SOD), catalase (CAT), glutathione peroxidase (GPx) and lipid peroxidationi mercury exposure workers. *IJSR* 2015 4(2): 517-528

Zulaikhah, S.T. and Sampurna, S. (2016).Tender Coconut Water To Prevent Oxidative Stress Due To Mercury Exposure. *IOSR Journal of Environmental Science, Toxicology and Food Technology (IOSR-JESTFT).* 2016; 10(6): 35-38

Zulaikhah, S.T., Anies, Ari S., Santosa(2015). Effects of Tender Coconut Water on Antioxidant Enzymatic Superoxida Dismutase (SOD), CATALASE (CAT), Glutathione Peroxidase (GPx) and Lipid Peroxidation In Mercury Exposure Workers. *International Journal of Science and Research (IJSR).* 4 (12): 517-524.

Niger. J. Physiol. Sci. 38 (December 2023): 125 – 128
www.njps.physiologicalsociety.com

Niger. J. Physiol. Sci.

Full length Research Article

The Use of Levels One and Two Dermatoglyphics for Sex Identification in University of Ibadan Community, Southwest Nigeria

***Adetona, M.O. and Preyor, E.**

Department of Anatomy, Faculty of Basic Medical Sciences, College of Medicine, University of Ibadan, Nigeria

Summary: Dermatoglyphic traits are genetically determined and remain constant until death. Dermatoglyphics features are arranged from patterns, minutiae and ridgeology. This study utilized patterns and minutiae details of fingerprints as a means of sexual differentiation amongst the University of Ibadan community. Three hundred and eighty-four (192 males and 192 females) participants from the University of Ibadan community were recruited using multistage sampling technique. Fingerprints were obtained using fingerprint scanner Dermalog LF10, Hamburg, Germany. GraphPad Prism 7.0 was used for the test of mean of variables. Ulnar loop, whorl and radial loop patterns were found to be predominantly distributed in both male and female in that order. However, the arch pattern was significantly different between female and male. The male subjects had significantly higher total finger ridge count (TFRC). All the analysed minutiae were significantly different between male and female except bridge. The arch pattern, TFRC and level 2 details (minutiae) of dermatoglyphics could be used as markers for sexual differentiation.

Keywords*: Dermatoglyphics, Sexual dimorphism, Pattern, Minutiae, Ibadan, Nigeria*

**Authors for correspondence: soladet@fastmail.fm , Tel: +234-7-87949572*

Manuscript received- April 2023; Accepted- September 2023

DOI: https://doi.org/10.54548/njps.v38i2.2

INTRODUCTION

Fingerprint had been found to be a useful tool in population studies and criminology and had been accepted as one of important means to differentiate gender (Reddy, 1975; Nte, 2012) because of its characteristic permanence, distinctiveness, reliability and accuracy. Accurate and efficient human identification or recognition have become crucial for forensic applications due to the large diversity of crime scenes, and because of the increasing need to accurately identify perpetrators in crime evidence. Identifying the gender of perpetrators from the crime scene is an important aspect in narrowing the scope of suspects in forensic investigation (Lee & Gaensslen, 2014; Abdullah *et al*., 2015).

Over the years, identification of the sex and identity of an individual has involved the use of several body features (Kumar *et al*., 2015). However, fingerprint was one of the oldest and one of the most important pieces of evidence with its infallible characteristic. Its use in forensic science has increased greatly because of the unique arrangement of the ridge on the finger of every individual which does not alter with growth and age (Gutiérrez-Redomero, 2017; Hariharan & Logeswari, 2019). Pattern details involve the use of the loop, whorl and arch, and their quantification. Minutiae features deal with specific ridge characteristics. Minutiae are minor or incidental details, and this makes level two features more unique for individual identity (Yager & Amin, 2004). Several studies (Nithin et.al; 2011, Wijerathne et.al., 2016, Paul and Paul, 2017 a & b) on dermatoglyphics have been carried out in different parts of the world including Nigeria for gender identification. But most of these studies have focused more on patterns and only few have explored the minutiae details for gender identification and most studies used the conventional ink method to obtain fingerprints samples.

The University of Ibadan is highly heterogeneous serving as habitat for people from different regions of Nigeria and other African countries. This study sought to increase the already existing knowledge, but with the use of both level one and two details of fingerprints. The study will also serve as a means of identification of latent print from crime scene in the community and may lead to creation of fingerprint data bank, as reported among Chinese sub-populations (Zhang *et al*., 2010).

MATERIALS AND METHODS

Location of Study: The University of Ibadan, occupying over 1,032 hectares of land, is in Ibadan North Local Government Area, Ibadan, Oyo State, Nigeria. The Institution was originally established on 17 November 1948 as University College, Ibadan. The name was later changed to the University of Ibadan in 1962 (Agbola *et al*., 2001).

Sampling Technique: This study was from a cross section of the population and a multistage sampling procedure was used.

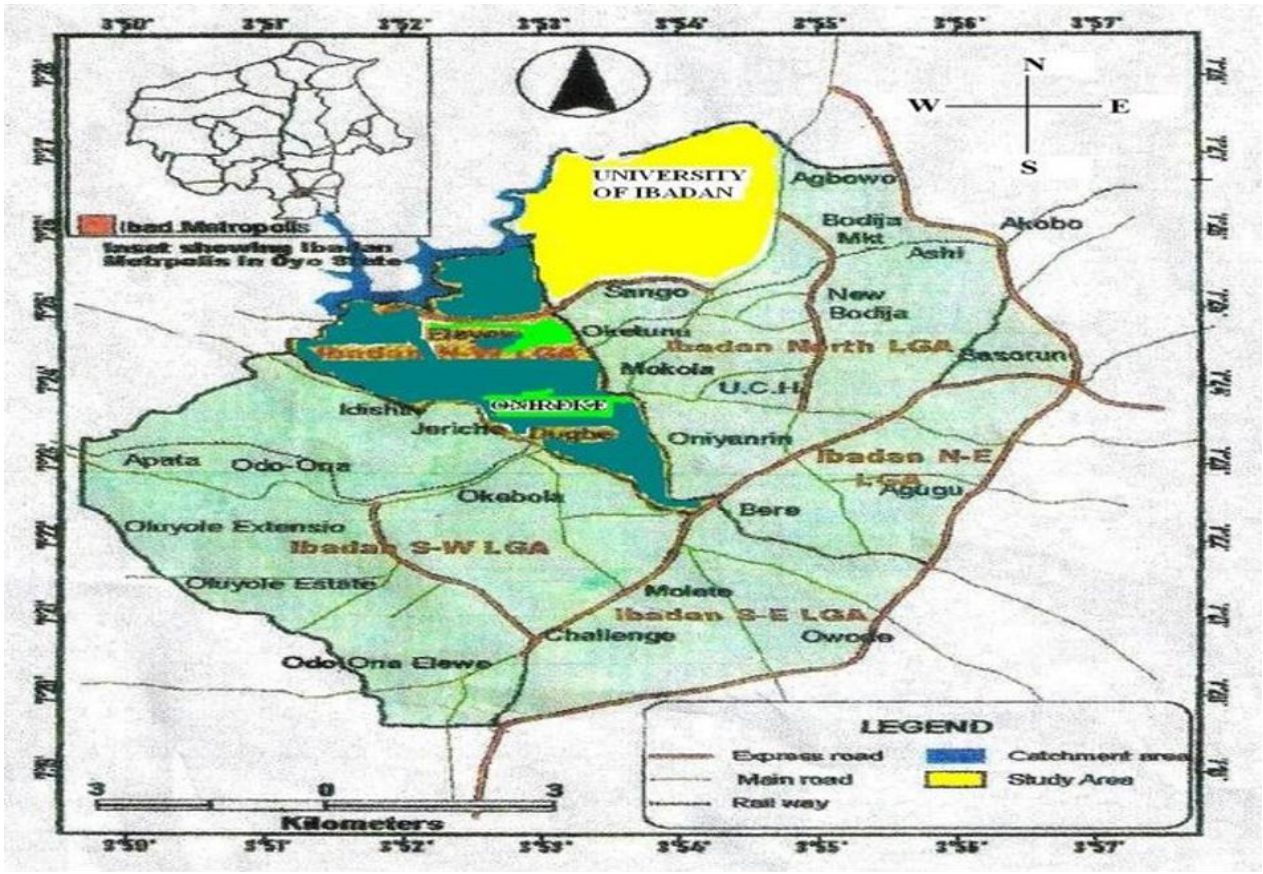

Plate 1:
Map of Ibadan Metropolis showing University of Ibadan (Mubarak & Samuel, 2015)

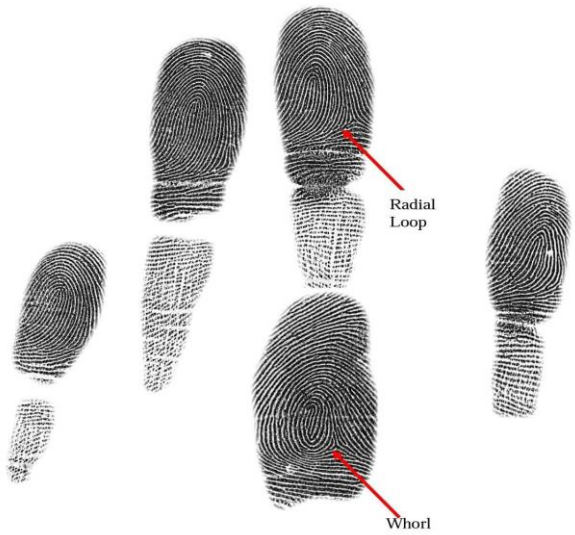

Fig. 2:
Fingers 1-5 Dermatoglyphs showing patterns.

Sample Size: Three hundred and eighty-four (384) participants, comprising 192 males and 192 females, volunteered for the study from the University of Ibadan.

Inclusion Criteria: An initial physical examination of the palmar surface of the fingers was done to exclude scarred fingers from the study.

Methodology: Bilateral digital prints of all the participants were obtained with Dermalog LF10 fingerprint scanner, Hamburg, Germany. The participants' fingers were thoroughly cleaned before prints were taken. The right and left thumbs of participants were first obtained separately for a clearer view. Each finger was pressed against the scanner with a little pressure applied for adequate contact with the scanner such that sharp fingerprints were obtained. Afterwards, the prints were adequately labelled. Interpretation of the patterns was carried out according to Cummins and Penrose (Penrose, 1969; Cummins, 1946). Automated Fingerprint Identification System (AFIS) software (Meadows, Pouratian 1999) was used to enhance the patterns and minutiae present (Fig. 2 and 3).

Fig. 3:
Fingers 1-5 Dermatoglyphs showing minutiae.

The patterns were identified and the minutiae studied were bifurcation, trifurcation, ridge ending, bridge, lake, double bifurcation, island, dot, ridge crossing, break, spur and opposed bifurcation. The parameters analysed included pattern frequency and total finger ridge count.

Statistical Analysis: GraphPad Prism 7.0 was used for statistical analysis and statistical significance was at $p \leq 0.005$.

Ethical Considerations: Ethical review guidelines of the University of Ibadan and University College Hospital (UI/UCH) relating to the use of human subjects for research were duly followed (UI/EC/19/0264). Informed consent was obtained from every volunteer before sampling.

RESULTS

The comparison of pattern type in both genders revealed significant differences between the arch pattern of males and females (Table 1). The female arch pattern was significantly higher than the male.

Table 1:
Comparison of pattern types of both hands of male and female

Pattern	Males (mean±SD)	Females (mean±SD)	P value
Ulna loop	122.3±30.0	113.0±32.8	0.52
Whorl	53.1±23.1	49.9±22.5	0.76
Arch	13.2±10.5	25.3±11.6	*0.025
Radial loop	3.4±5.4	3.8±5.1	0.87

$p \leq 0.05$

The male right and left hands ridge count were significantly higher than the female's right and left hands. There was also a significant difference of the TFRC. The male TFRC was significantly higher than the female (Table 2).
In male, the percentage distribution of minutiae characteristics in the right hand revealed that bifurcation (36.47%) and trifurcation (0.04%) were the most and least distributed respectively. In the left hands, bifurcation (35.77%) and trifurcation (0.02%) were also the most and least distributed respectively. In female, the percentage distribution of minutiae characteristics in the right hand revealed that bifurcation (35.67%) and trifurcation (0.10%) were the most and least distributed respectively. In the left hand, bifurcation (35.60%) and trifurcation (0.11%) were also the most and least distributed respectively (Table 3).

Table 2:
Distribution total finger ridge count in Male and female

	Male	Female	p-value
Digit	mean±SD	mean±SD	
Right	66.34±20.23	55.72±22.16	0.0006
Left	63.12±22.10	53.76±23.88	0.0044
TFRC	129.46±40.92	109.48±51.67	0.0001

Total Finger Ridge Count (TFRC), $p<0.005$

DISCUSSION

The ulnar loop predominance in this study is in conformity with previous studies on the Nigerian population (Adetona *et al*., 2008; Ekanem, 2008; Umana *et al*., 2014). This study showed no significant difference in the whorl, radial loops, and ulnar loop patterns between male and female, right and left hands, which agrees with previous studies (Eboh, 2012; Omuruka *et al*., 2017; Joseph & Ubaidullah, 2018; Adenowo & Dare, 2019). The arch was the only pattern in this study that showed significant gender difference with a higher distribution in female than male which was also reported by Adenowo and Dare (2019) among students of Bingham University, Nigeria and Ray *et al*., (2015) among Indian medical students. There was also a significant difference between male and female TFRC in this study. The male had higher finger ridge count than female, this was also previously reported by Anibor *et al*., (2011); Ekanem, (2008). This implies that the quantitative parameter of TFRC can be used for male and female differentiation within the population.

The minutiae revealed sexual dimorphism, there was a significant difference in the minutiae of right and left hands except the bridge.

Table 3:
Dermatoglyphic minutiae of male and female left and right hand.

	MALE				FEMALE			
MIN	**R**	**%**	**L**	**%**	R	%	L	%
BF	11461	36.47	12341	35.77	10330	35.66	11527	35.60
TF	11	0.04	6	0.02	31	0.10	36	0.11
RE	7567	24.08	8023	23.25	8398	28.99	8978	27.73
BG	324	1.03	333	0.97	290	0.99	387	1.20
LK	4960	15.79	6241	18.09	3888	13.42	4975	15.37
DBF	155	0.49	152	0.44	206	0.70	224	0.69
SR	2611	8.31	2309	6.69	2379	8.22	2032	6.28
DO	588	1.87	625	1.81	564	1.96	505	1.56
RC	16	0.05	21	0.06	71	0.23	105	0.32
OBF	324	1.03	311	0.90	164	0.56	207	0.64
BK	46	0.15	42	0.12	79	0.27	125	0.39
SP	3358	10.69	4098	11.88	2572	8.88	3272	10.11

MIN: Minutiae, R: Right hand, L: Left hand, BF: Bifurcation, TF: Trifurcation, RE: Ridge ending, BG: Bridge, LK: Lake, DBF: Double bifurcation, SR:Short ridge, DO: Dot, RC: Ridge crossing, OBF: Opposed bifurcation, BK: Break, SP: Spur

Table 4:
Comparison of dermatoglyphic minutiae of right and left hands of male and female

Minutiae	Males (Mean±SD)	Females (Mean±SD)	p value
Bifurcation	****12.40±4.16	11.38±4.09	0.0001
Trifurcation	0.01±0.09	****0.03±0.20	0.0001
Ridge Ending	8.12±3.27	****9.05±3.80	0.0001
Bridge	0.34±0.63	0.35±0.75	0.6232
Lake	****5.84±6.58	4.62±5.68	0.0001
Double Bifurcation	0.16±0.46	***0.22±0.60	0.0002
Short Ridge	*2.56±3.41	2.30±3.23	0.0134
Dot	*0.63±0.98	0.56±1.02	0.0202
Ridge Crossing	0.02±0.14	****0.09±0.35	0.0001
Opposed Bifurcatio	****0.33±0.57	0.19±0.44	0.0001
Break	0.05±0.24	****0.11±0.38	0.0001
Spur	****3.88±2.88	3.04±2.82	0.0001

p≤0.05

Bifurcation predominance and trifurcation as the least minutiae in both sexes and hands was similar to the findings of Paul and Paul, (2017a, b) among Kalabari and Ikwerre ethnic groups of Nigeria and Akpan *et al*., (2019) finding among University of Lagos community. Significant differences in the quantification of minutiae between male and female in this study had been reported by other researchers; Paul & Paul (2017a&b) among Nigerians; Thakar *et al*., (2018) among Indians; Gutierrez-Redomero *et al*., (2017) among Argentines. The lake minutiae also differentiate male and female in this study. Bridge minutiae showed no sexual dimorphism, this was also reported by Paul and Paul (2017b) among the Ikwerre ethnic group of Nigeria, and Gutierrez-Redomero *et al*., (2010) among Spanish population. All other minutiae in this study also revealed sexual dimorphism. This revealed that as previously reported and elucidated in this study, minutiae studies can be used for sexual differentiation in forensic analysis and human population studies.

In conclusion, gender disparity existed in the qualitative variable of arch pattern in University of Ibadan community, Nigeria. TFRC and minutiae details showed significant gender differences. This study can be used as a marker in conjunction with other markers in forensic investigation.

REFERENCES

Abdullah, S.F., Rahman, A.F. and Abas, Z.A. 2015. Classification of gender by using fingerprint ridge density in northern part of Malaysia. *Arpn journals of engineering and applied sciences* 10(22):10722-10726.

Adetona, M. O., Oladapo, O. O and Igbigbi, P. S. 2008. Palmar and digital dermatogylyphic patterns of the three major ethnic groups in Nigeria. *African Lournal of Medical Sciences* 37:333-337.

Adenowo, T.k. and Dare, B.J. 2019. Digital and palmar dermatoglyphic patterns of medical students of Bingham University, Karu, Nasarawa state Nigeria. *Journal of Applied Life Sciences International* 20(3): 1-10

Agbola, T., Olatubara, C.O. and Alabi, M. 2001. Students' on-campus housing at Bursting Point: A case study of the University of Ibadan. Ibadan. IFRA and African Book Builders 116-118

Akpan, U.U., Awe, T., Idowu, D.O. and Adekoya, K.O. 2019. Types and frequency of fingerprint minutiae in individuals of Igbo and Yoruba ethnic groups of Nigeria. *Ruhuna Journal of Science* 10(1)77–87.

Eboh, D.E.O. 2012. Digital dermatoglyphic patterns of Anioma and Urhobo students in two tertiary institutions of delta state, Southern Nigeria, A peer review. *Journal of biomedical sciences* 11(2):90 -96.

Ekanem, E., Eluwa, M., Udoaffah, G., Ekanem, T. and Akpantah, A. 2008. Digital dermatoglyphic patterns of Annang ethnic group in Akwa Ibom state of Nigeria. *The Internet Journal of Biological Anthropology* 3(1):1-4

Gutiérrez-Redomero, E., Galera, V., Martínez, J.M., Alonso-Rodriguez, C. 2017. Biological variability of the minutiae in the fingerprints of a sample of the Spanish population. *Forensic Science International* 172(2): 98–105.

Hariharan, R. and Logeswari, S. 2019. Fingerprint as a personal identification tool in forensic science. *Global journal for research analysis* 8(1):22-23

Kumar, P., Ritika, G., Rajinder, S. and Prakash, J. 2015. Effects of latent fingerprint development reagents on subsequent forensic DNA typing: A review. *Journal of Forensic and Legal Medicine* 32 (2015) 64e69

Langenburg, G.M. 2004. Pilot-study: A statistical analysis of the ACE-V methodology - analysis stage. *Journal of forensic identification* 54(1): 64-79.

Lee, H.C. and Gaensslen, R.E. 2001. Methods of latent fingerprint development. *Advances in fingerprint technology* 15;2(105-176):10.

Lipton, J. 2014. "Fingerprints: Unique to Us All." Jennifer Lipton, sites.psu.edu/jlipton/2014/06/03/fingerprints-unique-to-us-all/. Accessed 29 Jan. 2024.

Mubarak, A.F, and Samuel, O.O. 2015. Geophysical and geotechnical characterization of newly constructed Abadina-Ajibode road, University of Ibadan, Ibadan. *Journal of multidisciplinary engineering science* 2(1):363-378

Nithin, M.D., Balaraj, B.M., Manjunatha, B. and Shashidhar, C. 2009. Study of fingerprint classification and their gender distribution among South Indian population. *Journal of Forensic and Legal Medicine* 16:460–463

Nte, N. D. 2012. An evaluation of the challenges of forensic investigation and unsolved murders in Nigeria. *African journal of criminology and justice studies* 6(1/2)143.

Paul, C.W. and Paul, J.N. 2017a. Gender variation studies at level 2 dermatoglyphic details of the Ikwerre ethnic group in Rivers State, Nigeria. *Journal of pharmaceutical research international* 19(2): 1-8.

Paul, C.W. and Paul, J.N. 2017b. Gender variation studies at level 2 dermatoglyphic details of the Kalabari ethnic group in Rivers State, Nigeria. *Scholars journal of applied medical sciences* 5(11A):4297-4301

Reddy, G. G. 1975. Finger dermatoglyphics of the Bagathas of Araku Valley (AP), India. *American journal of physical anthropology* 42(2): 225-228.

Terhorst, P., Damer, N., Braun, A, and Kuijper, A. 2018. What can a single minutia tell about gender? International conference on information Fusion 2113-2120

Wijerathne, T.B., Robert, J.M., Thilini, C.A. and Suneth, B.A. 2015. Dermatoglyphics in hypertension: a review. *Journal of Physiological Anthropology* 34:29

Zhang, H.G., Chen, Y.F., Ding, M., Jin, L. and Case, D.T. 2010. Dermatoglyphics from all Chinese ethnic groups reveal geographic patterning. *Journal PLoS ONE* 5(1):e8783.

Niger. J. Physiol. Sci. 38 (December 2023): 125 – 128
www.njps.physiologicalsociety.com

Niger. J. Physiol. Sci.

Full length Research Article

The Use of Levels One and Two Dermatoglyphics for Sex Identification in University of Ibadan Community, Southwest Nigeria

***Adetona, M.O. and Preyor, E.**

Department of Anatomy, Faculty of Basic Medical Sciences, College of Medicine, University of Ibadan, Nigeria

Summary: Dermatoglyphic traits are genetically determined and remain constant until death. Dermatoglyphics features are arranged from patterns, minutiae and ridgeology. This study utilized patterns and minutiae details of fingerprints as a means of sexual differentiation amongst the University of Ibadan community. Three hundred and eighty-four (192 males and 192 females) participants from the University of Ibadan community were recruited using multistage sampling technique. Fingerprints were obtained using fingerprint scanner Dermalog LF10, Hamburg, Germany. GraphPad Prism 7.0 was used for the test of mean of variables. Ulnar loop, whorl and radial loop patterns were found to be predominantly distributed in both male and female in that order. However, the arch pattern was significantly different between female and male. The male subjects had significantly higher total finger ridge count (TFRC). All the analysed minutiae were significantly different between male and female except bridge. The arch pattern, TFRC and level 2 details (minutiae) of dermatoglyphics could be used as markers for sexual differentiation.

Keywords*: Dermatoglyphics, Sexual dimorphism, Pattern, Minutiae, Ibadan, Nigeria*

**Authors for correspondence: soladet@fastmail.fm , Tel: +234-7-87949572*

Manuscript received- April 2023; Accepted- September 2023

DOI: https://doi.org/10.54548/njps.v38i2.2

INTRODUCTION

Fingerprint had been found to be a useful tool in population studies and criminology and had been accepted as one of important means to differentiate gender (Reddy, 1975; Nte, 2012) because of its characteristic permanence, distinctiveness, reliability and accuracy. Accurate and efficient human identification or recognition have become crucial for forensic applications due to the large diversity of crime scenes, and because of the increasing need to accurately identify perpetrators in crime evidence. Identifying the gender of perpetrators from the crime scene is an important aspect in narrowing the scope of suspects in forensic investigation (Lee & Gaensslen, 2014; Abdullah *et al*., 2015).

Over the years, identification of the sex and identity of an individual has involved the use of several body features (Kumar *et al*., 2015). However, fingerprint was one of the oldest and one of the most important pieces of evidence with its infallible characteristic. Its use in forensic science has increased greatly because of the unique arrangement of the ridge on the finger of every individual which does not alter with growth and age (Gutiérrez-Redomero, 2017; Hariharan & Logeswari, 2019). Pattern details involve the use of the loop, whorl and arch, and their quantification. Minutiae features deal with specific ridge characteristics. Minutiae are minor or incidental details, and this makes level two features more unique for individual identity (Yager & Amin, 2004). Several studies (Nithin et.al; 2011, Wijerathne et.al., 2016, Paul and Paul, 2017 a & b) on dermatoglyphics have been carried out in different parts of the world including Nigeria for gender identification. But most of these studies have focused more on patterns and only few have explored the minutiae details for gender identification and most studies used the conventional ink method to obtain fingerprints samples.

The University of Ibadan is highly heterogeneous serving as habitat for people from different regions of Nigeria and other African countries. This study sought to increase the already existing knowledge, but with the use of both level one and two details of fingerprints. The study will also serve as a means of identification of latent print from crime scene in the community and may lead to creation of fingerprint data bank, as reported among Chinese sub-populations (Zhang *et al*., 2010).

MATERIALS AND METHODS

Location of Study: The University of Ibadan, occupying over 1,032 hectares of land, is in Ibadan North Local Government Area, Ibadan, Oyo State, Nigeria. The Institution was originally established on 17 November 1948 as University College, Ibadan. The name was later changed to the University of Ibadan in 1962 (Agbola *et al*., 2001).

Sampling Technique: This study was from a cross section of the population and a multistage sampling procedure was used.

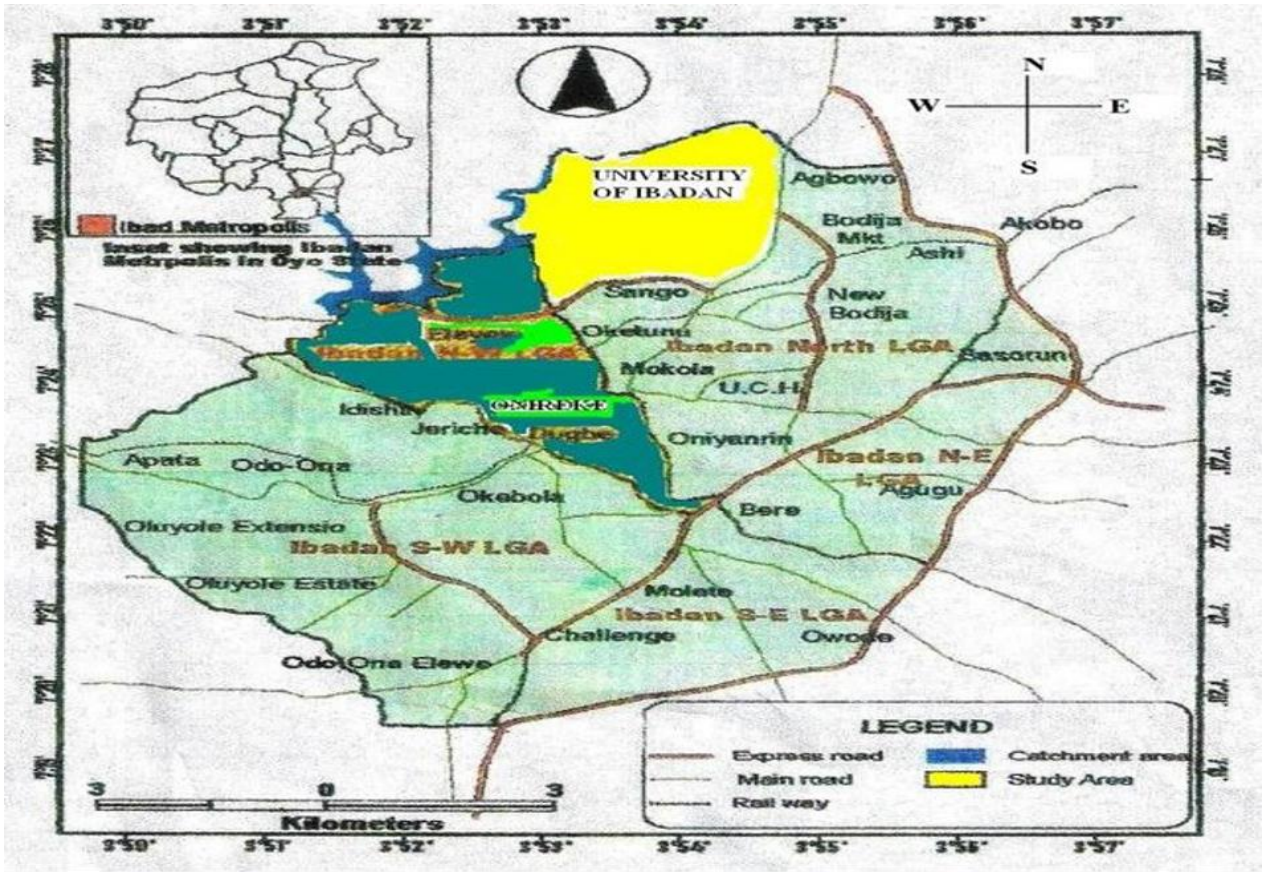

Plate 1:
Map of Ibadan Metropolis showing University of Ibadan (Mubarak & Samuel, 2015)

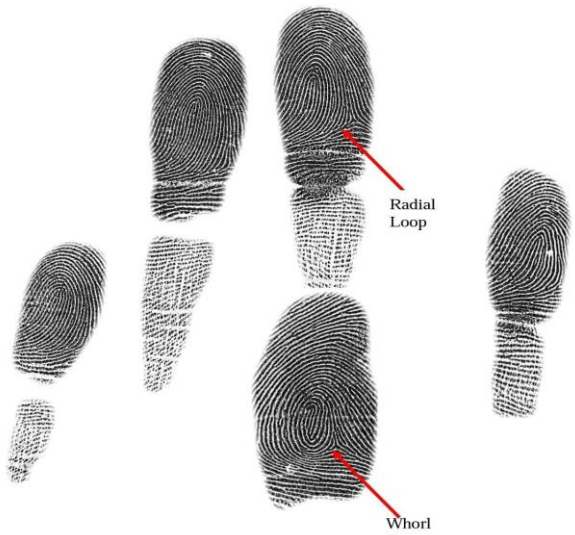

Fig. 2:
Fingers 1-5 Dermatoglyphs showing patterns.

Sample Size: Three hundred and eighty-four (384) participants, comprising 192 males and 192 females, volunteered for the study from the University of Ibadan.

Inclusion Criteria: An initial physical examination of the palmar surface of the fingers was done to exclude scarred fingers from the study.

Methodology: Bilateral digital prints of all the participants were obtained with Dermalog LF10 fingerprint scanner, Hamburg, Germany. The participants' fingers were thoroughly cleaned before prints were taken. The right and left thumbs of participants were first obtained separately for a clearer view. Each finger was pressed against the scanner with a little pressure applied for adequate contact with the scanner such that sharp fingerprints were obtained. Afterwards, the prints were adequately labelled. Interpretation of the patterns was carried out according to Cummins and Penrose (Penrose, 1969; Cummins, 1946). Automated Fingerprint Identification System (AFIS) software (Meadows, Pouratian 1999) was used to enhance the patterns and minutiae present (Fig. 2 and 3).

Fig. 3:
Fingers 1-5 Dermatoglyphs showing minutiae.

The patterns were identified and the minutiae studied were bifurcation, trifurcation, ridge ending, bridge, lake, double bifurcation, island, dot, ridge crossing, break, spur and opposed bifurcation. The parameters analysed included pattern frequency and total finger ridge count.

Statistical Analysis: GraphPad Prism 7.0 was used for statistical analysis and statistical significance was at $p \leq 0.005$.

Ethical Considerations: Ethical review guidelines of the University of Ibadan and University College Hospital (UI/UCH) relating to the use of human subjects for research were duly followed (UI/EC/19/0264). Informed consent was obtained from every volunteer before sampling.

RESULTS

The comparison of pattern type in both genders revealed significant differences between the arch pattern of males and females (Table 1). The female arch pattern was significantly higher than the male.

Table 1:
Comparison of pattern types of both hands of male and female

Pattern	Males (mean±SD)	Females (mean±SD)	P value
Ulna loop	122.3±30.0	113.0±32.8	0.52
Whorl	53.1±23.1	49.9±22.5	0.76
Arch	13.2±10.5	25.3±11.6	*0.025
Radial loop	3.4±5.4	3.8±5.1	0.87

$p \leq 0.05$

The male right and left hands ridge count were significantly higher than the female's right and left hands. There was also a significant difference of the TFRC. The male TFRC was significantly higher than the female (Table 2).
In male, the percentage distribution of minutiae characteristics in the right hand revealed that bifurcation (36.47%) and trifurcation (0.04%) were the most and least distributed respectively. In the left hands, bifurcation (35.77%) and trifurcation (0.02%) were also the most and least distributed respectively. In female, the percentage distribution of minutiae characteristics in the right hand revealed that bifurcation (35.67%) and trifurcation (0.10%) were the most and least distributed respectively. In the left hand, bifurcation (35.60%) and trifurcation (0.11%) were also the most and least distributed respectively (Table 3).

Table 2:
Distribution total finger ridge count in Male and female

	Male	Female	p-value
Digit	mean±SD	mean±SD	
Right	66.34±20.23	55.72±22.16	0.0006
Left	63.12±22.10	53.76±23.88	0.0044
TFRC	129.46±40.92	109.48±51.67	0.0001

Total Finger Ridge Count (TFRC), $p<0.005$

DISCUSSION

The ulnar loop predominance in this study is in conformity with previous studies on the Nigerian population (Adetona *et al*., 2008; Ekanem, 2008; Umana *et al*., 2014). This study showed no significant difference in the whorl, radial loops, and ulnar loop patterns between male and female, right and left hands, which agrees with previous studies (Eboh, 2012; Omuruka *et al*., 2017; Joseph & Ubaidullah, 2018; Adenowo & Dare, 2019). The arch was the only pattern in this study that showed significant gender difference with a higher distribution in female than male which was also reported by Adenowo and Dare (2019) among students of Bingham University, Nigeria and Ray *et al*., (2015) among Indian medical students. There was also a significant difference between male and female TFRC in this study. The male had higher finger ridge count than female, this was also previously reported by Anibor *et al*., (2011); Ekanem, (2008). This implies that the quantitative parameter of TFRC can be used for male and female differentiation within the population.

The minutiae revealed sexual dimorphism, there was a significant difference in the minutiae of right and left hands except the bridge.

Table 3:
Dermatoglyphic minutiae of male and female left and right hand.

	MALE				FEMALE			
MIN	**R**	**%**	**L**	**%**	R	%	L	%
BF	11461	36.47	12341	35.77	10330	35.66	11527	35.60
TF	11	0.04	6	0.02	31	0.10	36	0.11
RE	7567	24.08	8023	23.25	8398	28.99	8978	27.73
BG	324	1.03	333	0.97	290	0.99	387	1.20
LK	4960	15.79	6241	18.09	3888	13.42	4975	15.37
DBF	155	0.49	152	0.44	206	0.70	224	0.69
SR	2611	8.31	2309	6.69	2379	8.22	2032	6.28
DO	588	1.87	625	1.81	564	1.96	505	1.56
RC	16	0.05	21	0.06	71	0.23	105	0.32
OBF	324	1.03	311	0.90	164	0.56	207	0.64
BK	46	0.15	42	0.12	79	0.27	125	0.39
SP	3358	10.69	4098	11.88	2572	8.88	3272	10.11

MIN: Minutiae, R: Right hand, L: Left hand, BF: Bifurcation, TF: Trifurcation, RE: Ridge ending, BG: Bridge, LK: Lake, DBF: Double bifurcation, SR:Short ridge, DO: Dot, RC: Ridge crossing, OBF: Opposed bifurcation, BK: Break, SP: Spur

Table 4:
Comparison of dermatoglyphic minutiae of right and left hands of male and female

Minutiae	Males (Mean±SD)	Females (Mean±SD)	p value
Bifurcation	****12.40±4.16	11.38±4.09	0.0001
Trifurcation	0.01±0.09	****0.03±0.20	0.0001
Ridge Ending	8.12±3.27	****9.05±3.80	0.0001
Bridge	0.34±0.63	0.35±0.75	0.6232
Lake	****5.84±6.58	4.62±5.68	0.0001
Double Bifurcation	0.16±0.46	***0.22±0.60	0.0002
Short Ridge	*2.56±3.41	2.30±3.23	0.0134
Dot	*0.63±0.98	0.56±1.02	0.0202
Ridge Crossing	0.02±0.14	****0.09±0.35	0.0001
Opposed Bifurcatio	****0.33±0.57	0.19±0.44	0.0001
Break	0.05±0.24	****0.11±0.38	0.0001
Spur	****3.88±2.88	3.04±2.82	0.0001

p≤0.05

Bifurcation predominance and trifurcation as the least minutiae in both sexes and hands was similar to the findings of Paul and Paul, (2017a, b) among Kalabari and Ikwerre ethnic groups of Nigeria and Akpan *et al*., (2019) finding among University of Lagos community. Significant differences in the quantification of minutiae between male and female in this study had been reported by other researchers; Paul & Paul (2017a&b) among Nigerians; Thakar *et al*., (2018) among Indians; Gutierrez-Redomero *et al*., (2017) among Argentines. The lake minutiae also differentiate male and female in this study. Bridge minutiae showed no sexual dimorphism, this was also reported by Paul and Paul (2017b) among the Ikwerre ethnic group of Nigeria, and Gutierrez-Redomero *et al*., (2010) among Spanish population. All other minutiae in this study also revealed sexual dimorphism. This revealed that as previously reported and elucidated in this study, minutiae studies can be used for sexual differentiation in forensic analysis and human population studies.

In conclusion, gender disparity existed in the qualitative variable of arch pattern in University of Ibadan community, Nigeria. TFRC and minutiae details showed significant gender differences. This study can be used as a marker in conjunction with other markers in forensic investigation.

REFERENCES

Abdullah, S.F., Rahman, A.F. and Abas, Z.A. 2015. Classification of gender by using fingerprint ridge density in northern part of Malaysia. *Arpn journals of engineering and applied sciences* 10(22):10722-10726.

Adetona, M. O., Oladapo, O. O and Igbigbi, P. S. 2008. Palmar and digital dermatogylyphic patterns of the three major ethnic groups in Nigeria. *African Lournal of Medical Sciences* 37:333-337.

Adenowo, T.k. and Dare, B.J. 2019. Digital and palmar dermatoglyphic patterns of medical students of Bingham University, Karu, Nasarawa state Nigeria. *Journal of Applied Life Sciences International* 20(3): 1-10

Agbola, T., Olatubara, C.O. and Alabi, M. 2001. Students' on-campus housing at Bursting Point: A case study of the University of Ibadan. Ibadan. IFRA and African Book Builders 116-118

Akpan, U.U., Awe, T., Idowu, D.O. and Adekoya, K.O. 2019. Types and frequency of fingerprint minutiae in individuals of Igbo and Yoruba ethnic groups of Nigeria. *Ruhuna Journal of Science* 10(1)77–87.

Eboh, D.E.O. 2012. Digital dermatoglyphic patterns of Anioma and Urhobo students in two tertiary institutions of delta state, Southern Nigeria, A peer review. *Journal of biomedical sciences* 11(2):90 -96.

Ekanem, E., Eluwa, M., Udoaffah, G., Ekanem, T. and Akpantah, A. 2008. Digital dermatoglyphic patterns of Annang ethnic group in Akwa Ibom state of Nigeria. *The Internet Journal of Biological Anthropology* 3(1):1-4

Gutiérrez-Redomero, E., Galera, V., Martínez, J.M., Alonso-Rodriguez, C. 2017. Biological variability of the minutiae in the fingerprints of a sample of the Spanish population. *Forensic Science International* 172(2): 98–105.

Hariharan, R. and Logeswari, S. 2019. Fingerprint as a personal identification tool in forensic science. *Global journal for research analysis* 8(1):22-23

Kumar, P., Ritika, G., Rajinder, S. and Prakash, J. 2015. Effects of latent fingerprint development reagents on subsequent forensic DNA typing: A review. *Journal of Forensic and Legal Medicine* 32 (2015) 64e69

Langenburg, G.M. 2004. Pilot-study: A statistical analysis of the ACE-V methodology - analysis stage. *Journal of forensic identification* 54(1): 64-79.

Lee, H.C. and Gaensslen, R.E. 2001. Methods of latent fingerprint development. *Advances in fingerprint technology* 15;2(105-176):10.

Lipton, J. 2014. "Fingerprints: Unique to Us All." Jennifer Lipton, sites.psu.edu/jlipton/2014/06/03/fingerprints-unique-to-us-all/. Accessed 29 Jan. 2024.

Mubarak, A.F, and Samuel, O.O. 2015. Geophysical and geotechnical characterization of newly constructed Abadina-Ajibode road, University of Ibadan, Ibadan. *Journal of multidisciplinary engineering science* 2(1):363-378

Nithin, M.D., Balaraj, B.M., Manjunatha, B. and Shashidhar, C. 2009. Study of fingerprint classification and their gender distribution among South Indian population. *Journal of Forensic and Legal Medicine* 16:460–463

Nte, N. D. 2012. An evaluation of the challenges of forensic investigation and unsolved murders in Nigeria. *African journal of criminology and justice studies* 6(1/2)143.

Paul, C.W. and Paul, J.N. 2017a. Gender variation studies at level 2 dermatoglyphic details of the Ikwerre ethnic group in Rivers State, Nigeria. *Journal of pharmaceutical research international* 19(2): 1-8.

Paul, C.W. and Paul, J.N. 2017b. Gender variation studies at level 2 dermatoglyphic details of the Kalabari ethnic group in Rivers State, Nigeria. *Scholars journal of applied medical sciences* 5(11A):4297-4301

Reddy, G. G. 1975. Finger dermatoglyphics of the Bagathas of Araku Valley (AP), India. *American journal of physical anthropology* 42(2): 225-228.

Terhorst, P., Damer, N., Braun, A, and Kuijper, A. 2018. What can a single minutia tell about gender? International conference on information Fusion 2113-2120

Wijerathne, T.B., Robert, J.M., Thilini, C.A. and Suneth, B.A. 2015. Dermatoglyphics in hypertension: a review. *Journal of Physiological Anthropology* 34:29

Zhang, H.G., Chen, Y.F., Ding, M., Jin, L. and Case, D.T. 2010. Dermatoglyphics from all Chinese ethnic groups reveal geographic patterning. *Journal PLoS ONE* 5(1):e8783.

Niger. J. Physiol. Sci. 38 (December 2023): 129-137
www.njps.physiologicalsociety.com

Niger. J. Physiol. Sci.

Research Article

Electrocardiography, Blood Pressure Measurements, Vital Parameters and Anaesthetic Indices in the African Giant Rat (*Cricetomys Gambianus* Waterhouse) Immobilized with Diazepam or Ketamine

Igado, O.O.[1], *Abiola, J.O.[2], Anifowose, O.R.[2], Alaba, B.A.[2], Nottidge, H.O.[2] and Omobowale, T.O.[2]

[1] Department of Veterinary Anatomy, [2] Department of Veterinary Medicine, Faculty of Veterinary Medicine, University of Ibadan, Nigeria.

Summary: In spite of the increasing use and importance of the African giant rat (*Cricetomys Gambianus* Waterhouse) in research, and other fields, like location of landmines, there is still not enough information on their physiology. In this study, we assessed the electrocardiogram, blood pressure, vital parameters and anaesthetic indices of the African giant rat (*Cricetomys Gambianus* Waterhouse), both genders, using diazepam or ketamine as chemical restraints. A total of 24 adult African Giant Rats (AGR), 12 males and 12 females were used in this experiment. The animals were divided into two groups of twelve animals each (6 males and 6 females). One group was assessed for the effect of diazepam, and the other group ketamine. Diazepam (Roche®, Switzerland) was administered intraperitoneally at a dose rate of 7.5 mg/kg, while ketamine was administered intraperitoneally at a dose rate of 45 mg/kg. Parameters measured were recorded from the time desirable sedation was achieved, and every 15 minutes till the animal was awake. Animals administered diazepam took a longer time to sleep or achieve desirable sedative state, a longer time to respond to stimuli before waking up fully and a longer time to be fully awake, relative to ketamine-induced sedation. Ketamine caused a continuous increase in respiratory rate and blood pressure, while diazepam caused a continuous decrease in the respiratory rate. Electrocardiogram showed tachycardia throughout the experiment with the use of both drugs, although this was more pronounced with the use of diazepam, causing a decrease in QRS interval and a decrease in QT interval. Gender differences were observed in most parameters measured. Results obtained gave baseline values for electrocardiogram and blood pressure readings, while also detailing the changes and gender differences observed with sedation. In addition, results indicated ketamine is best used for short procedures and diazepam at a higher dose used for procedures requiring longer time in the African giant rat.

Keywords*: African giant rat, electrocardiogram, blood pressure, diazepam, ketamine, anaesthetic indices*.

**Address for correspondence: olusojiabiola1@gmail.com;, Tel: +234-8051495528*

Manuscript received- April 2023; Accepted: October 2023

DOI: https://doi.org/10.54548/njps.v38i2.3

INTRODUCTION

The African Giant Rat, AGR) belongs to the Order Rodentia, Family Nesomyidae, Genus *Cricetomys.* Scientific name *Cricetomys Gambianus* Waterhouse 1840 (Happold, 1987). It is the largest mammalian order with approximately 2016 species in 28 families including squirrels, beavers, chipmunks, rats, mice, lemmings. Gerbils, porcupines, cavies and the capybara. About 50% of the species of living mammals are reported to be rodents (Sheets, 1989). In Africa, these rats are considered to be a delicacy, and are therefore hunted for food. They are high in protein, and are increasingly becoming of interest (Ajayi *et al.*, 1978). More importantly, this rodent has been shown to have a good potential for use as a laboratory animal (Dipeolu *et al.*, 1981) and also, the rodent has been used to detect tuberculosis in patients and to sniff out landmines (Lindow, 2001).

In animals as active as the AGR, the use of chemical restraint is indicated while handling. Chemical restraint reduces excitement and hyper-activity trauma that may occur during handling, thereby reducing morbidity and mortality (Neiffer *et al.*, 2009). Diazepam and ketamine are anaesthetic drugs used to achieve a sedative or anaesthetic effect.

Diazepam, a benzodiazepine, is used clinically as a muscle relaxant, anticonvulsant, anxiolytic and a sedative-hypnotic (Gavish *et al.*, 1999). It is one of the most common sedatives in use, and it comes in different preparations – oral (tablets), injectable, inhalation and rectal forms (Mikota *et al.*, 2005). Ketamine is an NMDA receptor antagonist (Harrison *et al.*, 1985). It is a drug used in human and veterinary medicine, primarily for the induction and

maintenance of general anaesthesia, usually in combination with a sedative. At high, fully anaesthetic level doses, it has also been found to bind to μ-opioid receptors type 2 in cultured human neuroblastoma cells – however, without agonist activity (Hirota *et al.*, 1999) – and to sigma receptors in rats (Narita *et al.*, 2001). Other uses include sedation in intensive care, analgesia (particularly in emergency medicine), and treatment of bronchospasm. This drug has been reported to have a wide range of effects in humans, including analgesia, anaesthesia, hallucinations, elevated blood pressure, and bronchodilation (Peck *et al.*, 2008). Like other drugs of its class, such as tiletamine and phencyclidine (PCP), ketamine induces a state referred to as "dissociative anaesthesia" (Bergman, 1999), and is used as a recreational drug.

Despite the abundance of information on various aspects of the biology of the African Giant Rat (Adeyemo *et al.*, 1990; Oke *et al.*, 1995, 1999; Ali *et al.*, 2008; Akinloye, 2009; Olude *et al.*, 2011; Salami *et al.*, 2011; Akinloye *et al.*, 2012), there currently exists no information on the cardiological parameters of this animal such as electrocardiography and blood pressure measurements. This study was conducted to evaluate the ECG, BP, vital parameters and anaesthetic indices in the AGR immobilized with diazepam or ketamine.

MATERIALS AND METHODS

Ethical approval was obtained from the Ethical Committee, Faculty of Veterinary Medicine, University of Ibadan, Nigeria, ethical code number 02/14/01. All animals were humanely handled to ensure that they were not caused undue pain or stress, and all experiments were performed in accordance to the guidelines by the National Institute of Health (NIH), USA, and the Animal Care, Use and Research Ethics Committee (ACUREC), University of Ibadan, Nigeria. In addition, all methods were reported in accordance with ARRIVE guidelines for reporting of animal experiments.

A total of twenty-four (24) apparently healthy animals (12 males and 12 females) were used for this study. The animals were determined to be adults as earlier described using the weight (Ajayi *et al.*, 1978). They were housed in individual, but similar cages designed for the AGR, at the Giant Rat House. Acclimation to their new environment was done for two weeks prior to the commencement of the study. The rats were divided into two groups of 12 rats each (6 males and 6 females), one group to assess the effect of diazepam, and the other group to assess the effect of ketamine.

Sedation of experimental animals and recording of parameters: The rats in the first group were immobilised with 7.5mg/kg of Diazepam (Roche®, Switzerland), intraperitoneally while rats in the second group were immobilised with ketamine at the dosage of 45mg/kg intraperitoneally. The length of time to induce sedation was recorded. Parameters such as the electrocardiogram, blood pressure readings, respiratory rate, and rectal temperature were obtained from the time desirable sedation was achieved, and for every 15 minutes till the time the animal recovered from sedation.

Electrocardiography: Using a 6/7 lead computer ECG machine, (EDAN VE1010, Shanghai, China) lead-II electrocardiograms were recorded as earlier described by Omobowale et al. (Omobowale *et al.*, 2017). The machine was calibrated at a paper speed of 50mm/s and vertical at 20mm/mV. Briefly, each animal was placed on right lateral recumbency and the limbs were carefully positioned perpendicularly to the long axis of the body. Parameters such as heart rate, P-wave duration, PR-interval, QRS duration, R-amplitude and QT-interval and QTc (Bazett) were recorded (Fig. 1).

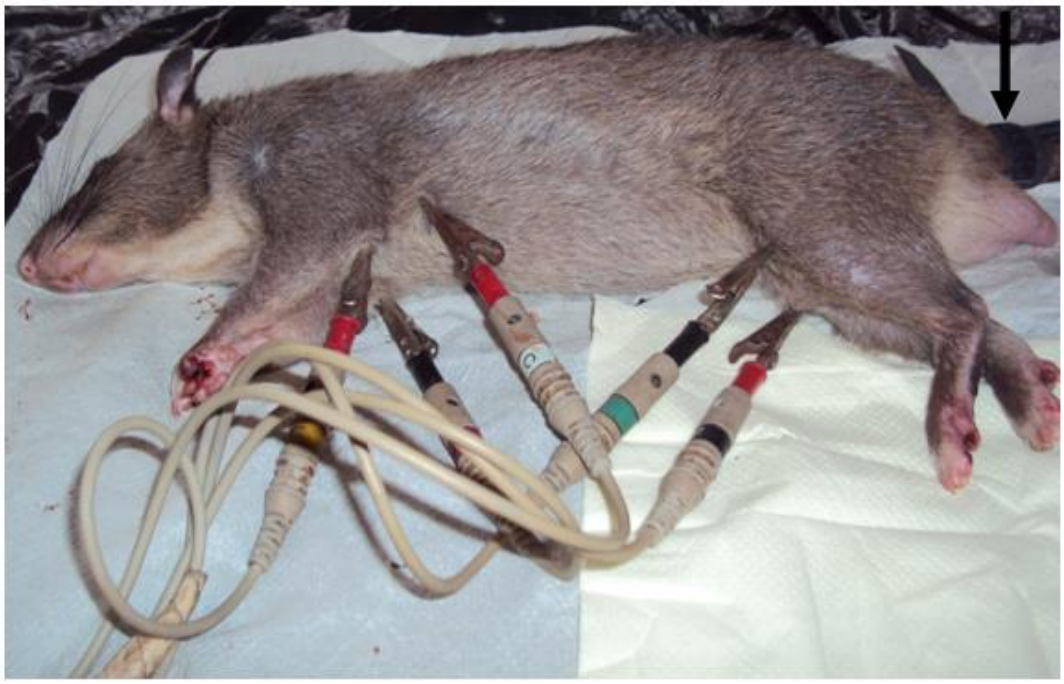

Plate 1:
An African giant rat sedated and placed on right lateral recumbency, showing the placement of the ECG electrodes. Note the blood pressure cuff on the tail (black arrow)

Rectal temperature and Respiratory rate: Values for the rectal temperature were obtained with the aid of a digital clinical thermometer and recorded in OC, while the respiratory rate was determined manually using a stop watch, and recorded as number of respirations / minute.

Blood Pressure Monitoring: Placing of cuffs: Blood pressure was monitored with a digital occilometric blood pressure monitor, model VET400A (Krutech®). The cuff was placed on the cranial aspect of the tail, close to the sacro-caudal joint (of the vertebral column) (Figure 1).

Statistical Analysis

All data obtained were analysed using Graphpad Prism® version 5 (GraphPad Software Inc., La Jolla, CA USA). Student's 't' test was used to test significant difference and $p<0.05$ was accepted as statistically significant.

RESULTS

Body Weight: The body weights (expressed as Mean ± Standard deviation) of the 12 AGRs used to assess the effect of diazepam was 826.7 ± 169.3 grams, with the males having a body weight of 863 ± 184.5 grams and the females 790.3 ± 160.8 grams. The ketamine group had a body weight of 836.7 ± 178.7 grams, with the males being 871 ± 206.7 grams, and the females 802 ± 157.2 grams. No statistically significant difference was observed in the weight of the two groups ($p>0.05$).

Other results are shown in Table 1 and Figures 2 – 7.

Electrocardiogram: Results are presented in Table 1.

Table 1:
LEAD-II ECG parameters in AGR administered diazepam and ketamine

Parameter	Diazepam				Ketamine			
	0 min	**15 min**	**30 min**	**45 min**	**0 min**	**15 min**	**30 min**	**45 min**
Heart Rate (/min)	259.2 ± 38.0	268.8 ± 37.9	266.6 ± 42.5	276.0 ± 40.3	178.2 ± 50.0	171.1 ± 46.0	184.2 ± 36.63	213.5 ± 13.4
P-wave duration (ms)	30.3 ± 2.0	37.6 ± 12.3	30.9 ± 6.4	28.8 ± 7.1	28.2 ± 4.3	29.8 ± 6.0	29.4 ± 4.83	27 ± 1.4
P-R interval (ms)	55.4 ± 7.1	57.7 ± 13.4	56.3 ± 7.43	51.3 ± 7.0	52.2 ± 8.6	55.4 ± 7.8	55.2 ± 14.27	47 ± 8.5
QRS duration (ms)	30.3 ± 7.0	29.9 ± 6.9	27.6 ± 10.50	23.5 ± 6.8	32.5 ± 10.7	31.6 ± 8.0	28.6 ± 5.86	26.5 ± 7.8
QT segment (ms)	109.4 ±18.4	98.2 ± 11.0	89.6 ± 12.0	84.3 ± 2.4	101.5 ± 15.8	97.9 ± 16.0	91.6 ± 17.18	88 ± 2.8
QTcB(ms)	225.1 ± 35.1	206 ± 19.0	187.9 ± 30.8	179.8 ± 10.5	172.6 ± 37.3	163.8 ± 37.0	158.8 ± 30.6	165.0 ± 0.0
R-amplitude (mV)	0.368 ± 0.15	0.372 ± 0.20	0.358 ± 0.17	0.389 ± 0.21	0.370 ± 0.2	0.408 ± 0.17	0.353 ± 0.11	0.365 ± 0.2

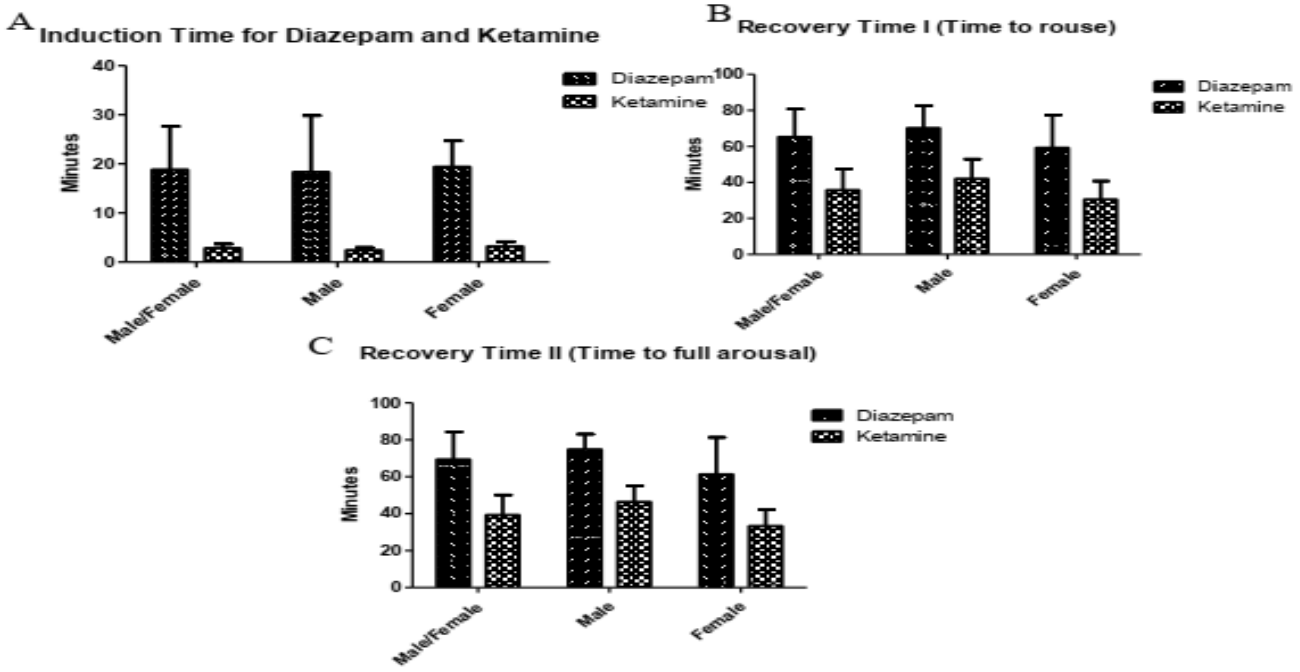

Figure 2A-C:
Bar charts showing time to induce sedation (A), time to arouse from sedation (B), and time to arouse completely from sedation (C), using diazepam or ketamine in AGR. Male/Female (n = 12), Male (n = 6) and Females (n = 6). Values obtained for ketamine were statistically significantly lower ($p<0.05$) in A – C, although values obtained for the males with ketamine administration was statistically significantly higher than the females ($p<0.05$) in C.

Both diazepam and ketamine caused an increase in the heart rate. Diazepam caused an increase, then a decrease in the P-wave duration. Ketamine caused the same change in the P-wave duration, although not as pronounced. This trend was also observed in the P-R interval. A progressive decrease was observed with the use of the two drugs in the QRS duration, the QT segment and the QTcB. The pattern observed for the R-amplitude was similar in both cases. At $p<0.05$, statistical significance was observed in the heart rate values between diazepam and ketamine at 0, 15 and 30 minutes ($p<0.05$), but not at 45 minutes ($p>0.05$). QTcB using the two drugs showed statistical significance at 0, 15 and 45 minutes ($p<0.05$). A decrease in QRS duration was observed from 0 to 45 minutes, with the use of both drugs.

Time to induce desirable sedation and time to recover from sedation (induction and recovery times): This was recorded in minutes (Figures 2A-C).
Statistically significant difference was observed between the time it took to achieve desirable sedation (induction time), the length of time from when the animal slept off to when it started to wake up, or respond to stimuli (recovery time I) and the length of time from when the animal slept off to when it was fully awake and could move around (recovery time II/ time to full arousal) values for diazepam versus ketamine ($p<0.05$). comparing male values with female values revealed statistical significance for time to attain full arousal, when ketamine was used, with the males having higher values (46.4 ± 8.71 minutes) relative to the females (33.33 ± 8.96 minutes) ($p<0.05$).
With the use of diazepam, at 15 minutes, all the animals (100%) were still sedated. At 30 minutes, 11 animals remained sedated (91.7%, of the AGR population, 100% male population, 83.3% female population). At 45 minutes, 7 animals (5 males, 2 females) remained sedated (58.3% of the AGR population, 33.3% of the females, and 83.3% of the males). Only one animal, male (16.7% of the male population, and 8.3% of the AGR population), remained sedated for up to 60 minutes throughout the experiment. This was during the administration of diazepam.
During ketamine sedation, at 15 minutes, all animals (100%) remained sedated. At 30 minutes, 7 animals remained sedated (4 males and 3 females) – 58.3% of the total AGR population, 66.7% of the male population and 50% of the female population. At 45 minutes, only two animals (both males) remained sedated (33.3% of the male population and 16.7% of the total AGR population).

Blood Pressure
Systolic Blood Pressure: Results are presented in Figures 3A-C. Ketamine appeared to result in a progressive increase in the systolic pressure of all the animals, both male and female. This is unlike that observed in diazepam-induced sedation where the males showed an increase, but the females recorded a decrease before an increase

Diastolic Blood Pressure: Results are presented in Figures 4A-C. As was observed in the systolic pressure, ketamine maintained a progressive increase in diastolic pressure, the pattern of which was similar in both male and female. Diazepam caused an initial increase, followed by a drop, and finally an increase. In the male, diazepam caused an increase in the last 15 minutes of the experiment (30 to 45 minutes), but a further decrease in the females for the last 15 minutes.

Mean Arterial Pressure: Results are presented in Figures 5A-C. Ketamine resulted in a progressive increase in the mean arterial (MA) pressure, also expressed in the same way in both genders. Diazepam caused an increase, a decrease and finally an increase, as was observed in the diastolic pressure in males.

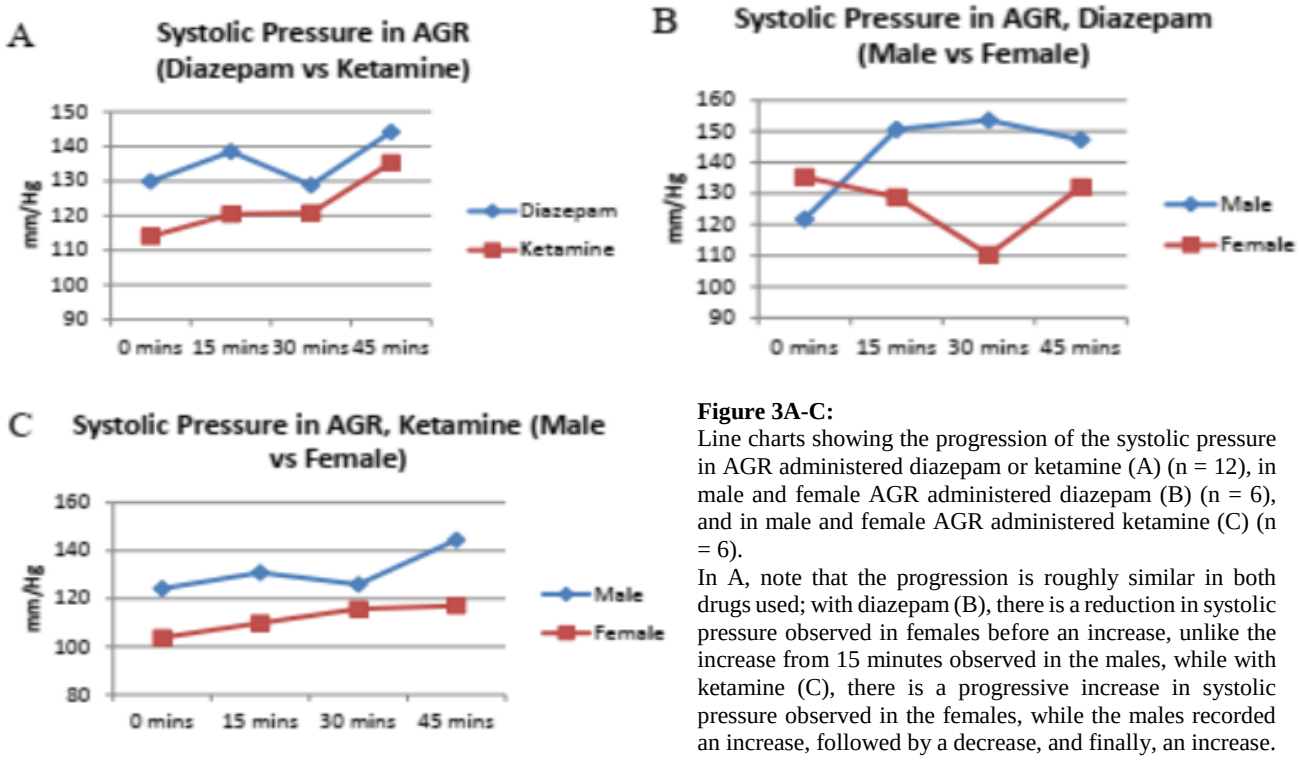

Figure 3A-C:
Line charts showing the progression of the systolic pressure in AGR administered diazepam or ketamine (A) (n = 12), in male and female AGR administered diazepam (B) (n = 6), and in male and female AGR administered ketamine (C) (n = 6).
In A, note that the progression is roughly similar in both drugs used; with diazepam (B), there is a reduction in systolic pressure observed in females before an increase, unlike the increase from 15 minutes observed in the males, while with ketamine (C), there is a progressive increase in systolic pressure observed in the females, while the males recorded an increase, followed by a decrease, and finally, an increase.

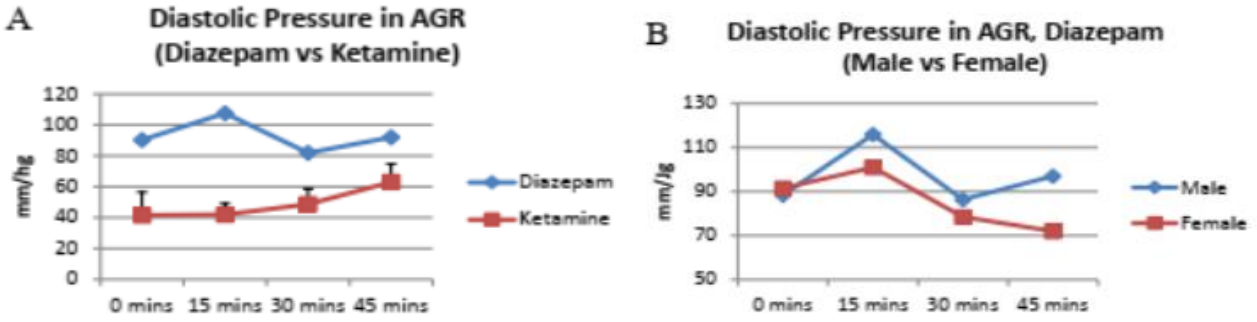

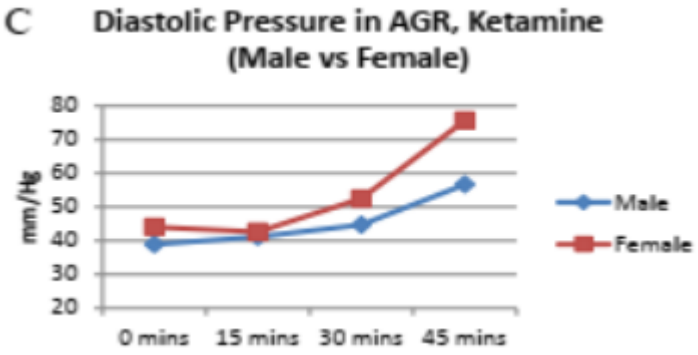

Figure 4A-C:
Line charts showing the progression of the diastolic pressure in AGR administered diazepam or ketamine (A) (n = 12), male and female AGR administered diazepam (B) (n = 6) and male and female AGR administered ketamine (C) (n = 6).
In A, note the progressive increase in diastolic pressure observed in ketamine induced sedation, and the increase, decrease and finally increase in diazepam-induced sedation. B (diazepam) shows a similar pattern of increase and decrease at 15 and 30 minutes respectively, followed by an increase in the male and a decrease in the female at 45 minutes, while C (ketamine) also displayed a similar pattern of increase in both genders throughout the experiment.

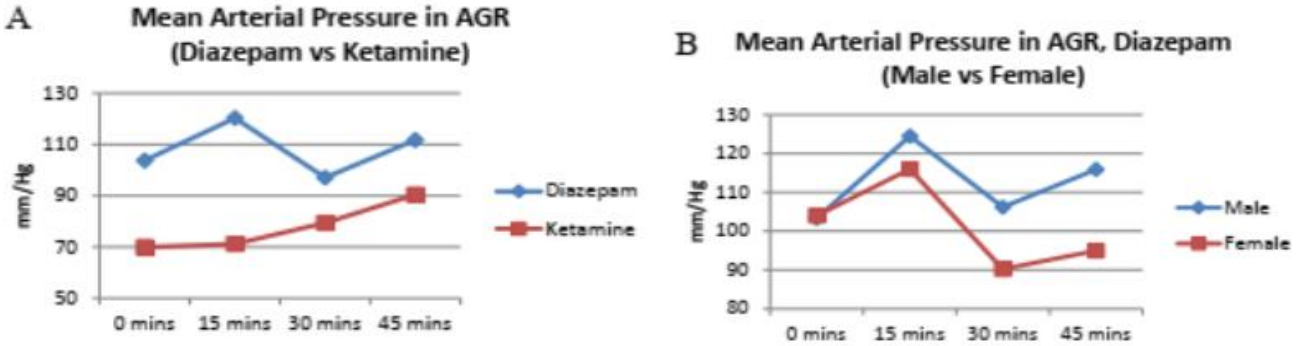

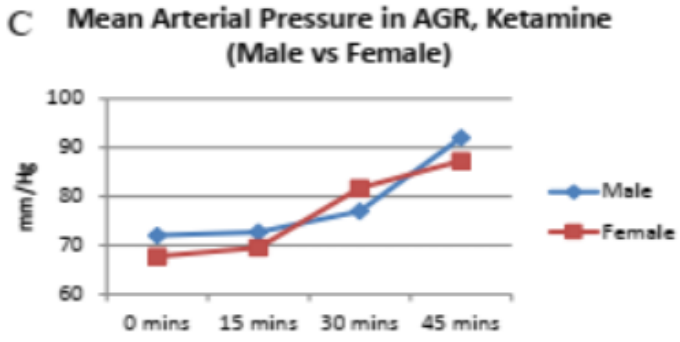

Figure 5A-C:
Line charts showing the progression of the mean arterial (MA) pressure in AGR administered diazepam or ketamine (A) (n = 12), male and female AGR administered diazepam (B) (n = 6), and male and female AGR administered ketamine (C) (n = 6).
In A, note the steady and consistent increase in MA pressure in ketamine induced sedation, and the increase, decrease and finally increase in the diazepam induced sedation; B (diazepam) showed a similar pattern of increase, decrease and then increase in both genders. Note also that although male and female values were similar at 0 minutes, and pattern was similar, the female MA pressure showed a decrease relative to the male; while in C (ketamine), both genders showed an increase in MA pressure.

Respiratory Rate: Results are presented in Figures 6A-C. Ketamine administration resulted in an increase in the respiratory rate while diazepam depressed it very slightly, although no significantly significant difference was observed between the two drugs. In comparing the genders, diazepam administration resulted in an increase in respiratory rate in the females, with a slight decrease observed at 30 minutes. The males however, showed a decrease in respiratory rate. Ketamine-induced sedation in the females showed an increase (15 mins), and then a slight decrease (30 mins), while the males had an increase up till the 45-minute mark. All ketamine-administered rats were awake before 60 mins.

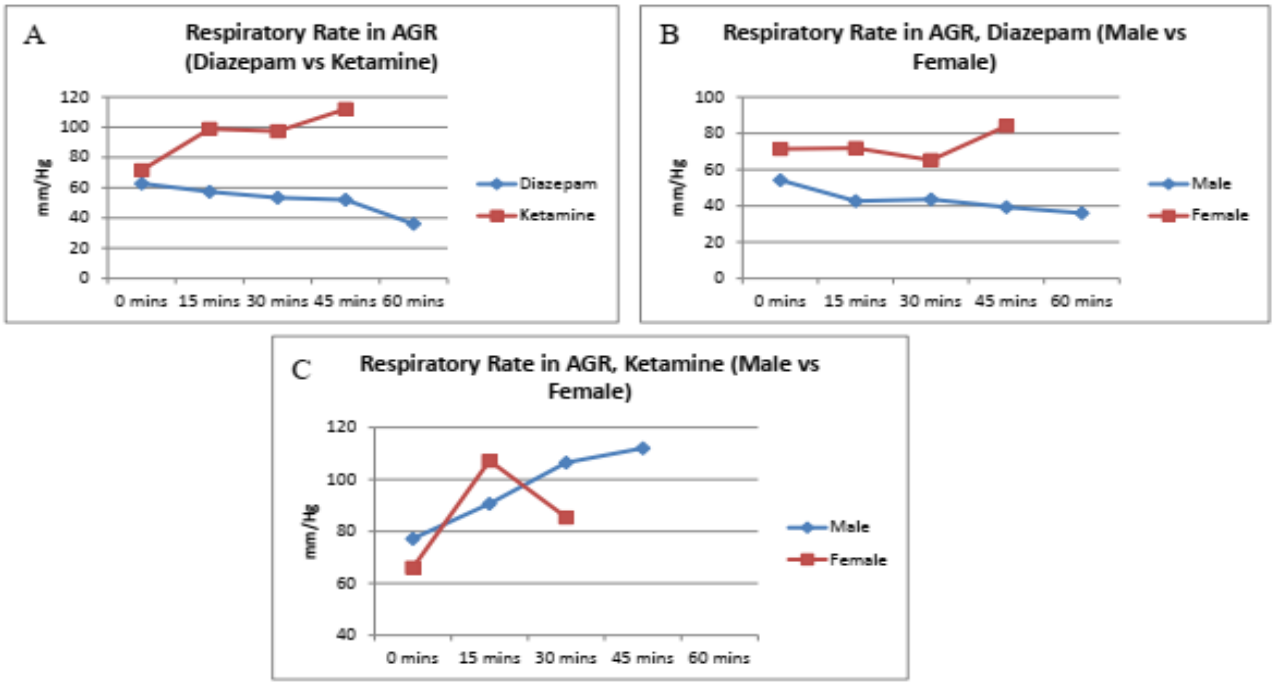

Figure 6A-C:
Line charts showing progression of respiratory rate in AGR administered diazepam or ketamine (A), male and female AGR administered diazepam (B) and male and female AGR administered ketamine (C).
In A, note the increase in respiratory rate in the ketamine group relative to the decrease in the diazepam group. No value was available for ketamine at 60 minutes, as all animals were fully awake by then; in B (diazepam), note the increase in respiratory rate in the females, although a slight dip occurred at 30 minutes. The males showed a depression or decrease in respiratory rate relative to the females; while in C (ketamine), there was an increase at 15 minutes, and then the dip at 30 minutes in values obtained in the females. The males showed a progressive increase in the rate of respiration up to 45 minutes. No animal hit the 60-minute mark.

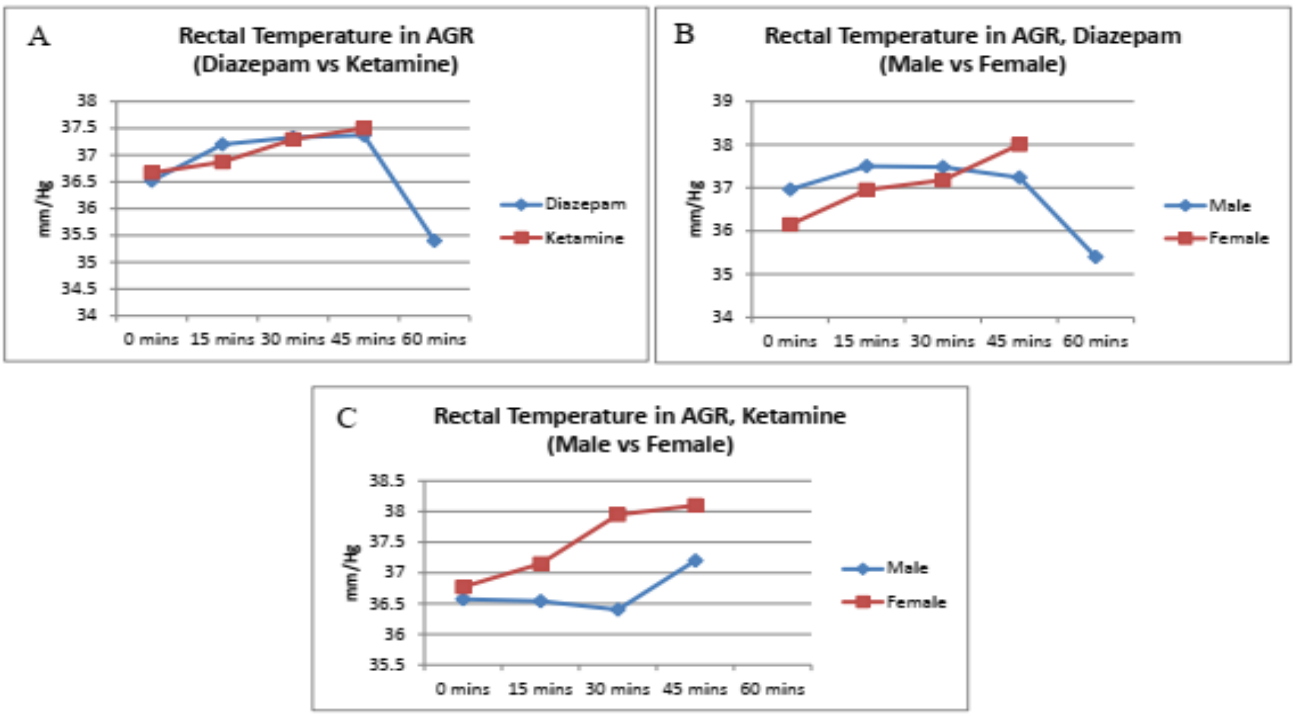

Figure 7A-C:
Line charts showing rectal temperature (Tr) in AGR administered diazepam or ketamine (A), male and female AGR administered diazepam (B) and male and female AGR administered ketamine (C).
In A, note the increase in both diazepam and ketamine up to 45 mins, and the subsequent decrease at 60 mins in the diazepam group. In B (diazepam), there was a consistent increase in Tr in the females, unlike the males. Also, all females were awake before 45 mins. In C (ketamine), the females also showed a consistent increase, while the males showed a slight decrease before an increase. All animals were awake before the 60 mins mark.

Electrocardiogram and blood pressure of the giant rat

Rectal Temperature: Results are presented in Figures 7A-C. In both males and females, using diazepam or ketamine, an increase in temperature was observed. The rate of increase was observed to decrease as the time was progressing towards the wearing off of sedation. By 60 minutes (observed for a single animal – male), a sharp decrease was observed in the value of the rectal temperature. Progression of temperature was observed to be similar with the use of the two sedatives. With the use of diazepam, progression of temperature change in both genders was similar till 30 minutes post-administration. By 45 minutes, an increase in temperature of 0.9OC was observed in the female, while a drop in temperature of 1.8OC was observed in the male. It should be noted however, that only a single male made it to the 60 minutes mark.

With the use of ketamine, the females showed a progressive increase in rectal temperature up to 45 minutes, while the males showed a slight drop from 0 to 30 minutes, which increased from 30 to 45 minutes.

No statistically significant difference was observed between values for diazepam and ketamine, and the time frames (0, 15, 30, 45 and 60 minutes) ($p>0.05$).

DISCUSSION

In this study, males had a higher mean body weight than the females. This observation is consistent with earlier reports in the fruit bat (Igado *et al.,* 2012) and that of Campbell (Campbell, 1990), who had earlier on made an observation that the males of most species are usually heavier than the females.

Anaesthetic management and handling of wildlife is often a challenge encountered by veterinarians or scientists. Ketamine at 45 mg/kg induced desirable sedation in a time considerably and statistically significantly lower ($p<0.05$) than diazepam (7.5 mg/kg). In spite of the fact that ketamine induced sedation faster, the period of sedation was considerably lower than that of diazepam., and the animals recovered faster from ketamine-induced sedation.

Ketamine is 10 times more lipid soluble than thiopentone and can quickly cross the blood-brain barrier. This makes it relatively rapid in the onset of effect and recovery due to redistribution, similar to the thiobarbiturates. The onset of anesthesia/sedation, in one study, was 45 seconds after intravenous injection (2 mg/kg) and 4 minutes after intramuscular injection (3 mg/kg) with recovery times of 18 minutes and 25 minutes respectively (Cotsen *et al.,* 1997). After intravenous injection in humans, the distribution half-life [t(½π)] was 24.1 seconds, redistribution half-life [t(½α)] was 4.68 minutes, and elimination half-life [t(½β) was 2.17 hours (Domino *et al.,* 1984) (Domino *et al.,* 1984). In our current study, ketamine (45 mg/kg) administered intra-peritoneally, gave an induction time of 2.818 ± 0.87 minutes, and recovery times of 35.73 ± 11.7 and 39.27 ± 10.82 minutes.

Ketamine at approximately 40 mg/kg body weight by intramuscular injection was shown to provide sedation that waned over approximately one hour (Fowler *et al.,* 2008). Flecknell (Flecknell, 1996) found that a combination of medetomidine (0.5 mg/kg) and ketamine (75 mg/kg) by intraperitoneal injection provided effective anaesthesia (although not necessarily for major surgery) in rats. In this current study, diazepam gave a longer period of sedation, but the sedative effect was not as effective as that of ketamine. This implies that ketamine is probably ideal for short procedures, while diazepam, at higher doses may probably be used for longer procedures, or in combination with other drugs.

Homeotherms (birds and mammals) employ physiologic mechanisms to maintain their body temperature within a narrow range, despite constant exothermic metabolism and wide ambient temperature fluctuations (Gordon, 2009). The rectal temperature is a good indicator of the core body temperature that is widely used in animals because of its accuracy, convenience and safety (Keim *et al.,* 2002; Zhao *et al.,* 2010). The rectal temperature of the AGR in this study did not display any statistically significant change, indicating that these drugs do not result in temperature changes. The decrease in temperature observed at some points may be due to the inactivity of the animal due to sedation. Also, it should be noted that the ambient temperatures on the days of the experiment remained relatively constant. The current experiment was carried out during the harmattan season (October to January), and results obtained were found to be similar to and within the same range as that obtained by Dzenda *et al.,* (Dzenda *et al.,* 2011), during the dry season (34.07 to 39.77^{O}C). It is noteworthy however, that the highest temperature obtained in the current experiment (39.0^{O}C), observed in a male during diazepam administration, was still lower than the maximum obtained by Dzenda *et al.,* (Dzenda *et al.,* 2011) in harmattan (39.77^{O}C), and the hot dry season (36.31^{O}C to 40.15^{O}C).

Based on the fact that results obtained with the two drugs administered were still within the range of normal rectal temperatures obtained during seasonal investigations in previous studies (Dzenda *et al.,* 2011), it can be safely deduced that neither diazepam nor ketamine exerted any significant change in the rectal temperature of the AGR.

Diazepam was observed to suppress the respiratory rate while ketamine elevated it. This is contradictory to Heshmati (Heshmati *et al.,* 2003), who reported that ketamine suppresses breathing more than other available anaesthetics. According to Peck *et al.,* (Peck *et al.,* 2008), ketamine causes bronchodilation, which may probably be responsible for the increased respiratory rate observed in ketamine induced sedation. This was more obvious in the males than the females who had a decrease in respiratory rate at 30 minutes. The reason for this decrease in respiratory rate needs further investigation to ascertain probable gender differences in response of AGR to ketamine.

Male and female response to diazepam in this study differed greatly, as the females recorded an elevation in respiratory rate, and the males, a depression. The reason for this could not be ascertained, and no record of gender difference in the reaction to diazepam could be obtained.

Respiration, heart rate, blood pressure and level of consciousness are controlled by numerous nuclei in the brainstem (Purves *et al.,* 2004). It is possible that the two drugs used in this experiment elicited differing responses from the respiratory centres.

The systolic pressure graph for diazepam and ketamine followed a similar pattern except for the decrease in diazepam at 30 minutes. An increase in systolic pressure

was also observed in both genders with the use of ketamine. Diastolic and mean arterial pressures were also observed to increase with the use of ketamine. This is consistent with the findings of West *et al.,* (West *et al.,* 2007) and Peck *et al.,* (Peck *et al.,* 2008), that ketamine causes increased mean arterial blood pressure and blood pressure respectively. This makes ketamine a drug to be considered in hypotensive animals, in cases of hypovolemic shock and in patients where blood volume status cannot be ascertained. No appreciable difference was observed between the male and the female, implying that ketamine might not necessarily cause gender specific reactions when administered, unlike what was observed with the use of diazepam.

Although diazepam caused an increase, then a decrease followed by an increase in systolic pressure, this trend was not the same when gender differences were considered. Diazepam showed a decrease in systolic pressure in the females, with an increase resulting at 45 minutes, unlike in males, where an increase was observed from 0 minutes. This same pattern was observed in the diastolic and mean arterial pressures. There was a great similarity between the male and female in mean arterial pressure with the use of diazepam. Results obtained may indicate the risk of hypotension at 30 minutes with the use of diazepam, in both sexes. This depression is consistent with the decrease in respiratory rate observed with the use of diazepam. Results from this experiment differs a bit from the findings of Kitajima *et al.,* (Kitajima *et al.,* 2004), that diazepam like all benzodiazepines cause hypotension (significant decrease of systolic and mean arterial blood pressure) by a central mechanism. Kitajima *et al.,* (Kitajima *et al.,* 2004), administered diazepam (5mg) intravenously to human subjects. The difference in this current experiment and the previous experiment may be due to difference in subjects (AGR versus humans). This may also show that AGR react differently to diazepam when compared with other subjects. This may need further investigation, in view of the increasing awareness of the AGR as a laboratory animal.
Ketamine resulted in an increase in blood pressure, coupled with an increase in respiratory rate, making it a seeming ideal drug for use in cases of respiratory arrest, in asthmatic patients or in cases of chronic obstructive pathway (Lankenau *et al.,* 2007). It can be concluded that when diazepam is to be used, more care should be employed in monitoring blood pressure and respiration.

The increase in heart rate in both groups can be attributed to one or more of the following mechanisms: a decrease in vagal tone, an increase in sympathetic tone, an increase in circulating catecholamines and a direct effect on the cardiac pacemaker and conduction (Dennis *et al.,* 2007). The duration of electrical conduction through atrioventricular node (PR interval) was similar between the diazepam and ketamine groups, implying that both drugs can result in delayed atrioventricular conduction when administered at a dose to result in prolonged sedation. There was a decrease observed in the QRS duration with the administration of diazepam and ketamine, from 0 minutes to 45 minutes. This may mean that the two drugs may cause a shortening of the interventricular and His bundle conduction times (Weber *et al.,* 1995). In dogs, QT interval was reported to be inversely related to the heart rate (Oguchi *et al.,* 1993). This is evident in this study as the heart rate was observed to increase while the QT interval decreased.

During the administration of ketamine, all animals were observed to have their eyes open throughout the period of sedation. Ketamine produces a unique anaesthetic state (dissociative anesthesia), characterized by dissociation between the thalamocortical and limbic systems. Patients are usually unconscious and cataleptic or partially conscious but unable to respond purposefully to physical stimulation or verbal command, depending on dose. Their vital reflexes are generally intact but can be depressed. Therefore, by definition, ketamine produces a unique state somewhere between deep sedation and general anesthesia (Bergman, 1999). This ability of ketamine to make patients partially conscious, but unable to respond to physical stimulation or verbal command may have been responsible for the non-closure of eyelid in spite of the fact that the animal appeared reasonably sedated.

During diazepam induced sedation, the animals were observed to move their mouths in a chewing manner. Also, upon recovery from diazepam sedation, they were observed to reach immediately for their food bowls. Diazepam has been reported to be used occasionally as an appetite stimulant. It is said to induce hyperphagia via a GABAergic action (Rahminiwati *et al.,* 1999). This may be responsible for the observed seemingly increased desire for food.

In conclusion, this study assessed the ECG readings, blood pressure values and vital parameters of the AGR. These values could not be obtained without sedation, therefore anaesthetic indices were recorded. Results obtained will provide baseline data in the field of internal medicine and surgery for these animals and other similar rodents.

The use of diazepam (7.5 mg/kg) and ketamine (45mg/kg) in the AGR may be ideal for short non-surgical procedures (when used without combination with other drugs). In order to make the animal more fully anaesthetised for surgery, higher doses may be recommended, or the use in combination with any other appropriate anaesthetics. With the increased use of these animals for research, further investigations need to be carried out to fully determine the reactions of this unique animal to these drugs, and the merits and demerits there are.

Acknowledgements
The authors appreciate the cooperation of the Staff of the Experimental Animal House, Faculty of Veterinary Medicine, University of Ibadan, Nigeria, during the period of this experiment.

REFERENCES

Adeyemo, O. and Oke, B.O. (1990), Comparison of the Testicular and Epididymal Proteins of the African Giant Rat (*Cricetomys Gambianus* Waterhouse) and the Laboratory Rat. *Tropical Veterinarian*, 8: 17-27.

Ajayi, S., Tewe, O. and Faturoti, E. (1978), Behavioural Changes in African Giant Rat (*Cricetomys Gambianus* Waterhouse) under Domestication. *East African Wildlife Journal*, 16(2): 137-143.

Akinloye, A.K. (2009), Structural and Hormonal Studies in the Female African Giant Rat (*Cricetomys Gambianus* Waterhouse).

Akinloye, A.K. and Oke, B.O. (2012), Sex Hormonal Pattern of the Female African Giant Rat (*Cricetomys Gambianus* Waterhouse) at Different Stages of the Oestrus Cycle. *Nigerian Veterinary Journal*, 33(3): 586-591.

Ali, M.N., Byanet, O., Salami, S.O., Imam, J., Maidawa, S.M., Umosen, A.D., Alphonsus, C. and Nzalak, J.O. (2008), Gross Anatomical Aspects of the Gastrointestinal Tract of the Wild African Giant Pouched Rat (*Cricetomys Gambianus*). *Scientific Research and Essay*, 3(10): 518–520.

Bergman, S.A. (1999), Ketamine: Review of Its Pharmacology and Its Use in Pediatric Anesthesia. *Anesthesia Progress*, 46(1): 10–20.

Campbell, N.A. (1990), Biology. The Benjamin/Cummings publishing Company Inc, New York.

Cotsen, MR., Donaldson, JS., Uejima, T. and Morello, FP. (1997), Efficacy of Ketamine Hydrochloride Sedation in Children for Interventional Radiologic Procedures. *Am J Roentgenol*., 169: 1019-1022.

Dennis, S.G., Wotton, P.R., Boswood, A. and Flaherty, D. (2007), Comparison of the Effects of Thiopentone and Propofol on the Electrocardiogram of Dogs. *Veterinary Record*, 160: 681–686.

Dipeolu, O.O., Akinboade, O.A. and Ogunji, F. (1981), Observation of the African Giant Rat (*Cricetomys Gambianus*). *Bulletin of Animal Health Production Africa*, 29: 393-397.

Domino, EF., Domino, SE. and Smith, RE. (1984), Ketamine Kinetics in Unmedicated and Diazepam Premedicated Subjects. *Clin Pharmacol Ther*, 36: 645-653.

Dzenda, T., Ayo, J.O., Lakpini, C.A.M. and Adelaiye, A.B. (2011), Diurnal, Seasonal and Sex Variations in Rectal Temperature of African Giant Rats (*Cricetomys Gambianus* , Waterhouse). *Journal of Thermal Biology*, 36: 255–263.

Flecknell, P.A. (1996), Laboratory Animal Anaesthesia. London, Academic Press.

Fowler, M.E. and Miller, R.E. (2008), Zoo and Wild Animal Medicine Current Therapy. Volume 6. *Saunders Elsevier* Inc.

Gavish, M., Bachman, I., Shoukrun, R., Yeshayahu, K., Veenamn, L., Weisinger, G. and Weizman, A. (1999), Enigma of the Peripheral Benzodiazepine Receptor. *Pharmacological Reviews*, 51(4): 629-650.

Gordon, C.J. (2009), Quantifying the Instability of Core Temperature in Rodents. *J. Therm. Biol.,* 34(5): 213–219.

Happold, D. C. D. (1987), The Mammals of Nigeria. Clarendon Press, Oxford, United Kingdom.

Harrison, N.L. and Simmonds, M.A. (1985), Quantitative Studies on Some Antagonists of N-Methyl D-Aspartate in Slices of Rat Cerebral Cortex. *British Journal of Pharmacology*, 84(2): 381–91.

Heshmati, F., Zeinali, M.B., Noroozinia, H., Abbacivash, R. and Mahoori, A. (2003), Use of Ketamine in Severe Status Asthmaticus in Intensive Care Unit. *Iranian Journal of Allergy, Asthma, and Immunology*, 2(4): 175–80.

Hirota, K., Sikand, K.S. and Lambert, D.G. (1999), Interaction of Ketamine with Mu2 Opioid Receptors in SH-SY5Y Human Neuroblastoma Cells. *Journal of Anesthesia*, 13(2): 107–109.

Igado, Olumayowa O, Omobowale, Temidayo O, Ajadi, Rasheed A and Nottidge, Helen O (2012), Craniofacial Morphometrics and Macro-Neurometrics of the Fruit Bat (Eidolon Helvum). *European Journal of Anatomy*, 16(3): 172–176.

Keim, S.M., Guisto, J.A. and Sullivan Jr., J.B. (2002), Environmental Thermal Stress. *Ann. Agric. Environ*. Med., 9: 1–15.

Kitajima, T., Kanbayashi, T., Saito, Y., Takahashi, Y., Ogawa, Y., Sugiyama, T., Kaneko, Y., Aizawa, R. and Shimizu, T. (2004), Diazepam Reduces Both Arterial Blood Pressure and Muscle Sympathetic Nerve Activity in Human. *Neuroscience Letters*, 355(1–2): 77–80.

Lankenau, S.E., Sanders, B., Bloom, J.J. and Al., Et (2007), First Injection of Ketamine among Young Injection Drug Users (IDUs) in Three U.S. Cities. *Drug and Alcohol Dependence*, 87(2–3): 183–93.

Lindow, M. (2001), The Landmines Sniffing Rats of Mozambique. Time Magazine.

Mikota, S.K. and Plumb, D.C. (2005), The Elephant Formulary. *Elephant Care International*.

Narita, M., Yoshizawa, K., Aoki, K., Takagi, M., Miyatake, M. and Suzuki, T. (2001), A Putative Sigma1 Receptor Antagonist NE-100 Attenuates the Discriminative Stimulus Effects of Ketamine in Rats. *Addiction Biology*, 6(4): 373–376.

Neiffer, D.L. and Stamper, M.A. (2009), Fish Sedation, Anaesthesia, Analgesia and Euthanasia: Considerations, Methods and Types of Drugs. *ILAR Journal*, 50(4): 343–360.

Oguchi, Y. and Hamlin, R.L. (1993), Duration of QT Interval in Clinically Normal Dogs. *Am J Vet Res*,, 54: 2145–2149.

Oke, B.O. and Aire, T.A. (1995), The Prostate Gland of the African Giant Rat (*Cricetomys Gambianus* Waterhouse). *Veterinaski Archiv*., 65: 125–135.

Oke, O.A. and Oke, B.O. (1999), Vaginal Cytological Changes during the Oestrus Cycle of the Adult Female African Giant Rat (*Cricetomys Gambianus* Waterhouse). *Tropical Veterinarian*, 17: 169–180.

Olude, M.A., Olopade, J.O., Igado, O.O., Mustapha, O A and Akinloye, A K (2011), Some Aspects of the Orbital and Ocular Morphometry of the African Giant Rat (*Cricetomys Gambianus* , Waterhouse). *Journal of Veterinary Anatomy*, 4(1): 11–18.

Omobowale, T.O., Otuh, P.I., Adejumobi, O.A., Abiola, J.O., Adebiyi, T., Ogunro, B.N. and Adeogun, A.O. (2017), Electrocardiography and Blood Pressure Measurements in Captive African Lions (Panthera Leo) Immobilized with Xylazine-Ketamine Combination. *Nigerian Journal of Physiological Sciences*, 32(1): 85 – 90.

Peck, T. E., Hill, S. A. and Williams, M. (2008), Pharmacology for Anaesthesia and Intensive Care. Cambridge: Cambridge University Press.

Purves, D., Augustine, G.J., Fitzpatrick, D., Hall, W.C., Lamantia, A.S., McNamara, J.O. and Williams, S.M. (2004), NEUROSCIENCE (3rd Edition, Ed.). Sinauer Associates, Inc.

Rahminiwati, M. and Nishimura, M. (1999), Effects of □9-Tetrahydrocannabinol and Diazepam on Feeding Behavior in Mice. *J. Vet. Med. Sci*., 61(4): 351–355.

Salami, S.O., Onwuama, K.T., Byanet, O., Ibe, S.C. and Ojo, S.A. (2011), Morphological Studies of the Appendicular Skeleton of the African Giant Pouched Rat (*Cricetomys Gambianus*) Part (Ii) Pelvic Limb. *Journal of Veterinary Medicine and Animal Health*, 3(7): 88-93.

Sheets, B.S. (1989), Cranial Anatomy of Jaculus Orientalis (Rodentia, Dipoidea): New Evidence for Close Relationship of Dipodoid and Muroid Rodents.

Weber, G., Stark, G. and Stark, U. (1995), Direct Cardiac Electrophysiologic Effects of Sufentanil and Vecuronium in Isolated Guinea-Pig Hearts. *Acta Anesthesiol Scand*, 39: 1071–1074.

West, G., Heard, D. and Caulkett, N. (2007), Zoo Animal and Wildlife Immobilization and Anaesthesia. Blackwell Publishing, USA.

Zhao, Z., Cao, J., Meng, X. and Li, Y. (2010), Seasonal Variations in Metabolism and Thermoregulation in the Striped Hamster (Cricetulus Barabensis. *J. Therm. Biol*, 35(1): 52–57

Niger. J. Physiol. Sci. 38 (December 2023): 171 – 185
www.njps.physiologicalsociety.com

Niger. J. Physiol. Sci.

Full length Research Article

Low Dose Potassium Bromate Enhances Ischemic Reperfusion-induced Gastric Ulcer Healing in Thyroidectomised Rats

***Salami, A.T.[1], Chukwukaeme, C.W.[1,2], Olagoke, O.C.[3,4], Olaleye, S.B.[1]**

[1]*Gastrointestinal Secretion and Inflammation Research Unit., Department of Physiology, University of Ibadan, Ibadan, Oyo State, Nigeria*

[2]*Department of Human Physiology, Nnamdi Azikiwe University, Awka, Nigeria*

[3]*Department of Physiology, Kampala International University, Uganda.*

[4]*Division of Gastroenterology, Department of Medicine, Beth Israel Deaconess Medical Center, Harvard Medical School, Boston, MA, USA*

Summary: Gastric ulcer healing is impaired in both hypothyroid and hyperthyroid conditions. Thyroid hormones regulate growth, energy metabolism and mitochondrial oxidative metabolism. Xenobiotics have been documented to negatively impact the thyroid gland at high doses but the redox and cellular interactions at low doses during wound healing process remains unclear. Potassium bromate has been documented to be toxic at high doses but there is dearth of information on its activities at a low dose in varied thyroid states which was evaluated in this study. 60 male Wistar rats (g, n=10) were randomised into 2 conditions: Normal, ulcerated untreated, ulcerated treated with 12.5mg/kg p.o KBrO3 and thyroidectomised groups: thyroidectomised ulcerated, thyroidectomised ulcer treated with KBrO3 and thyroidectomised treated with thyroxine (100µg/kg) Total thyroidectomy was used to model hypothyroidism, and ischaemia-reperfusion-induced gastric ulcers were monitored for healing. Daily body weights, Levels of thyroxine, Gastric mucin content, redox and sodium pump activity were examined alongside other markers of hepatic and haematological toxicity by days 3 and 7 post ulceration. Data were analysed using descriptive statistics and ANOVA α 0.05. The bromate-exposed hypothyroid rats showed increased gastric ulcer healing potential with reduced gastric epithelial oedema and inflammation; hepatic steatosis, and periportal inflammation. Haematological variables and markers of hepatic functions were normal. There were reduced levels of gastric and hepatic malondialdehyde levels. Thyroxine and potassium bromate treatment resolved the redox and cellular toxicity possibly via increasing catalase and sulfhydryl levels and increased Na+ K+ pump activity. We conclude that potassium bromate enhanced gastric ulcer healing in hypothyroid state, similar to thyroxine treatment.

Keywords*: Thyroidectomy, potassium bromate, inflammation, Gastric ulcer, renal function, hepatic function.*

**Author for correspondence: adeolathabitha@yahoo.com, Tel: +234-8038267882*

Manuscript received- August 2023; Accepted: November 2023

DOI: https://doi.org/10.54548/njps.v38i2.6

INTRODUCTION

Gastric ulcer healing is a complex process involving various phases such as haemostasis, inflammatory, angiogenesis, proliferative re-epithelization (Fagundes *et al*., 2020, Si *et al*., 2005; Miyake *et al*., 1980) just to mention a few. It is a process in which breached epithelium (gastric ulcer) mostly within the gut, heal formed wound. This involves several other systems like the blood, neuroendocrine (Hampton and Hale, 2011; Waldum *et al*., 2019) and endocrine cells/systems within the body (Sorbye and Svanes 1994, Salami *et al*., 2021). Various hormones have been documented to be implicated / enhanced during gastric ulcer healing few of these include testosterone (Machowska *et al*., 2004), growth (Beckert *et al*., 2004, Akpamu *et al*., 2016), gastrin (Batisa *et al*., 2015) gherline and leptin (Khalefa *et al*., 2010) as well as thyroid (Namulema *et al*., 2018) hormones.

The hypothalamic-pituitary-thyroid (HPT) axis primarily maintains circulating thyroid hormone levels via a negative feedback loop involving thyroid stimulating hormone (TSH; thyrotropin) release from the anterior pituitary gland, which is influenced by the hypothalamic thyrotropin-releasing hormone (TRH) and the thyroid hormones (Brent, 2012). The regulatory activity of the thyroid hormone requires activation of the prohormone thyroxine (T_4) to triiodothyronine (T_3). T_3 then interacts with cellular and tissue-specific thyroid hormone receptors, corepressors and coactivators both in the thyroid hormone signalling pathway and its cross-talk with other signalling pathways (Cheng *et al*., 2010). Thyroid hormones regulate energy metabolism while increasing basal metabolic rate (BMR) and oxidative metabolism (Shahid *et al*., 2022).

Consequently, reactive oxygen species (ROS) are generated as by-products of mitochondrial oxidative metabolism, which is exacerbated in the hyperthyroid state (Das and Chainy, 2001; Venditti and Di Meo, 2006). However, hypothyroidism may not influence existing oxidative stress, but increased levels of thiobarbituric acid reactive substances (TBARS) have been detected in the plasma of hypothyroid subjects, and T3 treatment mitigates the production of redox active species in hypothyroid rats (Das and Chainy, 2001; Gredilla *et al*., 2009; Kebapcilar *et al*., 2007), suggesting that both hypothyroidism and hyperthyroidism can predispose to redox imbalance. Conversely, the thyroid hormone is crucial for would healing in in vitro, in vivo and ex vivo systems as T3 has been linked with improved re-epithelialisation, angiogenesis, and vasodilation via the nitric oxide pathway (Adeniyi *et al*., 2018; Post *et al*., 2021; Salami *et al*., 2016; Zhang *et al*., 2019).

The solubility and stability of bromate in water, alongside the limitations in analytical methods and treatment technologies currently make bromate eradication from drinking water difficult, but a strict benchmark of 10 µl/L in drinking water is enforced across several regions (Bromate CASRN 15541-45-4 | IRIS | US EPA; Deangelo *et al*., 1998). Despite ozone's potential for disinfecting and reducing micropollutants in water, it may oxidize bromide in source water to form toxic bromate residue (Bonacquisti, 2006). Bromate may also be present in water due to other oxidation processes like chlorination, sulphate and ferrate-based oxidation, as well as from industrial effluents and road runoff into water bodies. (Zhang and Jiang, 2022). Bromide in water is oxidized to bromate, and bromate when ingested is converted to bromide invivo (Kurokawa *et al*., 1990; Abuelgasim *et al*., 2008). In individuals who have been accidentally exposed to higher bromate doses, there have been reports of rapid gastrointestinal absorption and irritation, renal failure, and reduced neurological function due to central nervous system depression (Gradus (Ben-Ezer) *et al*., 1984; Matsumoto *et al*., 1980). However, some bromide containing compounds and drugs like Methscopolamine bromide, Penthienate bromide (Ivey, 1975), Salt-bromine-iodine mineral water (Albertini *et al*., 2007), clidinium bromide (Eskander *et al*., 2013), Glycopyrronium bromide (Baume *et al*., 1972) and methantheline bromide (Liebowitz *et al*.,1952) have been used in the treatment of peptic ulcer.

Based on previous information on the displacement effect of halogens (-chloride and iodide) by bromide in vivo (Pavelka, 2004), it has been shown to concentrate majorly in the stomach and thyroid gland which contain halogens also called Schiff bases. Several researches have been documented as regards improved gastro-protective activities of chelated Schiff bases (halogens) especially chlorine (Jaisankar *et al*., 2018). Schiff based derived bromine exerts gastro-protection during ethanol induced gastric ulcer (Saremi *et al*., 2019). However, little information exists on the gastroprotective activities of bromine (a chelated Schiff base derived from potassium bromate) in hypothyroid states despite the ability of Schiff based bromine concentrates in the stomach and thyroid. This research was investigated to evaluate the gastro-protective activities of potassium bromate in hypothyroid states.

MATERIALS AND METHODS

Drugs and reagents: Levothyroxine Sodium was purchased from Mercury Pharma (Generics) Ltd., Croydon, UK and Procaine Penicillin was purchased from Guorui Pharmaceutical Co. Ltd., China. ELISA kits for Thyroid assay (T3, T4, TSH) were purchased from Cal Biotech Incorporation, Spring Valley, California, USA. All reagents were of analytical grade.

Potassium bromate: Animals were administered potassium bromate at a dose of 12.5mg/kg b.w orally. This dose is far lower than the LD50 of potassium bromate which is 215 mg/kg in Wistar rats and 464 mg/kg in ICR mice (Dongmei *et al*., 2015).

Experimental design: 60 male Wistar rats weighing 120 – 140 g were housed at the Central Animal House, Department of Physiology, College of Medicine, University of Ibadan, Nigeria. Approval was given before the commencement of experiment from the University of Ibadan, Animal Care and Use Research Ethics Committee (ACUREC) and assigned a number UI-ACUREC/19/0074. A two-week acclimatization period was ensured at standard experimental conditions, namely: 23 - 25oC room temperature, 55% relative humidity and 12 hr light / 12 hr dark cycle. Animals had free access to water and feed (Ladokun commercial rat diet, Nigeria), and were randomly assigned to groups (n=10), including: 1-Control [Normal], 2-Ulcer [UU], 3-Ulcer + 12.5 mg/kg KBrO3 (Kurokawa *et al*., 1990) [UK], 4-Ulcer + Thyroidectomy [UT], 5-Thyroidectomy + Ulcer + 100µg/kg thyroxine (Salami *et al*., 2016) [TUT], 6-Thyroidectomy + Ulcer + 12.5 mg/kg KBrO3 [TUK]

Thyroidectomy was induced at the start of the experimental period, then animals were observed for 35 days before gastric ulcer induction. Weights were recorded bi-weekly and animals were sacrificed on post-ulcer induction days 3 and 7 for further analysis.

Thyroidectomy and gastric ulcer induction: Animals were placed under anaesthesia (5 mg/kg b.w Xylazine and 60 mg/kg b.w Ketamine) for all surgical interventions. Thyroidectomy entailed removal of the thyroid gland via a midline incision in the neck, while leaving the parathyroid gland and recurrent laryngeal nerves intact (Salami *et al*., 2016). Gastric ulcer was induced by altering ischemia and reperfusion to the stomach (Wada *et al*., 1996, Salami *et al*., 2017). The left gastric artery was clamped for 30 mins and freed to allow reperfusion of the gastric tissue.

Thyroid function, haematology profile, renal and hepatic function test: Whole blood was collected from the rat retro orbital sinus into Ethylene Diamine Tetra acetic Acid (EDTA) bottles for thyroid function test, haematological profiling, plasma protein, plasma electrolyte and plasma lipid content, as well as renal and hepatic function test. Thyroid hormones were assayed via Enzyme-Linked Immuno-Sorbent Assay (ELISA) according to the protocols highlighted by the kit manufacturer (Cal biotech, El Cajon, CA). The reaction was based on a solid phase competitive ELISA with an analytical sensitivity of 1 µg/dl for thyroxine (T4), 0.25 ng/ml for triiodothyronine (T3) and 0.5 µlU/ml for thyroid stimulating hormone (TSH). Briefly,

samples were conjugated alongside the relevant enzyme to polyclonal antibody coated well. Unbound enzyme and enzyme conjugates were washed off before substrate addition. A standard curve was prepared and used to interpolate colour intensity to enzyme concentration.

Haematological profiling was based on established protocols. They included the evaluation of packed cell volume (PCV) (Sorokin, 1973), red blood cell count (RBC) (Rowan, 1983), haemoglobin concentration (Hb) (van Lerberghe *et al*., 1983), total white blood cell (TWBC) (Rowan, 1983), differential white blood cell count (Burstein, 2007) and platelet count (Brecher and Cronkite, 1950). Plasma protein, plasma electrolyte, plasma lipid content, as well as renal and hepatic function test were analysed as earlier described (Elinder *et al*., 1985; Gregor *et al*., 1977).

Macroscopic and microscopic examination of gastric epithelium: Excised rat stomach was cut open across the greater curvature, rinsed in normal saline to rid food debris and spread out to macroscopically examine for ulceration. Degree of ulceration was scored using a 2X magnifying lens as follows: normal stomach – 0; red coloration – 0.5; spot ulcer – 1; haemorrhagic streaks – 1.5; ulcers > 3mm < 5mm – 2; ulcers > 5mm – 3 (Kunchandy *et al*., 1985).
5µm stomach and liver sections were fixed in 10 % formalin and embedded in paraffin. Stained sections (Haematoxylin and Eosin (H&E) stain) were microscopically examined for inflammation, granulation, regeneration and vascular integrity. Pathophysiological changes were shown on a microphotograph.

Stomach and liver tissue preparation: Homogenised stomach and liver tissue was centrifuged (10,000 RPM x 4oC x 10 mins) and decanted supernatant was stored at -20oC for biochemical analysis. Protein concentration of gastric and hepatic tissue was estimated via a slight modification of the method described by (Gornall *et al*., 1949). CU2+ precipitation to Cuprous Oxide was prevented by the addition of Potassium the Biuret reagent.

Evaluation of oxidative stress (MDA, Protein Carbonyl) and antioxidant activity (SOD), Sulfhydryl, mucin, Nitric oxide and Sodium Potassium ATPase activity: The production of malondialdehyde (MDA) during lipid peroxidation of cellular membranes was used as a marker of oxidative stress, as thiobarbituric acid reactive substances (TBARs) react with MDA to form a pink solution whose light absorbance can be read at 532 nm (Varshney and Kale, 1990).

Protein carbonyl assay was based on the reaction of carbonyl groups with 2,4-dinitrophenylhydrazine to form the 2,4-dinitrophenylhydrazone (Levine *et al*., 1990).
Superoxide dismutase (SOD) and catalase activity were monitored as markers of antioxidant activity via the methods described by (Misra and Fridovich, 1972) and (Claiborne, 1985) respectively.

The estimation of nonprotein sulfhydryl content of gastric and hepatic tissues relied on (Ellman, 1959) determination that a mole 2-nitro-5-mercaptobenzoic acid is formed for each mole of sulfhydrl that reduces 5,5'-dithiobis-(2-nitrobenzoic acid) (Sedlak and Lindsay, 1968). The diazotizing agent – sulfanilamide, and the coupling agent – N-(1-naphthyl) ethylenediamine constitute the Griess reagent that reacts with nitrite to form a highly coloured azo dye readable at an absorbance of 548 nm (Ignarro *et al*., 1987). The estimated total nitrite is used as an indirect quantification of nitric oxide (NO) levels (Salami *et al*., 2016). Mucin contains hexose that reacts with orcinol (5-methyl resorcinol) in the presence of sulfuric acid, yielding a spectrophotometrically measurable coloured product (Winzler, 2006). Conversely, the incubation of biological membranes with adenosine triphosphate releases phosphate that is used as a measure of sodium potassium pump activity (Bewaji *et al*., 1985).

Statistical analysis: Data was analysed using two-way ANOVA with Tukey's post hoc test on GraphPad Prism 7 and presented as Mean ± Standard Error of Mean (S.E.M). p-value < 0.05 was considered statistically significant.

RESULTS

Body weight change and thyroid hormone levels: Thyroid hormone levels (TSH, T4, T3) were significantly reduced in thyroidectomised rats throughout the experimental period (Figure 1). There was also a significant reduction in percentage body weight in thyroidectomised (hypothyroid) rats exposed to potassium bromate compared with potassium bromate treated euthyroid rats (Figure 2).

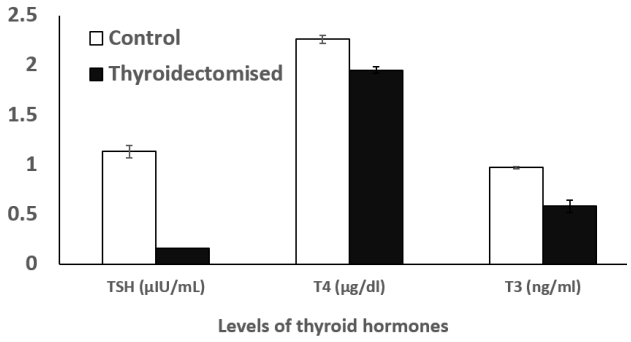

Figure 1
Thyroid hormones levels in control and thyroidectomised rats

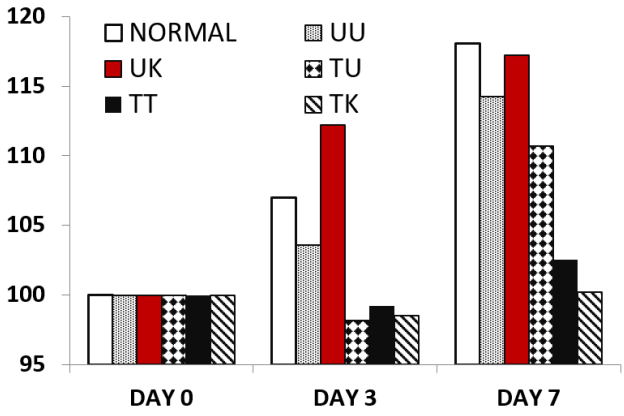

Figure 2:
Effect of potassium bromate on percentage body weight in euthyroid and hypothyroid states. NORMAL - Control; UU-ulcerated untreated; UK - Ulcerated treated with 12.5mg/kg/day of Potassium Bromate; TU - Thyroidectomised ulcerated untreated; TUT - Thyroidectomised ulcerated treated with (100µg/kg/day) of Levothyroxine; TUK - Thyroidectomised ulcerated treated with 12.5mg/kg/day of Potassium Bromate.

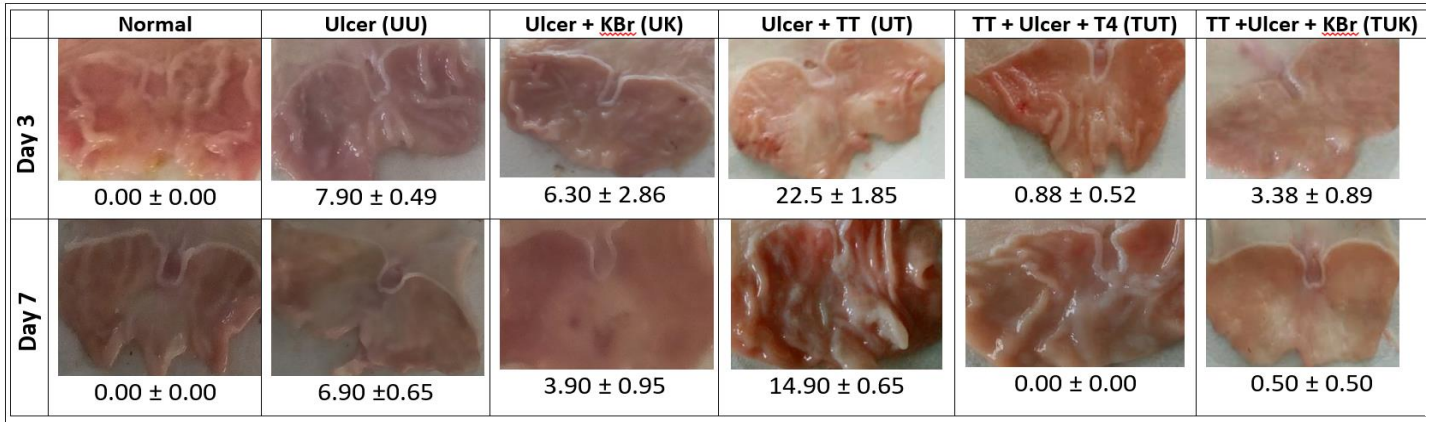

Plate 1:
Gastric tissue and mean ulcer score across groups

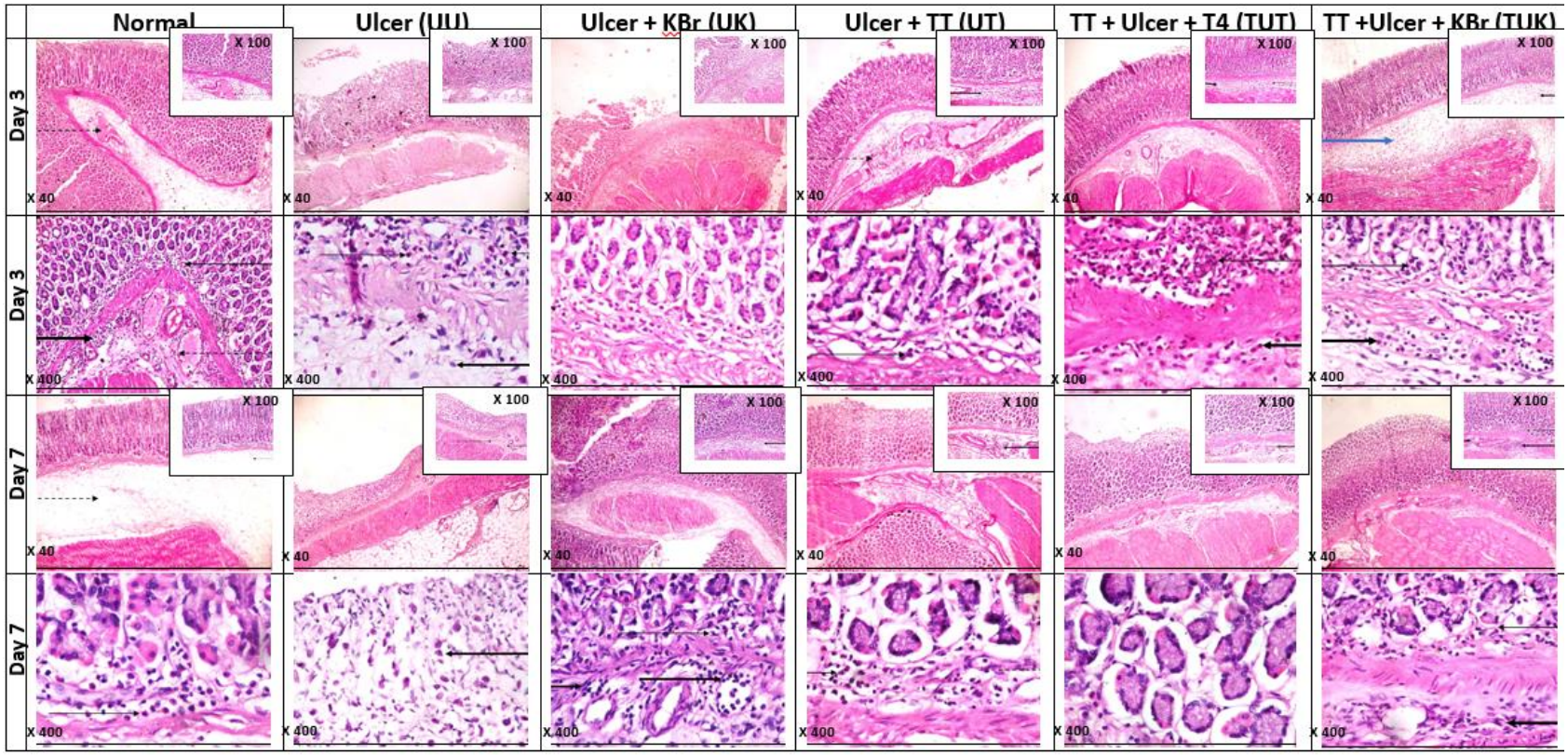

Plate 2:
Gastric tissue photomicrograph at Days 3 and 7, observed using haematoxylin and eosin stains at X 40, X 100 and X 400 magnification.

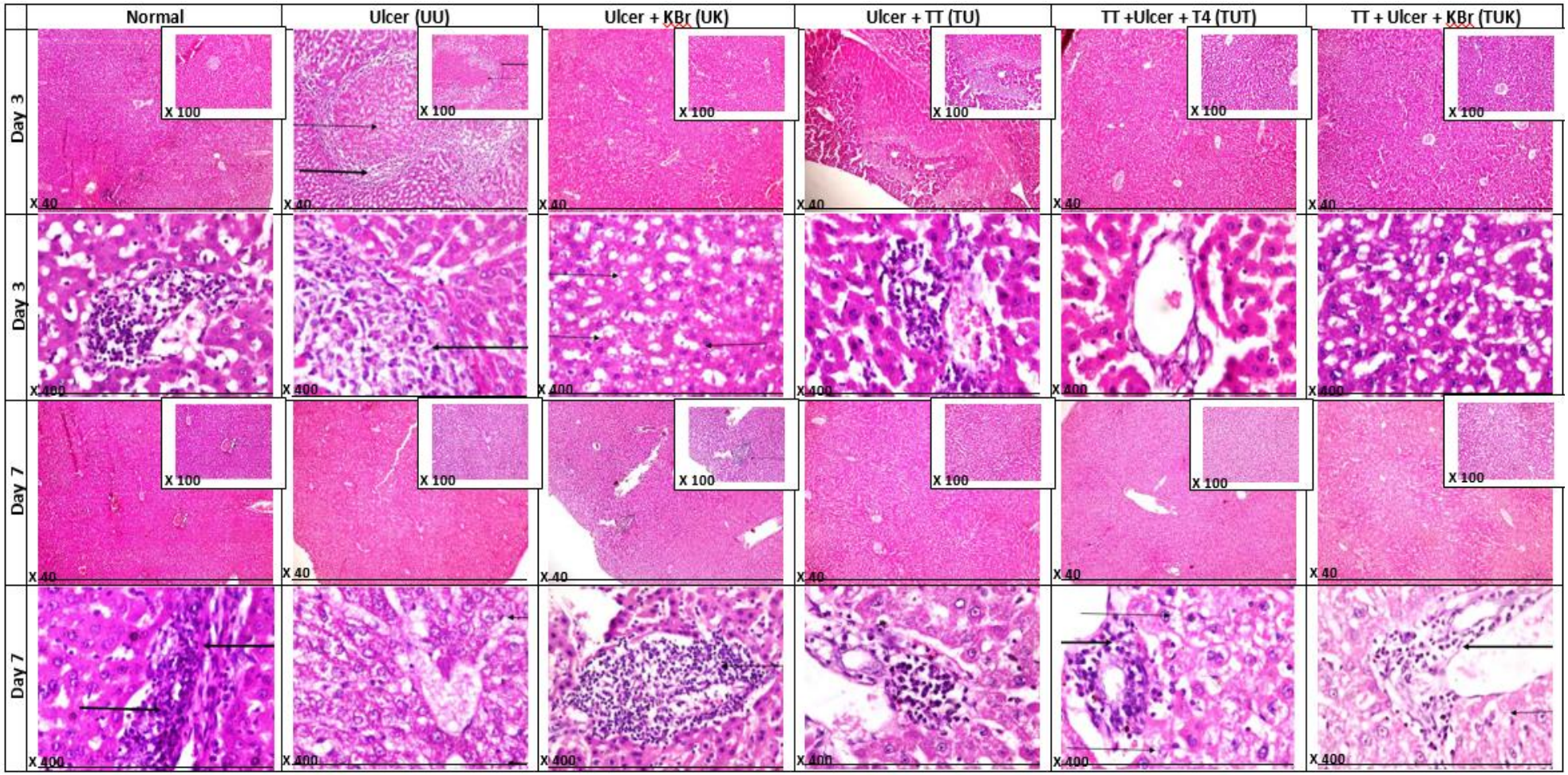

Plate 3:
Hepatic tissue photomicrograph at Days 3 and 7, observed using haematoxylin and eosin stains at X 40, X 100 and X 400 magnification

Gastric and hepatic epithelial integrity: Euthyroid and Hypothyroid state and/or potassium bromate exposure significantly decreased the severity of gastric ulcers formed during ischaemia and reperfusion of the gastric tissue compared with ulcerated untreated in euthyroid and hypothyroid states. Consequently, thyroxine treatment ameliorated the gastric ulcers in hypothyroid state (Plate 1).

Plate 2 shows gastric tissue photomicrographs during bromate exposure across thyroid states. By day 3, a focal area of angiogenesis with vascular congestion (dashed arrow) was observed in the control group. The Ulcer + 12.5 mg/kg KBrO3 and Ulcer + Thyroidectomy + 12.5 mg/kg KBrO3 groups showed mild ulceration of the mucosa with chronic inflammation of the submucosa and muscularis mucosa. The inflammatory cells were still present in the thyroxine treated group, but there was substantial adipocyte and fibroblast infiltration into the submucosa. By day 7, there were mild inflammatory cells into the mucosa and moderate infiltration into the submucosa persisted in the Ulcer + 12.5 mg/kg KBrO3 and Ulcer + Thyroidectomy + 12.5 mg/kg KBrO3 groups there were still mild inflammatory cells infiltration into the mucosa and submucosa in the thyroxine treated group.

Plate 3 shows hepatic tissue photomicrographs during bromate exposure across thyroid states. By day 3, the presence of vascular congestion, thrombosis, and cirrhosis with large regenerative nodules surrounded by thick fibrous connective tissue embedded with chronic inflammatory cells was observed in the ulcerated group. The Ulcer + 12.5 mg/kg KBrO3 and Ulcer + Thyroidectomy + 12.5 mg/kg KBrO3 groups showed focal area of mild steatosis, thrombosis, vascular congestion, periportal inflammation, the replacement of hepatocytes with fibrous connective tissue, and a focal area of well encapsulated cyst with heavy presence of inflammatory cells. However, normal hepatocytes were observed with no significant lesions in the thyroxine treated group. By day 7, the pathologies persisted with focal area of necrosis and mild steatosis in the ulcerated, in the Ulcer + 12.5 mg/kg KBrO3 and Ulcer + Thyroidectomy + 12.5 mg/kg KBrO3 groups there were disseminated mild steatosis, focal area of sinusoidal dilation and congestion, but there was no difference in photomicrographs of the control group and the Ulcer + Thyroidectomy + 100µg/kg thyroxine group.

Biochemical modifications: Figures 3 & 4 show alterations in oxidative stress, antioxidant activity markers, sodium pump activity, and mucin content in gastric tissue during bromate exposure across thyroid states. In all thyroidectomised groups (Ulcer + Thyroidectomy, Ulcer + Thyroidectomy + 100µg/kg thyroxine, Ulcer + Thyroidectomy + 12.5 mg/kg KBrO3), there was significant reduction in the detection of malondialdehyde (MDA), carbonyl and nitric oxide (NO). Conversely, there were increased nitric oxide (NO) levels, sodium pump (Na+ K+-ATPase) activity, and mucin content in potassium bromate and thyroxine treatment.

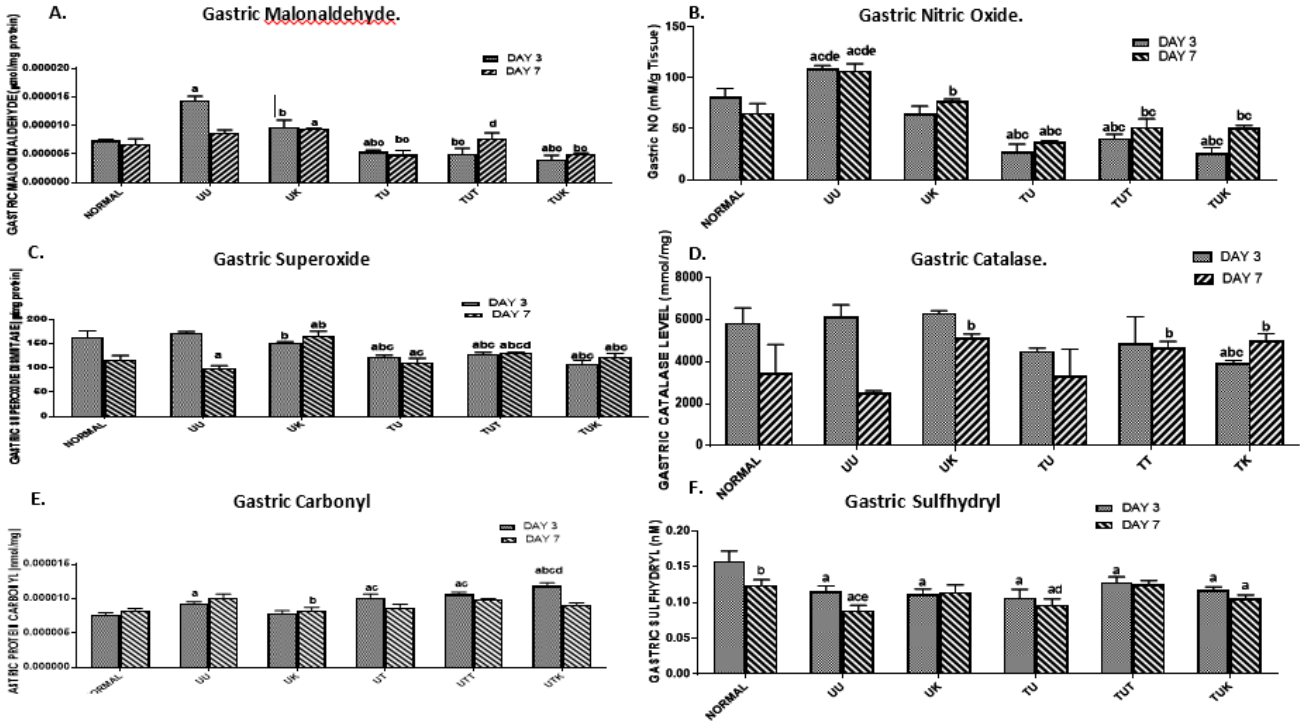

Figure 3:
Effect of potassium bromate on redox changes in the stomach in euthyroid and hypothyroid states. (A) Malonaldehyde levels across groups (B) Nitric oxide levels across groups (C) Superoxide dismutase activity across groups (D) Catalase activity across groups (E) Carbonyl levels across groups (F) Sulfhydrl levels across groups. [a] significant compared with animals in control (NORMAL), [b] significant compared with animals in ulcerated untreated group (UU), [c] significant compared with animals in ulcerated treated with potassium bromate group (UK), [d] significant compared with animals in thyroidectomized ulcerated untreated group (TU), [e] significant compared with animals in thyroidectomized ulcerated treated with levothyroxine group (TUT), [f] significant compared with animals in thyroidectomized ulcerated treated with potassium bromate group (TUK). Values are expressed as Mean ± SEM and are considered statistically significant when p value < 0.05

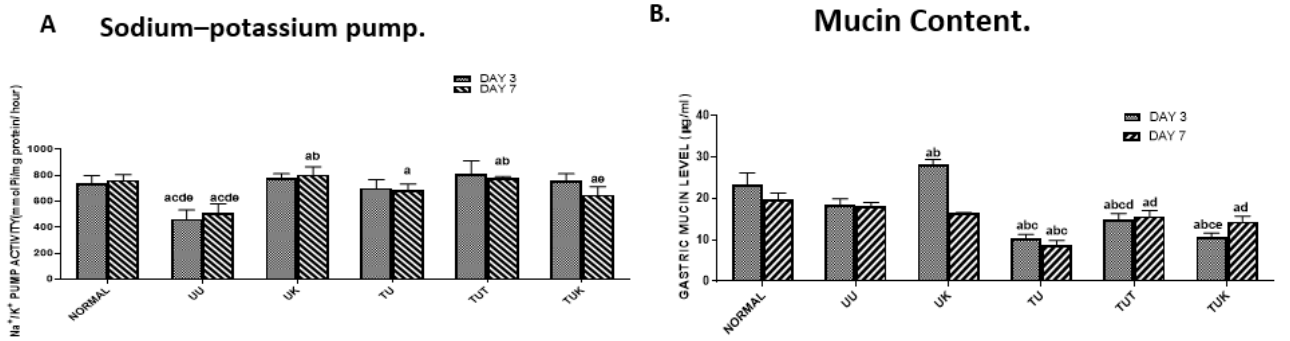

Figure 4:
Effect of potassium bromate on (A) sodium–potassium pump and (B) mucin content in the stomach during euthyroid and hypothyroid states. [a] significant compared with animals in control (NORMAL), [b] significant compared with animals in ulcerated untreated group (UU), [c] significant compared with animals in ulcerated treated with potassium bromate group (UK), [d] significant compared with animals in thyroidectomized ulcerated untreated group (TU), [e] significant compared with animals in thyroidectomized ulcerated treated with levothyroxine group (TUT), [f] significant compared with animals in thyroidectomized ulcerated treated with potassium bromate group (TUK). Values are expressed as Mean ± SEM and are considered statistically significant when p value < 0.05

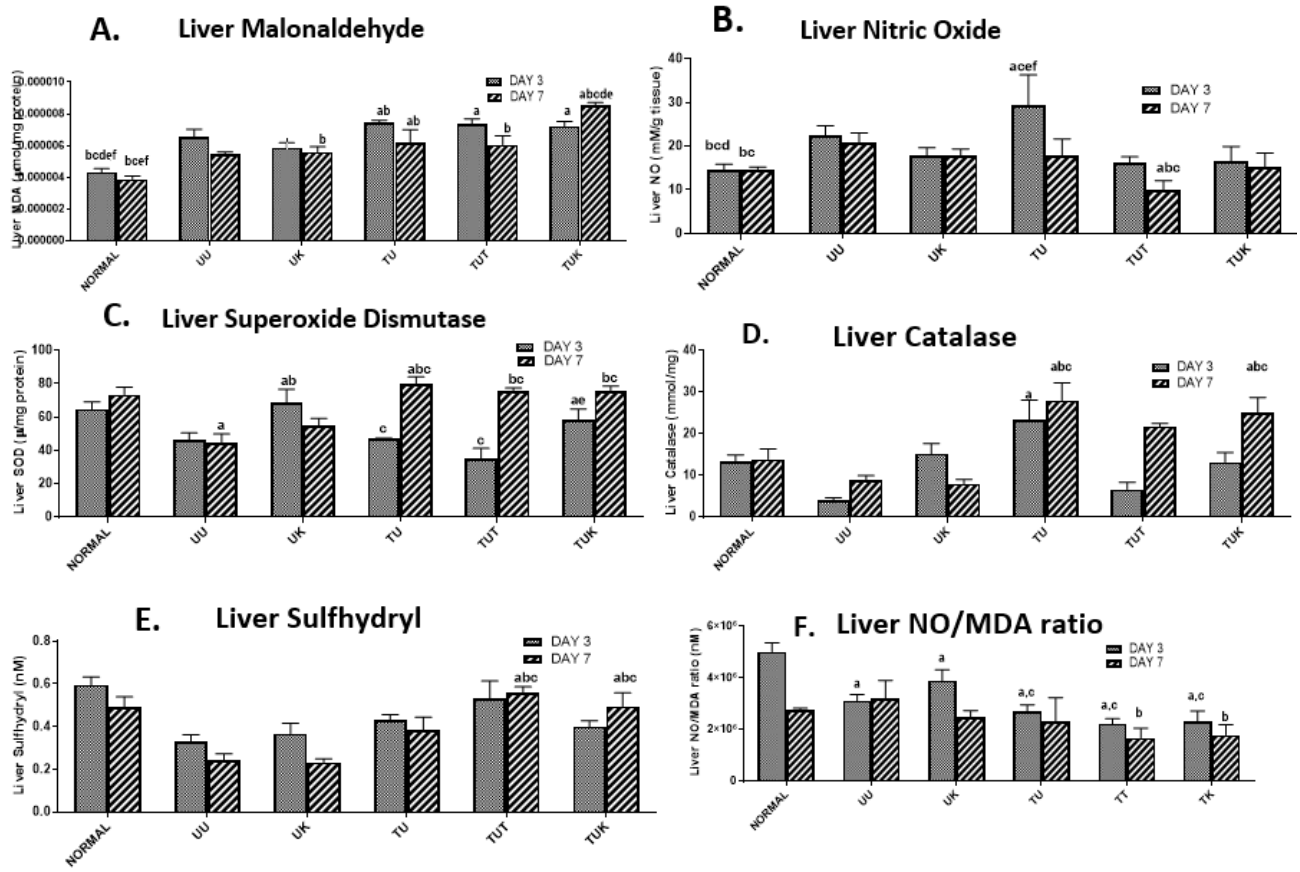

Figure 5:
Effect of potassium bromate on redox changes in the liver in euthyroid and hypothyroid states. (A) Malonaldehyde levels across groups (B) Nitric oxide levels across groups (C) Superoxide dismutase activity across groups (D) Catalase activity across groups (E) Sulfhydrl levels across groups (F) Nitric oxide / Malonaldehyde ratio across groups. a significant compared with animals in control (NORMAL), b significant compared with animals in ulcerated untreated group (UU), c significant compared with animals in ulcerated treated with potassium bromate group (UK), d significant compared with animals in thyroidectomized ulcerated untreated group (TU), e significant compared with animals in thyroidectomized ulcerated treated with levothyroxine group (TUT), f significant compared with animals in thyroidectomized ulcerated treated with potassium bromate group (TUK). Values are expressed as Mean ± SEM and are considered statistically significant when p value < 0.05

Figure 5 shows alterations in biochemical parameters in hepatic tissue during bromate exposure across thyroid states. Bromate exposure in hypothyroid state significantly increased hepatic MDA levels compared with bromate exposure in euthyroid state, and thyroxine treatment restored MDA levels within the control range (by day 7). SOD and catalase levels were also significantly increased in thyroidectomised groups, while thyroxine treatment increased sulfhydryl levels.

Table 1:
Effect of potassium bromate on red cell parameters and platelets (PLT) in euthyroid and hypothyroid states

	PCV (%)		Hb (g/dL)		RBC (x10^{6}L)		RTIC (%)		MCH (pg)		MCV (fL)		MCHC (%)		PLT (mm^3)	
GRP	**Day 3**	**Day 7**	**Day 3**	**Day 7**	**Day 3**	**Day 7**	**Day 3**	**Day 7**	**Day 3**	**Day 7**	**Day 3**	**Day 7**	**Day 3**	**Day 7**	**Day 3**	**Day 7**
NL	41.33 ± 1.33	42.0 ± 0.58	13.73 ± 0.29	14.3 ± 0.17	7.70 ± 0.24	7.24 ± 0.06	2.93 ± 0.03	2.93 ± 0.03	19.74 ± 0.15	19.74 ±0.15	60.38 ± 0.78	58.44± 0.07	32.91± 0.55	33.32± 0.37	142667± 1763.83	174000± 6429.10
UU	45.33± 0.33[a]	39± 1.00	14.7± 0.15	12.63± 0.19[a]	7.4 1± 0.04	7.16 ± 0.21	3.3 ± 0.06[a]	2.7 ± 0.00	19.55 ± 0.00	19.86 ±0.05	61.16 ±0.73	60.86 ± 0.13	32.37 ± 0.07	33.08 ± 0.33	110667 ± 3929.94[a]	244000 ± 8504.9[a]
UK	45.33± 0.33[a]	43.33± 0.33[b]	14.57± 0.13	14.53± 0.09[b]	7.34± 0.05	7.35± 0.02	3.17± 0.09	3.1± 0.06[b]	20.12± 0.09	19.78± 0.07	61.76 ± 0.31	60.29± 1.34	32.50± 0.16	33.5± 0.36	119333.33± 5696	244666.67± 6359.59[a]
TU	44 ± 0.58	39.33± 0.33[c]	14.37± 0.58	13.03± 0.28[c]	7.32± 0.03	6.66± 0.28	3.03± 0.15	2.13± 0.07[abc]	20.39± 0.26[b]	19.61± 0.38	61.05 ± 0.23	60.17± 0.96	32.92± 0.20	32.59± 0.13	162666.67± 7423.69[bc]	163333.33± 15025.90[bc]
TUT	42.67± 0.88	41.33± 0.33	13.93± 0.35	13.50± 0.25	7.16± 0.25	7.24± 0.25	3.20± 0.12	2.03 ± 0.03[abc]	19.47± 0.29[d]	20.12± 0.14	59.63 ± 0.98	61.09± 0.28	32.65± 0.16	32.47± 0.17	126000± 5131.6[d]	117000± 3214.55[abcd]
TUK	40.33± 0.33[bcd]	42.33± 1.20[b]	13.36± 0.12[b]	13.57± 0.47	6.55± 0.04[abcd]	6.89 ±0.22	3.20± 0.06	2.37 ± 0.03[abce]	20.39± 0.22[be]	19.69± 0.07	61.55 ± 0.38	58.94± 0.48	33.42± 0.29	33.23± 0.25	143000± 6806.86[b]	104666.67± 1763.83[abcd]

[a] *significant compared with animals in control (NORMAL),*
[b] *significant compared with animals in ulcerated untreated group (UU),*
[c] *significant compared with animals in ulcerated treated with potassium bromate group (UK),*
[d] *significant compared with animals in thyroidectomized ulcerated untreated group (TU),* [e] *significant compared with animals in thyroidectomized ulcerated treated with levothyroxine group (TUT),* [f] *significant compared with animals in thyroidectomized ulcerated treated with potassium bromate group (TUK). Values are expressed as Mean ± SEM and are considered statistically significant when p value < 0.05.*

Table 2
Effect of potassium bromate on white blood cells and differential count in euthyroid and hypothyroid states.

	WBC (× 105 µL)		EOS (%)		LYM (%)		NEUT (%)		MONO (%)		P-L RATIO		N-L RATIO		M-L RATIO	
GRP	**Day 3**	**Day 7**	**Day 3**	**Day 7**	**Day 3**	**Day 7**	**Day 3**	**Day 7**	**Day 3**	**Day 7**	**Day 3**	**Day 7**	**Day 3**	**Day 7**	**Day 3**	**Day 7**
NL	3666.67 ± 88.19	5450 ± 132.29	2.00 ± 0.58	2.00 ±0.58	71.0 ± 0.58	70.67 ± 0.67	25± 1	25.67± 0.58	2± 0	1± 0	1983.28± 56.22	2443.50± 127.45	0.35± 0.01	0.36 ± 0	0.03± 0.01	0.01 ±0
UU	5316.67± 187.82a	5733.33± 317.98	1.67± 0.88	2± 0.58	74± 0.58	64.67± 0.88a	22.0 ± 1.73	25.67± 3.06	2 ± 0.58	2± 0.58	1531.74± 70.30	3626.61± 32.78**a**	0.33± 0.03	0.41± 0.04	0.02± 0.00	0.04± 0.00**a**
UK	5216± 148.13a	6916.67± 268.22a	1.33± 0.33	2± 0.58	73± 0.58	74.33± 0.33ab	25 ±1	21± 2ab	1.67± 0.33	2± 0.00	2153.13± 203.39b	3152.68± 113.09**a**	0.33± 0.01	0.30± 0.01 **b**	0.02± 0.00	0.03± 0.00
TU	2983.33± 496.94bc	4966.67± 272.85c	1.67± 0.33	2.67± 0.33	72± 0	68.67± 1.20bc	24.67 ± 2.08	27.0 ± 1.73c	1.67± 0.67	1.67± 0.33	2305.01± 126.94b	2382.31± 238.16**bc**	0.34± 0.02	0.39± 0.02 **c**	0.02± 0.00	0.02± 0.00
TUT	4766.67± 683.943d	4933.33± 404.489c	2 ±0.58	1 ±0.00	71 ± 0.58	74 ± 0.58bd	26 ± 0.00	23 ± 0.00	1.67 ± 0.33	1.67± 0.33	1835.93± 68.29	1617.07± 22.77**abcd**	0.37± 0	0.31± 0**bd**	0.02± 0.00	0.03± 0.00
TUK	4216.67± 145.29	2866.67± 233.33abcde	1.00± 0.00	2.00± 0.00	70.6± 0.88	74.67± 1.45abd	26.33± 0.58b	23 ± 2.00	1.33 ± 0.33	2 ±0.58	2215.5± 145.18b	1429.82± 53.55**abcd**	0.37± 0.01	0.35± 0.02	0.02± 0.00	0.02± 0.01**b**

[a] *significant compared with animals in control (NORMAL),*
[b] *significant compared with animals in ulcerated untreated group (UU),*
[c] *significant compared with animals in ulcerated treated with potassium bromate group (UK),*
[d] *significant compared with animals in thyroidectomized ulcerated untreated group (TU),* [e] *significant compared with animals in thyroidectomized ulcerated treated with levothyroxine group (TUT),* [f] *significant compared with animals in thyroidectomized ulcerated treated with potassium bromate group (TUK). Values are expressed as Mean ± SEM and are considered statistically significant when p value < 0.05.*

Table 3
Erythrocyte sedimentation rate and plasma proteins, electrolytes and lipid profile across thyroidectomised groups

	Esr (Mm/Hr)		Total Protein (G/Dl)		Albumin (G/Dl)		Globulin (G/Dl)		Albumin-Globulin Ratio		Sodium Ion (Mmol/L)		Potassium Ion (Mmol/L)		Chloride Ion (Mmol/L)		Cholesterol (Mg/Dl)		Triglyceride (Mg/Dl)		Hdl (Mg/Dl)		Ldl (Mg/Dl)	
GRP	**Day 3**	**Day 7**	**Day 3**	**Day 7**	**Day 3**	**Day 7**	**Day 3**	**Day 7**	**Day 3**	**Day 7**	**Day 3**	**Day 7**	**Day 3**	**Day 7**	**Day 3**	**Day 7**	**Day 3**	**Day 7**	**Day 3**	**Day 7**	**Day 3**	**Day 7**	**Day 3**	**Day 7**
TU	1.3 ±.06 **a**	0.87 ± 0.07	7.40 ± 0.10	6.63 ± 0.32	2.67 ± 0.03	2.90 ± 0.15 **b**	4.73 ± 0.09	3.73 ± 0.32	0.57 ± 0.03	0.73 ± 0.09 **a**	138 ± 0.58	139 ± 2.08	4.73 ± 0.03	4.67 ± 0.27 **c**	104.33 ± 2.19	108.33 ± 2.73	71.33 ± 1.33	64.33 ± 2.33	43.67 ± 1.76	46.33 ± 0.88	40.67 ± 1.20	33 ± 1.53	21.40 ± 0.31	22.07 ± 1.38
TUT	1.2 ± 0.12 **a**	1 ± 0	7.47 ± 0.20	6.77 ± 0.12	2.93 ± 0.09	2.87± 0.03 **bc**	4.87 ± 0.09	3.73 ± 0.03	0.53 ± 0.03	0.70 ± 7.90E-17	141 ± 1	136.3 ± 0.33 **c**	4.83 ± 0.09	4.67 ± 0.03 **c**	106 ± 3.06	103 ± 0.58 **c**	73 ± 1.73	61.33 ± 0.88	47.33 ± 2.33	42.33 ± 0.88 **b**	43 ± 1.00	31 ± 0.58	21.87 ± 0.74	22.07 ± 0.37
TUK	1.2 ± 0.06 **a**	1.17± 0.09 **abc**	7.73 ± 0.20	6.83 ± 0.13	2.73 ± 0.07	2.90 ± 0.06 **b**	4.80 ± 0.10	3.83 ± 0.03	0.6 ± 0.00	0.70 ± 7.90E-17	138.6± 1.20	138 ± 1.15 **c**	4.50 ± 0.10	4.77 ± 0.09 **c**	108 ± 3.06	110.33 ± 5.24 **a**	70 ± 2.89	63.33 ± 1.20	47 ± 2.52	42.67 ± 1.20	41.33 ± 0.88	35.67 ± 0.33 **be**	22.13 ± 0.64	20.47 ± 0.24

[a] significant compared with animals in control (NORMAL), [b] significant compared with animals in ulcerated untreated group (UU), [c] significant compared with animals in ulcerated treated with potassium bromate group (UK), [d] significant compared with animals in thyroidectomized ulcerated untreated group (TU), [e] significant compared with animals in thyroidectomized ulcerated treated with levothyroxine group (TUT), [f] significant compared with animals in thyroidectomized ulcerated treated with potassium bromate group (TUK). Values are expressed as Mean ± SEM and are considered statistically significant when p value < 0.05.

Table 4:
Effect of potassium bromate on organ weight, renal and hepatic function in euthyroid and hypothyroid states

	Stomach weight		Liver weight		BUN (mg/dL)		CR (mg/dL)		AST (µL)		ALT (µL)		ALP (µL)		TBIL (mg/dL)	
GRP	**Day 3**	**Day 7**	**DAY 3**	**Day 7**	**Day 3**	**Day 7**	**Day 3**	**Day 7**	**Day 3**	**Day 7**	**Day 3**	**Day 7**	**Day 3**	**Day 7**	**Day 3**	**Day 7**
NL	0.90 ± 0.03	1.09 ± 0.06	4.92 ± 0.32	5.43 ± 0.18	16.40 ± 0.21	16.40 ± 0.21	0.70 ± 7.9E-17	0.70 ± 7.9E-17	40.67± 0.67	40.33± 0.33	31± 0.58	29.33 ± 0.33	103 ± 1.00	80.33 ± 1.45	0.30 ± 0	0.10 ± 9.8E-18
UU	0.98 ± 0.00	0.97 ± 0.05	5.04 ± 0.13	6.76 ± 0.18 **acdef**	16.70 ± 0.06	15.43 ± 0.15**a**	0.80 ± 7.9E-17	0.70 ± 7.9E-17	43 ± 0	38.33 ± 0.33	31.67± 0.33	26 ± 0.58	102.67 ± 1.45	88.67 ± 1.20	0.33 ± 0.03	0.10 ± 9.8E-18
UK	0.74 ± 0.00	1.08 ± 0.03	4.98 ± 0.12	4.89 ± 0.09	16.47 ± 0.03	16.57 ± 0.15**b**	0.80 ± 7.9E-17	0.80 ± 7.9E-17	42.67± 0.33	41.67± 0.33	30 ± 0	27 ± 1.15	96.67 ± 2.67	104.67 ± 0.88 **ab**	0.20 ± 2E-17**ab**	0.20 ± 2E-17 **ab**
TU	1.26 ± 0.09 **c**	1.67 ± 0.22 **abcef**	4.23 ± 0.06	4.81 ± 0.46	16.77 ± 0.15	17.67 ± 0.18	0.60 ± 0**bc**	0.70 ± 0.06	42.33± 0.88	37.33± 1.33 **c**	31 ± 0.58	27 ± 1.15	112 ± 2.08**c**	94.33 ± 5.55 **ac**	0.30 ± 0 **c**	0.23 ± 0.03**ab**
TUT	1.12 ± 0.06 **c**	1.11 ± 0.04	4.43 ± 0.11	4.89 ± 0.19	17.97 ± 0.15	17.47 ± 0.12	0.70 ± 7.9E-17	0.67 ± 0.03**c**	43.67± 0.88	37 ± 0.58 **c**	32 ± 1.15	27 ± 1.15	115 ± 1.15**abc**	111 ± 1.53**abd**	0.40 ± 3.9E-17	0.20 ± 2E-17**ab**
TUK	1.23 ± 0.08 **c**	1.09 ± 0.09	4.57 ± 0.19	5.21 ± 0.58	18.13 ± 0.23	17.43 ± 0.12	0.67 ± 0.03	0.67 ± 0.03**c**	44.33± 1.33	37 ± 1.00**c**	31.33± 0.88	29.67 ± 0.88	120.33 ± 0.88**abc**	106.67 ± 1.76 **abd**	0.30 ± 0	0.27 ± 0.03**ab**

: [a] significant compared with animals in control (NORMAL), [b] significant compared with animals in ulcerated untreated group (UU), [c] significant compared with animals in ulcerated treated with potassium bromate group (UK), [d] significant compared with animals in thyroidectomized ulcerated untreated group (TU), [e] significant compared with animals in thyroidectomized ulcerated treated with levothyroxine group (TUT), [f] significant compared with animals in thyroidectomized ulcerated treated with potassium bromate group (TUK). Values are expressed as Mean ± SEM and are considered statistically significant when p value < 0.05.

Haematological profile, plasma content, renal and hepatic function.: Table 1 shows alterations in haematological parameters during bromate exposure across thyroid states. Packed cell volume (PCV) and red blood cell (RBC) count were reduced, but haemoglobin content in red blood cell relative to the cells volume (Mean corpuscular haemoglobin concentration (MCHC)) was significantly increased in bromate exposed hypothyroid rats by day 3. The values tended towards normal by day 7.

Table 2 depicts white blood cell (WBC) and differential count during bromate exposure across thyroid states, while Table 3 shows no alterations in plasma protein, electrolyte and lipid content during bromate exposure across thyroid states. There was significant increase in plasma chloride but significant decrease in plasma potassium and cholesterol levels in bromate exposed hypothyroid rats by day 3. The values tended towards normal by day 7. Table 4 shows no alterations in renal and hepatic function during bromate exposure across thyroid states.

DISCUSSION

Loss of body weight is an indicator towards pathology or efficacy of a treatment regime during a disease state (Dietze *et al*., 2016). Hypothyroidism has been linked with weight gain in humans and rodents (Carlwe *et al*., 2013; Dale *et al*., 2001). High doses of potassium bromate exposure has been reported to cause a decrease in body weight (Kurokawa *et al*., 1990; Ajarem *et al*., 2016), probably indicative of toxicity while Abuelgasim *et al*., 2008, Dongmei *et al*., 2015; Salami *et al*., 2020) noted no changes in body weight between potassium bromate treated animals and control in euthyroid state. In this study, potassium bromate (at a low dose) increased body weight in euthyroid animals but not in hypothyroid animals. These variations in body weight (increase or decrease) might be due to dosage exposure, a high dose of potassium bromate is indicative of toxicity hence loss of body weight while low dose exposure might be beneficial to the system.

Hypothyroidism has been linked with a prolonged proliferative phase of wound healing (Cannon, 1994; Thá Nassif *et al*., 2009). In this study thyroidectomised animals treated with thyroxine had the highest percentage inhibition ulcer score which is similar to observations of other studies (Oluwole and Saka, 2007; Adeniyi *et al*., 2014; Salami *et al*., 2016). Potassium bromate greatly reduced the mean ulcer score in thyroidectomised ulcerated rats. Bromide ion (from reduction of bromate in vivo) has been shown to replace iodine in the thyroid forming brominated analogues of thyroid hormone (Velicky *et al*., 1998; Pavelka, 2004) mimicking the functions of iodine more (Vobecky *et al*., 1996). However, in a recent study, cadexomer iodine has been documented to reduce ulcer size and facilitate complete healing of wounds (Raju *et al*., 2019, Gupta *et al*., 2022). It may be that in the absence of thyroid hormone synthesis in the thyroid gland, bromide ion mimicks the action of iodine and release of thyroid stimulating hormone (Allain and MacGregor, 1993) thus bringing about ulcer healing. Thus it is safe to conclude that a normal level of thyroxine is required for optimal healing of gastric ulcer.

Hypothyroidism predisposes to a drastic reduction in the pace of metabolic processes, leading to metabolic anomalies like anaemia. In fact, about half of hypothyroid patients present with at least one type of anaemia (Bashir *et al*., 2012; Shah *et al*., 1999). In the same vein, potassium bromate has been shown to elicit in vitro erythrocytic lysis and a diagnosis of anaemia in humans (Ahmad *et al*., 2014; SONG *et al*., 2001, Omer *et al*., 2008; Stuti and D'Souza, 2013; Altoom *et al*., 2017). However, in this study it was observed that potassium bromate prevented anemia by maintaining RBC, PCV, Hb and reticulocyte values similar to that of normal animals in non-thyroidectomised animals. This is similar to the findings of Kurokawa *et al*., (1990) and Achukwu *et al*., (2009). However in thyroidectomised animals, potassium bromate did not prevent anemia as RBC, PCV and Hb values were decreased, which leads us to infer that the decrease was as a result of ulceration rather than treatment of bromate.

Though previous studies noted a decrease in white blood cells (WBC) when potassium bromate was administered (Achukwu *et al*., 2009; Altoom *et al*., 2017), while the bromate treated rats had decreased WBC count. Potassium bromate increased lymphocyte count in both thyroidectomised and non-thyroidectomised animals. Inflammatory biomarkers, such as the neutrophil-to-lymphocyte ratio (NLR), platelet-to- lymphocyte ratio (PLR), or Monocyte-to-lymphocyte ratio (MLR), have been used as markers in the assessment of disease activity in gastric ulcer (Adeniyi *et al*., 2018) and inflammatory bowel disease (IBD) (Erademir *et al*., 2016). Nitric Oxide – Malondialdehyde ratio (NO/MDA) may be considered as an integrated marker of degree of inflammation and lipid peroxidation (Caimi *et al*., 2014) in tissues. NO/MDA is low when there is more inflammation compared to vasodilation. NO/MDA is high when there is more vasodilation than inflammation. NO has been shown to decrease mitochondrial MDA content (He *et al*., 2019). Potassium bromate treated animals had NO/MDA ratios similar to that of normal animals even in the presence or absence of the thyroid gland. This suggests that potassium bromate at the administered dose modulated inflammatory response in ulcerated animals both in the presence or absence of the thyroid gland.

Erythrocyte sedimentation rate (ESR), plasma viscosity and fibrinogen are less predictive markers of inflammation in diseased conditions like gastric ulceration (Salami *et al*., 2017). Potassium bromate increased ESR in non-thyroidectomised animals but it was decreased in thyroidectomised animals. The increase in ESR of animals with intact thyroid may have been as a result of inflammation resulting from ulceration (Bridgen, 1999). The decrease noted in thyroidectomised animals may have been due to plasma protein abnormalities (Bridgen, 1999) since decrease in thyroid hormones affects plasma protein synthesis (Graninger *et al*., 1986). Fibrinogen, an inflammatory marker and a major coagulation protein in the blood, has been found to be increased in patients with diabetic foot ulcer (Li *et al*., 2016). Fibrinogen levels were normal in potassium bromate treated rats. Lower serum albumin levels has been shown to delay peptic ulcer healing and cause peptic ulcer bleeding (PUB) and other complications (Hu *et al*., 2017; Cheng *et al*., 2018). Potassium bromate increased albumin levels in animals with intact thyroid gland which contradicts reports of lowered albumin and serum protein levels in potassium bromate treated animals (Omer *et al*., 2008; Stuti and D'Souza,

2013); while a general decrease was observed in all thyroidectomized ulcerated rats at day 3 which reverted back to normal by day 7.

In this study, animals with intact thyroid gland treated with potassium bromate had high sodium, potassium and chloride ions. The thyroidectomised potassium bromate treated ulcerated animals with had normal electrolyte levels. Kurokawa *et al*., (1990) reported increased sodium levels and decreased potassium levels, while Abuelgasim *et al*., (2008) reported the inverse in potassium bromate treated animals. The increased chloride may have been as a result of bromide ion displacing body chloride (Pavelka, 2004).

Changes in their activities of Aspartate aminotransferase (AST), Alanine transaminase (ALT), Alkaline phosphatase (ALP) are indicative of liver damage by toxicants or in disease conditions (Oseni *et al*., 2018). The AST and ALT levels were normal in potassium bromate treated animals with or without the thyroid gland indicating absence of liver toxicity. This contradicts several studies done on potassium bromate which reported liver toxicity and increased AST and ALT in animals treated with potassium bromate (Omer *et al*., 2008; Oloyede and Sunmonu, 2009; Oseni *et al*., 2015; Oseni *et al*., 2018). This may be because the dose of potassium bromate administered in this study is much lower than that used in the other studies which ranged from 30 to 200 mg/kg. Increased ALP has been associated with growth spurts (Shipman, 2013) which was evident in these groups. Blood urea nitrogen and creatinine levels which are used to evaluate kidney function were normal for both thyroidectomised and normal ulcerated animals treated with potassium bromate. This means that potassium bromate had no adverse effect on kidney function and is in line with DeAngelo *et al*., (1998) and Abuelgasim *et al*., (2008).

Increased lipid peroxidation has been reported to contribute to mucosal inflammation (Biswas *et al*., 2003; Omayone *et al*., 2016). Malondialdehyde (MDA) level has been shown to be elevated in potassium bromate treated animals (Josiah *et al*., 2011; Josiah *et al*., 2012; Oseni *et al*., 2015; Ahmad *et al*., 2015; Oseni *et al*., 2018). This study observed that non-thyroidectomised rats treated with potassium bromate had lower gastric MDA levels (unlike in the ulcer untreated group), while thyroidectomised rats had minimal peroxidation. However, liver of potassium bromate treated rats showed elevated MDA levels by day 7.

Increased protein carbonyl levels have been found in the intestine of animals treated with potassium bromate (Ahmad *et al*., 2015). However, it had no such effect on thyroidectomised animals as elevated carbonyl levels were observed in all the treatment groups by day 7. The reason for this may be the oxidative stress known to be associated with thyroidectomy and ulceration (Salami *et al*., 2016).

Endogenous antioxidants (Superoxide dismutase (SOD), catalase and Sulfhydryl) have been reported to be decreased in gastric ulcer, as a result of increased lipid peroxidation (Omayone *et al*., 2016). However, potassium bromate protected against tissue damage from oxidative stress in both normal and thyroidectomised animals in this study contrary to earlier reports (Oseni *et al*., 2015; Silva *et al*., 2015; Costa *et al*., 2019).

In contrast, the thyroid hormones play crucial roles in the wound healing process, including enhancing collagen formation, mitochondrial oxidative phosphorylation, inducing protein synthesis, and diminishing fibroblast function (Kivirikko *et al*., 1967; Natori *et al*., 1999; Sterling, 2010). This explains the increased gastric mucin content that we found in the thyroxine treated group, as adequate mucin production is important for the protection of gastric epithelial layers from perturbations like gastric acid secretion (Adeniyi *et al*., 2018; Bansil and Turner, 2006; Salami *et al*., 2021). This study observed an increased mucin content in ulcerated animals treated with potassium bromate both in the thyroidectomised and non-thyroidectomised states.

Nitric oxide production under normal physiological conditions mediates many aspects of inflammation but in abnormal conditions, it is regarded as pro-inflammatory mediator that induces inflammation due to its excess production (Odukanmi *et al*., 2017). This may explain why in the non-thyroidectomised animals, the ulcer untreated group had the highest nitric oxide level at both days 3 and 7, probably due to ulcer formation. Potassium bromate did not alter nitric oxide levels in both non-thyroidectomised and thyroidectomised animals.

The sodium potassium pump helps in maintaining resting membrane potential and controlling the intracellular ion concentration inside the cell, which are important for numerous of the cell's enzymatic functions (Sherwood, 2012; Clausen *et al*., 2017). The thyroid hormone influences metabolic energy generation via enhanced mitochondrial function for Adenosine triphosphate (ATP) production (Harper and Seifert, 2008). Consequently, similar patterns of recovery from toxin-related injury have been recorded in thyroxine-treated rats and their ATP-MgCl2 treated counterparts (Siegel *et al*., 1984). Given that tissue repair is energy-intensive (Schulte-Wissermann *et al*., 1977), we investigated how different thyroid states affect gastric ulcer healing during low oral dose bromate exposure. This study observed that potassium bromate increased gastric sodium potassium pump activity in non-thryoidectomised ulcerated rats while it maintained pump activity within normal range in thyroidectomised animals.

Previous study Salami *et al*., 2020, documented that Protocatechuic acid ameliorated gastric ulceration during potassium bromate exposure at a low dose however, similar activities of increased antioxidant status, gastric sodium potassium pump activities and angiogenesis in the bromate treated groups were also observed in this study. This observation needs critical evaluation as both studies reveals angiogenesis, increased gastric sodium potassium pump activities and antioxidant activities at the dose of potassium bromate administered.

In conclusion, this study showed that in the absence or decrease of the thyroid hormones, low-dose potassium bromate mimicks the effect of thyroxine thereby promoting gastric ulcer healing. Potassium bromate at low dose prevented anemia associated with ulcer contrary to reports of anemia after treatment with high doses of potassium bromate. From the results of our study, low dose potassium bromate was found to be gastroprotective in both non-thyroidectomised and thyroidectomised states and had no toxic effect on the liver or blood, unlike reports of toxicity at high doses.

REFERENCES

Abuelgasim, A.I., Omer, R., and Elmahdi, B. (2008): Serrobiochemical Effects of Potassium Bromate on Wistar

Albino Rats. *American Journal of Food Technology* 3(5): 303-309

Achukwu, P.U., Ufelle, S.A., Ukaejiofo, E.O., Ejezie, F.E., Nwachukwu, D.N., Nwagha, U.I, Nworie, W.C, and Anyaehie, U.S.B. (2009): The Effect of Potassium Bromate on some Haematological Parameters of Wistar Rats. *Nigerian Journal of Physiological Sciences* 24 (1): 59 – 61

Adeniyi, O.S., Emikpe, B.O., and Olaleye, S.B. (2014): Gastric Mucosa Re-epithelisation, Oxidative Stress and Apoptosis during Healing of Acetic Acid-Induced Ulcerations in Thyroxine Treatment and Thyroidectomy on Rats. *J. Afr. Ass. Physiol. Sci.* 2 (1): 57-67.

Adeniyi, O.S., Emikpe, B.O., and Olaleye, S.B. (2018). Accelerated gastric ulcer healing in thyroxine-treated rats: roles of gastric acid, mucus, and inflammatory response. https://doi.org/10.1139/cjpp-2017-0399 96, 597–602. https://doi.org/10.1139/CJPP-2017-0399

Ahmad, M.K., Amani, S., and Mahmood, R. (2014). Potassium bromate causes cell lysis and induces oxidative stress in human erythrocytes. *Environ Toxicol* 29, 138–145. https://doi.org/10.1002/TOX.20780

Ahmad, M.K., Khan, A.A., Ali, S.N., and Mahmood, R. (2015): Chemoprotective Effect of Taurine on Potassium Bromate-Induced DNA Damage, DNA Protein Cross-Linking and Oxidative Stress in Rat Intestine. *PLoS ONE* 10(3): e0119137. doi:10.1371/journal.pone.0119137

Ajarem, J., Altoom, N.G., Allam, A.A, Maodaa, S.N, Abdel-Maksoud, M.A., and Chow, B.K.C. (2016): Oral administration of potassium bromate induces neurobehavioral changes, alters cerebral neurotransmitters level and impairs brain tissue of swiss mice. *Behav Brain Funct* 12:14. DOI 10.1186/s12993-016-0098-8

Akpamu, U., Otamere, H.O., Ernest-Nwoke, I. O., Ekhator, C. N., Osifo, U.C. (2016). The protective effect of testosterone on Indomethacin induced gastric ulcer in female Sprague Dawley rats. *Advances in Endocrinology*, 2016, Article ID 3452760, 5 pages. https://doi.org/10.1155/2016/3452760

Allain, T. J., and McGregor, A. M. (1993). Thyroid hormones and bone. *Journal of Endocrinology*, 139(1), 9-18.

Al-Mareed, A.A., Farah, M.A., Al-Anazi, K.M., Hailan, W.A.Q., and Ali, M.A., (2022). Potassium bromate-induced oxidative stress, genotoxicity and cytotoxicity in the blood and liver cells of mice. *Mutation Research/Genetic Toxicology and Environmental Mutagenesis* 878, 503481. https://doi.org/10.1016/J.MRGENTOX.2022.503481

Altoom, N.G., Ajarem, J., Allam, A.A., Maodaa, S.N., and Abdel-Maksoud, M.A., (2018). Deleterious effects of potassium bromate administration on renal and hepatic tissues of Swiss mice. *Saudi J Biol Sci* 25, 278–284. https://doi.org/10.1016/J.SJBS.2017.01.060

Bansil, R., and Turner, B.S., (2006). Mucin structure, aggregation, physiological functions and biomedical applications. *Curr Opin Colloid Interface Sci* 11, 164–170. https://doi.org/10.1016/J.COCIS.2005.11.001

Bashir, H., Bhat, M.H., Farooq, R., Majid, S., Shoib, S., Hamid, R., Mattoo, A.A., Rashid, T., Bhat, A.A., Wani, H.A., and Masood, A. (2012). Comparison of hematological parameters in untreated and treated subclinical hypothyroidism and primary hypothyroidism patients. *Med J Islam Repub Iran* 26, 172.

Batista, L.M., Lima, G.R.D.M., De Almeida, A.B.A. *et al*. (2015) Ulcer healing and mechanism(s) of action involved in the gastroprotective activity of fractions obtained from Syngonanthus arthrotrichus and Syngonanthus bisulcatus. *BMC Complement Altern Med* 15, 391 https://doi.org/10.1186/s12906-015-0923-x

Beckert, S., Class, N., Farrahi, F., and Coerper, S. (2004). Growth hormone enhances gastric ulcer healing in rats. Med Sci Monit. 10(8):BR255-8. *Epub* 2004 Jul 23. PMID: 15277985.)

Bewaji, C.O., Olorunsogo, O.O., and Bababunmi, E.A. (1985). Comparison of the membrane-bound (Ca2+ + Mg2+)-ATPase in erythrocyte ghosts from some mammalian species. *Comparative Biochemistry and Physiology -- Part B: Biochemistry* and 82, 117–122. https://doi.org/10.1016/0305-0491(85)90138-5

Bhattacharyya, A., Chattopadhyay, R., Mitra, S., and Crowe, S.E. (2014). Oxidative Stress: An Essential Factor in the Pathogenesis of Gastrointestinal Mucosal Diseases. *Physiol Rev* 94, 329. https://doi.org/10.1152/PHYSREV.00040.2012

Biswas, K., Bandyopadhyay, U., Chattopadhyay, I., Varadaraj, A., Ali, E., and Banerjee, R.K. (2003): Mechanism of antiulcer effect of omeprazole. *The American Society for Biochemistry and Molecular Biology*, Manuscript M210328200

Bonacquisti, T.P. (2006). A drinking water utility's perspective on bromide, bromate, and ozonation. Toxicology 221, 145–148. https://doi.org/10.1016/J.TOX.2006.02.010

Brecher, G., and Cronkite, E.P. (1950). Morphology and Enumeration of Human Blood Platelets. https://doi.org/10.1152/jappl.1950.3.6.365 3, 365–377. https://doi.org/10.1152/JAPPL.1950.3.6.365

Brent, G.A. (2012). Mechanisms of thyroid hormone action. J Clin Invest 122, 3035–3043. https://doi.org/10.1172/JCI60047

Bridgen, M.L. (1999): Clinical utility of the erythrocyte sedimentation rate. *Am. Fam. Physician*; 60(5): 1443-50

Bromate CASRN 15541-45-4 | IRIS | US EPA, ORD [WWW Document], n.d. URL https://iris.epa.gov/ChemicalLanding/&substance_nmbr=1002 (accessed 4.23.23).

Burstein, C. (2007). Hematology: Clinical principles and applications. LaboratoriumsMedizin 31, 278–279. https://doi.org/10.1515/JLM.2007.040

Cannon, C.R. (1994). Hypothyroidism in head and neck cancer patients: Experimental and clinical observations. Laryngoscope 104, 1–21. https://doi.org/10.1288/00005537-199411001-00001

Caimi, G., Presti, R.L., Montana, M., Noto, D., Canino, B., Averna, M.R., and Hopps, E. (2014): Lipid peroxidation, nitric oxide metabolites, and their ratio in a group of subjects with metabolic syndrome. *Oxidative Medicine and Cellular Longevity;* Volume 2014, Article ID 824756, 8 pages

Carlwe, M., Schaffer, T., and Sjöberg, S. (2013). Short-term Withdrawal of Levothyroxine, Induced Increase of Thyroid-stimulating Hormone and an Increase Ratio of Triiodothyronine to Thyroxine. *Eur Endocrinol* 9, 37. https://doi.org/10.17925/EE.2013.09.01.37

Cheng, S.Y., Leonard, J.L., and Davis, P.J. (2010). Molecular aspects of thyroid hormone actions. *Endocr Rev* 31, 139–170. https://doi.org/10.1210/ER.2009-0007

Chipman, J.K., Davies, J.E., Parsons, J.L., Nair, J., O'Neill, G., and Fawell, J.K. (1998). DNA oxidation by potassium bromate; a direct mechanism or linked to lipid peroxidation? Toxicology 126, 93–102. https://doi.org/10.1016/S0300-483X(97)00174-1

Christ-Crain, M., Huber, P.R., Keller, U., Meier, C., Müller, B., Puder, J., and Staub, J.-J. (2004). Changes in Liver Function correlate with the Improvement of Lipid Profile after Restoration of Euthyroidism in Patients with Subclinical Hypothyroidism. *EXCLI J* 3, 1–9. https://doi.org/10.17877/DE290R-14916

Claiborne, A. (1985). Catalase activity, in: Handbook of Methods for Oxygen Radical Research. CRC Press, Boca Raton, pp. 283–284.

Clausen, M.V., Hilbers, F. and Poulsen, H. (2017): The structure and function of the Na,K-ATPase isoforms in health and disease. *Frontiers in Physiology*; 8:371

Costa, P., Somensi, L.B., Silva, R.C.S., Mariano, L.N.B., Boeing, T., Longo, B., Perfoll, E., Souza, P., Gushiken, L.F.S., Pellizzon, C.H., Rodrigues, D.M., Bastos, J.K., Andrade, S.F., and Silva, L.M. (2019): Role of the antioxidant properties in the gastroprotective and gastric healing activity promoted by Brazilian green propolis and the healing efficacy of Artepillin C. *Inflammopharmacology.* DOI: https://doi.org/10.1007/s10787-019-00649-7

Dale, J., Daykin, J., Holder, R., Sheppard, M.C., and Franklyn, J.A. (2001). Weight gain following treatment of hyperthyroidism. *Clin Endocrinol* (Oxf) 55, 233–239. https://doi.org/10.1046/J.1365-2265.2001.01329.X

Das, K., and Chainy, G.B.N. (2001). Modulation of rat liver mitochondrial antioxidant defence system by thyroid hormone. Biochimica et Biophysica Acta (BBA) - Molecular Basis of Disease 1537, 1–13. https://doi.org/10.1016/S0925-4439(01)00048-5

Deangelo, A.B., George, M.H., Kilburn, S.R., Moore, T.M., and Wolf, D.C. (1998)

. Carcinogenicity of Potassium Bromate Administered in the Drinking Water to Male B6C3F, Mice and F344/N Rats*. Safety Assessment TOXICOLOGIC PATHOLOGY 26, 587–594.

Dietze, S., Lees, K.R., and Voigt, J. (2016): Food deprivation, body weight loss and anxiety-related behavior in rats. Animals (Basel). 6(1): 4.

Dongmei, L., Zhiwei, W., Qi, Z., Fuyi, C., Yujuan, S., and Xiaodong, L. (2015). Drinking water toxicity study of the environmental contaminant—Bromate. Regulatory Toxicology and Pharmacology 73, 802–810. https://doi.org/10.1016/J.YRTPH.2015.10.015

Elinder, C.G., Edling, C., Lindberg, E., Kågedal, B., and Vesterberg, O. (1985). Assessment of renal function in workers previously exposed to cadmium. *Occup Environ Med* 42, 754–760. https://doi.org/10.1136/OEM.42.11.754

Ellman, G.L. (1959). Tissue sulfhydryl groups. *Arch Biochem Biophys* 82, 70–77. https://doi.org/10.1016/0003-9861(59)90090-6

Erion, M.D., Cable, E.E., Ito, B.R., Jiang, H., Fujitaki, J.M., Finn, P.D., Zhang, B.H., Hou, J., Boyer, S.H., Van Poelje, P.D., and Linemeyer, D.L. (2007). Targeting thyroid hormone receptor-β agonists to the liver reduces cholesterol and triglycerides and improves the therapeutic index. *Proc Natl Acad* Sci U S A 104, 15490–15495. https://doi.org/10.1073/PNAS.0702759104/SUPPL_FILE/02759SUPPAPPENDIX.PDF

Fagundes, F.L., Piffer, G.d.M., Périco, L.L., Rodrigues, V.P., Hiruma-Lima, C.A., dos Santos, R.d.C., (2020) Chrysin Modulates Genes Related to Inflammation, Tissue Remodeling, and Cell Proliferation in the Gastric Ulcer Healing. International *Journal of Molecular Sciences*. 21(3):760. https://doi.org/10.3390/ijms21030760

Graninger, W., Pirich, K.R., Speiser, W., Deutsch, E., and Waldhäusl, W.K. (1986): Effect of Thyroid Hormones on Plasma Protein Concentrations in Man. *The Journal of Clinical Endocrinology & Metabolism*, Volume 63, Issue 2, Pages 407–411, https://doi.org/10.1210/jcem-63-2-407

Gornall, A., Bardawill, M., and David, M. (1949). Determination of serum proteins by means of the biuret reaction. *J. Biol. Chem* 177, :751-66.

Gradus (Ben-Ezer), D., Rhoads, M., Bergstrom, L.B., and Jordan, S.C. (1984). Acute Bromate Poisoning Associated with Renal Failure and Deafness Presenting as Hemolytic Uremic Syndrome. *Am J Nephrol* 4, 188–191. https://doi.org/10.1159/000166804

Grasselli, E., Voci, A., Canesi, L., De Matteis, R., Goglia, F., Cioffi, F., Fugassa, E., Gallo, G., and Vergani, L., (2011). Direct effects of iodothyronines on excess fat storage in rat hepatocytes. *J Hepatol* 54, 1230–1236. https://doi.org/10.1016/J.JHEP.2010.09.027

Gredilla, R., Barja, G., and López-Torres, M. (2009). Thyroid hormone-induced oxidative damage on lipids, glutathione and DNA in the mouse heart. https://doi.org/10.1080/10715760100300931 35, 417–425. https://doi.org/10.1080/10715760100300931

Gregor, A., Kostrzewska, E., and Godorowska, W. (1977). Determination of Serum Proteins in the Presence of Dextran by means of the Biuret Reaction. *Transfusion Medicine and Hemotherapy* 4, 48–50. https://doi.org/10.1159/000219790

Gupta, S., Shinde, R. K., and Shinde, S. (2022). Comparison of the outcomes of cadexomer iodine and povidone-iodine ointments in wound management. Cureus, 14(5).

Hampton, D.D., and Hale, L.P (2011). Mast Cells Are Critical for Protection against Peptic Ulcers Induced by the NSAID Piroxicam. *PLoS ONE* 6(8): e23669. https://doi.org/10.1371/journal.pone.0023669

Harper, M.E., and Seifert, E.L. (2008). Thyroid hormone effects on mitochondrial energetics. Thyroid 18, 145–156. https://doi.org/10.1089/THY.2007.0250

He, W., An, X., Li, L., Shao, X., Li, Q., Yao, Q., and Zhang, J.A. (2017). Relationship between Hypothyroidism and Non-Alcoholic Fatty Liver Disease: A Systematic Review and Meta-analysis. *Front Endocrinol* (Lausanne) 8, 335. https://doi.org/10.3389/FENDO.2017.00335/BIBTEX

Ignarro, L.J., Buga, G.M., Wood, K.S., Byrns, R.E., and Chaudhuri, G. (1987). Endothelium-derived relaxing factor produced and released from artery and vein is nitric oxide. Proc *Natl Acad Sci* U S A 84, 9265–9269. https://doi.org/10.1073/pnas.84.24.9265

Josiah, S.J., Nwangwu, S.C.O., Akintola, A.A., Allu, T., Usunobun, U., Njoya, H., and Adejumo, B.I (2011): The Protective Effect of Ethanolic Extract of Unripe Pulp of Carica papaya (Pawpaw) Against Potassium Bromate Induced Tissue Damage in Wistar Rats. *Current Research Journal of Biological Sciences* 3(6): 597-600

Kebapcilar, L., Akinci, B., Bayraktar, F., Comlekci, A., Solak, A., Demir, T., Yener, S., Küme, T., and Yesil, S. (2007). Plasma thiobarbituric acid-reactive substance levels in subclinical hypothyroidism. *Medical Principles and Practice* 16, 432–436. https://doi.org/10.1159/000107747

Khalefa, A. A., Abd-Alaleem, D. I., and Attiaa, K. I. (2010). The protective effects of ghrelin and leptin against stress-induced gastric ulcer in rats. *Arab Journal of Gastroenterology*, 11(2), 74-78. https://doi.org/10.1016/j.ajg.2010.04.005

Kivirikko, K.I., Laitinen, O., Aer, J., and Halme, J. (1967). Metabolism of collagen in experimental hyperthyroidism and hypothyroidism in the rat. *Endocrinology* 80, 1051–1061. https://doi.org/10.1210/endo-80-6-1051

Köroğlu, E., Canbakan, B., Atay, K., Hatemi, İ., Tuncer, M., Dobrucalı, A., Sonsuz, A., Gültepe, İ., and Şentürk, H. (2016). Role of oxidative stress and insulin resistance in disease severity of non-alcoholic fatty liver disease. *Turk J Gastroenterol* 27, 361–367. https://doi.org/10.5152/tjg.2016.16106

Kumar, S., and Pankaj, P. (2012). Accidental Potassium Bromate Poisoning in Nine Adults. *Journal of Indian Academy of Forensic Medicine* 34.

Kunchandy, J., Khanna, S., and Kulkarni, S.K. (1985). Effect of alpha2 agonists clonidine, guanfacine and B-HT 920 on gastric acid secretion and ulcers in rats. *Arch Int Pharmacodyn Ther* 275, 123–138.

Kurokawa, Y., Maekawa, A., Takahashi, M., and Hayashi, Y. (1990). Toxicity and carcinogenicity of potassium bromate - A new renal carcinogen. *Environ Health Perspect* 87, 309–335. https://doi.org/10.1289/EHP.9087309

Levine, R.L., Garland, D., Oliver, C.N., Amici, A., Climent, I., Lenz, A.G., Ahn, B.W., Shaltiel, S., and Stadtman, E.R. (1990). [49] Determination of carbonyl content in oxidatively modified proteins. *Methods Enzymol* 186, 464–478. https://doi.org/10.1016/0076-6879(90)86141-H

Lu, S.C. (2009). Regulation of glutathione synthesis. Mol Aspects Med 30, 42–59. https://doi.org/10.1016/j.mam.2008.05.005

Machowska, A., Szlachcic, A., Pawlik, M., Brzozowski, T., Konturek, S.J., and Pawlik, W.W. (2004). The role of female and male sex hormones in the healing process of preexisting lingual and gastric ulcerations. *J Physiol Pharmacol.55 Suppl* 2:91-104. PMID: 15608364.

Mandato, C., D'Acunzo, I., and Vajro, P. (2018). Thyroid dysfunction and its role as a risk factor for non-alcoholic fatty liver disease: What's new. *Digestive and Liver Disease* 50, 1163–1165. https://doi.org/10.1016/j.dld.2018.08.026

Mantovani, A., Nascimbeni, F., Lonardo, A., Zoppini, G., Bonora, E., Mantzoros, C.S., and Targher, G., (2018). Association between Primary Hypothyroidism and Nonalcoholic Fatty Liver Disease: A Systematic Review and Meta-Analysis. *Thyroid* 28, 1270–1284. https://doi.org/10.1089/THY.2018.0257/ASSET/IMAGES/LARGE/FIGURE3.JPEG

Matsumoto, I., Morizono, T., and Paparella, M.M. (1980). Hearing Loss following Potassium Bromate: Two Case Reports. Otolaryngology–Head and Neck Surgery 88, 625–629. https://doi.org/10.1177/019459988008800519

Misra, H.P., and Fridovich, I. (1972). The Role of Superoxide Anion in the Autoxidation of Epinephrine and a Simple Assay for Superoxide Dismutase. *J Biol Chem* 247, 3170–3175.

Miyake, T., Suzaki, T., and Oishi, M. (1980): Correlation of gastric ulcer healing features by endoscopy, stereoscopic microscopy, and histology, and a reclassification of the epithelial regenerative process. *Dig Dis Sci*. 25(1):8-14. doi: 10.1007/BF01312726. PMID: 7353454.

Namulema, J., Nansunga, M., Kato, C.D. *et al*. (2018). Thyroid hormones increase stomach goblet cell numbers and mucin expression during indomethacin induced ulcer healing in Wistar rats. Thyroid Res 11, 6. https://doi.org/10.1186/s13044-018-0050-0

Natori, J., Shimizu, K., Nagahama, M., and Tanaka, S. (1999). The influence of hypothyroidism on wound healing An experimental study. Journal of Nippon Medical School 66, 176–180. https://doi.org/10.1272/JNMS.66.176

Nogueira, L., Sanches, A.L.M., da Silva, D.G.H., Ferrizi, V.C., Moreira, A.B., and de Almeida, E.A. (2011). Biochemical biomarkers in Nile tilapia (Oreochromis niloticus) after short-term exposure to diesel oil, pure biodiesel and biodiesel blends. Chemosphere 85, 97–105. https://doi.org/10.1016/J.CHEMOSPHERE.2011.05.037

Odukanmi, O.A., Salami, A.T., Ashaolu, O.P., Adegoke, A.G., and Olaleye, S.B. (2017): Kolaviron attenuates ischemia-reperfusion injury in the stomach of rats. *Appl. Physiol. Nutr. Metab*. 43(1):30-37. doi: 10.1139/apnm-2017-0138. Epub 2017 Aug 25. PMID: 28841395.

Oliveira, M., Pacheco, M., and Santos, M.A. (2008). Organ specific antioxidant responses in golden grey mullet (Liza aurata) following a short-term exposure to phenanthrene. *Science of The Total Environment* 396, 70–78. https://doi.org/10.1016/J.SCITOTENV.2008.02.012

Oluwole, S.O and Saka, M.T. (2007): Effect of thyroid hormone on gastric mucous secretion around indomethacin-induced gastric ulcers in rats. *J Med Sci* 7(4): 678-681.

Omayone, T.P., Salami, A.T., Oluwole, F.S. and Olaleye, S.B. (2016): Gastroprotective effect of vanadium in rats - the roles of gastric acid and nitric oxide. *J. Afr. Ass. Physiol. Sci*. 4 (1): 32-40

Omer, R., Abuelgasim, A.I., and Elmahdi, B. (2008): Effect of Potassium Bromate on Liver and Blood Constituents of Wistar Albino Rats. *American Journal of Food Technology*, 3: 310-314.

Oseni, O. A., Ogunmoyole T., and Idowu K. A. (2015): Lipid Profile and Cardio-Protective Effects of Aqueous Extract of Moringa Oleifera (Lam) Leaf on Bromate- Induced Cardiotoxicity on Wistar Albino Rats. *European Journal of Advanced Research in Biological and Life Sciences* Vol. 3 (2)

Pagadala, M.R., Zein, C.O., Dasarathy, S., Yerian, L.M., Lopez, R., and McCullough, A.J. (2012). Prevalence of hypothyroidism in nonalcoholic fatty liver disease. *Dig Dis Sci* 57, 528–534. https://doi.org/10.1007/S10620-011-2006-2/METRICS

Post, H., Hundt, J.E., Zhang, G., Depping, R., Rose, C., Langan, E.A., and Paus, R. (2021). Thyroxine restores severely impaired cutaneous re-epithelialisation and angiogenesis in a novel preclinical assay for studying human skin wound healing under "pathological" conditions ex vivo. Arch Dermatol Res 313, 181–192. https://doi.org/10.1007/S00403-020-02092-Z/FIGURES/4

Raju, R., Kethavath, S.N., Sangavarapu, S.M., and Kanjarla, P. (2019). Efficacy of cadexomer iodine in the treatment of chronic ulcers: A randomized, multicenter, controlled trial.Wounds 31 85–90.

Recknagel, R.O., Glende, E.A., and Britton, R.S. (2020). Free Radical Damage and Lipid Peroxidation. *Hepatotoxicology* 401–436. https://doi.org/10.1201/9780367812041-9

Rowan, R.M. (1983). Blood Cell Volume Analysis: A New Screening Technology for the Haematologist., in: Albert Clark.

Salami, A.T., Odukanmi, O.A., Olagoke, C.O., Iyiola, T.O., and Olaleye, S.B. (2016). Role of nitric oxide and endogenous antioxidants in thyroxine facilitated healing of ischemia-reperfusion induced gastric ulcers. *Nigerian Journal of Pharmaceutical Research* 12, 189–206. https://doi.org/10.4314/njpr.v12i2.

Salami A.T., Odukanmi O. A., Faniyan O. F., Omayone T.P., and Olaleye S. B. (2017): Seeds of Buchholzia coriacea in Diet Mitigate Ischemic Reperfusion–Induced Gastric Ulceration in Experimental Rats, *Journal of Dietary Supplements*, DOI: 10.1080/19390211.2017.1404544

Salami, A.T., Adebimpe, M.A., Olagoke, O.C., Iyiola, T.O., and Olaleye, S.B., (2020). Potassium bromate cytotoxicity in the Wister rat model of chronic gastric ulcers: Possible reversal by protocatechuic acid. *J Food Biochem* 44(12), e13501. https://doi.org/10.1111/JFBC.13501

Salami, A.T., Okonkwo, C.E., Attah, F.A., and Olagoke, O.C., (2021). Bioactive Moringa olifera seed extracts attenuates cholesterol gall stones in hyperglycaemic Swiss mice. *Comparative Clinical Pathology*, 30(2), 207–216. https://doi.org/10.1007/S00580-021-03206-3

Salami, A.T., Odukanmi, A.O., Adeola A., Iyiola T.O. and Olaleye S.B (2021). Artesunate, with or without Mefloquine, alters activities of Mast cells, Anti-inflammatory markers and Antioxidants in Rats with Acetic acid induced Gastric ulcers. *Arch. Bas. App. Med*. 9 (2021): 45– 57.

Schulte-Wissermann, H., Straub, E., and Funke, P.J. (1977). Influence of L-thyroxine upon enzymatic activity in the renal tubular epithelium of the rat under normal conditions and in mercury-induced lesions. I. Histochemical studies of alkaline phosphatase, acid phosphatase, adenosine- tri-phosphatase and leucine-aminopeptidase. *Virchows Arch B Cell Pathol* 23, 163–173. https://doi.org/10.1007/BF02889128

Sedlak, J., and Lindsay, R.H. (1968). Estimation of total, protein-bound, and nonprotein sulfhydryl groups in tissue with Ellman's reagent. *Anal Biochem* 25, 192–205. https://doi.org/10.1016/0003-2697(68)90092-4

Senese, R., Cioffi, F., de Lange, P., Leanza, C., Iannucci, L.F., Silvestri, E., Moreno, M., Lombardi, A., Goglia, F., and Lanni, A. (2017). Both 3,5-diiodo-L-thyronine and 3,5,3'-triiodo-L-thyronine prevent short-term hepatic lipid accumulation via distinct mechanisms in rats being fed a high-fat diet. *Front Physiol* 8, 706. https://doi.org/10.3389/FPHYS.2017.00706/BIBTEX

Shah, S., Begum, M., Akter, D.M., Rahman, A.A.T.M., Uddin, F., and Rahman, J. (1999). [Anemia in hypothyroidism]. *Med Pregl* 52, 136–140. https://doi.org/10.3329/bmrcb.v46i1.47470

Shahid, M.A., Ashraf, M.A., and Sharma, S. (2022). Physiology, Thyroid Hormone. StatPearls.

Sherwood L. (2012): The digestive system. Fundamentals of Human Physiology. 4th Edition.

Shu, W., Yang, M., Yang, J., Lin, S., Wei, X., and Xu, X. (2022). Cellular crosstalk during liver regeneration: unity in diversity. *Cell Communication and Signaling* 2022 20:1 20, 1–13. https://doi.org/10.1186/S12964-022-00918-Z

Si, M., Cao, Q., and Wu, G. (2005). Quality of gastric ulcer healing evaluated by endoscopic ultrasonography. *World Journal of Gastroenterology* : WJG, 11(22), 3461-3464. https://doi.org/10.3748/wjg.v11.i22.346;

Siegel, N.J., Gaudi0, K.M., Katz, L.A., Reilly, H.F., Ardito, T.A., Hendler, F.G., and Kashgarian, M. (1984). Beneficial effect of

thyroxin on recovery from toxic acute renal failure. *Kidney Int* 25, 906–911. https://doi.org/10.1038/ki.1984.108

Silva, L.M., Boeing, T., Somensi, L.B., Cury, B.J., Steimbach, V.M.B., Silveria, A.C.O., Niero, R., Filho, V.C., Santin, J.R., and Andrade S.F. (2015): Evidence of gastric ulcer healing activity of Maytenus robusta Reissek: In vitro and invivo studies. *Journal of Ethnopharmacology* 175:75–85

Song, K.I., Kim, S.H., Jang, J.G., and Choi, J.S. (2001). Bromate Intoxication Associated with Acute Renal Failure. *Korean Journal of Nephrology* 732–735.

Sørbye, H., and Svanes, K. (1994). The role of blood flow in gastric mucosal defence, damage and healing. *Dig Dis*. 1994 Sep-Oct;12(5):305-17. doi: 10.1159/000171465. PMID: 7533677.

Sorokin, C. (1973). Dry weight, packed cell volume and optical density. pp. 321–343.

Sterling, K. (2010). Thyroid Hormone Action at the Cell Level. https://doi.org/10.1056/NEJM197901183000304 300, 117–123. https://doi.org/10.1056/NEJM197901183000304

Stuti, M., and D'souza, D. (2013): Effects of Potassium Bromate on the Kidney and Haematological Parameters of Swiss Albino Mice. *The Bioscan* 8(3): 1011-1014

Suzuki, H., Nishizawa, T., Tsugawa, H., Mogami, S., and Hibi T. (2012). Roles of oxidative stress in stomach disorders. *J Clin Biochem Nutr* 50, 35. https://doi.org/10.3164/JCBN.11-115SR

Thá Nassif, A.C., Hintz Greca, F., and Graf, H., Domingues Repka, J.C., Nassif, L.S. (2009). Wound Healing in Colonic Anastomosis in Hypothyroidism. *European Surgical Research* 42, 209–215. https://doi.org/10.1159/000208519

van Lerberghe, W., Keegels, G., Cornelis, G., Ancona, C., Mangelschots, E., and van Balen, H. (1983). Haemoglobin measurement: the reliability of some simple techniques for use in a primary health care setting. *Bull World Health Organ* 61, 957.

Varshney, R., and Kale, R.K. (1990). Effects of calmodulin antagonists on radiation-induced lipid peroxidation in microsomes. *Int J Radiat Biol* 58, 733–743. https://doi.org/10.1080/09553009014552121

Velicky J., Titlbach M., Lojda Z., Duskova J., Vobecky M., Strbak V., and Raska I. (1998): Long-term action of potassium bromide on the rat thyroid gland. *Acta histochem*. 100, 11-23

Venditti, P., and Di Meo, S. (2006). Thyroid hormone-induced oxidative stress. *Cell Mol Life Sci* 63, 414–434. https://doi.org/10.1007/S00018-005-5457-9

Villabona, C., Sahun, M., Roca, M., Mora, J., Gómez, N., Gómez, J.M., Puchal, R., and Soler, J. (1999). Blood Volumes and Renal Function in Overt and Subclinical Primary Hypothyroidism. *Am J Med Sci* 318, 277–280. https://doi.org/10.1016/S0002-9629(15)40631-7

Wada, K., Kamisaki, Y., Kitano, M., Kishimoto, Y., Nakamoto, K., and Itoh, T. (1996). A new gastric ulcer model induced by ischemia-reperfusion in the rat: Role of leukocytes on ulceration in rat stomach. *Life Sci* 59, PL295–PL301. https://doi.org/10.1016/0024-3205(96)00500-0

Waldum, H. L., Sørdal, Ø. F., and Mjønes, P. G. (2019). The Enterochromaffin-like [ECL] Cell—Central in Gastric Physiology and Pathology. *International Journal of Molecular Sciences*, 20(10). https://doi.org/10.3390/ijms20102444

Winzler, R.J. (2006). Determination of Serum Glycoproteins, in: Methods of Biochemical Analysis. John Wiley & Sons, Ltd, pp. 279–311. https://doi.org/10.1002/9780470110188.ch10

Wong, V.W.S., and Singal, A.K. (2019). Emerging medical therapies for non-alcoholic fatty liver disease and for alcoholic hepatitis. Transl *Gastroenterol Hepatol* 4. https://doi.org/10.21037/TGH.2019.06.06

Zhang, G.Y., Langan, E.A., Meier, N.T., Funk, W., Siemers, F., and Paus, R. (2019). Thyroxine (T4) may promote re-epithelialisation and angiogenesis in wounded human skin ex vivo. *PLoS One* 14, e0212659. https://doi.org/10.1371/JOURNAL.PONE.0212659

Zhang, S., and Jiang, J.Q. (2022). Synergistic Effect of Ferrate with Various Water Processing Techniques—A Review. *Water* 2022, Vol. 14, Page 2497 14, 2497. https://doi.org/10.3390/W14162497.

Niger. J. Physiol. Sci. 38 (December 2023): 249 – 258
www.njps.physiologicalsociety.com

Niger. J. Physiol. Sci.

Full length Research Article

Morphologic and Histologic Studies on the Tongue of the Juvenile Cattle Egret (*Bubulcus ibis*)

Azeez I.A.[a], Omirinde J.O.[a], Elisha J.[a], Plang N.J.[a] and *Olopade J.O.[b].

[a]*Department of Veterinary Anatomy, Faculty of Veterinary Medicine, University of Jos, Nigeria.*
[b]*Department of Veterinary Anatomy, Faculty of Veterinary Medicine, University of Ibadan, Nigeria*

Summary: Cattle egret (*Bubulcus ibis*) is a cosmopolitan heron species, with least concern conservation status. There are limited literatures on the anatomy of this bird, especially in relation to its sensory organs, hence this study described the morphologic and histologic features of its tongue. The tongues of twelve juvenile cattle egrets were examined in situ for morphological features and morphometric measurements were determined ex situ. Histological assessment was conducted on the tongue section with parameters such as epithelial and lamina propia heights, lingual muscle and entoglossal cartilage heights evaluated. Grossly, the tongue was divided into three parts namely; apex, body and the root. It was arrow shaped, conforming to the shape of the beak, with a laryngeal mound bounded caudally by the pharyngeal papillae at its root. A massive entoglossal cartilage formed the core of the cranial apex, ventral body portion, and caudal aspect of the root. Histologically, the lingual mucosa possessed keratinized squamous epithelium in all its divisions, with spinous conical papillae being characteristic of the cranial apical mucosa. The body lingual mucosa possessed foliate papillae on the dorsal aspects, while filiform papillae were prominent in the ventral portions. The lingual root uniquely possessed numerous glandular ducts in its lamina propia as well as localized adipocytes. Overall, the regression analysis showed that the bird's body weight can be conveniently predicted from tongue parameters. This study, thus provided additional knowledge on the anatomy of the birds and, the generated data could be useful in comparative regional avian anatomy.

Keywords*: cattle egret, entoglossal cartilage, histomorphometry, lingual papillae, morphometry*

**Authors for correspondence: jkayodeolopade@yahoo.com, Tel: +234-8023860829*

Manuscript received- June 2022; Accepted- February 2023

DOI: https://doi.org/10.54548/njps.v38i1.15

INTRODUCTION

The bird, Cattle Egret (*Bubulcus ibis*) is a species of heron found all over the world, with least concern conservation status (Telfair and Raymond, 2006). The bird belongs to the order Pelecaniformes, family Ardeidae and, are native to Africa; mostly found in dry grassy habitats, in association with wildlife and livestock (Hancock, 1984). They are associated with both small and large flocks, feeding in loose aggregates. The birds feed on insects, earthworms, spider, frogs and most especially ticks present on cattle (Siegfried, 1971). Other prey of the birds include grasshoppers, crickets, and moths (McKilligan, 2005). Generally, cattle egrets are colonial in nature and whitish in colour. Both sexes of this bird are similar, and the male is slightly bigger and possess marginally longer breeding plumes than the female. The juvenile age group lacks coloured plumes and have a black beak (Mckilligan, 2005), with the adult possessing greyish-yellow feet and sharply pointed yellow short bill (Seedikkoya *et al*., 2007).

Studies on the gross morphometry and histomorphomtery of the cattle egret are scarce. The descriptive anatomy on its appendicular (Rezk 2015a) and axial skeletons (Rezk, 2015b), gross morphometrics of the fore- and hind-limb skeleton (Ekeolu *et al*., 2016), the gross and morphometrical studies on the humerus (Sasan *et al*., 2019), and more recently, the craniofacial and ocular morphometrics (Azeez *et al*., 2022a) of the cattle egret have been published. With the exception of the report of Al-Zahaby (2016) on gross and histological description of tongue of the adult egret, there is a dearth of information on the gross and histo-morphometric parameters of the tongue of the juvenile cattle egret and this study objective was to fill part of that knowledge gap. Aging-associated morphological and morphometric indices are very important for comparative, developmental and evolutionary assessments. Hence, the description of the lingual macro-anatomical structure and histology of cattle egret juvenile age category can provide supplementary data to the basic information on the adult egret tongue, as studies across age groups are of great value to set standards of comparison for research. Furthermore, considering the vital sentinelling role played by cattle egrets in the assessment of agro-ecosystem pollution and its importance in serving as excellent animal model in foraging study as well as biological insect pest control agent in the agro-ecosystem, there is need to comprehensively study its tongue morphology, a suitable indicator of its feeding habit, more particularly in a juvenile cattle egret which is yet to be

investigated.The tongue is a very muscular organ, constituting a larger part of the oral cavity. Structurally, it possesses a free apex, body and an attached root. It is a very sensitive organ owing to it's very rich innervation, possesses a huge mass of skeletal muscles that rest on the floor of the oral cavity (Abayomi *et al*., 2009; Igado *et al*., 2015). The lingual gross and histological features such as its' lateral boundary and median sulcus conformation, papillae types and predominance, degree of keratinization of lingual epithelia and the placement of the lingual glands are crucial considerations that determine the level of tongues' mobility and its ability to capture preys as well as manipulate and swallow food items (Jackowiak and Godynicki, 2005; Emura *et al*., 2008).

This study described the morphologic and histologic features of the tongue of juvenile *Bubulcus ibis* (cattle egret) found in Nigeria.

MATERIALS AND METHODS

Animals: The animals, cattle egret, used were captive and of the juvenile age group. They were aged according to the detailed morphologic description by Mckilligan (2005) and Seedikkoya *et al*., (2007), while the juveniles possess black feet and beaks, and lack coloured plumes, the adults in contrast possess yellow feet and sharply-pointed short yellow bill. Of note, cattle egret is a medium sized bird, possessing short-legs and thick necks, in comparison to other egrets (Ivory, 2000). Twelve apparently healthy juvenile cattle egrets (mixed sexes) were used in this study. The birds were captured alive in a single batch from their habitat at Yelwa Fulani Community, Naraguta B Ward in Jos North Local Government Area of Plateau State, Nigeria (GPS coordinates: 9°59'21.5"N; 8°52'49.7"E). The birds were then transported to the Gross Anatomy Laboratory of the Department of Veterinary Anatomy, Faculty of Veterinary Medicine, University of Jos, Nigeria. Live body weight was measured and recorded using the mechanical laboratory weighing scale sensitive to 0.1 gm (Camry Emperor Table Scale J1712420834, China). Care was taken to ensure the bird did not experience undue pain or discomfort. The ethical clearance (Reference number: UJ/FPS/F17-00379) for the use of this bird was obtained from the Animal Care and Use Committee of the University of Jos, Nigeria. The experimental protocols used were also in conformity with the National Institute of Health Guide for the Care and Use of Animals (NIH Publications No. 80–23) and the European Communities Council Directive of November 24, 1986 (86/609/EEC).

Sedation and Organ Excision: The birds were euthanized by the administration of ketamine (40 mg/kg) and xylazine (10 mg/kg) through the intravenous route (Lierz and Korbel, 2012). Following deep anaesthesia, the birds were exsanguinated by cardiac puncture. The head was carefully dissected and the upper beak reflected to expose the tongue in situ.

Morphological Studies: Gross observations were made on the tongue in both in situ and ex situ positions. Gross features of the dorsal and ventral surfaces of the tongue were captured using a Sony® Digital Camera (DSC-H300 20.1 megapixels with 35x Optical Zoom). Tongue weight was obtained using the analytical weighing balance (Ohaus GmbH, Nänikon, Switzerland), sensitive to 0.01 gram, following its careful dissection from the lower jaw (ex situ). Linear morphometric parameters (defined in subsequent section) were measured with the aid of graded ruler (in centimeters). The nomenclature adopted in this study for the anatomical descriptions was as described in the sixth edition of the Nomina Anatomica Avium (2017).

Morphometric Parameters: The parameters measured are highlighted below, with weight recorded in grams (g) and linear measurements in centimeters (cm):
a). Weight of the animal (WOA) - measured with the aid of a mechanical laboratory weighing scale. b). Weight of the tongue (TOW) - measured using the analytical weighing balance.
c). Apex width (AW): The widest distance between the lateral margins of the apex of the tongue.
d). Body width (BW): The widest distance between the lateral margins of the body of the tongue.
e). Root width (RW): The widest distance between the lateral margins of the root of the tongue
f). Tongue length (TL): The longitudinal distance between the tip of the apex and the caudal-most part of the tongue (i.e the cranial margin of the laryngeal mound).
g). Apex length (AL): The longitudinal distance between the tip and the terminal end of the apex of the tongue.
h). Body length (BL): The longitudinal distance between the caudal end of the apex and the terminal end of the body of the tongue.
i) Root length (RL): The distance between the caudal end of the body and the terminal end of the root of the tongue (i.e. the cranial margin of the laryngeal mound).

Histological Studies: Immediately after the birds were euthanized, the tongues were dissected out and fixed in 4% phosphate-buffered paraformaldehyde (Loba Chemie PVT Ltd, India). The tissue samples were processed using the routine histological technique for light microscopic examination, as described by Azeez *et al*., (2022b). Surgifield SM-202A rotatory microtome was used for the sectioning at 7 µm. Longitudinal sections were obtained and stained using Haematoxylin (CDH Lab Reagent, New Delhi, India) and Eosin (Kem Light Lab Reagent, Mumbai, India). Histological examination was carried out on the processed tissue samples and photomicrographs taken at ×40, 100 and 400 magnifications through an Olympus Microscope equipped with industrial digital camera using an imaging software, MII ImageView version 3.7.9229 (YSC Technologies, Fremont, CA, USA). Photomicrographs of the sections of the apex, body and root were evaluated for regional variations.

Histomorphometry: Lingual histomorphometry was carried out using Motic Image Plus (MIP) 2.0 software by following the modified approach of Ahmed (2018). The parameters evaluated based on the tongue's division (as illustrated in Figure 2) of the cattle egret include:
(a) At the cranial (ACC I) and caudal (ACC II) aspects of the lingual apex, the following measurements were done:
- lingual epithelial height (EH) – the distance between the epithelial mucosal apex and its base border with laminal propria,

- lamina propria height (LP) – the distance between the base of the epithelial mucosa and the cranial border of the dorsal lingual muscle,
- dorsal lingual muscle length (DM) – the distance between the caudal most part of the lamina propria and the most cranial part of the endochondrial sheath of the entoglossal cartilage,
- entoglossal cartilage width/height (EC) – The distance between the dorsal and ventral endochodrial sheath summits.
- ventral lingual muscle- (VM) – The distance between the ventral border of endochodrial sheath and the outermost layer of the ventral lingual muscle.

(b). At the dorso-ventral (BDV) divisions (I, II and III) of the lingual body, the morphometric parameters (EH, LP, DM, EC and VM) assessed for the apex were recorded, except for the absence of the dorsal lingual muscle, entoglossal cartilage in DV I, and also, the same ventral lingual muscle shared by DV I and DV II.

(c). For the dorso-ventral (DV) divisions (1, II, III and IV) of the lingual root, the complete lingual parameters described for the apex (i.e., EH, LP, DM, EC and VM) were determined.

Data analysis: The numeric data generated were analyzed and expressed as mean ± SD, and the Scatter plot and the Pearson correlation coefficient (R two-tailed test) were used to measure the direction and strength of relationship between the variables. The regression analysis was done to forecast the imapact of the lingual parameters on the body weight prediction were also done. The John's Macintosh Project Statistical Analysis Software (JMP SAS/STATR) software version 10.0 (SAS Institute Inc., Carry, NC, USA) was used for statistical analyses.

RESULTS

Gross Characteristics: The tongue of the juvenile cattle egret revealed a long, protrusible structure, bounded; on the dorsal surface by the palate, laterally by the paired lower beak, and ventrally by visibly folded oral mucosa with patterned longitudinal fold (Plate. 1). It conforms to the shape of the lower beak which is V-shaped in outline (Plates. 1A and B). Grossly, it is divided into three parts; apex, body and the root. The apex of the tongue of the *Bubulcus ibis* evaluated in this study and their surrounding oral mucosa were reddish in colour in situ. The body and root of the tongue had a similar coloration as the apex. The apical aspect of the tongue is pointed assuming a spear-like shape and wider at its base. On its dorsal surface, it is characterized by a longitudinal furrow known as median groove (Figs. 1A and C). At the point of transition into the body of the tongue, a dorsally located transverse rows of caudally pointing papillae were situated (Plates 1A and C). The significant core of the apex is constituted by entoglossal cartilage. Similarly, the body of the tongue is supported by entoglossal cartilage. The ventral surface of the tongue of egret more specifically at the body of the tongue is anchored to the oral floor by mucosal fold referred to as frenulum (Plate. 1B). The root has the widest outline compared to other divisions of the tongue. Its caudal relation is formed by the laryngeal mound which is characterized by a median slit (glottis), an entrance into the laryngeal cavity and raised caudally pointing projections (pharyngeal papillae) on its dorsal summit (Plates 1A and C).

Morphometrics and analysis: Body and organ weights and, the morphometric parameters results are presented in Table 1. The scatter plot matrix and the Pearson's correlation co-efficient values of the variables from Table 1 are presented in Fig. 1. The regression analysis for the body weight prediction from lingual parameters is shown in Table 2. The apex had the longest length relative to the body and root. Conversely, the root had the longest width, in comparison with the apex and the body. Correlation of the body weight of the birds with tongue parameters using Pearson's correlation showed highest values for tongue weight (r=0.9351).

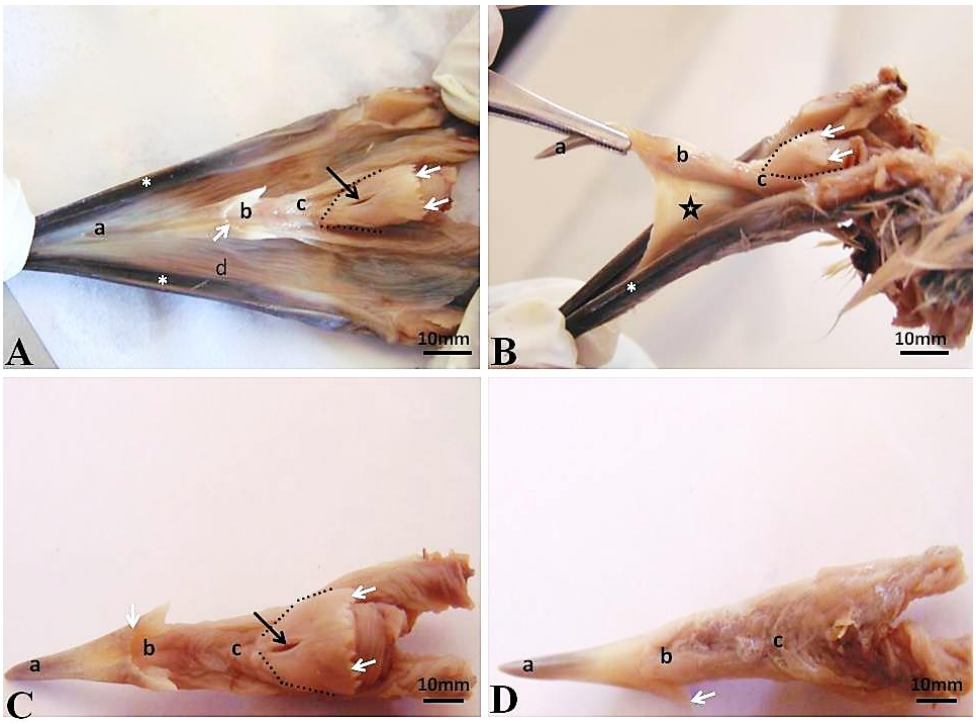

Plate 1.
Photographs of the tongue of juvenile cattle egret (*Bubulcus ibis*) following post-fixation. **A. Dorsal view** (*in situ*) **B. Dorso-lateral view** (*in situ*) **C. Dorsal view** (*ex situ*) **D. Ventral view** (*ex situ*). Note the divisions of the tongue (a- apex, b- body c- root) and these lingual and paralingual features; White arrow – pharyngeal papillae, Black star – frenulum linguae, Black arrow – glottis (laryngeal cleft), Dashed lines – laryngeal mounds, d – oral mucosa (folded and numerous), white asterisk – (lower beak).

Juvenile cattle egret tongue morphology

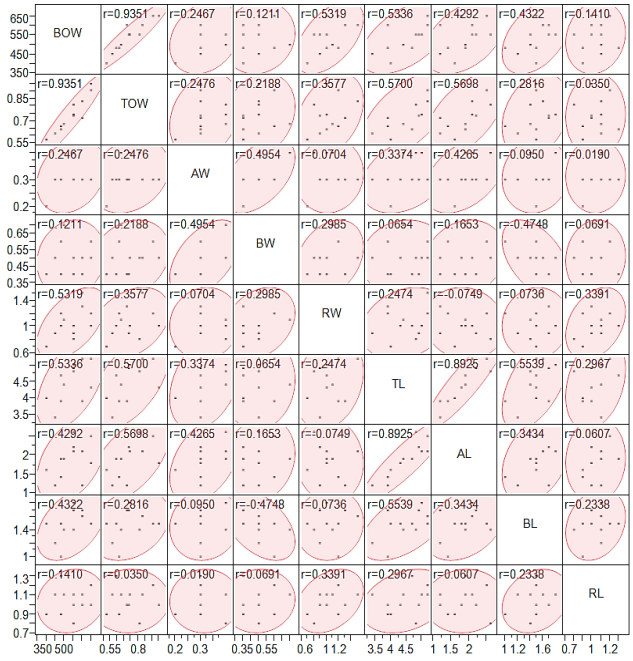

Figure 1:
Correlation analysis and scatter plot matrix of the measured parameters Correlation coefficients (r) were captured within the scatter plots. The scatterplot showed the relationships of the different variables as well as the density ellipses in the shaded portions.

Table 1.
Morphometric characteristics of the tongue in the juvenile cattle egret

Variables (n=12)	mean±SD
Weight of the animal (BOW) (g)	538.33±78.72
Weight of the tongue (TOW) (g)	0.74±0.12
Apex width (AW) (cm)	0.32±0.06
Body width (BW) (cm)	0.50±0.10
Root width (RW) (cm)	1.05±0.22
Tongue length (TL) (cm)	4.48±0.58
Apex length (AL) (cm)	1.88±0.46
Body length (BL) (cm)	1.48±0.22
Root length (RL) (cm)	1.04±0.13

Regression analysis was done to predict the weight of the bird animal from tongue morphometric data. As shown in Table 2 below, the equation for the predictor of the weight of the body is Y= a+bx, where Y= predictor value for the body weight, a=intercept, b=regression coefficient and x=explanatory variable. Hence, Y= -18.14+582.08TOW+85.54RW-22.62TL+93.43BL, where R2 = 0.9665 and adjusted R2 = 0.9473.

Histological Examination: For easy identification at histological examination, a schematic illustration of the tongue was made from the gross appearance shown in Fig. 1. As shown in Fig. 2 the apex was divided into cranial (illustrated as ACC I) and caudal (illustrated as ACC II) portions.The body was divided into 3; dorsal and ventral (BDV): I, II and III. The root was divided into 4; dorsal and ventral (RDV): I, II, III and IV.

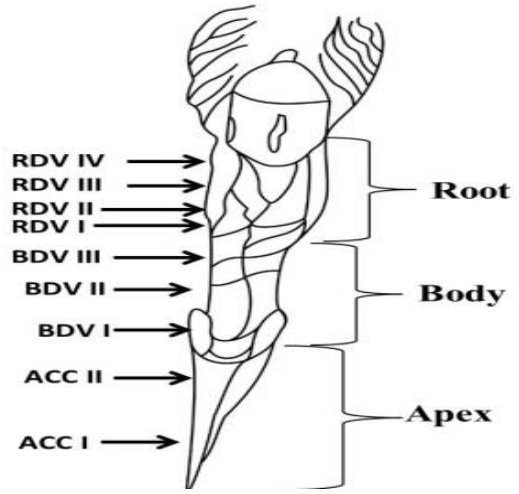

Figure 2.
Schematic diagram of the lingual (tongue) divisions of the juvenile cattle egret (*Bubulcus ibis*). Note the three main divisions of the tongue; Apex, body and root. Drawing was done using the modified approach of Erdogan and Iwasaki, (2014).

Table 2.
Regression analysis for the prediction of body weight from tongue parameters.
Current Estimates

Lock	Entered	Parameter	Estimate	nDF	SS	"F Ratio"	"Prob>F"
X	X	Intercept	-18.141929	1	0	0.000	1
	X	TOW	582.079385	1	32210.37	98.681	2.24e-5
		AW	0	1	164.8324	0.467	0.52009
		BW	0	1	5.006322	0.013	0.91236
	X	RW	85.5405486	1	3482.197	10.668	0.01375
	X	TL	-22.619614	1	964.149	2.954	0.12937
		AL	0	1	202.1073	0.582	0.47436
	X	BL	93.4361198	1	3224.848	9.880	0.01631
		RL	0	1	24.38251	0.065	0.80768

RSquare	RSquare Adj
0.9665	0.9473

The analysis shows the stepwise fit for body weight (BOW) in relation to other measured parameters. The BOW value can successfully be predicted from the intercept, explanatory variable and regression coefficient values generated. TOW – tongue weight, RW – root width, TL – tongue length, AW – apex width, BW- body width, RW – root width, AL – apex length and BL – body length

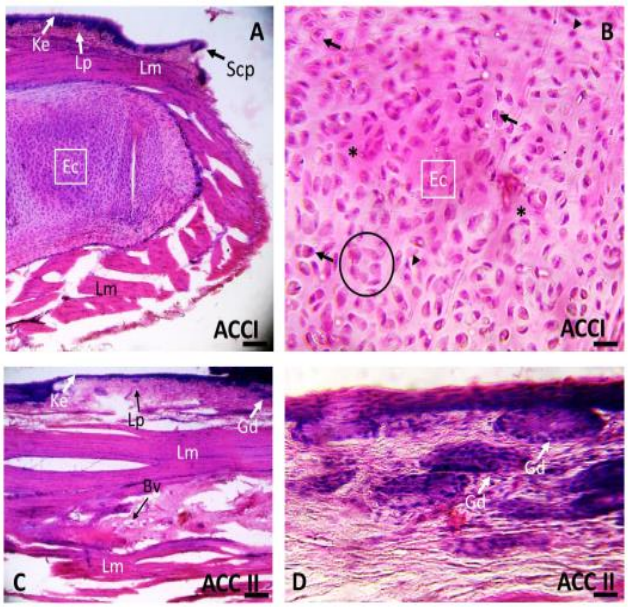

Plate 2.
Photomicrographs of the longitudinal section of the apical aspect of the tongue of the juvenile cattle egret (*Bubulcus ibis*). A. Cranial apical part. B. High power micrograph of the entoglossal cartilage (Ec) in A. C. Caudal apical part. D. High power micrograph of the glandular duct (Gd) in C. Lp – Lamina propria, Bv – Blood vessel, Ke - keratinized squamous epithelium, Lm - lingual muscles, Scp - spinous conical papillae, ACC I and ACC II are the cranial and caudal apical portions, respectively. Stain: H&E. Scale bar: A-D = 100 µm

The Apex: The histological profile of the longitudinal section of the cranial apex (the early and later part) of juvenile egret tongue is characterized by lingual mucosa containing keratinized squamous epithelium with exclusive presence of spinous conical papillae (Scp) in the mucosa of the early part of the apex. The bulk of the cranial part is typified by the presence of a centrally located entoglossal cartilage (Ec) bounded dorsally and ventrally by lingual muscles (Lm) (Plate 2A and B). However, although the histological appearances of the caudal apex of the tongue also featured keratinized squamous epithelium (Ke), lingual muscles predominate its architecture, with few glandular ducts (Gd) (Plate 2C and D).

The Body: The histology of the body aspect (early dorsal part) of the egret tongue is characterized by the presence of keratinized squamous epithelium and appearance of foliate papillae on the lingual mucosa (Plate 3A). The later dorsal part of the tongue's body bears both keratinized and non-keratinized epithelium most especially on the ventral aspect. It also has on its dorsal most part foliate and on the ventral part filiform papillae (Flp) as well as a prominent entoglossal cartilage (Plate 3D). The final dorsal part (i.e. caudal-most part) of the tongue's body (Plate 4A) showed keratinized squamous epithelium and foliate papillae on the lingual mucosa. Moreover, there was a presence of relatively thin lingual muscle layer dorsal to centrally located massive entoglossal cartilage layer (Plate 4A). Conversely, the final ventral part of the tongue's body is characterized by the presence of entoglossal cartilage layer and a thin layer of lingual muscle (Plate 4B and C).

The Root: The histo-architecture of the root (cranio-dorsal part) of the tongue is typified by the presence of keratinized squamous epithelium, multiple glandular ducts within the lamina propria and uneven distribution of lingual muscles (Plate 5A). The later dorsal part (mid-portion) of the tongue's root was observed to be lined by both keratinized and non-keratinized epithelia most especially on the cranio-ventral aspect. It also bears on the dorsal most part foliate papillae and filiform on the cranio-ventral part coupled with the presence of substantial entoglossal cartilage and few lingual muscles (Plate 5B).

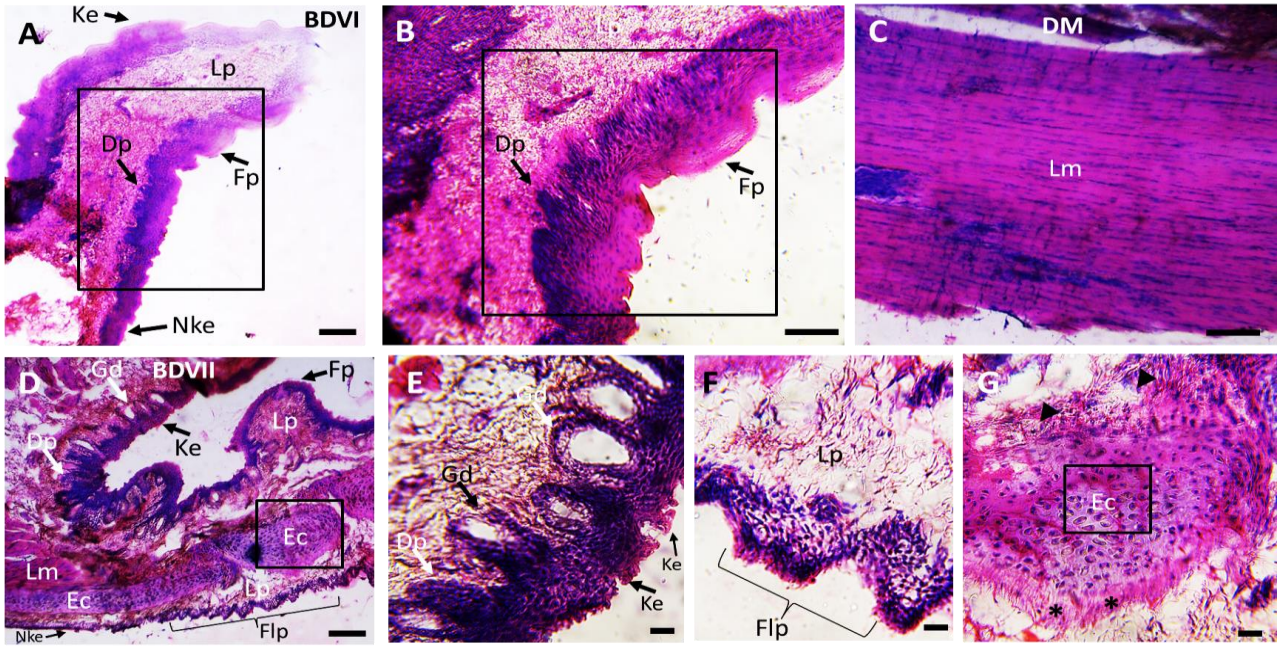

Plate 3.
Photomicrographs of the longitudinal section of the body aspect of the tongue of the juvenile cattle egret (*Bubulcus ibis*). **A.** Early dorsal part of the tongue's body **B.** Higher power micrograph of the boxed area in A. **C.** Early ventral part of the tongue's body **D.** Mid-dorsal part of the tongue's body. **E-G:** These are high power micrographs of keratinized squamous epithelium (Ke), filiform papillae (Flp) and entoglossal cartilage (Ec) (boxed area) of D. Stain: H&E. Scale bar: A-G = 100 µm

For the more later dorsal part of the tongue's root (Plate 5C), the following features were recognized; Keratinized squamous epithelium, localized adipocytes, glandular ducts within lamina propria and lingual muscles. On the other hand, there was presence of substantial entoglossal cartilage and more lingual muscles in the most caudal dorsal part (Plate 5D). With respect to the ventral aspect of the tongue's root, its' bulk is constituted by lingual muscles.

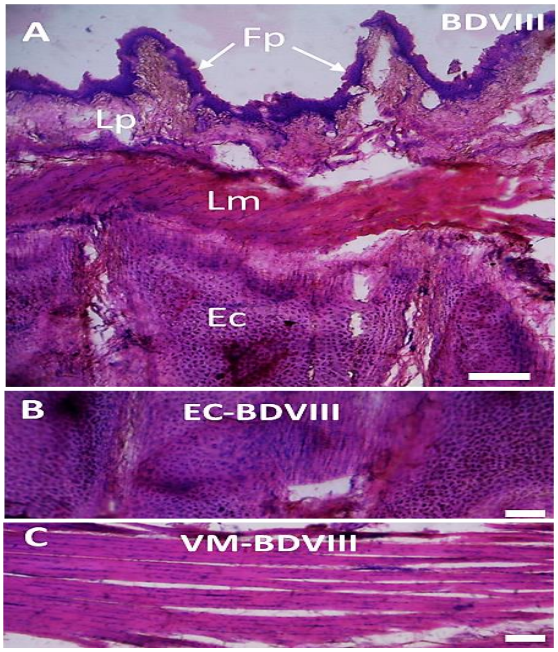

Plate 4.
Photomicrographs of the longitudinal section of the body aspect of the tongue of the juvenile cattle egret (*Bubulcus ibis*). A. Dorso-caudal extremity of the tongue's body. B-C. Dorso-ventral extremity of the tongue's body. Fp – foliate papillae, Lp – lamina propia, and entoglossal cartilage (Ec). Scale bar: A-C = 100 µm

Histomorphometry: The epithelial height (EH) was found to be highest in the cranial aspect of the body of the tongue compared to the apex and root. For the lamina propia height (LP), the highest value was recorded in the cranial aspect of the dorsoventral segment of the root of the tongue compared to the apex and body (Table 3). Similar values were recorded for the dorsal lingual muscles of the body (middle portion) and the root (the most caudal part) (352.88±15.60 µm and 310.31±22.54 µm, respectively) compared to the lesser value recorded for the apex (188.26±17.83 µm). In contrast, the ventral lingual muscle (VM) was most dominant in the caudal portion of the body in comparison with the apex and root. With regards to the entoglossal cartilage (EC), it was massive in the caudal portions of the root and in the body. Of note, the lamina propia height (LP) values of the body and the root decreased cranio-caudally (Table 3).

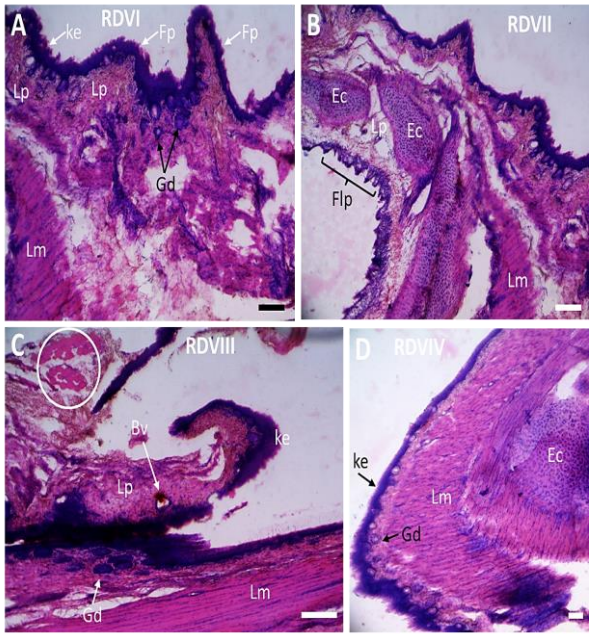

Plate 5.
Photomicrographs of the longitudinal section of the root aspect of the tongue of the juvenile cattle egret (*Bubulcus ibis*). **A-B.** Cranial dorsal portions of the tongue's root. **C-D.** Caudal dorsal portions of the tongue's root. Ke - keratinized squamous epithelium, Fp - filiform papillae, Ec - entoglossal cartilage, Lp – lamina propia, Lm - lingual muscles, Flp - filiform papillae and Gd – glandular ducts Stain: H&E. Scale bar: A-D = 100 µm.

Table 3.
Histomorphometric measurements of the tongue in the juvenile cattle egret

Apex Parameters (µm)	**EH-ACCI**	**LP-ACCI**	**DM-ACCI**	**EC-ACCI**	**VM-ACCI**	**EH-ACCII**	**LP-ACCII**	**DM-ACCII**	**EC-ACCII**	**VM-ACCII**
	33.91 ±3.97	29.35 ±4.63	159.61 ±10.76	454.96 ±11.44	254.39 ±16.62	24.62 ±2.09	50.56 ±4.65	188.26 ±17.83	335.18 ±18.41	231.66 ±6.99
Body Parameters	EH-BDV1	LP-BDV1	EH-BDVII	LP-BDVII	EC-BDVII	DM-BDVII	VM-BDVII	EH-BDVIII	LP-BDVIII	EC-BDVIII
	54.69 ±6.6	139.02 ±10.74	48.8 ±4.54	112.73 ±12.47	166.67 ±15.07	352.88 ±15.6	398.8 ±22.59	53.72 ±6.41	101.01 ±11.71	830.13 ±100.9
	DM-BDVIII	VM-BDVIII	EH-RDV1	LP-RDV1	EC-RDV1	VM-RDVI	EH-RDVII	LP-RDVII	EC-RDVII	VM-RDVII
	256.5 ±13.97	637.74 ±42.15	43.78 ±10.15	164.43 ±16.87	775.53 ±30.06	458.02 ±24.24	49.99 ±6.27	82.05 ±6.55	177.41 ±13.49	454.83 ±18.08
Root Parameters	EH-RDVIII	LP-RDVIII	EC-RDVIII	DM-RDVIII	VM-RDVIII	EH-RDVIV	LP-RDVIV	EC-RDVIV	DM-RDVIV	VM-RDVIV
	36.73 ±6.79	27.62 ±5.88	1173.52 ±157.26	254.3 ±21.15	526.13 ±14.7	32.7 ±4.49	35.21 ±5.22	503.65 ±18.24	310.31 ±22.54	525.61 ±28.29

The parameters were expressed as mean±SD. Measurements were based on the schematic illustration in Fig. 2. Legends: EH, LP, DM, EH, VM, ACC, BDV and RDV were as earlier state

DISCUSSION

The tongue constitutes a major part of the lingual apparatus and it is situated on the lower beak (mandible) floor. Lingual apparatus components include: the tongues' hyoid apparatus (a cartilaginous and bony structure), blood vessels, connective tissues and innervations (Homberger, 1989). The tongue is endowed with the intrinsic and extrinsic muscles; while the extrinsic muscles in conjunction with the extrinsic connective tissues link the lingual apparatus with the skull, the intrinsic tongue muscles join the hyoid apparatus bones, thereby enhancing their relative movements and changing lingual conformation (Crole and soley, 2009). Meanwhile, in contrast to most mammalian tongues, only the extrinsic muscle is consistently present in almost all birds (Huang *et al*., 1999), except the Parrot (Homberger, 1989).

Variations exist in the morphological and structural adaptations of the avian tongue to the various ecological conditions, especially their feeding patterns and behaviours, with correlations documented between the food intake type and lingual morphology (Iwasaki 2002; Sabry, 2015). The disparity in lingual features such as the lateral boundary and median sulcus conformations, papillae types and predominance, degree of keratinization of lingual epithelia and the placement of the lingual glands determine the level of tongues' mobility and its ability to capture preys as well as manipulate and swallow food items (Jackowiak and Godynicki, 2005; Emura *et al*., 2008).

The avian tongue is a triangular shaped organ, assuming the shape of the oral cavity, and it is non-protrusible. Generally, birds possess a poorly developed sense of taste (Dyce *et al*., 2016). In the present study, the tongue of the juvenile cattle egret (*Bubulcus ibis*) was observed to be divided into three portions namely; the apex, body and root. The observed divisions of egret tongue were consistent with the reports of Erdogan and Iwasaki (2014) on the avian tongue. The juvenile cattle egret has a V-shaped outline, with its apical part assuming a spear-like shape cranially, dorsally possessing a median groove. The arrow shaped tongue of the juvenile egret and its observed conformation to the shape of the beak could largely be associated with their kind of diet and the mechanism of food intake. Seedikkoya *et al*., (2007) proposed that the dagger-like apex of the egrets' tongue provides suitable eating prospects for searching small food items, especially insects in waste dumps and ticks on cattle's body. This morpho-functional attribute with respect to the shape of egret tongue concur with our observation and the previous report by Harrison, (1964).

The laryngeal mound of birds is caudal to the base of the tongue and the glottis is found on it, appearing as a median slit. Interestingly, the glottis of birds is not guarded by the epiglottis (Dyce *et al*., 2016). In this study, there was a laryngeal mound that is bounded caudally by the pharyngeal papillae at the root end of the tongue. These pharyngeal papillae are believed to perform functions connected with the retaining of food in the oral cavity and directing food into the oesophagus. The observations on the pharyngeal papillae gross appearance in the egret further validate the findings of McLelland (1979), Kobayashi *et al*. (1998), and Erdogan and Iwasaki (2014).

The average body weight of the juvenile cattle egret in this study was 538.33±78.72 g. This is in line with the weight range (270 - 512 g) of the cattle egret as documented by Telfair and Raymond, (2006). The whole length of the juvenile cattle egret tongue was recorded as 4.48 mm, this is less than the value recorded for the length of the adult cattle egret tongue (6.00 mm) by Al-Zahaby (2016). Conversely, in this study,a slightly higher value (4.40 mm) for the whole tongue width was recorded, relatively to the reported value (4.00 mm) by Al-Zahaby (2016). Overall, the regression analysis data indicates that the weight of the bird can be excellently predicted from weight of the tongue, width of the root, length of the tongue and the breadth of the body. With respect to the earlier investigations on the gross morphometry of the tongue of other avian species, Bello *et al*., (2015) observation on the tongue of Muscovy duck revealed that the duck's tongue was triangular in shape with a mean length of 55 mm, the apex and root mean widths of 10mm and 16mm, respectively and the root length of 7.5 mm. Also, Pourlis (2014) observed that the tongue of the quail was triangular in shape with a slightly rounded apex and an average length of 1.2 cm. More recently, İlgün *et al*., (2020) equally reported in Guinea fowl tongue, features like flattened, pointed and triangular shaped tongue with the mean length of 18.21 mm.

The presence of frenulum, a membrane fold attaching the lingual ventral aspect to the floor of oral cavity and the free nature of the tongue at the apex seen in this study seemed to be morphological features that assist in the anchorage of the tongue within the oral cavity. These gross findings on the tongue of the juvenile egret have structural resemblance with the typical morphological appearance of the tongue documented by McLelland (1979), Homberger and Meyers, (1989) in chicken.

Histologically, previous reports indicated that the dorsal surface of the apex of avian tongue was lined by slightly keratinized stratified squamous epithelium comprised of six to eight layers of polyhedral cells with coverings by a few-layered keratinized epithelia (Farouk and Hassan, 2015), and the ventral surface possessed thinner and highly keratinized epithelium with a slightly wavy basement membrane (El-Bakary, 2011). The adult cattle egret was documented by Al-Zahaby *et al*., (2016) to possess keratinized lingual epithelia, with its' largely parakeratinized epithelia leading to the slough-off and desquamation of its superficial cells to varying degrees, except for epithelia of the tongues' root which was smooth and less exfoliated.

The epithelial keratinization type (stratified squamous) and the papillae (conical and filiform) distribution observed on the lingual mucosa of the different divisions of the juvenile cattle egret tongue seemed to vary with the regions, with the exclusive presence of numerous glandular ducts and localized adipocytes in the lamina propia of the apex and body. The present study also showed that the lamina propia height of the tongue was higher in the body and root of the tongue compared to the apex. This could be due to the constant external assaults on the apex of the tongue since it is the first line of contact with food. The relatively larger proportions of the lingual body muscles could be attributed to the tapered nature of the tongue. Qureshi *et al*., (2017) reported that the mean thickness of the lingual epithelium, submucosa and muscularis and lamina propia of the immature Duck (Anas platyrhynchos) were 96.13±12.04, 150.87±0.002, 232.67±24.78 and 118.93±7.03 µm,

respectively, although the authors did not state from which region(s) of the tongue the measurements were made. The authors also reported that there was an increase in thickness from the immature stages to the adult stages after which it remained fixed till old age.

The observed variations in the nature of the epithelial stratification and keratinization as well as the progressive cranio-caudal decrease in the epithelial thickness of the tongue from the apex to the root in the cattle egret here studied could be attributed to the functional resistance of the lingual epithelium to external assaults. The lingual epithelial nature described in this study wholly concurs with reports of Iwasaki *et al*. (1997) and Skieresz-Szewczyk *et al*. (2014) in the tongue of Middendorf's bean goose and the tongue of the domestic duck, respectively. It however, contrasted the lingual epithelial nature described by Crole and Soley (2009) in Emu tongue.

The dense irregular connective tissue, adipose cells, strong layer of striated muscle fibres and numerous blood vessels observed as components of the lamina propria in the egret tongue could be responsible for the firmness of the tongue of this species. The lamina propria profile seen in this work is similar to Erdogan and Iwasaki (2014) report on function-related morphological characteristics and specialized structures of the avian tongue. This presence of tubulo-alveolar glands surrounded by connective tissue beneath the dorsal lingual epithelium in the egret tongue could be suggestive of higher demands for lubricating fluid for ingested food particles. McLelland, (1990) mentioned that the structure of lingual glands is more developed and complex in birds that feed on dry food compared to those consuming naturally well-lubricated food. Therefore, their presence validates the above statement.

The histological features of the entoglossal cartilage of the juvenile cattle egret were typical of hyaline cartilage. Importantly, the massive nature of the entoglossal cartilage of the juvenile cattle egret tongue and its envelop formed by a definite perichondrium consisting of a fibrous connective tissue and striated muscle fibres could provide an important morphological support to the tongue and could also be suggested to be of importance in the movement of the tongue out of the oral cavity. The morpho-physiological details of entoglossal cartilage of egret assessed are similar to those reported by Erdogan and Alan, (2012) in Chukar partridges' tongue, Igwebuike and Anagor (2013) in Muscovy duck, Pasand *et al*. (2010) in male ostrich, and Parchami and Dehkordi (2011) in domestic pigeon.

This study revealed that the tongue of the juvenile cattle egret is divided into three portions of the apex, body and the root, grossly. It demonstrated that the shape of the tongue of the juvenile cattle egret is in conformation with the shape of the beak and this is largely associated with their kind of diet and mechanism of feed intake. Altogether, the above datasets could come handy in the clinical and regional anatomical studies of this bird. Further studies are required especially on the histochemical and immunohistochemical demonstration of the tissue components in the tongue of the juvenile cattle egret as this will further elucidate its morphology, and as well studies could be carried out on the variation of the tongue morphology across different age groups of the cattle egret.

REFERENCES

Abayomi, T. A., Ofusori, D. A., Ayoka, O. A., Odukoya, S. A., Omotoso, E. O., Amegor, F. O., Ajayi, S. A., Ojo, G. B. and Oluwayinka, O. P. (2009): A comparative histological study of the tongue of rat (Rattus Norvegicus), bat (Eidolon Helvum) and pangolin (Manis Tricuspis). *Int. J. Morphol*. 27, 1111–1119.

Ahmed, S. (2018). Histological and Histomorphometric Evaluation of Anterior Part of Rats Tongue Exposed to Passive Cigarette Smoking. *Egypt J Oral Maxillofac Surg*. 9:174-178 https://doi.org/10.21608/omx.2019.5326.1018

Al-Zahaby, A-AS. (2016). Light and scanning electron microscopic features of the tongue in cattle egret. *Microsc Res Tech* 79:595–603. https://doi.org/10.1002/jemt.22672

Azeez, I.A., Ekeolu, O.K., Usende I.L., Adejumobi, O.A. and Adetogun, A. (2022a). Anatomical investigation on the craniofacial and ocular morphometrics of the male Western Cattle egret (*Bubulcus ibis*). *Anatomy Journal of Africa*, 11(1), 2033-2042.

Azeez, I.A., Hena, S.A., Ogwujo, P.O., Omirinde, J.O., Akinsola, O.M., Plang N.J. and Gosomji I.J. (2022b). Comparative skin anatomy of the Nigerian local dogs and pigs. *Savannah Veterinary Journal*, 5(1), 20-27.

Bello, A., Onu, J.E., Jimoh, M.I. and Olushola, O. (2015). Morphometric observations of the tongue of the domestic duck (Anas platyrhynchos domestica) *Research Journal of Phytomedine* 1(1): 30-2

Crole, M.R and Soley, J.T (2009). Morphology of the tongue of the Emu (Dromaius novaehollandiae). Gross anatomical features and topography. *Ondersteport Journal of Veterinary Research* 76: Pp 335-345.

Dyce, K. M., W. O. Sack, and C. J. G. Wensing. (2016). Textbook of Veterinary Anatomy. 5th edn. Philadelphia: Saunders Company. ISBN: 9780323442640.

Ekeolu, O.K., Usende, I.L., Adejumobi, O.A., Azeez, I.A. and Orolu-Adedeji, M.O. (2016). Comparative morphometric study of the right and left pectoral and pelvic bones of cattle egret (Bulbucus ibis). *Int J Vet Sci* 5:285–289

El-Bakary, N.E. (2011). Surface morphology of the Hoopee (UpupaEpops). *Journal of American Science* 7(1): 394-399.

Emura S, Okumura T, Chen H. 2008. Scanning electron microscopic study of the tongue in the peregrine falcon and common kestrel. *Okajimas Folia Anat Jpn* 85:11–15.

Erdogan, S., and Iwasaki, S. (2014). Function-related morphological characteristics and specialized structures of the avian tongue. *Annals of Anatomy* 196(2-3): 75-87.

Erdogan, S. and Alan A. (2012). Gross anatomical and scanning electron microscopic studies of the oropharyngeal cavity in the European Magpie (Pica pica) and the Common raven (Corvus corax). *Microscopy Research and Techniques* 75: 379-387.

Farouk, S.M. and Hassan, S.A. (2015). Tongue of the laughing dove (Stigmatopelia senegalensis): Histochemical and Ultrastructural characteristics. *Journal of cytology and histology*, 6:363.

Hancock, J. (1984). Field Identification of West Palearctic White Herons and Egret. *Brit Birds*, 77: 451-457.

Harrison, J.G. (1964). Tongue. A new dictionary of birds. A.L Thomson, Nelson. Pp. 825-827.

Homberger, D. G. and Meyers, R.A. (1989). Morphology of the lingual apparatus of the domestic chicken (Gallus gallus) with special attention to the structure of the fasciae. *American Journal of Anatomy* 186: Pp 217-257.

Huang R., Zhi Q., Izpisua-Belmonte J., Chist B., Patel K., (1999). "Origin and development of avian tongue muscles" *Ana Embryo* 200:137-152.

Igado, O.O., Omobowale, T.O., Ajadi, R.A., and Nottidge, H.O. (2015). Gross Morphometric Studies on the Tongue, Buccal Cavity and Hard Palate of the Fruit Bat (Eidolon helvum). *J Vet Med Ser C Anat Histol Embryol* 44:283–287. https://doi.org/10.1111/ahe.12138

Igwebuike, U.M., and Anagor, T.A. (2013). Morphology of the oropharynx and tongue of the Muscovy duck (Anas platyrhynchos) *Veterinary Archives* 83:685-693.

İlgün, R., Kuru, N., Bölükbaş, F. and Gür, F.M., (2020). Histological and electron microscopical structure of tongue and lingual papillae of guinea fowl (Numida meleagris). *Pakistan J. Zool.*, Vol. 52, Iss. 3, pp 949-956.

Ivory, A. 2000. "*Bubulcus ibis*" (On-line), Animal Diversity Web. https://animaldiversity.org/accounts/Bubulcus_ibis/

Iwasaki, S.I. (2002). Evolution of the structure and function of the vertebrate tongue. *J. Anat*. 201:1-13

Iwasaki, S., Asami, T., and Chiba, A. (1997). Ultrastructural study of the keratinization of the dorsal epithelium of the tongue of Middendorf's bean goose, Anser fabalis middendorfii (Anseres, Antidae). *Anatomical Record* 247: 147-163.

Jackowiak, H., and Godynicki, S. (2005(. Light and scanning electron microscopic study of the tongue in the white tailed eagle (Haliaeetus albicilla, Accipitridae, Aves). *Ann Anat* 187:251–259.

Kobayashi, K., Kumakura, M., Yoshimura, K, Inatomi, M., and Asami, T. (1998). Fine structure of the tongue and lingual papillae of penguin. *Archves of Histology and Cytology* 61: 37-46.

Lierz, M., and Korbel, R. (2012). Anesthesia and Analgesia in Birds. *J Exot Pet Med*. https://doi.org/10.1053/j.jepm.2011.11.008

Mckilligan, N. (2005). Herons , Egrets and Bitterns: Their Biology and Conservation Status in Australia. Csiro Publishing, Collingwood, Australia. ISBN: 9780643092099.

McLelland, J. (1979). Digestive system, in form and function in birds. Volume 1, edited by A.S King and J Mclelland. San Diego, California Academic Press. Pp. 69-92.

McLelland, J. (1990). A colour atlas of avian anatomy. Published by Mosby. Pp. 1-127. ISBN 9780723415756.

Nomina Anatomica Avium (2017). Handbook of Avian Anatomy.

Parchami, A. and Dehkordi, R.A. (2011). Lingual structure in the domestic pigeon (Columba livia domestica). A light and scanning microscopic study. *World Applied Sciences Journal*. 12(9): 1517-22.

Pasand A., Tadjalli M., and Mansouri H. (2010). Microscopic study on the tongue of male ostrich. Eur. J. Bio, Sci. 2(2): 24-31.

Pourlis, A.F. (2014). Morphological features of the tongue in the quail (Cortunix cortunix japonica). *Journal of Morphological sciences* 31(3): 177-181.

Qureshi, A.S., Faisal, T., Saleemi, M.K. and Ali, M.Z., 2017. Histological and histometric alterations in the digestive tractand accessory glands of duck (anasplatyrhynchos) with sex andprogressive age. *Journal of Animal & Plant Sciences*, 27(5); 1528-1533

Rezk, H.M. (2015a). Anatomical investigation on the appendicular skeleton of the cattle egret (*Bubulcus ibis*). *J Exp Clin Anat* 14:5–12.

Rezk, H.M. (2015b). Anatomical Investigation on the Axial Skeleton of the Cattle Egret, *Bubulcus ibis*. *Assiut Vet. Med. J*. 61:12-21

Sabry, D. (2015). Comparative studies on tongue of Egretta ibis and Gallus gallus. *Res Opin Anim Vet Sci* 5:375-382.

Sasan, J.S., Sarma, K., Suri, S., and Nabi, N. (2019). Gross and morphometrical studies on humerus of cattle egret (*Bubulcus ibis*). *Explor Anim Med Res*. 9(1):93-96.

Seedikkoya, K, Azeez, P.A., Abdul Shukkur, E.A. (2007). Cattle egret as a biocontrol agent. *Zoos' Print J*. https://doi.org/10.11609/jott.zpj.1731.2864-6

Siegfried, W.R. (1971). The Food of the Cattle Egret. *J Appl Ecol.* 8:447–468. https://doi.org/10.2307/2402882

Skieresz-szewczyk, K., Jackowiak H., and Ratajckzak, M. (2014). LM and TEM study of the orthokeratinized and parakeratinized epithelium of the tongue in the domestic duck (Anas platyrhynchos f. domestica). Micron 67: 117-124.

Telfair, R.C. and Raymond, C. 2006. Cattle Egret (*Bubulcus ibis*), The Birds of North America. Ed. Poole, A. thaca: *Cornell Lab of Ornithology*. http://bna.birds.cornell.edu.hal.weber.edu:2200/bna/species/113doi:10.2173/bna.113.